



TECHNISCHE
UNIVERSITÄT
WIEN

D I S S E R T A T I O N

Coupling and numerical integration of the Landau–Lifshitz–Gilbert equation

(Kopplung und numerische Integration der Landau–Lifshitz–Gilbert-Gleichung)

ausgeführt zum Zwecke der Erlangung des akademischen Grades
eines Doktors der technischen Wissenschaften unter der Leitung von

Prof. Dr. Dirk Praetorius

E101 – Institut für Analysis und Scientific Computing – TU Wien

eingereicht an der Technischen Universität Wien
Fakultät für Mathematik und Geoinformation
von

Dott.mag. Michele Ruggeri

Matrikelnummer: 1328691

Oswaldgasse 118/5/10, 1120 Wien

Diese Dissertation haben begutachtet:

1. **Prof. Dr. Sören Bartels**
Abteilung für Angewandte Mathematik, Albert-Ludwigs-Universität Freiburg
2. **Prof. Dr. Ansgar Jüngel**
Institut für Analysis und Scientific Computing, TU Wien
3. **Prof. Dr. Dirk Praetorius**
Institut für Analysis und Scientific Computing, TU Wien

Wien, am 25. Oktober 2016

Abstract

The understanding of the magnetization dynamics plays an essential role in the design of many technological applications, e.g., magnetic sensors, actuators, storage devices, electric motors, and generators. The availability of reliable numerical tools to perform large-scale micromagnetic simulations of magnetic systems is therefore of fundamental importance. Time-dependent micromagnetic phenomena are usually described by the Landau–Lifshitz–Gilbert (LLG) equation. The numerical integration of the LLG equation poses several challenges: strong nonlinearities, a nonconvex pointwise constraint, an intrinsic energy law, which combines conservative and dissipative effects, as well as the presence of nonlocal field contributions, which prescribes the coupling with other partial differential equations (PDEs). This dissertation is concerned with the numerical analysis of a tangent plane integrator for the LLG equation. The method is based on an equivalent reformulation of the equation in the tangent space, which is discretized by first-order finite elements and requires only the solution of one linear system per time-step. The pointwise constraint is enforced at the discrete level by applying the nodal projection mapping to the computed solution at each time-step. In this work, we provide a unified abstract analysis of the tangent plane scheme, which includes the effective discretization of the field contributions. We prove that the sequence of discrete approximations converges towards a weak solution of the problem. Under appropriate assumptions, the convergence is unconditional, i.e., the numerical analysis does not require to impose any CFL-type condition on the time-step size and the spatial mesh size. Moreover, we show that a fully linear projection-free variant of the method preserves the (unconditional) convergence result. One particular focus of this work is on the efficient treatment of coupled systems, for which we show that an approach based on the decoupling of the time integration of the LLG equation and the coupled PDE is very attractive in terms of computational cost and still leads to time-marching algorithms that are unconditionally convergent. As an application of the abstract theory, we analyze several extensions of the micromagnetic model for the simulation of spintronic devices. These range from extended forms of the LLG equation to more involved coupled systems, in which, e.g., the nonlinear coupling with a diffusion equation, which describes the evolution of the spin accumulation in the presence of spin-polarized currents, is considered. Numerical experiments support our theoretical findings and demonstrate the applicability of the method for the simulation of practically relevant problem sizes.

Kurzfassung

Das Verständnis des dynamischen Verhaltens der Magnetisierung spielt beim Design vieler technologischer Anwendungen – z.B. magnetischer Sensoren, Aktoren, Datenspeicher, Elektromotoren und elektrischer Generatoren – eine essentielle Rolle. Die Verfügbarkeit zuverlässiger numerischer Methoden für die umfassende Simulation von magnetischen Systemen ist dazu sehr wichtig, um die kosten- und zeitintensive Produktion von Prototypen zu vermeiden. Zeitabhängige mikromagnetische Phänomene werden üblicherweise durch die Landau-Lifshitz-Gilbert-Gleichung (LLG-Gleichung) beschrieben. Die numerische Integration der LLG-Gleichung führt auf einige mathematische Herausforderungen: Nichtlinearitäten, eine nichtkonvexe punktweise Nebenbedingung, ein Energieerhaltungsgesetz und nichtlokale Effekte, die die Kopplung mit anderen partiellen Differentialgleichungen notwendig machen. Diese Arbeit befasst sich mit der numerischen Analyse des sogenannten Tangent-Plane-Verfahrens für die LLG-Gleichung. Diese Methode basiert auf der äquivalenten Formulierung der Gleichung im Tangentialraum, die durch ein Finite-Elemente-Verfahren erster Ordnung diskretisiert wird. Pro Zeitschritt muss bei diesem Verfahren ein lineares Gleichungssystem gelöst werden. Die punktweise Nebenbedingung der diskreten Lösung wird durch die knotenweise Projektion auf die Einheitssphäre sichergestellt. In dieser Arbeit erweitern wir die Analysis des Tangent-Plane-Verfahrens. Wir beweisen, dass die Folge der Näherungslösungen gegen eine schwache Lösung der LLG-Gleichung konvergiert. Unter gewissen Voraussetzungen konvergiert das Verfahren unbedingt, d.h. in der numerischen Analysis muss keine CFL-Bedingung zwischen der Zeitschrittweite und Ortsgitterweite gefordert werden. Außerdem zeigen wir, dass das Verfahren ohne nodale Projektion ebenfalls unbedingt konvergiert. Ein zentrales Thema dieser Arbeit ist die Behandlung einiger gekoppelter Systeme. Wir erweitern die Diskretisierung der LLG-Gleichung auf diese Kopplungen. Das resultierende, unbedingt konvergente Verfahren entkoppelt die Zeitintegration der LLG-Gleichung und der gekoppelten Gleichung, was zu einem günstigeren Rechenaufwand führt. Als Anwendung analysieren wir einige Erweiterungen des mikromagnetischen Modells in der Spintronik. Wir betrachten erweiterte Formen der LLG-Gleichung sowie (nichtlineare) Kopplungen der LLG-Gleichung mit einer Diffusionsgleichung für die Spin-Akkumulation. Numerische Experimente bestätigen die theoretischen Resultate und damit die Anwendbarkeit der entwickelten Algorithmen auf die Simulation praktisch relevanter Problemgrößen.

Riassunto

La comprensione dei fenomeni di evoluzione nei corpi ferromagnetici riveste un ruolo fondamentale per la progettazione di numerose applicazioni tecnologiche: sensori magnetici, attuatori, supporti di memoria, motori elettrici e generatori. La disponibilità di metodi affidabili per eseguire simulazioni numeriche di sistemi magnetici su larga scala è pertanto di vitale importanza. I fenomeni micromagnetici di tipo evolutivo sono normalmente descritti dall'equazione di Landau–Lifshitz–Gilbert, la cui approssimazione numerica pone diverse difficoltà: non-linearità, un vincolo puntuale e non-convesso, una legge di conservazione dell'energia (che combina effetti conservativi e dissipativi) e la presenza di contributi non-locali, che richiedono lo studio di sistemi in cui l'equazione di Landau–Lifshitz–Gilbert è accoppiata ad altre equazioni alle derivate parziali. Questa tesi si occupa dell'analisi numerica di un metodo di tipo 'tangent plane' per l'equazione di Landau–Lifshitz–Gilbert. Il metodo si fonda su una formulazione variazionale del problema basata sullo spazio tangente, che viene discretizzata mediante elementi finiti di primo ordine, in modo da richiedere soltanto la soluzione di un sistema lineare sparso per ogni time-step. La validità del vincolo puntuale a livello discreto viene assicurata attraverso la proiezione nodale della soluzione calcolata. In questa tesi, si propone un'analisi astratta del metodo 'tangent plane'. In particolare, si dimostra che la successione delle approssimazioni discrete converge verso una soluzione debole del problema. Assumendo la validità di ipotesi appropriate, la convergenza è incondizionata, ossia risulta valida senza che sia necessario imporre alcuna condizione CFL tra i parametri associati alla discretizzazione temporale e a quella spaziale. Inoltre, si mostra che l'omissione della proiezione, pur determinando la violazione del vincolo, non intacca il risultato di convergenza (incondizionata). Nel lavoro, si evidenzia come il disaccoppiamento della discretizzazione temporale dell'equazione di Landau–Lifshitz–Gilbert da quella dell'equazione a essa accoppiata costituisca una valida strategia per lo studio di sistemi. Tale approccio non solo risulta essere molto interessante dal punto di vista del costo computazionale, ma conduce anche ad algoritmi incondizionatamente convergenti. Come applicazione della teoria presentata, si analizzano alcune tra le più comuni estensioni del modello micromagnetico utilizzate per la simulazione di dispositivi spintronici. Esse spaziano da forme generalizzate dell'equazione di Landau–Lifshitz–Gilbert a sistemi complessi di equazioni non-lineari, in cui, per esempio, l'equazione di evoluzione per la magnetizzazione viene accoppiata a un'equazione di diffusione per lo spin, che incorpora nel modello la presenza di correnti elettriche polarizzate. Alcuni esperimenti numerici supportano i risultati teorici e dimostrano l'efficacia dei metodi proposti anche per la risoluzione di problemi derivanti da applicazioni concrete.

Acknowledgments

This thesis would not have been possible without the support of many people and institutions.

First and foremost, I would like to express my gratitude to my supervisor, Prof. Dirk Praetorius, for his guidance over the past three and a half years. His patience, knowledge, and invaluable assistance have been fundamental for my growth both as an individual and as a mathematician. One could not wish for a better supervisor.

I would like to thank Prof. Sören Bartels and Prof. Ansgar Jüngel for their reports on this thesis and their interest in my work.

I wish to thank all the colleagues of the working group I had the opportunity to meet during my doctoral studies for the fabulous work atmosphere and for all the fun we have had together: Michael Feischl, Thomas Führer, Gregor Gantner, Alexander Haberl, Josef Kemetmüller, Marcus Page, Carl-Martin Pfeiler, and Stefan Schimanko, as well as the foster members (at least for the recreational activities) Markus Faustmann and Alexander Rieder. A special mention is deserved by my office mate Bernhard Stiftner for his fundamental help during the preparation of the numerical experiments of this thesis.

I would like to extend my appreciation to Claas Abert, Florian Bruckner, Gino Hrkac, Thomas Schrefl, Dieter Suess, and Christoph Vogler. The interdisciplinary collaboration with them has been very important to broaden my horizons. Mathematicians sometimes forget the practical implications of their work.

I am very grateful to Ms Ursula Schweigler for her precious support during my countless battles against the Austrian bureaucracy and for her help during the organization of workshops.

I would like to thank the colleagues and friends of the doctoral program in *Dissipation and dispersion in nonlinear PDEs* for many interesting discussions.

Moreover, I would like to acknowledge the support of TU Wien through the *Innovative Projekte* initiative, the Austrian Science Fund (FWF) under grant W1245, and the Vienna Science and Technology Fund (WWTF) under grant MA14-44.

Deepest gratitude is also due to my family for their constant support throughout my studies.

Finally, I wish to thank my beloved wife Nicole for her encouragement, understanding, and patience, even during hard times. This thesis is dedicated to her and to *who is growing inside her*.

Vienna, October 25, 2016

Michele Ruggeri



Contents

1	Introduction	1
1.1	Motivation	1
1.2	State of the art	4
1.3	Contributions and general outline of the dissertation	6
2	Mathematical modeling	9
2.1	Maxwell's equations	9
2.2	Classical micromagnetic theory	11
2.3	Metal spintronics	21
3	Preliminaries	31
3.1	Nondimensionalization	31
3.2	Notation for Lebesgue/Sobolev/Bochner spaces	36
3.3	Time discretization	38
3.4	Finite element discretization	38
4	Tangent plane integrators	47
4.1	Model problem	47
4.2	Numerical algorithm	49
4.3	Convergence analysis	52
5	Application to metal spintronics	77
5.1	Spin diffusion model	77
5.2	Spintronic extensions of the LLG equation	91
6	Numerical results	101
6.1	Solution of the system	101
6.2	Numerical experiments	106
7	Perspectives and future work	115
A	Physical quantities, constants and units	119
A.1	Physical quantities	119
A.2	Physical constants	120
B	Auxiliary results	121
B.1	Linear algebra	121
B.2	Useful (in)equalities	122
B.3	Vector calculus	123
	References	125
	Curriculum Vitae	137

Chapter 1

Introduction

1.1 Motivation

The understanding of the magnetization dynamics plays an important role in the design of many technological applications, e.g., magnetic sensors, actuators, storage devices, electric motors, and generators. In magnetic recording devices, e.g., in hard disk drives (HDDs), the magnetization of ferromagnetic materials is used for the storage of data. The information is stored as tiny areas of either positive or negative magnetization on the surfaces of the disks. Each tiny area corresponds to a bit of information and the total storage capacity depends directly on how small the area needed to represent one bit of information can be made: The smaller the bits are, the greater becomes the capacity.

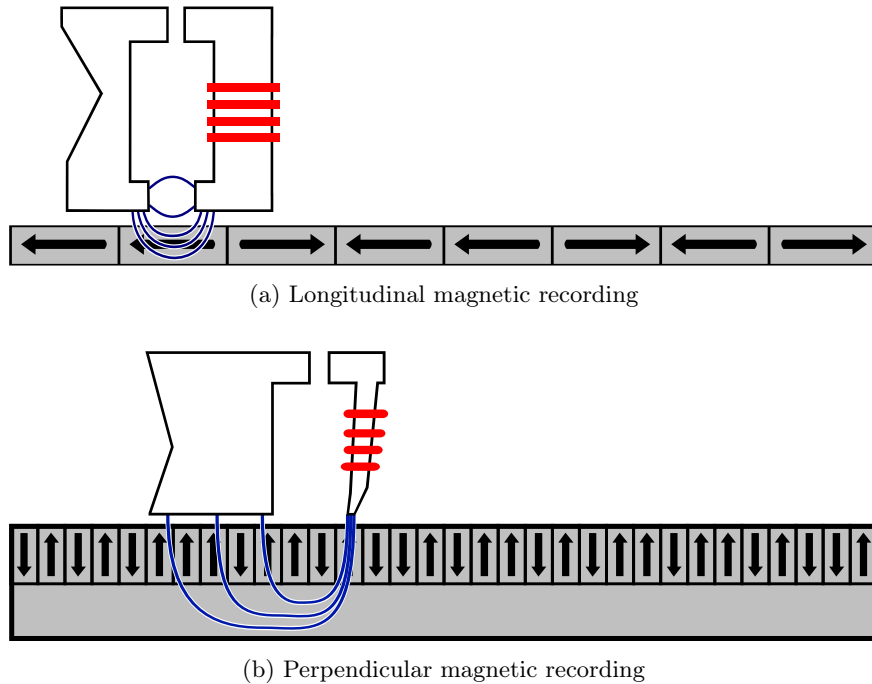


Figure 1.1: Different technologies for data recording in HDDs [1]: Longitudinal magnetic recording (a) vs. perpendicular magnetic recording (b).

Figure 1.1(a) shows the operating principle of an HDD based on the so-called longitudinal magnetic recording (LMR). This technique has been used for nearly 50 years in the industry and has nowadays been replaced by a more effective method, the perpendicular magnetic recording (PMR);

see Figure 1.1(b). In LMR-based HDDs, the magnetization of each bit is aligned horizontally with respect to the spinning platter of the drive. The areas which correspond to two adjacent bits with opposing magnetizations must be separated by a sufficiently wide transition region, in order to prevent the random magnetization flipping due to the superparamagnetic effect. In PMR-based HDDs, the perpendicular geometry allows the recording head field to penetrate the medium more efficiently, which substantially increases the number of magnetic elements that can be stored in a given area of the platter [172, 209].

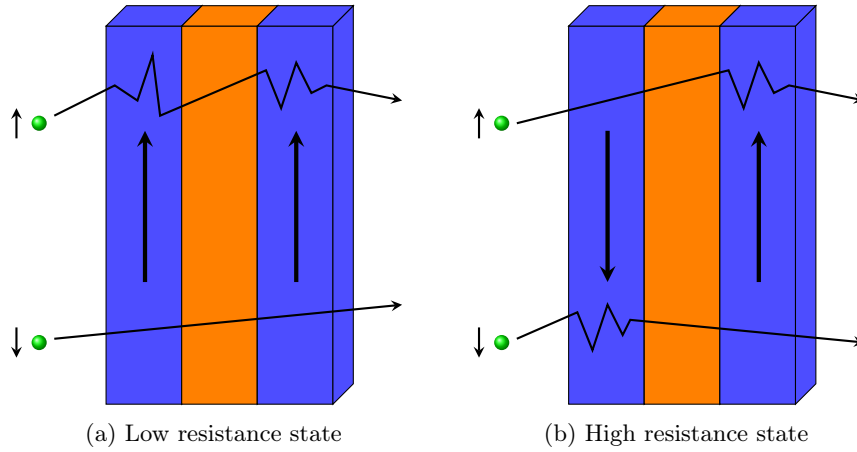


Figure 1.2: Giant magnetoresistance effect. The electrical resistance of a magnetic multi-layer depends on whether the magnetization configurations of consecutive ferromagnetic sublayers are in parallel alignment (a) or in antiparallel alignment (b).

The discovery of the giant magnetoresistance effect (GMR) in 1988 [19, 49], for which A. FERT and P. GRÜNBERG were awarded the Nobel Prize in physics in 2007, determined a breakthrough in magnetic HDD storage capacity. This effect occurs in magnetic multilayers (systems constituted by alternating ferromagnetic and nonmagnetic sublayers) and consists in the dependence of the electrical resistance on the relative orientation of the magnetization in the ferromagnetic layers. The electrical resistance changes from low for a parallel alignment to high for an antiparallel alignment; see Figure 1.2.

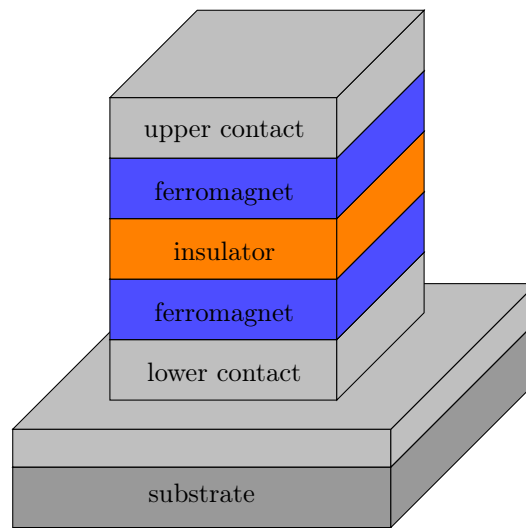


Figure 1.3: Schematic of a magnetic tunnel junction.

The GMR effect is the fundamental ingredient to understand the operating principle of a magnetic (or magnetoresistive) random access memory (MRAM) [80]. Unlike conventional solid-state RAMs, in MRAMs the information is stored neither as electric charge in a capacitor nor as electric current in an electronic circuit, but rather by magnetic storage elements. Every cell of a MRAM contains a magnetic tunnel junction (MTJ), such as the one depicted in Figure 1.3, which consists of a magnetic trilayer with two ferromagnetic sublayers separated by a thin nonmagnetic sublayer. One of the ferromagnetic layers (the so-called pinned or fixed layer) is a permanent magnet set with a fixed orientation of the magnetization. The information is stored in the relative orientation of the two ferromagnetic sublayers. Both the writing and the reading processes are performed by applying an electric current which flows perpendicularly with respect to the plane of the layers. On the one hand, in the writing process, the orientation of the magnetization of the free layer is switched by the resulting Oersted field. On the other hand, the reading process is based on the GMR effect and consists in measuring the electrical resistance of the structure.

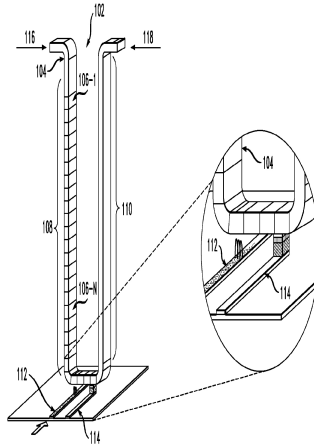


Figure 1.4: Unit cell of a domain wall racetrack memory [162, 201].

The storage density of MRAMs is limited by the use of the Oersted field in the writing process, which causes difficulties in terms of power consumption and scaling [65]. The input to overcome these problems came from the concept of spin transfer torque (STT), proposed independently by J. C. SLONCZEWSKI and L. BERGER in 1996, which predicts that the magnetization of a ferromagnetic layer can be switched by a spin-polarized current, even in the absence of a magnetic field [191, 44]. This theoretical progress allowed for the design of new recording devices. The STT random access memory (STTRAM) is another type of nonvolatile RAM which differs from the MRAM for the writing process only [115]: the magnetization reversal mechanism exploits the interactions with spin-polarized currents and is not based on the generated Oersted field. The same principle lies behind the operating principle of the domain wall racetrack memory [162], proposed by S. S. P. PARKIN in 2008, a new type of nonvolatile memory device which promises to provide the performance and reliability of solid-state memories, but at the low cost of standard HDDs. The unit cell of a racetrack memory is a ferromagnetic nanowire (see Figure 1.4), in which the information is stored as a pattern of magnetic domains and domain walls. Pulses of spin-polarized current move the entire pattern along the length of the wire close to the reading/writing units.

For the design and the realization of the described recording devices, the influence of a variety of different physical effects needs to be taken into account. Numerical simulations represent an invaluable tool to explore and gain new insights into these new technologies. This dissertation investigates the mathematical models which describe the physics behind the presented recording devices. Our aim is the development and the rigorous analysis of numerical algorithms to perform fast and reliable micromagnetic simulations. One particular focus is on the study of the convergence of the numerical solutions towards the solutions of the underlying (systems of) partial differential equations (PDEs).

1.2 State of the art

Micromagnetism, or micromagnetics¹, is the study of magnetic processes on a submicrometer length scale. Started with pioneering works by P.-E. WEISS, F. BLOCH, L. D. LANDAU, and E. M. LIFSHITZ, the theory was developed in the 1940s by W. F. BROWN, JR, who gave the first extended treatment of the topic in his 1963 book [54]. For several years, the micromagnetic theory essentially consisted of applications of, on the one hand, standard variational techniques to the so-called static micromagnetic problem, i.e., a constrained minimization problem for the micromagnetic energy [139], and, on the other hand, classical nucleation theory to model different magnetization reversal mechanisms [134, 135]. In the 1980s, with the simultaneous development of new magnetic materials (used, e.g., for permanent magnets, media and heads in recording devices, or magnetic sensors) and the widespread availability of large scale computational resources, one of the main focuses of the micromagnetic theory became the development of fast and reliable tools to perform large-scale simulations of magnetic systems.

Applications to magnetic recording, in which the external field can change fast so that the hysteresis properties are not accurately described by a static approach, encouraged the study of numerical methods to deal with the the so-called dynamic micromagnetic problem, i.e., the solution of the Landau–Lifshitz–Gilbert (LLG) equation which governs the time evolution of the magnetization [139, 107, 108]. In this framework, one of the main issues concerns the computation of the nonlocal magnetostatic interactions, which turns out to be, in many situations, the most time-consuming part of micromagnetic simulations [188, 177, 159].

Most of the micromagnetic codes (both commercial and open-source) are based on either the finite difference method (FDM) or the finite element method (FEM); see, e.g., [152, 185]. In finite-difference-based codes, the computation of the magnetostatic interactions is usually based on the fast Fourier transform (FFT). As an example, we mention the widely used Object-Oriented MicroMagnetic Framework (OOMMF) software [4, 82], a FDM-FFT micromagnetic code developed at the National Institute of Standards and Technologies (NIST) of Gaithersburg (USA). The application of the FEM in micromagnetics, more suitable to capture possible irregular shapes and grain structures of the magnets, was proposed by D. R. FREDKIN and T. R. KOEHLER [98, 125]. The efficiency of finite-element-based micromagnetic simulations was improved by the work of the groups of J. FIDLER, T. SCHREFL, and D. SUESS at TU Wien [181, 182, 97, 194, 180]. The magnetostatic interaction is formulated in terms of a scalar potential and discretized by combining the FEM with the boundary element method (BEM).

Nowadays, important lines of research in micromagnetics, from both the modeling and the computational point of view, concern the spintronic extensions of micromagnetics, e.g., with the concepts of spin transfer torque [202, 191, 212] or spin-orbit coupling [85, 197, 91], the study of enucleation processes, stability, and dynamics of magnetic skyrmions [157, 173, 175, 200, 127], and the incorporation of thermal effects [55, 100, 105, 90].

For a long time, the investigation of micromagnetic phenomena has been a prerogative of physicists and engineers. However, in the last three decades, the growing need of fast and reliable numerical simulations encouraged several mathematical studies, from both the analytical and the numerical point of view.

The first existence result for weak solutions to the LLG equation can be traced back to [203], where the coupling of the LLG equation with the Maxwell equations and with a balance law for the linear momentum to model the magnetoelastic interaction was considered. Since then, existence and regularity questions for the LLG equation have been the subject of intense research. The so-called small particle limit of the LLG equation, in which the effective field comprises only the exchange contribution, was studied, almost simultaneously, in [17, 114]. In particular, [17] adapted the proof of the analogous result for the harmonic maps heat flow [78, 48] and established global existence and nonuniqueness of weak solutions of the LLG equation. If the initial condition is sufficiently regular, strong solutions of the LLG equation exist locally in time and are unique [63].

¹Throughout the literature, these terms are usually used as synonyms of each other. To specify the precise acceptance of each of these words, we might say that micromagnetism refers to the underlying science, while micromagnetics is more concerned with the application of that science.

These two notions of solutions are connected by a weak-strong uniqueness principle, in the sense that if a strong solution exists up to some time $T > 0$, then any global weak solution coincides with it up to time T [84]. Extended versions and coupled problems have also been considered; see, e.g., an extended LLG equation with an additional spin transfer torque term [151], the coupling of the LLG equation with the full Maxwell equations [62], with a conservation law for the linear momentum [61], with a spin diffusion equation [103], with a system of drift-diffusion equations [210, 211] to model the magnetization dynamics in semiconductors. Further analytical results for (coupled problems for) the LLG equation can be found, e.g., in the papers [148, 154, 73, 74, 77, 149], in the monograph [113], in the recent preprint [94], as well as in the references therein. Recently, to include thermal effects, also the stochastic LLG equation has been investigated; see, e.g., [126, 59, 160, 60].

In parallel, the numerical integration of the LLG equation has also been the subject of many mathematical studies. The main challenges concern the strong nonlinearity of the equation, the nonconvex pointwise constraint satisfied by the solutions, an intrinsic energy law, which combines conservative and dissipative effects and has to be preserved by the numerical scheme, as well as the presence of nonlocal field contributions, which prescribes the (possibly nonlinear) coupling with other PDEs; see the review articles [21, 137, 101, 75], the papers [20, 71, 22, 72], and the monographs [169, 26]. One important aspect of the research is related to the development of unconditionally convergent (stable) methods, for which the numerical analysis does not require to impose any CFL-type condition on the spatial and temporal discretization parameters. For a numerical integrator of the LLG equation, such a property is highly desirable, since the application of standard ‘off-the-shelf’ explicit schemes usually enforces severe constraints on the time-step size which are sometimes unfeasible in practice or lead to unnecessary long computational time. As an example for numerical schemes based on the finite difference method, we mention the unconditionally stable Gauss–Seidel projection method [87, 207] and the scheme introduced in [79] based on the midpoint rule in time.

The works [40, 12] proposed numerical integrators, based on lowest-order finite elements in space, that are proven to be (unconditionally) convergent towards a weak solution of the small particle limit of the LLG equation. Both approaches were successfully applied to similar geometrically constrained evolution equations, such as the harmonic maps heat flow or the wave maps heat flow [41, 38, 35, 37], and extended to the case of the stochastic LLG equation [27, 25, 26, 13, 112].

On the one hand, the implicit midpoint scheme [40], proposed by S. BARTELS and A. PROHL in 2006, is formally of 2nd order in time and inherently preserves some of the fundamental properties of the LLG equation, such as the pointwise constraint (at the nodes of the mesh) and the energy law, but requires the solution of a nonlinear system of equations per time-step. To deal with it, the authors proposed a linear fixed-point iteration, which is still constraint-preserving, but requires the condition $k = \mathcal{O}(h^2)$ for the time-step size k and the mesh size h in order to be stable. The analysis of the algorithm was extended allowing the inexact solution of the nonlinear system in [34, 76]. In the recent preprint [167], we extended the analysis of the algorithm to the full effective field and proposed an implicit-explicit treatment of the field contributions, attractive from the computational point of view, which formally preserves the convergence of 2nd order in time. Extensions of the scheme for the coupling of the LLG equation with the Maxwell equations [24] and for an extended LLG equation which models the dynamics of the magnetization when the temperature is not constant were also considered [30, 31].

On the other hand, the θ -method [12], proposed by F. ALOUGES, is based on an equivalent reformulation of the LLG equation in the tangent space and requires only the solution of one linear system per time-step. Moreover, it is (unconditionally) convergent and formally of 1st order in time. The pointwise constraint, which characterizes the solutions of the LLG equation, is enforced at a discrete level by applying the nodal projection mapping to the computed solution at each time step. The stability of the scheme requires restrictive conditions either on the discretization parameters or on the underlying mesh. The method improves the explicit scheme introduced in [14] and analyzed in [39], where also the finite time blow-up of the solutions, motivated by the analogous result for the harmonic maps heat flow, was numerically investigated. An implicit-explicit approach for the full effective field was introduced and analyzed in [109, 16] and [56],

where the discretization of the field contributions and the coupling with a nonlinear material law were also considered. Strategies to improve the convergence order in time of the method were proposed in [16, 15]. Extensions of the tangent plane scheme for the discretization of the coupling of the LLG equation with the full Maxwell equations, the eddy current equation, a balance law for the linear momentum (magnetostriction), and a spin diffusion equation for the spin accumulation were considered in [142, 161, 29, 141, 28, 6]. In [161, 29, 141, 28, 6] one particular focus is on the decoupling of the time integration of the LLG equation and the coupled PDE, which is very attractive in terms of computational cost and leads to algorithms that are still unconditionally convergent. Inspired by [37], the projection-free version of the tangent plane scheme, which avoids the use of the nodal projection mapping, was introduced and analyzed in [6]. The violation of the constraint at the nodes of the triangulation occurring in this case is controlled by the time-step size, independently of the number of iterations. The projection-free tangent plane scheme was combined with a FEM-BEM coupling method for the discretization of the coupling of the LLG equation with the magnetoquasistatic Maxwell equations in full space in [92, 93]. There, assuming the existence of a unique sufficiently regular solution, the authors proved also convergence rates of the method.

1.3 Contributions and general outline of the dissertation

In the present dissertation, we contribute to the study of reliable and effective numerical methods for the LLG equation. Our algorithm is an extension of the tangent plane scheme [12]. We transfer ideas from [37] and propose a projection-free variant of the scheme. Moreover, we investigate its applicability for the efficient discretization of coupled systems of PDEs, in which the LLG equation is coupled with another equation that describes a particular nonlocal effective field contribution. One of the main focuses is on the development of unconditionally convergent finite element methods for the numerical approximation of LLG-based models for metal spintronic devices.

The thesis is the continuation of a successful cooperation between the Institute of Solid State Physics (group of D. SUESS) and the Institute for Analysis and Scientific Computing (group of D. PRAETORIUS) of TU Wien [111, 110, 58, 57, 56, 6, 7, 174, 205, 204, 8].

The remainder of this work is organized as follows:

- In Chapter 2, we describe the physical background which is behind the mathematical models considered in the dissertation. We start with a concise and micromagnetics-oriented presentation of the Maxwell equations (Section 2.1), the fundamental system of PDEs for the modeling of electromagnetic phenomena. In Section 2.2, we give a brief introduction on the classical theory of micromagnetics, with a careful description of the involved energy and field contributions as well as a formal derivation of the LLG equation. We conclude the chapter with an organic presentation of the, in our opinion, most relevant spintronic extensions of the LLG equation (Section 2.3).
- In Chapter 3, as a preparation for the following analysis, we collect some auxiliary results. To start with, we analyze the rigorous nondimensionalization of the problems introduced in Chapter 2 (Section 3.1). Then, we briefly describe the notation used for Lebesgue, Sobolev, and Bochner spaces (Section 3.2). Finally, we discuss some preliminary results about the time discretization (Section 3.3) and the spatial discretization (Section 3.4), which is based on 1st order finite elements.
- In Chapter 4, we propose a unified analysis of the tangent plane scheme for a generalized form of the LLG equation, which improves and extends those of [12, 16, 56, 6]. The proposed framework considers both the standard tangent plane scheme and its projection-free variant (Algorithm 4.2.1). We introduce a set of general assumptions (on the discretization parameters, on the field contributions as well as on their numerical approximations) which guarantee the (unconditional) convergence of the sequence of discrete solutions towards a weak solution of the problem (Theorem 4.3.2). The abstract framework covers most of the classical contributions that are usually included into the effective field.

- Chapter 5 is devoted to the numerical approximation of the extensions of the LLG equation, which are currently used for the micromagnetic modeling of spintronic devices. These models, which take the effects of the interaction between the magnetization and spin-polarized electric currents into account, can be classified into two main categories. On the one hand, there are extended forms of the LLG equation, in which the classical energy-based effective field is augmented by (local or nonlocal) additional terms which include the effect of the spin transfer torque [191, 213, 174, 8]. In this case, we show that the resulting extended forms of the LLG equation are covered by the abstract framework of Chapter 4, which ensures the convergence of the numerical scheme. On the other hand, the LLG equation is nonlinearly coupled with a diffusion equation for the spin accumulation [212, 103]. We show that the approach of [29, 141, 28], introduced to deal with the coupling of the LLG equation with the Maxwell equations (both the full system and the eddy current approximation) and the conservation of momentum (magnetostriction) and based on the decoupling of the time integration of the LLG equation and the coupled PDE, can be successfully applied. Here, differently from those cases, the magnetization affects not only the right-hand side of the coupled equation, but also the main part of the involved differential operator, which leads to a slightly more involved analysis.
- In Chapter 6, we propose some effective strategies for the solution of the constrained linear system which arises when the LLG equation is discretized by the tangent plane scheme (Section 6.1). In Section 6.2, to support our theoretical findings, we present some numerical results, which investigate both the general performance of our methods as well as their applicability for the simulation of practically relevant problem sizes.
- For most of the results and the methods of the present dissertation, there are a number of possible extensions and related open questions, which are, in our opinion, worth to be investigated. In Chapter 7, we give a short outlook on some of them.
- For the convenience of the reader, we conclude this work with two appendices. In Appendix A, we summarize the physical quantities and the physical constants considered throughout the thesis. In Appendix B, we collect some useful linear algebra definitions, vector identities, and well-known product rules of classical vector calculus.

Some of the presented results have been partially published in our papers [56, 6, 7, 174, 8]. However, in the present work, we propose an extended treatment of the topic with several additional comments. In particular, some results are more general or slightly sharper and some proofs have even been improved.

Chapter 2

Mathematical modeling

In this chapter, we introduce the partial differential equations that are considered throughout the thesis. When we refer to physical quantities, we use physical units in the International System of Units (SI). For an overview of the considered physical quantities/constants and the corresponding units, we refer the reader to Appendix A.

2.1 Maxwell's equations

The Maxwell system is a set of four fundamental equations in the theory of electromagnetism [145]. A classical reference for the physics of electromagnetism is, e.g., the book [119]. Here, we consider the macroscopic Maxwell equations, namely

$$\nabla \cdot \mathbf{D} = \rho, \quad (2.1a)$$

$$\nabla \cdot \mathbf{B} = 0, \quad (2.1b)$$

$$\nabla \times \mathbf{E} = -\partial_t \mathbf{B}, \quad (2.1c)$$

$$\nabla \times \mathbf{H} = \mathbf{J}_e + \partial_t \mathbf{D}. \quad (2.1d)$$

The physical quantities which appear in (2.1) are the magnetic flux density \mathbf{B} (in T), the electric displacement field \mathbf{D} (in C/m²), the electric field \mathbf{E} (in V/m), the magnetic field \mathbf{H} (in A/m), and the electric current density \mathbf{J}_e (in A/m²), which are three-dimensional vector fields, and the scalar-valued electric charge density ρ (in C/m³). For the orientation of the electric field and the electric current density, we adopt the standard convention: The direction of the electric field is chosen to be the direction of the force exerted on a positive test charge; consistently, the direction of electric current is arbitrarily defined as the direction of a flow of positive charges. The Maxwell system comprises the Gauss law (2.1a), the Gauss law for magnetism (2.1b), the Faraday law of induction (2.1c), and the Maxwell–Ampère circuital law (2.1d). The above equations are posed on the full space \mathbb{R}^3 . However, the charge density ρ and the electric current density \mathbf{J}_e are supported on a limited region of space, which we assume to be a bounded domain $\Omega \subset \mathbb{R}^3$, which represents the volume occupied by a conducting body. We assume $\mathbb{R}^3 \setminus \bar{\Omega}$ to be vacuum.

Formally, the summation of the time derivative of (2.1a) with the divergence of (2.1d) yields a conservation law for the electric charge on the conducting domain Ω , i.e., the continuity equation

$$\partial_t \rho + \nabla \cdot \mathbf{J}_e = 0.$$

Moreover, if the initial condition for \mathbf{B} satisfies (2.1b), the equation will be satisfied for all time. This follows by taking the divergence of (2.1c) and noting that the divergence of the curl is zero.

In the case of linear materials, one usually assumes the constitutive laws

$$\mathbf{D} = \varepsilon \mathbf{E}, \quad (2.2a)$$

$$\mathbf{B} = \mu \mathbf{H}, \quad (2.2b)$$

where the electric permittivity ε (in F/m) and the magnetic permeability μ (in N/A²) are symmetric and uniformly positive definite matrices in $\mathbb{R}^{3 \times 3}$. In particular, in vacuum, e.g., in $\mathbb{R}^3 \setminus \overline{\Omega}$, it holds that $\varepsilon = \varepsilon_0 \mathbf{I}_{3 \times 3}$ as well as $\mu = \mu_0 \mathbf{I}_{3 \times 3}$, where the positive constants ε_0 and μ_0 are the vacuum permittivity (in F/m) and the vacuum permeability (in N/A²), respectively. Under this assumption, the Maxwell system (2.1) can be rewritten as

$$\nabla \cdot (\varepsilon \mathbf{E}) = \chi_\Omega \rho, \quad (2.3a)$$

$$\nabla \cdot (\mu \mathbf{H}) = 0, \quad (2.3b)$$

$$\nabla \times \mathbf{E} = -\mu \partial_t \mathbf{H}, \quad (2.3c)$$

$$\nabla \times \mathbf{H} = \chi_\Omega \mathbf{J}_e + \varepsilon \partial_t \mathbf{E}. \quad (2.3d)$$

The characteristic function χ_Ω is a reminder that the charge density and the electric current density vanish in $\mathbb{R}^3 \setminus \overline{\Omega}$. The electromagnetic energy (in J) is the sum of the electric energy and the magnetic energy

$$\mathcal{E}(\mathbf{E}, \mathbf{H}) = \frac{1}{2} \int_{\mathbb{R}^3} \varepsilon \mathbf{E} \cdot \mathbf{E} \, dx + \frac{1}{2} \int_{\mathbb{R}^3} \mu \mathbf{H} \cdot \mathbf{H} \, dx. \quad (2.4)$$

Using the product rule

$$\nabla \cdot (\mathbf{E} \times \mathbf{H}) = (\nabla \times \mathbf{E}) \cdot \mathbf{H} - (\nabla \times \mathbf{H}) \cdot \mathbf{E}, \quad (2.5)$$

together with the equations (2.3c)–(2.3d), we obtain

$$\begin{aligned} \frac{d}{dt} \mathcal{E}(\mathbf{E}, \mathbf{H}) &= \int_{\mathbb{R}^3} \frac{\delta \mathcal{E}}{\delta \mathbf{E}} \cdot \partial_t \mathbf{E} \, dx + \int_{\mathbb{R}^3} \frac{\delta \mathcal{E}}{\delta \mathbf{H}} \cdot \partial_t \mathbf{H} \, dx \\ &\stackrel{(2.4)}{=} \int_{\mathbb{R}^3} \varepsilon \partial_t \mathbf{E} \cdot \mathbf{E} \, dx + \int_{\mathbb{R}^3} \mu \partial_t \mathbf{H} \cdot \mathbf{H} \, dx \\ &\stackrel{(2.3)}{=} \int_{\mathbb{R}^3} (\nabla \times \mathbf{H}) \cdot \mathbf{E} \, dx - \int_{\Omega} \mathbf{J}_e \cdot \mathbf{E} \, dx - \int_{\mathbb{R}^3} (\nabla \times \mathbf{E}) \cdot \mathbf{H} \, dx \\ &\stackrel{(2.5)}{=} - \int_{\mathbb{R}^3} \nabla \cdot (\mathbf{E} \times \mathbf{H}) \, dx - \int_{\Omega} \mathbf{J}_e \cdot \mathbf{E} \, dx. \end{aligned}$$

We conclude the energy law

$$\frac{d}{dt} \mathcal{E}(\mathbf{E}, \mathbf{H}) + \int_{\mathbb{R}^3} \nabla \cdot (\mathbf{E} \times \mathbf{H}) \, dx = - \int_{\Omega} \mathbf{J}_e \cdot \mathbf{E} \, dx.$$

The vector $\mathbf{S} = \mathbf{E} \times \mathbf{H}$, usually referred to as Poynting vector (in W/m²), plays the role of energy flux density, while the term on the right-hand side refers to the so-called Joule heating, i.e., the energy which is converted into heat when an electric current flows through a resistance.

Associated with the Maxwell equations, one usually considers a constitutive law for conduction that relates the fields to the sources. The usual choice for a conducting material is the Ohm law, i.e.,

$$\mathbf{J}_e = \sigma \mathbf{E}, \quad (2.6)$$

where $\sigma \in \mathbb{R}^{3 \times 3}$, a symmetric and uniformly positive definite matrix, is the conductivity (in A/(m V)). Under this assumption, the Faraday law of induction (2.3c) and the Maxwell–Ampère circuital law (2.3d), namely

$$\begin{aligned} \mu \partial_t \mathbf{H} + \nabla \times \mathbf{E} &= \mathbf{0}, \\ \varepsilon \partial_t \mathbf{E} - \nabla \times \mathbf{H} + \chi_\Omega \sigma \mathbf{E} &= \mathbf{0}, \end{aligned}$$

are sufficient to determine the electromagnetic fields, and the charge density ρ becomes a ‘leftover quantity’, which can be obtained from (2.3a) once the electric field is known. Moreover, in this case the energy law becomes

$$\frac{d}{dt} \mathcal{E}(\mathbf{E}, \mathbf{H}) + \int_{\mathbb{R}^3} \nabla \cdot (\mathbf{E} \times \mathbf{H}) \, dx = - \int_{\Omega} \sigma \mathbf{E} \cdot \mathbf{E} \, dx < 0.$$

The negative right-hand side reveals the dissipative nature of the Joule heating.

In many practical situations, since wave phenomena usually occur on a very short time scale, for an appropriate description of the electromagnetic fields it is sufficient to consider truncated versions of the Maxwell equations, where the time derivative of either the magnetic field or the electric field (quasistatic approximation) or both of them (static approximation) are omitted. In these cases, the electromagnetic waves, which result from the coupling of the magnetic field and the displacement current, are neglected.

The magnetoquasistatic Maxwell equations can be considered whenever $|\varepsilon \partial_t \mathbf{E}| \ll |\nabla \times \mathbf{H}| + |\boldsymbol{\sigma} \mathbf{E}|$, e.g., when $\mu_{\max} \varepsilon_{\max} L^2 T^{-2} \ll 1$ and $\varepsilon_{\max} \sigma_{\min}^{-1} T^{-1} \ll 1$, where ε_{\max} and μ_{\max} (resp. σ_{\min}) denote the maximal (resp. minimal) eigenvalues of ε and $\boldsymbol{\mu}$ (resp. $\boldsymbol{\sigma}$), while $L > 0$ and $T > 0$ denote some typical length (in m) and typical time (in s) of the problem; see [10, Section 1.2]. For a material which satisfies the Ohm law (2.6), the resulting system is given by

$$\nabla \cdot (\varepsilon \mathbf{E}) = \chi_{\Omega} \rho, \quad (2.7a)$$

$$\nabla \cdot (\boldsymbol{\mu} \mathbf{H}) = 0, \quad (2.7b)$$

$$\nabla \times \mathbf{E} = -\boldsymbol{\mu} \partial_t \mathbf{H}, \quad (2.7c)$$

$$\nabla \times \mathbf{H} = \chi_{\Omega} \boldsymbol{\sigma} \mathbf{E}. \quad (2.7d)$$

Replacing the electric field \mathbf{E} in (2.7c) by the expression that can be derived from (2.7d), which is admissible in the conducting region Ω , we obtain the so-called eddy current equation

$$\boldsymbol{\mu} \partial_t \mathbf{H} = -\nabla \times (\boldsymbol{\sigma}^{-1} \nabla \times \mathbf{H}).$$

In the static case, the equations for the electric field and the magnetic field can be decoupled. The resulting systems are the electrostatic Maxwell equations

$$\nabla \cdot (\varepsilon \mathbf{E}) = \chi_{\Omega} \rho,$$

$$\nabla \times \mathbf{E} = \mathbf{0},$$

and the magnetostatic Maxwell equations

$$\nabla \cdot (\boldsymbol{\mu} \mathbf{H}) = 0,$$

$$\nabla \times \mathbf{H} = \chi_{\Omega} \mathbf{J}_e.$$

2.2 Classical micromagnetic theory

In this section, we briefly introduce the classical theory of micromagnetism. For further details, we refer the interested reader to the monographs [9, 118, 47, 136] and the review articles [97, 96, 183, 184].

Micromagnetics can be defined as the study of magnetic processes at submicrometer length scales. The considered length scale, which ranges from few nanometers to micrometers, is large enough to average the atomic structure of the material, which allows to replace the individual atomistic magnetic moments by a continuous function in space (the so-called continuous medium approximation). At the same time, the length scale is small enough to resolve magnetic structures such as domain walls or vortices. The magnetic condition of a ferromagnetic body is described by a physical quantity called magnetization. It is defined as the quantity of magnetic moment per unit volume and it is measured in A/m. Mathematically, the magnetization is represented by a three-dimensional vector field \mathbf{M} , defined on a bounded domain $\Omega \subset \mathbb{R}^3$, which represents the volume occupied by the ferromagnetic body, with boundary denoted by $\Gamma := \partial\Omega$.

If the temperature is constant and far below the so-called Curie temperature of the ferromagnetic material (in K), the modulus of the magnetization is assumed to be constant, i.e.,

$$|\mathbf{M}| = M_s. \quad (2.8)$$

The constant $M_s > 0$ is called saturation magnetization and is a measure of the maximal amount of field that can be generated by a material (in A/m). We define the normalized magnetization by $\mathbf{m} := \mathbf{M}/M_s$, for which the modulus constraint (2.8) becomes $|\mathbf{m}| = 1$, i.e., the normalized magnetization assumes values on the unit sphere

$$\mathbb{S}^2 = \{\mathbf{x} \in \mathbb{R}^3 : |\mathbf{x}| = 1\}.$$

In the case of linear ferromagnetic materials, the constitutive law (2.2b) takes the form

$$\mathbf{B} = \mu_0(\mathbf{H} + M_s \chi_\Omega \mathbf{m}). \quad (2.9a)$$

Moreover, for the sake of simplicity, we restrict ourselves to the case of scalar-valued electric permittivity $\varepsilon > 0$ and conductivity $\sigma > 0$, i.e., we consider the constitutive laws

$$\mathbf{D} = \varepsilon \mathbf{E}, \quad (2.9b)$$

$$\mathbf{J}_e = \sigma \mathbf{E}, \quad (2.9c)$$

instead of (2.2a) and (2.6).

2.2.1 Total magnetic Gibbs' free energy

In micromagnetism, the study of magnetic processes is characterized by an energy-based approach. The key quantity is the total magnetic Gibbs free energy of the ferromagnetic body (in J), which depends on the magnetization and on possible applied external fields. The total magnetic Gibbs free energy comprises several energy contributions.

2.2.1.1 Exchange energy

The exchange energy contribution stems from the exchange interactions between the spins theorized by W. K. HEISENBERG. According to this quantum mechanical effect, neighboring magnetic moments tend to be parallel to each other. This is reflected by an energy contribution which penalizes disuniformities of the magnetization, i.e.,

$$\mathcal{E}_{\text{ex}}(\mathbf{m}) = A \int_{\Omega} |\nabla \mathbf{m}|^2 \, d\mathbf{x},$$

where $A > 0$ is the so-called exchange stiffness constant. Its value for standard ferromagnetic materials is usually of the order of 10^{-11} J/m.

2.2.1.2 Magnetocrystalline anisotropy energy

The crystalline structure of the material implies the existence of preferred directions for the magnetization, usually referred to as easy axes. This is mathematically modelled by a smooth function $\Phi : \mathbb{S}^2 \rightarrow \mathbb{R}$ with values in J/m³, which takes the anisotropy of the ferromagnetic material into account. It is usually a nonnegative function which takes the value 0 if and only if the direction belongs to the set of preferred directions. As an example, we mention three important cases:

- Uniaxial anisotropy: There is one preferred direction $\mathbf{a} \in \mathbb{S}^2$. The function $\Phi : \mathbb{S}^2 \rightarrow \mathbb{R}$ is given by

$$\Phi(\mathbf{u}) = K_u [1 - (\mathbf{a} \cdot \mathbf{u})^2], \quad (2.10)$$

with $K_u > 0$; see Figure 2.1(a).

- Planar anisotropy: The magnetization tends to remain in a plane. The anisotropy function $\Phi : \mathbb{S}^2 \rightarrow \mathbb{R}$ is given by

$$\Phi(\mathbf{u}) = K_p (\mathbf{a} \cdot \mathbf{u})^2,$$

where $K_p > 0$ is constant and $\mathbf{a} \in \mathbb{S}^2$ denotes the normal vector to the plane; see Figure 2.1(b).

- Cubic anisotropy: There are three mutually orthogonal easy directions $\mathbf{a}_i \in \mathbb{S}^2$, $1 \leq i \leq 3$. A possible expression for the function $\Phi : \mathbb{S}^2 \rightarrow \mathbb{R}$ is given by

$$\begin{aligned} \Phi(\mathbf{u}) = & K_{c1} [(\mathbf{a}_1 \cdot \mathbf{u})^2(\mathbf{a}_2 \cdot \mathbf{u})^2 + (\mathbf{a}_1 \cdot \mathbf{u})^2(\mathbf{a}_3 \cdot \mathbf{u})^2 + (\mathbf{a}_2 \cdot \mathbf{u})^2(\mathbf{a}_3 \cdot \mathbf{u})^2] \\ & + K_{c2}(\mathbf{a}_1 \cdot \mathbf{u})^2(\mathbf{a}_2 \cdot \mathbf{u})^2(\mathbf{a}_3 \cdot \mathbf{u})^2, \end{aligned}$$

with $K_{c1}, K_{c2} \in \mathbb{R}$; see Figure 2.1(c).

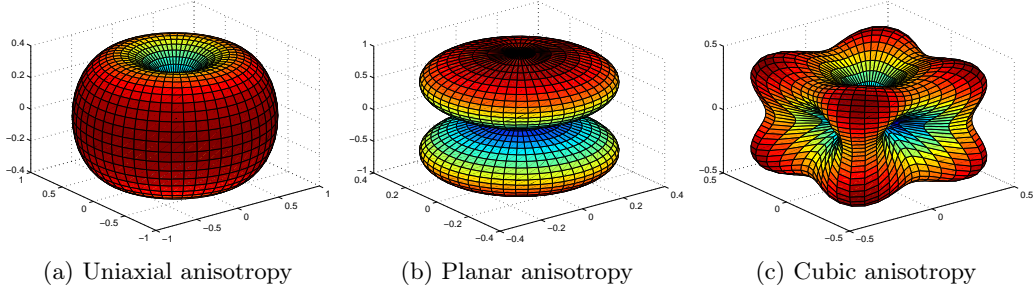


Figure 2.1: Anisotropy functions. (a) Plot of the uniaxial anisotropy function with $K_u = 1$ and $\mathbf{a} = \mathbf{e}_3$. (b) Plot of the planar anisotropy function with $K_p = 1$ and $\mathbf{a} = \mathbf{e}_3$. (c) Plot of the cubic anisotropy function with $K_{c1} = 2$, $K_{c2} = 0$ and $\mathbf{a}_i = \mathbf{e}_i$ for all $1 \leq i \leq 3$.

The above constants K_u, K_p, K_{c1}, K_{c2} are material parameters and are measured in J/m^3 .

Throughout this work, we consider a general anisotropy function of the form $\Phi = K\phi$, where $K > 0$ is a general anisotropy constant in J/m^3 , while $\phi : \mathbb{S}^2 \rightarrow \mathbb{R}$ is a (nondimensional) smooth function. Clearly, the three aforementioned examples can be recasted into this framework. The magnetocrystalline anisotropy energy is given by

$$\mathcal{E}_{\text{ani}}(\mathbf{m}) = K \int_{\Omega} \phi(\mathbf{m}) \, d\mathbf{x}$$

and can be defined as the work required to rotate the magnetization out of the easy axes.

2.2.1.3 Zeeman's energy

In the presence of an external field, the magnetization tends to align itself to it. The Zeeman energy, named after P. ZEEMAN, is an energy contribution which penalizes any deviation of the magnetization from this field inside the body. The corresponding term is

$$\mathcal{E}_{\text{ext}}(\mathbf{m}, \mathbf{H}_{\text{ext}}) = -\mu_0 M_s \int_{\Omega} \mathbf{H}_{\text{ext}} \cdot \mathbf{m} \, d\mathbf{x},$$

where \mathbf{H}_{ext} denotes the applied external field (in A/m).

2.2.1.4 Antisymmetric exchange energy

Chiral magnets are characterized by an atomic structure which lacks inversion symmetry. The associated interaction is called antisymmetric exchange interaction, also referred to as Dzyaloshinskii–Moriya (DM) interaction. It is a short-range effect which tries to twist the magnetization (neighboring magnetic moments tend to be perpendicular to each other) and it is thus in direct competition with the exchange interaction which favors uniform magnetization configurations. It was found that the mechanism behind this effect is based on spin-orbit coupling [86, 156]. The corresponding energy contribution takes the form

$$\mathcal{E}_{\text{DM}}(\mathbf{m}) = D \int_{\Omega} (\nabla \times \mathbf{m}) \cdot \mathbf{m} \, d\mathbf{x},$$

where $D \in \mathbb{R}$ is the DM constant (in J/m²). The Dzyaloshinskii–Moriya interaction turns out to be one of the main ingredient for the formation of magnetic skyrmions [95, 157, 175, 127].

2.2.1.5 Magnetostatic energy

Taking the constitutive law (2.9a) for ferromagnetic materials into account, it turns out that the magnetization ‘generates’ a magnetic field, which is described by the Maxwell equations; see Section 2.1. Since the electromagnetic wavelength is much larger than the standard dimensions of a ferromagnet, an appropriate description of this magnetic field usually employs the magnetostatic Maxwell equations, which for a ferromagnet are given by

$$\nabla \cdot \mathbf{H} = -M_s \nabla \cdot (\chi_\Omega \mathbf{m}), \quad (2.11a)$$

$$\nabla \times \mathbf{H} = \chi_\Omega \mathbf{J}_e. \quad (2.11b)$$

We decompose the magnetic field into two components, i.e., $\mathbf{H} = \mathbf{H}_s + \mathbf{H}_c$. Here, \mathbf{H}_s is the so-called stray field (or demagnetizing field, since it acts on the magnetization so as to reduce the total magnetic moment), ‘generated’ by the magnetization \mathbf{m} , while \mathbf{H}_c is usually referred to as Oersted field, ‘generated’ by the electric current density \mathbf{J}_e . From the superposition principle, it follows that \mathbf{H}_s and \mathbf{H}_c satisfy

$$\nabla \cdot \mathbf{H}_s = -M_s \nabla \cdot (\chi_\Omega \mathbf{m}), \quad (2.12a)$$

$$\nabla \times \mathbf{H}_s = \mathbf{0}, \quad (2.12b)$$

and

$$\nabla \cdot \mathbf{H}_c = 0, \quad (2.13a)$$

$$\nabla \times \mathbf{H}_c = \chi_\Omega \mathbf{J}_e, \quad (2.13b)$$

respectively. Note that the stray field and the Oersted field are nothing but the gradient part and the curl part of the Helmholtz decomposition of \mathbf{H} , respectively. From (2.12b), it turns out that the stray field \mathbf{H}_s is an irrotational field in a simply connected domain (the full space), from which it follows that it can be understood as the gradient of a scalar potential. It holds that $\mathbf{H}_s = -\nabla u$, where u denote the magnetostatic potential (in A). With the usual transmission conditions (the normal component of the magnetic flux density must be continuous at the interface) and a suitable radiation condition at infinity, from (2.12) it follows that the magnetostatic potential solves the scalar full-space transmission problem

$$-\Delta u^{\text{int}} = -M_s \nabla \cdot \mathbf{m} \quad \text{in } \Omega, \quad (2.14a)$$

$$-\Delta u^{\text{ext}} = 0 \quad \text{in } \mathbb{R}^3 \setminus \overline{\Omega}, \quad (2.14b)$$

$$u^{\text{ext}} - u^{\text{int}} = 0 \quad \text{on } \Gamma, \quad (2.14c)$$

$$(\nabla u^{\text{ext}} - \nabla u^{\text{int}}) \cdot \mathbf{n} = -M_s \mathbf{m} \cdot \mathbf{n} \quad \text{on } \Gamma, \quad (2.14d)$$

$$u(\mathbf{x}) = \mathcal{O}(1/|\mathbf{x}|) \quad \text{as } |\mathbf{x}| \rightarrow \infty. \quad (2.14e)$$

Here, the superscripts ‘int’ and ‘ext’ denote the restriction of the magnetostatic potential to Ω and its complement. This interpretation explains why, in analogy with the electrostatic case, the quantities $-M_s \nabla \cdot \mathbf{m}$ and $-M_s \mathbf{m} \cdot \mathbf{n}$ are usually referred to as magnetic volume charge and magnetic surface charge, respectively. As for the Oersted field, using the vector identity

$$\nabla \times (\nabla \times \mathbf{H}_c) = \nabla(\nabla \cdot \mathbf{H}_c) - \Delta \mathbf{H}_c, \quad (2.15)$$

we obtain that

$$\nabla \times (\chi_\Omega \mathbf{J}_e) \stackrel{(2.13b)}{=} \nabla \times (\nabla \times \mathbf{H}_c) \stackrel{(2.15)}{=} \nabla(\nabla \cdot \mathbf{H}_c) - \Delta \mathbf{H}_c \stackrel{(2.13a)}{=} -\Delta \mathbf{H}_c.$$

With the usual transmission conditions (the tangential component of the magnetic field must be continuous at the interface) and a suitable radiation condition at infinity, we deduce that the Oersted field solves the vector full-space transmission problem

$$-\Delta \mathbf{H}_c^{\text{int}} = \nabla \times \mathbf{J}_e \quad \text{in } \Omega, \quad (2.16a)$$

$$-\Delta \mathbf{H}_c^{\text{ext}} = \mathbf{0} \quad \text{in } \mathbb{R}^3 \setminus \bar{\Omega}, \quad (2.16b)$$

$$\mathbf{H}_c^{\text{ext}} - \mathbf{H}_c^{\text{int}} = \mathbf{0} \quad \text{on } \Gamma, \quad (2.16c)$$

$$(\nabla \mathbf{H}_c^{\text{ext}} - \nabla \mathbf{H}_c^{\text{int}}) \mathbf{n} = \mathbf{n} \times \mathbf{J}_e \quad \text{on } \Gamma, \quad (2.16d)$$

$$\mathbf{H}_c(\mathbf{x}) = \mathcal{O}(1/|\mathbf{x}|) \quad \text{as } |\mathbf{x}| \rightarrow \infty. \quad (2.16e)$$

The decomposition of the magnetic field into stray field and Oersted field is reflected by a decomposition of the magnetic energy

$$\mathcal{E}(\mathbf{H}) = \frac{\mu_0}{2} \int_{\mathbb{R}^3} |\mathbf{H}|^2 d\mathbf{x} = \frac{\mu_0}{2} \int_{\mathbb{R}^3} |\mathbf{H}_s|^2 d\mathbf{x} + \frac{\mu_0}{2} \int_{\mathbb{R}^3} |\mathbf{H}_c|^2 d\mathbf{x}.$$

In micromagnetics, the (magnetization-dependent) magnetic energy of the stray field is usually referred to as magnetostatic energy. It can be understood as the energy of the magnetization associated with the interactions with its own demagnetizing field

$$\mathcal{E}_{\text{stray}}(\mathbf{m}) = \frac{\mu_0}{2} \int_{\mathbb{R}^3} |\mathbf{H}_s|^2 d\mathbf{x} = -\frac{\mu_0 M_s}{2} \int_{\Omega} \mathbf{H}_s \cdot \mathbf{m} d\mathbf{x}.$$

The classical theory of micromagnetism usually models the behavior of ferromagnetic materials in the absence of electric currents, i.e., without Oersted field. However, for conducting materials and certain geometries, e.g., in the case of ferromagnetic nanowires, the effect of the electric current and the associated Oersted field cannot be ignored.

2.2.1.6 Magnetoelastic energy

Ferromagnetic bodies are also sensible to mechanical stresses and deformations: Changes in the magnetization cause strains in the crystal lattice. Conversely, if an applied force produces a strain in a ferromagnetic material, this stress affects the magnetization. This bidirectional coupling between magnetic and elastic properties is usually referred to as magnetostriction.

According to the second Newton law, the displacement $\mathbf{u} \in \mathbb{R}^3$, i.e., the distance of the deformed configuration from the reference configuration (in m), satisfies

$$\kappa \partial_{tt} \mathbf{u} = \nabla \cdot \boldsymbol{\sigma} + \mathbf{f}, \quad (2.17)$$

where $\kappa > 0$ is the density of the medium (in kg/m³), $\boldsymbol{\sigma} \in \mathbb{R}^{3 \times 3}$ is the stress tensor (in Pa), and $\mathbf{f} \in \mathbb{R}^3$ represents an applied body force (in N/m³). Let $\boldsymbol{\varepsilon}(\mathbf{u}) \in \mathbb{R}^{3 \times 3}$ denote the (nondimensional) strain tensor. In linear elasticity, the displacement-strain relation is given by the symmetrized Jacobian

$$\boldsymbol{\varepsilon}(\mathbf{u}) = \frac{1}{2} (\nabla \mathbf{u} + \nabla \mathbf{u}^\top);$$

see, e.g., [69, Section 6.3]. We assume that the strain tensor can be decomposed into two components, i.e., $\boldsymbol{\varepsilon} = \boldsymbol{\varepsilon}_{\text{el}} + \boldsymbol{\varepsilon}_{\text{m}}$, where $\boldsymbol{\varepsilon}_{\text{el}}$ denotes the elastic strain tensor, whereas $\boldsymbol{\varepsilon}_{\text{m}}$ denotes the magnetostrain tensor. In a linear elastic material, the elastic strain tensor $\boldsymbol{\varepsilon}_{\text{el}}$ is related to the stress tensor by the Hooke law

$$\boldsymbol{\sigma} = \mathbf{C} \boldsymbol{\varepsilon}_{\text{el}},$$

where \mathbf{C} is a symmetric and positive definite 4th order tensor, usually referred to as stiffness tensor (in Pa)¹. As for the magnetostrain tensor, several expressions can be found in the literature; see,

¹In the case of homogeneous and isotropic materials, e.g., it holds that $\boldsymbol{\sigma} = \lambda \text{tr}(\boldsymbol{\varepsilon}_{\text{el}}) \mathbf{I} + 2\mu \boldsymbol{\varepsilon}_{\text{el}}$, with $\lambda \in \mathbb{R}$ and $\mu > 0$ being the so-called Lamé constants (both in Pa); see, e.g., [69, Section 3.8]. The corresponding stiffness tensor is given by $C_{ijkl} = \lambda \delta_{ij} \delta_{kl} + \mu (\delta_{ik} \delta_{jl} + \delta_{il} \delta_{jk})$.

e.g., [118, Section 3.2.6] or [136, Section 2.2.4]. Here, we restrict ourselves to the form

$$\varepsilon_m(\mathbf{m}) = \boldsymbol{\lambda}(\mathbf{m} \otimes \mathbf{m} - \mathbf{I}_{3 \times 3}/3),$$

with $\boldsymbol{\lambda}$ also being a symmetric and positive definite 4th order tensor (nondimensional). Within this framework, the conservation of momentum (2.17) can be rewritten as

$$\kappa \partial_{tt} \mathbf{u} = \nabla \cdot [\mathbf{C} \varepsilon_{\text{el}}(\mathbf{u}, \mathbf{m})] + \mathbf{f}, \quad (2.18)$$

where $\varepsilon_{\text{el}}(\mathbf{u}, \mathbf{m}) = \varepsilon(\mathbf{u}) - \varepsilon_m(\mathbf{m})$. This equation is usually supplemented with the mixed boundary conditions

$$\begin{aligned} \mathbf{u} &= \mathbf{0} & \text{on } \Gamma_D, \\ \boldsymbol{\sigma} \mathbf{n} &= \mathbf{t} & \text{on } \Gamma_N, \end{aligned}$$

for a given partition of the boundary $\Gamma = \overline{\Gamma_D} \cup \overline{\Gamma_N}$ into relatively open parts $\Gamma_D, \Gamma_N \subset \Gamma$ such that $\Gamma_D \cap \Gamma_N = \emptyset$ and $|\Gamma_D| > 0$. The homogeneous Dirichlet condition imposes that the body is clamped on Γ_D , whereas the Neumann condition allows the possible effect of a contact force $\mathbf{t} \in \mathbb{R}^3$ (traction, in N/m²). The expression of the elastic energy is given by

$$\mathcal{E}_{\text{el}}(\mathbf{m}, \mathbf{u}) = \frac{1}{2} \int_{\Omega} \kappa |\partial_t \mathbf{u}|^2 d\mathbf{x} + \frac{1}{2} \int_{\Omega} \varepsilon_{\text{el}}(\mathbf{u}, \mathbf{m}) : [\mathbf{C} \varepsilon_{\text{el}}(\mathbf{u}, \mathbf{m})] d\mathbf{x} - \int_{\Omega} \mathbf{f} \cdot \mathbf{u} d\mathbf{x} - \int_{\Gamma_N} \mathbf{t} \cdot \mathbf{u} dS. \quad (2.19)$$

It comprises four terms: the kinetic energy, the elastic energy, and the work done by the body force and the contact force, respectively. In many practical situations, the deformation of the ferromagnetic body can be considered at equilibrium, see, e.g., [190]. It is thus sufficient to consider the stationary case of (2.18)

$$\nabla \cdot [\mathbf{C} \varepsilon_{\text{el}}(\mathbf{u}, \mathbf{m})] + \mathbf{f} = \mathbf{0}.$$

In this case, the kinetic energy is not taken into account.

2.2.2 The Landau–Lifshitz–Gilbert equation

According to the theory of micromagnetism, the admissible configurations of the magnetization are those which minimize the total Gibbs free energy of the ferromagnetic body, i.e., we are led to consider the minimization problem

$$\min_{|\mathbf{m}|=1} \mathcal{E}(\mathbf{m}). \quad (2.20)$$

The qualitative structure of the stable configurations are the result of the balance between the different energy contributions [118, Section 3.3]. Minimizing the exchange energy is achieved by a uniform magnetization configuration, which is however characterized by a significant magnetostatic energy. As a compromise, the magnetization in ferromagnetic materials exhibits intricate domain structures, which consist of areas where the magnetization is almost uniform or varies slowly (magnetic domains), separated by sharp transition layers, where the orientation of the magnetization rotates coherently from the direction in one domain to that in the next domain on a much shorter lengthscale (domain walls). The presence of an applied external field has an influence on the size of the domains, while the anisotropy of the material tends to favor the easy directions. The domain wall width is a compromise between the tendency of the exchange energy to enlarge the layers, since minimizing the exchange energy implies that the magnetization changes slowly as function of position, and that of the anisotropy energy to reduce their thickness, in order to reduce the region in which the magnetization deviates from a preferred direction. The interplay between the exchange interaction and the Dzyaloshinskii–Moriya interaction is the fundamental ingredient for the stabilization of magnetic skyrmions [175].

Important quantitative parameters in micromagnetics, which are usually considered for the comparison of ferromagnetic materials, are

- the magnetostatic energy density (in J/m³)

$$K_s = \frac{\mu_0 M_s^2}{2}, \quad (2.21)$$

- the exchange length (in m)

$$\lambda_{\text{ex}} = \sqrt{\frac{A}{K_s}}, \quad (2.22)$$

that is the length below which the exchange interaction dominates typical magnetostatic fields,

- the Bloch parameter (in m)

$$\delta_0 = \sqrt{\frac{A}{K}},$$

that is the length below which the exchange interaction dominates anisotropy effects and is proportional to the Bloch wall width $\delta = \pi\delta_0$ (in m),

- the magnetic hardness parameter (nondimensional)

$$q = \frac{\lambda_{\text{ex}}}{\delta_0} = \sqrt{\frac{K}{K_s}}, \quad (2.23)$$

whose value is used to classify the ferromagnetic materials into hard magnetic materials ($q \gg 1$) and soft magnetic materials ($q \ll 1$).

A key quantity of the micromagnetic theory is the effective field. It is defined, up to constants, as the negative functional derivative of the Gibbs free energy with respect to \mathbf{m} , i.e.,

$$\mu_0 M_s \mathbf{H}_{\text{eff}} = - \frac{\delta \mathcal{E}}{\delta \mathbf{m}}. \quad (2.24)$$

It has the physical dimensions of a magnetic field (A/m) and can be understood as the local field affected by the magnetization. The effective field appears in the Euler–Lagrange equations associated with the minimization problem (2.20). Indeed, any solution of (2.20) is a weak solution of the boundary value problem

$$\mathbf{m} \times \mathbf{H}_{\text{eff}} = \mathbf{0} \quad \text{in } \Omega, \quad (2.25a)$$

$$\frac{\delta \mathcal{E}}{\delta (\nabla m_i)} \cdot \mathbf{n} = 0 \quad \text{on } \Gamma, \text{ for all } 1 \leq i \leq 3. \quad (2.25b)$$

The equation (2.25a) states that the magnetization is parallel to the effective field at a minimizer or, equivalently, that the local torque exerted on a minimizing magnetization is zero. If the only term of the energy involving derivatives of \mathbf{m} is the exchange energy, the boundary conditions (2.25b) turn out to be homogeneous Neumann boundary conditions

$$\partial_{\mathbf{n}} \mathbf{m} = \mathbf{0}. \quad (2.26)$$

In this case, the Euler–Lagrange equations (2.25) are usually referred to as Brown’s equations. If the energy comprises both the exchange and the Dzyaloshinskii–Moriya interaction, then the resulting boundary condition is

$$2A \partial_{\mathbf{n}} \mathbf{m} + D \mathbf{m} \times \mathbf{n} = \mathbf{0}.$$

Under these assumptions, for each energy contribution considered in Section 2.2.1, a direct computation of the functional derivative in (2.24) yields an explicit expression of the corresponding

effective field:

$$\begin{aligned}
\mathcal{E}_{\text{ex}}(\mathbf{m}) &= A \int_{\Omega} |\nabla \mathbf{m}|^2 \, d\mathbf{x} & \implies & \mathbf{H}_{\text{eff,ex}} = \frac{2A}{\mu_0 M_s} \Delta \mathbf{m}, \\
\mathcal{E}_{\text{ani}}(\mathbf{m}) &= K \int_{\Omega} \phi(\mathbf{m}) \, d\mathbf{x} & \implies & \mathbf{H}_{\text{eff,ani}} = -\frac{K}{\mu_0 M_s} \nabla \phi(\mathbf{m}), \\
\mathcal{E}_{\text{ext}}(\mathbf{m}, \mathbf{H}_{\text{ext}}) &= -\mu_0 M_s \int_{\Omega} \mathbf{H}_{\text{ext}} \cdot \mathbf{m} \, d\mathbf{x} & \implies & \mathbf{H}_{\text{eff,ext}} = \mathbf{H}_{\text{ext}}, \\
\mathcal{E}_{\text{DM}}(\mathbf{m}) &= D \int_{\Omega} (\nabla \times \mathbf{m}) \cdot \mathbf{m} \, d\mathbf{x} & \implies & \mathbf{H}_{\text{eff,DM}} = -\frac{2D}{\mu_0 M_s} \nabla \times \mathbf{m}, \\
\mathcal{E}_{\text{stray}}(\mathbf{m}) &= \frac{\mu_0}{2} \int_{\mathbb{R}^3} |\mathbf{H}_s|^2 \, d\mathbf{x} & \implies & \mathbf{H}_{\text{eff,stray}} = \mathbf{H}_s, \\
\mathcal{E}_{\text{el}}(\mathbf{m}, \mathbf{u}) &= \frac{1}{2} \int_{\Omega} \varepsilon_{\text{el}}(\mathbf{u}, \mathbf{m}) : [\mathbf{C} \varepsilon_{\text{el}}(\mathbf{u}, \mathbf{m})] \, d\mathbf{x} + \dots & \implies & \mathbf{H}_{\text{eff,el}} = \frac{2}{\mu_0 M_s} (\lambda \boldsymbol{\sigma}) \mathbf{m}.
\end{aligned}$$

In concrete applications of the micromagnetic model, the energy comprises the terms that are relevant for the process which is considered. The choice usually depends on the material and the geometry of the sample. The most common contributions are exchange energy, anisotropy energy, Zeeman energy, and magnetostatic energy, which already allow to describe a large variety of phenomena. In this case, the effective field takes the form

$$\mathbf{H}_{\text{eff}} = \frac{2A}{\mu_0 M_s} \Delta \mathbf{m} + \frac{2K}{\mu_0 M_s} (\mathbf{a} \cdot \mathbf{m}) \mathbf{a} + \mathbf{H}_{\text{ext}} + \mathbf{H}_s.$$

So far, we have discussed the equilibrium configurations for a magnetized body, but we have not described how the magnetization, starting from an unstable configuration, reaches the equilibrium. Following [108], we formally derive the equation of motion for the magnetization dynamics. The magnetic moment of a particle, e.g., of an electron, is defined as the vector which relates the torque on the particle when it is subjected to a magnetic field to the magnetic field itself. The relation is

$$\boldsymbol{\tau} = \boldsymbol{\mu} \times \mathbf{B}$$

where $\boldsymbol{\tau}$ is the torque (in J) and $\boldsymbol{\mu}$ is the magnetic moment (in J/T). The equation for the rotational motion of a rigid body is

$$\boldsymbol{\tau} = \partial_t \mathbf{L},$$

where \mathbf{L} is the angular momentum of the particle (in Js). The magnetic moment of an electron is related to the angular momentum by

$$\boldsymbol{\mu} = \gamma \mathbf{L},$$

where $\gamma < 0$ is the gyromagnetic ratio of the electron (in rad/(s T)). Altogether, we thus obtain

$$\partial_t \boldsymbol{\mu} = \gamma \boldsymbol{\mu} \times \mathbf{B}.$$

This equation of motion is satisfied by each discrete magnetic moment in the ferromagnetic sample. In micromagnetism, we replace this set of differential equations (one for each magnetic moment) with a single differential equation for the continuous magnetization. The role of the magnetic induction (the origin of the torque) is played by the effective field \mathbf{H}_{eff} . Moreover, we define the rescaled gyromagnetic ratio by $\gamma_0 = -\gamma \mu_0$ (in m/(A s)). We obtain the equation

$$\partial_t \mathbf{m} = -\gamma_0 \mathbf{m} \times \mathbf{H}_{\text{eff}}. \quad (2.27)$$

Equation (2.27) describes the precession of the magnetization around the effective field; see Figure 2.2(a).

It is clear from experiments that the magnetization dynamics is a dissipative process. The microscopic nature of the dissipation is still not clear, and it is probably too complex to be explicitly

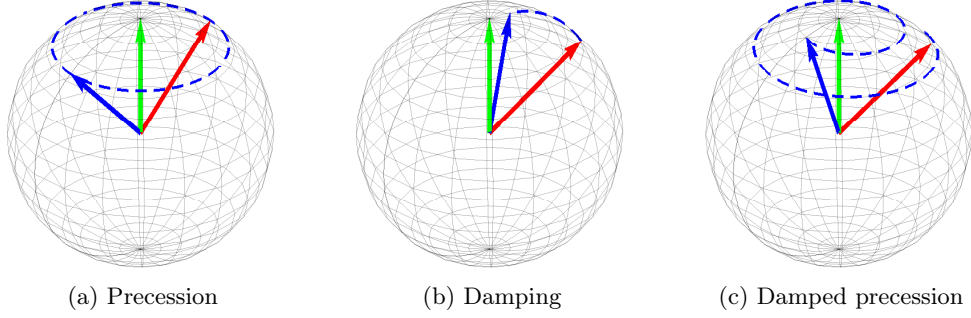


Figure 2.2: Dynamics of the magnetization with respect to the effective field. The red and the blue arrows visualize the magnetization at two different times $t_{\text{red}} < t_{\text{blue}}$. The green arrow refers to the effective field.

included into the equation of motion. A possible approach for this problem is to introduce the effect of the (unspecified) energy loss mechanisms into the equation in a phenomenological way. This can be done by adding to (2.27) a damping term which can be tuned by means of a damping parameter to be experimentally determined, without knowing the details of the transfer mechanisms.

In 1935, the Russian physicists L. D. LANDAU and E. M. LIFSHITZ introduced dissipation by way of a torque term proportional to the component of \mathbf{H}_{eff} orthogonal to \mathbf{m} , which pushes the magnetization towards the effective field; see Figure 2.2(b). The resulting equation is the so-called Landau–Lifshitz equation

$$\partial_t \mathbf{m} = -\gamma_0 \mathbf{m} \times \mathbf{H}_{\text{eff}} - \gamma_0 \lambda \mathbf{m} \times (\mathbf{m} \times \mathbf{H}_{\text{eff}}), \quad (2.28)$$

where $\lambda > 0$ is a nondimensional phenomenological damping parameter; see [139, equation (21)]. Taking both precession and damping into account, equation (2.28) describes a magnetization that rotates around the effective field while being damped towards it; see Figure 2.2(c). In 1955, the American physicist T. L. GILBERT proposed to add a different damping term to the precession equation (2.27); see [107]. He considered a viscous-type ‘damping field’, which is directly proportional to the rate of change of the magnetization and can modify the effective field and thus change the torque exerted on the magnetization. The resulting equation is

$$\partial_t \mathbf{m} = -\gamma_0 \mathbf{m} \times (\mathbf{H}_{\text{eff}} - \eta \partial_t \mathbf{m}),$$

where η is a viscosity parameter (in A s/m). The latter can be rewritten as

$$\partial_t \mathbf{m} = -\gamma_0 \mathbf{m} \times \mathbf{H}_{\text{eff}} + \alpha \mathbf{m} \times \partial_t \mathbf{m}, \quad (2.29)$$

which is usually referred to as Gilbert equation. The constant $\alpha = \gamma_0 \eta$ is the so-called (nondimensional) Gilbert damping parameter. Actually, it turns out that (2.28) and (2.29) are equivalent (up to rescaling the constants); see Proposition 3.1.1. Indeed, equation (2.28) can be equivalently rewritten as

$$\partial_t \mathbf{m} = -\gamma_0(1 + \lambda^2) \mathbf{m} \times \mathbf{H}_{\text{eff}} + \lambda \mathbf{m} \times \partial_t \mathbf{m},$$

whereas (2.29) can be restated as

$$\partial_t \mathbf{m} = -\frac{\gamma_0}{1 + \alpha^2} \mathbf{m} \times \mathbf{H}_{\text{eff}} - \frac{\gamma_0 \alpha}{1 + \alpha^2} \mathbf{m} \times (\mathbf{m} \times \mathbf{H}_{\text{eff}}). \quad (2.30)$$

The latter is commonly referred to as the Landau–Lifshitz–Gilbert (LLG) equation. Throughout the thesis, without loss of generality, we will always consider the Gilbert form of the damping.

Concerning the boundary conditions to be imposed on Γ , in many situations they are chosen to be consistent with the stationary case², i.e., with (2.25b). A justification that the choice of a

²Note that a stationary solution of the LLG equation (2.30) or, equivalently, of (2.29) is a solution of the Euler–Lagrange equations (2.25a).

homogeneous Neumann boundary condition (2.26), in the pure exchange case and in the absence of surface effects, is physically meaningful also in the dynamic case can be found in [171].

Taking the scalar product of (2.29) with \mathbf{m} , we deduce the orthogonality condition

$$\mathbf{m} \cdot \partial_t \mathbf{m} = 0. \quad (2.31)$$

In particular, since

$$\partial_t |\mathbf{m}|^2 = 2\mathbf{m} \cdot \partial_t \mathbf{m} = 0,$$

it follows that the modulus constraint $|\mathbf{m}| = 1$ is always satisfied, provided it is satisfied by the initial condition.

We now aim at studying the evolution of the energy during the dynamics. Taking the vector product of (2.29) with \mathbf{m} , we obtain

$$\mathbf{m} \times \partial_t \mathbf{m} = -\gamma_0 \mathbf{m} \times (\mathbf{m} \times \mathbf{H}_{\text{eff}}) + \alpha \mathbf{m} \times (\mathbf{m} \times \partial_t \mathbf{m}).$$

Taking (2.31) and the constraint $|\mathbf{m}| = 1$ into account, the vector triple product expansion formula

$$\mathbf{a} \times (\mathbf{b} \times \mathbf{c}) = (\mathbf{a} \cdot \mathbf{c})\mathbf{b} - (\mathbf{a} \cdot \mathbf{b})\mathbf{c} \quad \text{for all } \mathbf{a}, \mathbf{b}, \mathbf{c} \in \mathbb{R}^3,$$

yields the equality

$$\mathbf{m} \times \partial_t \mathbf{m} = -\gamma_0 (\mathbf{m} \cdot \mathbf{H}_{\text{eff}}) \mathbf{m} + \gamma_0 \mathbf{H}_{\text{eff}} - \alpha \partial_t \mathbf{m}.$$

Taking the scalar product of the latter with $\partial_t \mathbf{m}$ and exploiting the orthogonality (2.31), we obtain the relation

$$\gamma_0 \mathbf{H}_{\text{eff}} \cdot \partial_t \mathbf{m} = \alpha |\partial_t \mathbf{m}|^2. \quad (2.32)$$

A formal application of the chain rule yields the energy law

$$\begin{aligned} \frac{d}{dt} \mathcal{E}(\mathbf{m}) &= \int_{\Omega} \frac{\delta \mathcal{E}}{\delta \mathbf{m}} \cdot \partial_t \mathbf{m} \, d\mathbf{x} + \int_{\Omega} \frac{\delta \mathcal{E}}{\delta \mathbf{H}_{\text{ext}}} \cdot \partial_t \mathbf{H}_{\text{ext}} \, d\mathbf{x} \\ &\stackrel{(2.24)}{=} -\mu_0 M_s \int_{\Omega} \mathbf{H}_{\text{eff}} \cdot \partial_t \mathbf{m} \, d\mathbf{x} - \mu_0 M_s \int_{\Omega} \partial_t \mathbf{H}_{\text{ext}} \cdot \mathbf{m} \, d\mathbf{x} \\ &\stackrel{(2.32)}{=} -\frac{\mu_0 M_s \alpha}{\gamma_0} \int_{\Omega} |\partial_t \mathbf{m}|^2 \, d\mathbf{x} - \mu_0 M_s \int_{\Omega} \partial_t \mathbf{H}_{\text{ext}} \cdot \mathbf{m} \, d\mathbf{x}. \end{aligned}$$

If the applied field \mathbf{H}_{ext} is constant in time, the energy law reduces to

$$\frac{d}{dt} \mathcal{E}(\mathbf{m}) = -\frac{\mu_0 M_s \alpha}{\gamma_0} \int_{\Omega} |\partial_t \mathbf{m}|^2 \, d\mathbf{x} \leq 0,$$

which reveals the dissipative behavior of the model and the Lyapunov structure of the LLG equation [164].

In several practical situations, the effect of eddy currents must be taken into account [46, 117, 196]. Taking the constitutive laws (2.9) for ferromagnetic materials into account, the magnetoquasistatic Maxwell equations (2.7) take the form

$$\nabla \cdot (\varepsilon \mathbf{E}) = \chi_{\Omega} \rho, \quad (2.33a)$$

$$\nabla \cdot \mathbf{H} = -M_s \nabla \cdot (\chi_{\Omega} \mathbf{m}), \quad (2.33b)$$

$$\nabla \times \mathbf{E} = -\mu_0 \partial_t \mathbf{H} - \mu_0 M_s \chi_{\Omega} \partial_t \mathbf{m}, \quad (2.33c)$$

$$\nabla \times \mathbf{H} = \chi_{\Omega} \sigma \mathbf{E}. \quad (2.33d)$$

In the mathematical literature, see, e.g., [203, 62, 155, 24, 28], also the coupling of the LLG equation with the full Maxwell system

$$\mu_0 \partial_t \mathbf{H} + \nabla \times \mathbf{E} = -\mu_0 M_s \chi_{\Omega} \partial_t \mathbf{m}, \quad (2.34a)$$

$$\varepsilon \partial_t \mathbf{E} - \nabla \times \mathbf{H} + \chi_{\Omega} \sigma \mathbf{E} = \mathbf{0}, \quad (2.34b)$$

is studied, but, due to the short time scales of wave phenomena, this is essentially of no practical concern. In both cases, the magnetic field \mathbf{H} then interacts with the magnetization during the dynamics as an additional field contribution to be added to the energy-based effective field, i.e.,

$$\partial_t \mathbf{m} = -\gamma_0 \mathbf{m} \times (\mathbf{H}_{\text{eff}} + \mathbf{H}) + \alpha \mathbf{m} \times \partial_t \mathbf{m}.$$

The identity (2.32) in this case turns out to be

$$\gamma_0 (\mathbf{H}_{\text{eff}} + \mathbf{H}) \cdot \partial_t \mathbf{m} = \alpha |\partial_t \mathbf{m}|^2. \quad (2.35)$$

In the case of the full Maxwell system (2.34), the evolution of the energy, defined as the sum of the electromagnetic energy (2.4) and the micromagnetic Gibbs free energy, follows the law

$$\begin{aligned} \frac{d}{dt} \mathcal{E}(\mathbf{E}, \mathbf{H}, \mathbf{m}) &= \int_{\mathbb{R}^3} \frac{\delta \mathcal{E}}{\delta \mathbf{E}} \cdot \partial_t \mathbf{E} \, d\mathbf{x} + \int_{\mathbb{R}^3} \frac{\delta \mathcal{E}}{\delta \mathbf{H}} \cdot \partial_t \mathbf{H} \, d\mathbf{x} + \int_{\Omega} \frac{\delta \mathcal{E}}{\delta \mathbf{m}} \cdot \partial_t \mathbf{m} \, d\mathbf{x} \\ &= \int_{\mathbb{R}^3} \varepsilon \mathbf{E} \cdot \partial_t \mathbf{E} \, d\mathbf{x} + \mu_0 \int_{\mathbb{R}^3} \mathbf{H} \cdot \partial_t \mathbf{H} \, d\mathbf{x} - \mu_0 M_s \int_{\Omega} \mathbf{H}_{\text{eff}} \cdot \partial_t \mathbf{m} \, d\mathbf{x} \\ &\stackrel{(2.35)}{=} \int_{\mathbb{R}^3} \varepsilon \mathbf{E} \cdot \partial_t \mathbf{E} \, d\mathbf{x} + \mu_0 \int_{\mathbb{R}^3} \mathbf{H} \cdot \partial_t \mathbf{H} \, d\mathbf{x} + \mu_0 M_s \int_{\Omega} \mathbf{H} \cdot \partial_t \mathbf{m} \, d\mathbf{x} - \frac{\mu_0 M_s \alpha}{\gamma_0} \int_{\Omega} |\partial_t \mathbf{m}|^2 \, d\mathbf{x} \\ &\stackrel{(2.34)}{=} \int_{\mathbb{R}^3} (\nabla \times \mathbf{H}) \cdot \mathbf{E} \, d\mathbf{x} - \int_{\Omega} \sigma |\mathbf{E}|^2 \, d\mathbf{x} - \int_{\mathbb{R}^3} (\nabla \times \mathbf{E}) \cdot \mathbf{H} \, d\mathbf{x} - \frac{\mu_0 M_s \alpha}{\gamma_0} \int_{\Omega} |\partial_t \mathbf{m}|^2 \, d\mathbf{x} \\ &\stackrel{(2.5)}{=} - \int_{\mathbb{R}^3} \nabla \cdot (\mathbf{E} \times \mathbf{H}) \, d\mathbf{x} - \int_{\Omega} \sigma |\mathbf{E}|^2 \, d\mathbf{x} - \frac{\mu_0 M_s \alpha}{\gamma_0} \int_{\Omega} |\partial_t \mathbf{m}|^2 \, d\mathbf{x}. \end{aligned}$$

We conclude the section by formally computing the energy law for the Gibbs free energy, assumed to include the elastic energy (2.19), when its evolution is driven by the coupling of the LLG equation and the conservation of momentum law (2.18). It holds that

$$\begin{aligned} \frac{d}{dt} \mathcal{E}(\mathbf{m}, \mathbf{u}) &= \int_{\Omega} \frac{\delta \mathcal{E}}{\delta \mathbf{m}} \cdot \partial_t \mathbf{m} \, d\mathbf{x} + \int_{\Omega} \frac{\delta \mathcal{E}}{\delta \mathbf{u}} \cdot \partial_t \mathbf{u} \, d\mathbf{x} + \int_{\Omega} \frac{\delta \mathcal{E}}{\delta (\partial_t \mathbf{u})} \cdot \partial_{tt} \mathbf{u} \, d\mathbf{x} - \int_{\Omega} \partial_t \mathbf{f} \cdot \mathbf{u} \, d\mathbf{x} - \int_{\Gamma_N} \partial_t \mathbf{t} \cdot \mathbf{u} \, dS \\ &= -\mu_0 M_s \int_{\Omega} \mathbf{H}_{\text{eff}} \cdot \partial_t \mathbf{m} \, d\mathbf{x} + \int_{\Omega} [\mathbf{C} \varepsilon_{\text{el}}(\mathbf{u}, \mathbf{m})] : \varepsilon(\partial_t \mathbf{u}) \, d\mathbf{x} - \int_{\Omega} \mathbf{f} \cdot \partial_t \mathbf{u} \, d\mathbf{x} - \int_{\Gamma_N} \mathbf{t} \cdot \partial_t \mathbf{u} \, dS \\ &\quad + \int_{\Omega} \kappa \partial_{tt} \mathbf{u} \cdot \partial_t \mathbf{u} \, d\mathbf{x} - \int_{\Omega} \partial_t \mathbf{f} \cdot \mathbf{u} \, d\mathbf{x} - \int_{\Gamma_N} \partial_t \mathbf{t} \cdot \mathbf{u} \, dS \\ &= -\frac{\alpha \mu_0 M_s}{\gamma_0} \int_{\Omega} |\partial_t \mathbf{m}|^2 \, d\mathbf{x} + \int_{\Omega} \boldsymbol{\sigma} : \varepsilon(\partial_t \mathbf{u}) \, d\mathbf{x} - \int_{\Omega} \mathbf{f} \cdot \partial_t \mathbf{u} \, d\mathbf{x} - \int_{\Gamma_N} \mathbf{t} \cdot \partial_t \mathbf{u} \, dS \\ &\quad + \int_{\Omega} \kappa \partial_{tt} \mathbf{u} \cdot \partial_t \mathbf{u} \, d\mathbf{x} - \int_{\Omega} \partial_t \mathbf{f} \cdot \mathbf{u} \, d\mathbf{x} - \int_{\Gamma_N} \partial_t \mathbf{t} \cdot \mathbf{u} \, dS \\ &\stackrel{(2.18)}{=} -\frac{\alpha \mu_0 M_s}{\gamma_0} \int_{\Omega} |\partial_t \mathbf{m}|^2 \, d\mathbf{x} - \int_{\Omega} \partial_t \mathbf{f} \cdot \mathbf{u} \, d\mathbf{x} - \int_{\Gamma_N} \partial_t \mathbf{t} \cdot \mathbf{u} \, dS. \end{aligned}$$

2.3 Metal spintronics

Spintronics, a portmanteau for spin electronics, is a recent field of research, which can be defined as the study of active control and manipulation of the spin degree of freedom in solid-state systems [206]. Its roots can be traced back to the discoveries on the influence of the spin on the electrical conduction in ferromagnetic metals obtained during the 1980s, e.g., the observation of spin-polarized electron injection from a ferromagnetic metal to a normal metal [120] or the discovery of the giant magnetoresistance (GMR) effect, independently carried out by the groups of A. FERT [19] and P. GRÜNBERG [49] in 1988.

The GMR effect consists in a relevant change in the electrical resistance observed in magnetic multilayers composed of alternating ferromagnetic and nonmagnetic sublayers. The resistance turns out to depend on whether the magnetization configurations of consecutive ferromagnetic sublayers are in a parallel alignment (lower resistance) or in an antiparallel alignment (higher resistance), which shows that the magnetic state of a material has an influence on its conduction properties.

Conversely, the magnetization can be manipulated by spin-polarized currents, even without applying any external magnetic field. The fundamental physics underlying this phenomenon is understood as a mutual transfer of spin angular momentum between the conduction electrons and the magnetization. The concept of spin transfer was proposed independently by J. C. SLONCZEWSKI and L. BERGER in 1996 [191, 44]. The key mechanism was named spin transfer torque (STT) and involves the so-called s-d exchange interaction between the nonequilibrium itinerant 4s conduction electrons and the localized 3d magnetic electrons. The original ballistic model for multilayer structures proposed in [191] was then extended in [212, 189] by including the effects of the spin diffusion and the electric conduction in the bulk of the layer. The derivation of the model does not follow the typical energy-based approach of micromagnetics.

In this section, we present some of the most used extensions of the classical micromagnetic model in metal spintronics.

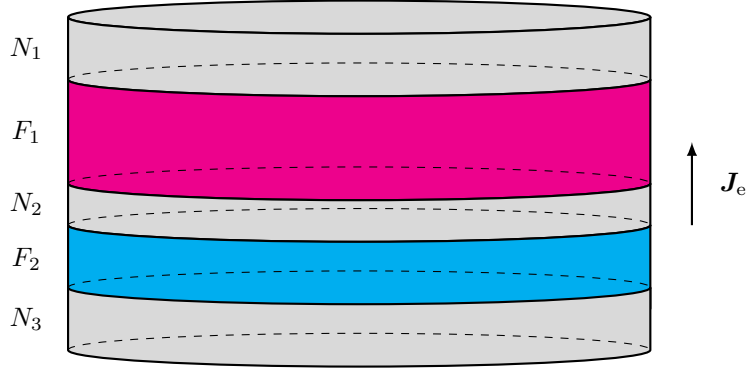


Figure 2.3: Schematic of a magnetic nanopillar structure. The multilayer consists of two ferromagnetic sublayers (F_1 and F_2) separated by a nonmagnetic spacer (N_2). The top and the bottom layers (N_1 and N_3) are made of nonmagnetic material and play the role of electrodes. The electric current is assumed to flow perpendicularly from N_1 to N_3 .

2.3.1 Slonczewski models

We consider a metallic multilayer structure consisting of two ferromagnetic sublayers (F_1 and F_2) separated by three nonmagnetic sublayers (N_1 , N_2 , and N_3) such as the one depicted in Figure 2.3. All the sublayers have the same cross section area $A > 0$ (in m^2). An applied electric current flows perpendicularly to the plane of the layers. This experimental setup is usually referred to as current-perpendicular-to-plane (CPP) injection geometry. For $i = 1, 2$, the magnetic state of the ferromagnetic sublayer F_i is assumed to be described by the vector \mathbf{S}_i , which is the macroscopic total spin momentum per unit area (in $1/\text{m}^2$), i.e., the corresponding total angular momentum of the sublayer is given by $\mathbf{L}_i = \hbar A \mathbf{S}_i$, where $\hbar > 0$ denotes the reduced Planck constant (in Js). Moreover, let $\mathbf{s}_i = \mathbf{S}_i / |\mathbf{S}_i|$ be the unit vector pointing in the \mathbf{S}_i direction.

If no additional interaction or damping is considered, the mutual influence of the ferromagnetic layers can be modelled by the system

$$\partial_t \mathbf{S}_{1,2} = \frac{J_e G(\mathbf{s}_1 \cdot \mathbf{s}_2)}{e} \mathbf{s}_{1,2} \times (\mathbf{s}_1 \times \mathbf{s}_2); \quad (2.36)$$

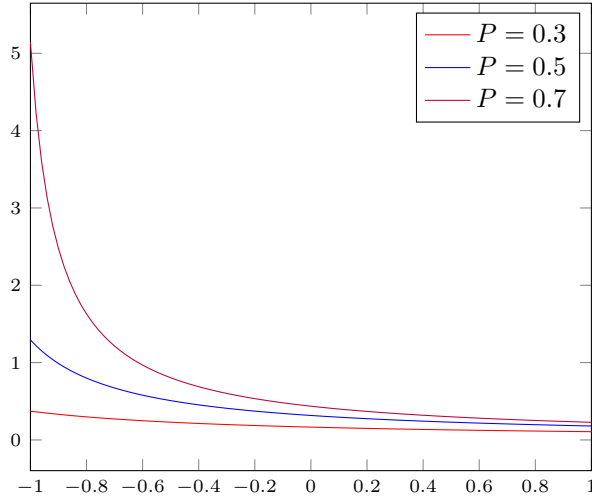


Figure 2.4: Plot of the ballistic function G from (2.37) for different values of the spin polarization parameter $0 < P < 1$.

see [191, equation (13)], where the function $G : [-1, 1] \times (0, 1) \rightarrow \mathbb{R}_{>0}$ is given by

$$G(x, P) = \left[\frac{(1+P)^3(3+x)}{4P^{3/2}} - 4 \right]^{-1}; \quad (2.37)$$

see [191, equation (14)] and Figure 2.4. Here, $0 < P < 1$ is a nondimensional spin polarization parameter (roughly speaking, the percentage of flowing electrons that are polarized in the \mathbf{s}_1 direction), J_e denotes the intensity of the perpendicular electric current density (in A/m²), with the convention that $J_e > 0$ if the electron flows from F_1 to F_2 , whereas e is the (positive) charge of the electron (in As).

We assume that the magnetic sublayer F_1 (the so-called fixed layer) is characterized by a constant value of the magnetization. Starting from (2.36), we aim at deriving an expression for the spin transfer torque exerted by the polarized conduction electrons on the magnetization of the sublayer F_2 (the so-called free layer), under the assumption that they conserve the polarization gained in F_1 , which is reasonable if the nonmagnetic sublayer N_2 is sufficiently thin. The total magnetic moment of the sublayer F_2 (in J/T) is given by $\boldsymbol{\mu}_2 = \gamma \mathbf{L}_2 = \gamma \hbar A \mathbf{S}_2$, so that the magnetization of the layer reads

$$\mathbf{M}_2 = \frac{\boldsymbol{\mu}_2}{V} = \frac{\boldsymbol{\mu}_2}{Ad} = \frac{\gamma \hbar}{d} \mathbf{S}_2 = -\frac{g_e \mu_B}{d} \mathbf{S}_2,$$

where $V > 0$ and $d > 0$ denote the volume (in m³) and the thickness (in m) of the free layer F_2 , $g_e \approx 2$ is the g-factor of the electron (nondimensional), $\mu_B > 0$ is the Bohr magneton (in A m²). From the latter, it follows that the normalized magnetization of the free layer, which is denoted by \mathbf{m} , satisfies $\mathbf{m} = \mathbf{M}_2/M_s = -\mathbf{s}_2$. Let $\mathbf{p} \in \mathbb{S}^2$ be the constant magnetization of the fixed layer, which satisfies $\mathbf{p} = -\mathbf{s}_1$ for the same reason. Multiplying (2.36) by $-g_e \mu_B/d$, we derive the following expression for the spin transfer torque term

$$\partial_t \mathbf{m} = -\frac{g_e \mu_B J_e G(\mathbf{m} \cdot \mathbf{p}, P)}{e M_s d} \mathbf{m} \times (\mathbf{m} \times \mathbf{p}).$$

Taking the identity $\gamma = -g_e \mu_B/\hbar$ and the definition of the rescaled gyromagnetic ratio $\gamma_0 = -\gamma \mu_0$ into account, we obtain the relation $\gamma_0 \hbar = \mu_0 g_e \mu_B$. We conclude that the normalized magnetization \mathbf{m} of the free layer satisfies the Landau–Lifshitz–Gilbert–Slonczewski (LLGS) equation

$$\partial_t \mathbf{m} = -\gamma_0 \mathbf{m} \times \mathbf{H}_{\text{eff}} + \alpha \mathbf{m} \times \partial_t \mathbf{m} - \frac{\gamma_0 \hbar J_e G(\mathbf{m} \cdot \mathbf{p}, P)}{e \mu_0 M_s d} \mathbf{m} \times (\mathbf{m} \times \mathbf{p}). \quad (2.38)$$

The Gilbert form (2.29) of the LLG equation is supplemented with a term which is parallel to the orthogonal projection of \mathbf{p} onto the plane perpendicular to \mathbf{m} . Besides some physical constants, the coefficient in front of it depends on the angle between \mathbf{m} and \mathbf{p} , on the electric current density, and on the free layer thickness. Arguing as in Section 2.2.2, from (2.38) one easily derives the equality

$$\gamma_0 \mathbf{H}_{\text{eff}} \cdot \partial_t \mathbf{m} = \alpha |\partial_t \mathbf{m}|^2 - \frac{\gamma_0 \hbar J_e G(\mathbf{m} \cdot \mathbf{p}, P)}{e \mu_0 M_s d} (\mathbf{m} \times \mathbf{p}) \cdot \partial_t \mathbf{m},$$

the counterpart of (2.32). We obtain that the Gibbs free energy, which is related to the effective field via (2.24), satisfies the energy law

$$\frac{d}{dt} \mathcal{E}(\mathbf{m}) = -\frac{\alpha \mu_0 M_s}{\gamma_0} \int_{\Omega} |\partial_t \mathbf{m}|^2 d\mathbf{x} + \frac{\hbar J_e}{ed} \int_{\Omega} G(\mathbf{m} \cdot \mathbf{p}, P) (\mathbf{m} \times \mathbf{p}) \cdot \partial_t \mathbf{m} d\mathbf{x}.$$

The LLGS equation has been phenomenologically extended with the inclusion of an additional torque term. Currently, most of the micromagnetic simulations of spintronic devices with CPP injection geometry are usually based on the equation

$$\partial_t \mathbf{m} = -\gamma_0 \mathbf{m} \times \mathbf{H}_{\text{eff}} + \alpha \mathbf{m} \times \partial_t \mathbf{m} - \frac{\gamma_0 \hbar J_e P}{2e \mu_0 M_s d} \mathbf{m} \times (\mathbf{m} \times \mathbf{p}) - \frac{\gamma_0 \hbar J_e P \xi}{2e \mu_0 M_s d} \mathbf{m} \times \mathbf{p}. \quad (2.39)$$

see, e.g., [124, 175, 176]. Up to physical constants, the two additional terms which supplement the LLG equation take the form

$$\mathbf{m} \times (\mathbf{m} \times \mathbf{p}) \quad \text{and} \quad \mathbf{m} \times \mathbf{p}.$$

The first term, which is already present in the LLGS equation (2.38), is the so-called adiabatic (or Slonczewski-type) term. Note that the adiabatic term of (2.39) exactly coincides with the one of (2.38) if we choose a constant (independent of \mathbf{m}) ballistic function according to $G(\mathbf{m} \cdot \mathbf{p}, P) = P/2$ instead of (2.37). The second term is usually referred to as nonadiabatic (or field-like) term and models the precession of the magnetization of the free layer around the ‘field’ \mathbf{p} associated with the magnetization of the fixed layer. In (2.39), $\xi > 0$ is the ratio of nonadiabaticity (nondimensional). In this case, the Gibbs free energy evolves according to the law

$$\frac{d}{dt} \mathcal{E}(\mathbf{m}) = -\frac{\alpha \mu_0 M_s}{\gamma_0} \int_{\Omega} |\partial_t \mathbf{m}|^2 d\mathbf{x} + \frac{\hbar J_e P}{2ed} \int_{\Omega} (\mathbf{m} \times \mathbf{p} + \xi \mathbf{p}) \cdot \partial_t \mathbf{m} d\mathbf{x}.$$

2.3.2 Spin diffusion model

We consider a three-dimensional extension of the one-dimensional model proposed in [212]; see also [189, 102]. Let $\Omega \subset \Omega'$ be two bounded domains in \mathbb{R}^3 with corresponding boundaries $\Gamma := \partial\Omega$ and $\Gamma' := \partial\Omega'$. The larger domain Ω' refers to the volume occupied by a conducting material, while Ω denotes its ferromagnetic part. This setting covers, e.g., the case of the multilayer structure of Figure 2.3, where Ω' is the volume of the entire multilayer, while Ω corresponds to the volume occupied by the two magnetic sublayers ($F_1 \cup F_2$).

In Ω the magnetization is governed by the equation of motion

$$\partial_t \mathbf{m} = -\gamma_0 \mathbf{m} \times \mathbf{H}_{\text{eff}} + \alpha \mathbf{m} \times \partial_t \mathbf{m} - \frac{1}{\tau_J M_s} \mathbf{m} \times \mathbf{s}; \quad (2.40)$$

see [212, equation (11)]. This is the Gilbert form (2.29) of the LLG equation supplemented by an additional term which models the spin transfer torque exerted on the magnetization by the flowing conduction electrons. In the last term on the right-hand side, \mathbf{s} denotes the spin accumulation (in A/m), or nonequilibrium spin density, while $\tau_J := \hbar/J$ denotes the characteristic time of the spin transfer torque (in s), defined as the quotient of the reduced Planck constant (in Js) and the exchange integral $J > 0$ (in J). From (2.40), it is clear that only the transverse (i.e., perpendicular to \mathbf{m}) component of the spin accumulation contributes to the torque. The dynamics of the spin accumulation in Ω' is governed by the continuity equation

$$\partial_t \mathbf{s} + \nabla \cdot \mathbf{J}_s = -\frac{1}{\tau_{\text{sf}}} \mathbf{s} - \frac{1}{\tau_J} \mathbf{s} \times \mathbf{m}, \quad (2.41)$$

where \mathbf{J}_s is the matrix-valued spin current density (in A/s), such that, for all $1 \leq i, j \leq 3$, the coefficient $(\mathbf{J}_s)_{ij}$ is the flow of the i component of the spin accumulation in the j direction, while $\tau_{\text{sf}} > 0$ is the spin-flip relaxation time (in s). From the nonvanishing right-hand side of (2.41), we observe that the spin accumulation is not conserved: this is due to the spin relaxation (first term) and the interaction with the local magnetic moments (second term). According to [212], phenomenological expressions for the spin current density \mathbf{J}_s and the electric current density \mathbf{J}_e are given by

$$\mathbf{J}_e = \sigma \mathbf{E} - \beta' \frac{e}{\mu_B} D_0 \nabla \mathbf{s}^\top \mathbf{m} \quad (2.42)$$

and

$$\mathbf{J}_s = \beta \frac{\mu_B}{e} \sigma \mathbf{m} \otimes \mathbf{E} - D_0 \nabla \mathbf{s}, \quad (2.43)$$

respectively. Here, $0 < \beta, \beta' < 1$ are nondimensional spin polarization parameters, while D_0 and σ denote the diffusion coefficient (in m^2/s) and the conductivity (in $\text{A}/(\text{m V})$) of the material, respectively, which are related to each other via the Einstein relation

$$\sigma = e^2 N_0 D_0, \quad (2.44)$$

with the constant $N_0 > 0$ being the density of states at Fermi level (in $1/(\text{J m}^3)$). Note that (2.42) reduces to the classical Ohm law for conducting materials in the nonmagnetic part of the domain; see (2.6) or (2.9c). Extracting the expression of the electric field from (2.42) and substituting it into (2.43), we obtain

$$\mathbf{J}_s = \frac{\beta \mu_B}{e} \mathbf{m} \otimes \mathbf{J}_e - D_0 (\mathbf{I}_{3 \times 3} - \beta \beta' \mathbf{m} \otimes \mathbf{m}) \nabla \mathbf{s}.$$

Using this expression into (2.41) we obtain the quasilinear diffusion equation

$$\partial_t \mathbf{s} - \nabla \cdot [D_0 (\mathbf{I}_{3 \times 3} - \beta \beta' \mathbf{m} \otimes \mathbf{m}) \nabla \mathbf{s}] + \frac{1}{\tau_{\text{sf}}} \mathbf{s} + \frac{1}{\tau_J} \mathbf{s} \times \mathbf{m} = -\frac{\beta \mu_B}{e} \nabla \cdot (\mathbf{m} \otimes \mathbf{J}_e). \quad (2.45)$$

As for the energy law, we have the equality

$$\gamma_0 \mathbf{H}_{\text{eff}} \cdot \partial_t \mathbf{m} = \alpha |\partial_t \mathbf{m}|^2 - \frac{1}{\tau_J M_s} \mathbf{s} \cdot \partial_t \mathbf{m},$$

from which we deduce that the Gibbs free energy satisfies

$$\frac{d}{dt} \mathcal{E}(\mathbf{m}) = -\frac{\alpha \mu_0 M_s}{\gamma_0} \int_{\Omega} |\partial_t \mathbf{m}|^2 d\mathbf{x} + \frac{\mu_0}{\gamma_0 \tau_J} \int_{\Omega} \mathbf{s} \cdot \partial_t \mathbf{m} d\mathbf{x}.$$

The dynamics of the spin accumulation is much faster than the one of the magnetization, e.g., the relaxation time of the spin accumulation is two orders of magnitude below the typical reaction time of the magnetization [212, 7, 174]. As long as one is interested in the magnetization dynamics, it is therefore reasonable to treat the spin accumulation as in equilibrium, i.e., to consider the stationary case of (2.45), namely

$$-\nabla \cdot [D_0 (\mathbf{I}_{3 \times 3} - \beta \beta' \mathbf{m} \otimes \mathbf{m}) \nabla \mathbf{s}] + \frac{1}{\tau_{\text{sf}}} \mathbf{s} + \frac{1}{\tau_J} \mathbf{s} \times \mathbf{m} = -\frac{\beta \mu_B}{e} \nabla \cdot (\mathbf{m} \otimes \mathbf{J}_e).$$

As for the boundary conditions for the spin accumulation, a possible choice is given by homogeneous Neumann boundary conditions

$$\partial_n \mathbf{s} = \mathbf{0} \quad \text{on } \Gamma',$$

as done, e.g., in [6, 7, 102, 174]. As an alternative, given a partition of the boundary $\Gamma' = \overline{\Gamma'_D} \cup \overline{\Gamma'_N}$ into relatively open disjoint parts $\Gamma'_D, \Gamma'_N \subset \Gamma'$, also the mixed boundary conditions

$$\mathbf{s} = \mathbf{0} \quad \text{on } \Gamma'_D \quad \text{and} \quad \mathbf{J}_s \mathbf{n} = \mathbf{0} \quad \text{on } \Gamma'_N$$

can be considered. In the case of the multilayer structure of Figure 2.3, a physically meaningful choice for the Dirichlet boundary Γ'_D is represented by the top and the bottom surfaces (electric contacts), while the insulating boundary Γ'_N includes the lateral surfaces. The homogeneous Dirichlet condition for the spin accumulation is physically meaningful if the electrodes are sufficiently large when compared to the spin diffusion length $\lambda_{\text{sd}} = \sqrt{2(1 - \beta \beta') D_0 \tau_{\text{sf}}}$ (in m); see [212].

2.3.3 Zhang–Li model

Starting from a simplified version of the spin diffusion equation (2.45), in [213] the authors model the effect of the electric current density on the magnetization dynamics by the equation

$$\partial_t \mathbf{m} = -\gamma_0 \mathbf{m} \times \mathbf{H}_{\text{eff}} + \alpha \mathbf{m} \times \partial_t \mathbf{m} + b_J \mathbf{m} \times [\mathbf{m} \times (\mathbf{J}_e \cdot \nabla) \mathbf{m}] + b_J \xi \mathbf{m} \times (\mathbf{J}_e \cdot \nabla) \mathbf{m}, \quad (2.46)$$

where $b_J = \mu_B P / [e M_s (1 + \xi^2)]$ (in m^3/C). Here, the nondimensional parameters $0 < P < 1$ and $\xi > 0$ are the spin polarization parameter of the ferromagnet and the ratio of nonadiabaticity; see [213, equation (11)]. A similar equation was obtained in a phenomenological way in [198] for the description of the current-driven domain wall motion in patterned nanowires. There, the authors proposed the equation

$$\partial_t \mathbf{m} = -\gamma_0 \mathbf{m} \times \mathbf{H}_{\text{eff}} + \alpha \mathbf{m} \times \partial_t \mathbf{m} + (\mathbf{u} \cdot \nabla) \mathbf{m} - \xi \mathbf{m} \times (\mathbf{u} \cdot \nabla) \mathbf{m}, \quad (2.47)$$

where $\mathbf{u} = -[\mu_B g_e P / (2e M_s)] \mathbf{J}_e = -[\gamma_0 \hbar P / (2e \mu_0 M_s)] \mathbf{J}_e$ and ξ is the ratio of nonadiabaticity (in the original publication denoted by β); see [198, equation (3)]. From the identity

$$(\mathbf{J}_e \cdot \nabla) \mathbf{m} = -\mathbf{m} \times [\mathbf{m} \times (\mathbf{J}_e \cdot \nabla) \mathbf{m}],$$

which follows from the orthogonality $(\nabla \mathbf{m})^\top \mathbf{m} = \mathbf{0}$ (which in turn is a consequence of the constraint $|\mathbf{m}| = 1$), it turns out that, up to the different constants, the two additional terms coincide and are proportional to

$$\mathbf{m} \times [\mathbf{m} \times (\mathbf{J}_e \cdot \nabla) \mathbf{m}] \quad \text{and} \quad \mathbf{m} \times (\mathbf{J}_e \cdot \nabla) \mathbf{m}.$$

The first term is the adiabatic (Slonczewski-like) one and was already proposed in [42, 18, 143]. The contribution can be understood as the continuous limit of the Slonczewski spin-transfer term from Section 2.3.1 for a multilayer with infinite sublayers of infinitesimal thickness; see, e.g., [151]. The second term is the nonadiabatic (field-like) one, which models the precession around the ‘field’ $(\mathbf{J}_e \cdot \nabla) \mathbf{m}$ generated whenever an electric current flows in a nonuniformly magnetized material.

Arguing along [213], we show that a similar equation can be obtained from a formal simplification of the spin diffusion model considered in Section 2.3.2. The model is based on two main assumptions:

1. The spin accumulation is treated as in equilibrium, i.e., $\partial_t \mathbf{s} = \mathbf{0}$;
2. The spin accumulation is assumed to vary slowly in space, i.e., $|\nabla \mathbf{s}| \ll 1$, so that the terms of (2.45) which contain $\nabla \mathbf{s}$ can be neglected.

Due to the second assumption, the model is not suitable for the simulation of multilayer structures, while it is adequate, e.g., for the study of the current-driven motion of domain walls in single-phase samples characterized by a current-in-plane (CIP) injection geometry.

Under these assumptions, the governing equation for the spin accumulation (2.45) reduces to

$$\frac{1}{\tau_{\text{sf}}} \mathbf{s} + \frac{1}{\tau_J} \mathbf{s} \times \mathbf{m} + \frac{\beta \mu_B}{e} \nabla \cdot (\mathbf{m} \otimes \mathbf{J}_e) = \mathbf{0}.$$

Using the product rule $\nabla \cdot (\mathbf{m} \otimes \mathbf{J}_e) = (\mathbf{J}_e \cdot \nabla) \mathbf{m} + (\nabla \cdot \mathbf{J}_e) \mathbf{m}$ for the last term of the left-hand side, we obtain

$$\frac{1}{\tau_{\text{sf}}} \mathbf{s} + \frac{1}{\tau_J} \mathbf{s} \times \mathbf{m} + \frac{\beta \mu_B}{e} [(\mathbf{J}_e \cdot \nabla) \mathbf{m} + (\nabla \cdot \mathbf{J}_e) \mathbf{m}] = \mathbf{0},$$

which is equivalent to

$$\mathbf{s} = \frac{\tau_{\text{sf}}}{\tau_J} \mathbf{m} \times \mathbf{s} - \frac{\tau_{\text{sf}} \beta \mu_B}{e} [(\mathbf{J}_e \cdot \nabla) \mathbf{m} + (\nabla \cdot \mathbf{J}_e) \mathbf{m}]. \quad (2.48)$$

Taking the vector product of (2.48) with \mathbf{m} and using the constraint $|\mathbf{m}| = 1$, an application of the triple product expansion formula $\mathbf{m} \times (\mathbf{m} \times \mathbf{s}) = (\mathbf{m} \cdot \mathbf{s})\mathbf{m} - \mathbf{s}$ yields

$$\begin{aligned}\mathbf{m} \times \mathbf{s} &= \frac{\tau_{\text{sf}}}{\tau_{\text{J}}} \mathbf{m} \times (\mathbf{m} \times \mathbf{s}) - \frac{\tau_{\text{sf}}\beta\mu_B}{e} \mathbf{m} \times (\mathbf{J}_e \cdot \nabla)\mathbf{m} \\ &= \frac{\tau_{\text{sf}}}{\tau_{\text{J}}} (\mathbf{m} \cdot \mathbf{s})\mathbf{m} - \frac{\tau_{\text{sf}}}{\tau_{\text{J}}} \mathbf{s} - \frac{\tau_{\text{sf}}\beta\mu_B}{e} \mathbf{m} \times (\mathbf{J}_e \cdot \nabla)\mathbf{m}.\end{aligned}$$

In the first two terms on the right-hand side of the latter, we replace \mathbf{s} by its expression from (2.48). Since $(\mathbf{J}_e \cdot \nabla)\mathbf{m} \cdot \mathbf{m} = 0$, we obtain

$$\begin{aligned}\mathbf{m} \times \mathbf{s} &= \frac{\tau_{\text{sf}}}{\tau_{\text{J}}} \left(-\frac{\tau_{\text{sf}}\beta\mu_B}{e} \nabla \cdot \mathbf{J}_e \right) \mathbf{m} - \frac{\tau_{\text{sf}}}{\tau_{\text{J}}} \left(\frac{\tau_{\text{sf}}}{\tau_{\text{J}}} \mathbf{m} \times \mathbf{s} - \frac{\tau_{\text{sf}}\beta\mu_B}{e} [(\mathbf{J}_e \cdot \nabla)\mathbf{m} + (\nabla \cdot \mathbf{J}_e)\mathbf{m}] \right) \\ &\quad - \frac{\tau_{\text{sf}}\beta\mu_B}{e} \mathbf{m} \times (\mathbf{J}_e \cdot \nabla)\mathbf{m} \\ &= -\frac{\tau_{\text{sf}}^2\beta\mu_B}{\tau_{\text{J}}e} (\nabla \cdot \mathbf{J}_e)\mathbf{m} - \frac{\tau_{\text{sf}}^2}{\tau_{\text{J}}^2} \mathbf{m} \times \mathbf{s} + \frac{\tau_{\text{sf}}^2\beta\mu_B}{\tau_{\text{J}}e} (\mathbf{J}_e \cdot \nabla)\mathbf{m} + \frac{\tau_{\text{sf}}^2\beta\mu_B}{\tau_{\text{J}}e} (\nabla \cdot \mathbf{J}_e)\mathbf{m} \\ &\quad - \frac{\tau_{\text{sf}}\beta\mu_B}{e} \mathbf{m} \times (\mathbf{J}_e \cdot \nabla)\mathbf{m} \\ &= -\frac{\tau_{\text{sf}}^2}{\tau_{\text{J}}^2} \mathbf{m} \times \mathbf{s} + \frac{\tau_{\text{sf}}^2\beta\mu_B}{\tau_{\text{J}}e} (\mathbf{J}_e \cdot \nabla)\mathbf{m} - \frac{\tau_{\text{sf}}\beta\mu_B}{e} \mathbf{m} \times (\mathbf{J}_e \cdot \nabla)\mathbf{m}\end{aligned}$$

Rearranging the terms, we get

$$\mathbf{m} \times \mathbf{s} = \frac{\tau_{\text{J}}\beta\mu_B}{e(1 + \tau_{\text{J}}^2/\tau_{\text{sf}}^2)} \left[(\mathbf{J}_e \cdot \nabla)\mathbf{m} - \frac{\tau_{\text{J}}}{\tau_{\text{sf}}} \mathbf{m} \times (\mathbf{J}_e \cdot \nabla)\mathbf{m} \right].$$

We define the nondimensional ratio of nonadiabacity by $\xi = \tau_{\text{J}}/\tau_{\text{sf}} = \hbar/(\tau_{\text{sf}}J)$. Moreover, to simplify the notation, we define the quantity $b_\xi = \beta\mu_B/[eM_s(1 + \xi^2)]$ (in m^3/C). Note the analogy with the constant b_{J} , which appears in the original Zhang–Li model; see (2.46). The above expression then becomes

$$\mathbf{m} \times \mathbf{s} = b_\xi \tau_{\text{J}} M_s [(\mathbf{J}_e \cdot \nabla)\mathbf{m} - \xi \mathbf{m} \times (\mathbf{J}_e \cdot \nabla)\mathbf{m}]. \quad (2.49)$$

With this computation, we have obtained an expression of the spin transfer torque $\mathbf{m} \times \mathbf{s}$ that is actually independent of \mathbf{s} . Hence, in the LLG equation (2.40) we can replace $\mathbf{m} \times \mathbf{s}$ by its expression from (2.49). The resulting equation is the extended LLG equation

$$\partial_t \mathbf{m} = -\gamma_0 \mathbf{m} \times \mathbf{H}_{\text{eff}} + \alpha \mathbf{m} \times \partial_t \mathbf{m} - b_\xi (\mathbf{J}_e \cdot \nabla)\mathbf{m} + b_\xi \xi \mathbf{m} \times (\mathbf{J}_e \cdot \nabla)\mathbf{m}. \quad (2.50)$$

It is clear that all three equations (2.46), (2.47), and (2.50) can be rewritten in the form

$$\partial_t \mathbf{m} = -\gamma_0 \mathbf{m} \times \mathbf{H}_{\text{eff}} + \alpha \mathbf{m} \times \partial_t \mathbf{m} - \mathbf{m} \times [\mathbf{m} \times (\mathbf{v} \cdot \nabla)\mathbf{m}] - \xi \mathbf{m} \times (\mathbf{v} \cdot \nabla)\mathbf{m}, \quad (2.51)$$

with $\mathbf{v} = -b_{\text{J}}\mathbf{J}_e$ for (2.46), $\mathbf{v} = \mathbf{u}$ for (2.47), and $\mathbf{v} = -b_\xi \mathbf{J}_e$ for (2.50). The vector \mathbf{v} can be understood as a given spin velocity vector (in m/s). Finally, the usual calculations lead to the following energy law for the Gibbs free energy

$$\frac{d}{dt} \mathcal{E}(\mathbf{m}) = -\frac{\alpha\mu_0 M_s}{\gamma_0} \int_{\Omega} |\partial_t \mathbf{m}|^2 dx + \frac{\mu_0 M_s}{\gamma_0} \int_{\Omega} [\mathbf{m} \times (\mathbf{v} \cdot \nabla)\mathbf{m} + \xi (\mathbf{v} \cdot \nabla)\mathbf{m}] \cdot \partial_t \mathbf{m} dx.$$

2.3.4 Self-consistent model

The Slonczewski model presented in Section 2.3.1 provides an adequate description of the spin transfer torque exerted on the free layer by the fixed layer of a multilayer structure characterized by a CPP injection geometry. The Zhang–Li model considered in Section 2.3.3 describes the spin transfer torque induced by the presence of magnetization gradients and is appropriate, e.g., for

the description of current-driven domain wall motion in structures with a CIP injection geometry. Both the situations can be described by the spin diffusion model considered in Section 2.3.2, which provides a generalization based on the interaction of the local magnetization with the spin accumulation. However, in all three approaches, the effects of the magnetic state of the system on the electronic transport are neglected. Indeed, the electric current density is always assumed to be known and the models can be used only to investigate how the electronic transport affects the magnetization dynamics, but not vice versa.

In this section, we introduce a model, which includes a bidirectional coupling of the magnetization to the electric current, for the self-consistent computation of magnetization dynamics and spin-polarized currents. The model has been applied to a magnetic nanowire geometry for the prediction of current-driven motion of domain walls [193] and for investigating the magnetization-dependent resistivity related to the GMR effect in composite multilayer structures [8].

The three basic ingredients of the model are the LLG equation (2.40) with spin transfer torque for the magnetization dynamics, the continuity equation (2.41) for the spin accumulation, and the Maxwell equations for the electromagnetic fields discussed in Section 2.1. As in Section 2.3.2, we consider two bounded domains $\Omega \subset \Omega'$ in \mathbb{R}^3 which represent the volume occupied by a conducting body and its ferromagnetic part, respectively. We assume that Ω' is a simply connected domain and denote by $\Gamma := \partial\Omega$ and $\Gamma' := \partial\Omega'$ the respective boundaries.

To obtain a self-consistent and well-defined system of equations, we introduce some appropriate assumptions. Since the dynamics of both the spin accumulation and the electromagnetic fields is indeed much faster than the one of the magnetization, we treat the spin accumulation and the electromagnetic fields as in equilibrium and thus consider the stationary cases of the corresponding governing equations.

The magnetostatic Maxwell equations, namely

$$\nabla \cdot \mathbf{H} = -M_s \nabla \cdot (\chi_\Omega \mathbf{m}), \quad (2.52a)$$

$$\nabla \times \mathbf{H} = \chi_{\Omega'} \mathbf{J}_e, \quad (2.52b)$$

can be treated as in Section 2.2.1 and give rise to the stray field \mathbf{H}_s and the Oersted field \mathbf{H}_c ; see page 14. Moreover, from the static Maxwell–Ampère law (2.52b), we deduce that the electric current density is divergence-free. Together with the stationary case of (2.41), we thus obtain the following conservation laws for the electric current and the spin accumulation

$$\nabla \cdot \mathbf{J}_e = 0,$$

$$\nabla \cdot \mathbf{J}_s = -\frac{1}{\tau_{sf}} \mathbf{s} - \frac{1}{\tau_J} \mathbf{s} \times \mathbf{m}.$$

The electrostatic Maxwell equations are given by

$$\nabla \cdot (\varepsilon \mathbf{E}) = \chi_{\Omega'} \rho, \quad (2.53a)$$

$$\nabla \times \mathbf{E} = \mathbf{0}. \quad (2.53b)$$

The static Faraday law (2.53b) shows that the electric field \mathbf{E} is irrotational. Since Ω' is simply connected, it is also conservative, i.e., $\mathbf{E} = -\nabla V$, with V being the electric potential (in V). Let $c := eN_0\mu_B$, so that the Einstein relation (2.44) can be rewritten as $\sigma = c(e/\mu_B)D_0$. Under these assumptions, the phenomenological expressions (2.42)–(2.43) for the electric current density and the spin current density take the form

$$\begin{aligned} \mathbf{J}_e &= -c \frac{e}{\mu_B} D_0 \nabla V - \beta' \frac{e}{\mu_B} D_0 \nabla \mathbf{s}^\top \mathbf{m}, \\ \mathbf{J}_s &= -\beta c D_0 \mathbf{m} \otimes \nabla V - D_0 \nabla \mathbf{s}. \end{aligned}$$

We conclude that the magnetization, the spin accumulation and the electric potential solve the

system

$$\partial_t \mathbf{m} = -\gamma_0 \mathbf{m} \times (\mathbf{H}_{\text{eff}} + \mathbf{H}_c) + \alpha \mathbf{m} \times \partial_t \mathbf{m} - \frac{1}{\tau_J M_s} \mathbf{m} \times \mathbf{s} \quad (2.54a)$$

$$-c \nabla \cdot (D_0 \nabla V) - \beta' \nabla \cdot (D_0 \nabla \mathbf{s}^\top \mathbf{m}) = 0, \quad (2.54b)$$

$$-\beta c \nabla \cdot (D_0 \mathbf{m} \otimes \nabla V) - \nabla \cdot (D_0 \nabla \mathbf{s}) = -\frac{1}{\tau_{\text{sf}}} \mathbf{s} - \frac{1}{\tau_J} \mathbf{s} \times \mathbf{m}. \quad (2.54c)$$

In (2.54a) the energy-based effective field, besides the stray field, comprises the contributions that are relevant for the specific model under consideration.

To complete the setting, we need to impose appropriate boundary conditions. To this end, we consider a partition of the boundary $\Gamma' = \overline{\Gamma'_D} \cup \overline{\Gamma'_N}$ into relatively open parts $\Gamma'_D, \Gamma'_N \subset \Gamma'$ such that $\Gamma'_D \cap \Gamma'_N = \emptyset$. On Γ'_D , we impose Dirichlet boundary conditions for both the electric potential and the spin accumulation, i.e.,

$$V = V_D \quad \text{and} \quad \mathbf{s} = \mathbf{0} \quad \text{on } \Gamma'_D$$

for some given electric potential V_D . On Γ'_N , we prescribe no flux conditions, i.e.,

$$\mathbf{J}_e \cdot \mathbf{n} = 0 \quad \text{and} \quad \mathbf{J}_s \cdot \mathbf{n} = \mathbf{0} \quad \text{on } \Gamma'_N.$$

The appropriate boundary condition for the magnetization on Γ depends on the contributions that are included in the effective field.

Chapter 3

Preliminaries

In this chapter, in view of the forthcoming analysis, we collect some auxiliary results. We start with the rigorous nondimensionalization of the problems considered in Chapter 2. Then, we introduce the notation and discuss some preliminary results about the discretization methods considered in the following chapters.

3.1 Nondimensionalization

Let $\Omega \subset \mathbb{R}^3$ be a bounded domain representing the volume occupied by a ferromagnetic body and let $T > 0$ be some finite time. The magnetization is mathematically represented by a vector field $\mathbf{m} : \Omega \times (0, T) \rightarrow \mathbb{S}^2$, where

$$\mathbb{S}^2 = \{\mathbf{x} \in \mathbb{R}^3 : |\mathbf{x}| = 1\}$$

denotes the unit sphere.

We start by rescaling the time variable: We perform the substitution $t^* = \gamma_0 M_s t$ with t^* being the so-called reduced time. Recall that the physical units of the rescaled gyromagnetic ratio γ_0 and the saturation magnetization M_s are m/(A s) and A/m, respectively, from which it follows that the reduced time is nondimensional. Consistently, we define $T^* := \gamma_0 M_s T$.

We rescale the effective field and the Gibbs free energy by $\mathbf{h}_{\text{eff}} = \mathbf{H}_{\text{eff}}/M_s$ and $\mathcal{E}^* = \mathcal{E}/(2K_s)$, where $K_s = \mu_0 M_s^2/2$ is the magnetostatic energy density introduced in (2.21). Moreover, we rescale the quantities which appear in the expression of the elastic energy (2.19) as $\kappa^* = \kappa \gamma_0^2/M_s$, $\mathbf{C}^* = \mathbf{C}/K_s$, $\mathbf{f}^* = \mathbf{f}/K_s$, and $\mathbf{t}^* = \mathbf{t}/K_s$, and define $\boldsymbol{\sigma}^* := \mathbf{C}^* \boldsymbol{\varepsilon}_{\text{el}}$, so that the expression of the energy with the rescaled constants remains the same. Indeed, it holds that

$$\begin{aligned} \mathcal{E}_{\text{el}}^*(\mathbf{m}, \mathbf{u}) &= \frac{\mathcal{E}_{\text{el}}(\mathbf{m}, \mathbf{u})}{2K_s} \\ &= \frac{\gamma_0^2}{2\mu_0} \int_{\Omega} \kappa |\partial_t \mathbf{u}|^2 \, d\mathbf{x} + \frac{1}{2\mu_0 M_s^2} \int_{\Omega} \boldsymbol{\varepsilon}_{\text{el}}(\mathbf{u}, \mathbf{m}) : [\mathbf{C} \boldsymbol{\varepsilon}_{\text{el}}(\mathbf{u}, \mathbf{m})] \, d\mathbf{x} \\ &\quad - \frac{1}{\mu_0 M_s^2} \int_{\Omega} \mathbf{f} \cdot \mathbf{u} \, d\mathbf{x} - \frac{1}{\mu_0 M_s^2} \int_{\Gamma_N} \mathbf{t} \cdot \mathbf{u} \, dS \\ &= \frac{1}{2} \int_{\Omega} \kappa^* |\partial_t \mathbf{u}|^2 \, d\mathbf{x} + \frac{1}{2} \int_{\Omega} \boldsymbol{\varepsilon}_{\text{el}}(\mathbf{u}, \mathbf{m}) : [\mathbf{C}^* \boldsymbol{\varepsilon}_{\text{el}}(\mathbf{u}, \mathbf{m})] \, d\mathbf{x} - \int_{\Omega} \mathbf{f}^* \cdot \mathbf{u} \, d\mathbf{x} - \int_{\Gamma_N} \mathbf{t}^* \cdot \mathbf{u} \, dS. \end{aligned}$$

As a consequence, the rescaled effective field is related to the rescaled energy via the relation

$$\mathbf{h}_{\text{eff}} = -\frac{\delta \mathcal{E}^*}{\delta \mathbf{m}}.$$

In particular, for each of the energy contributions introduced in Section 2.2.1, it holds that

$$\begin{aligned}
\mathcal{E}_{\text{ex}}^*(\mathbf{m}) &= \frac{\lambda_{\text{ex}}^2}{2} \int_{\Omega} |\nabla \mathbf{m}|^2 \, \mathrm{d}\mathbf{x} & \implies & \mathbf{h}_{\text{eff,ex}} = \lambda_{\text{ex}}^2 \Delta \mathbf{m}, \\
\mathcal{E}_{\text{ani}}^*(\mathbf{m}) &= \frac{q^2}{2} \int_{\Omega} \phi(\mathbf{m}) \, \mathrm{d}\mathbf{x} & \implies & \mathbf{h}_{\text{eff,ani}} = -\frac{q^2}{2} \nabla \phi(\mathbf{m}), \\
\mathcal{E}_{\text{ext}}^*(\mathbf{m}, \mathbf{h}_{\text{ext}}) &= - \int_{\Omega} \mathbf{h}_{\text{ext}} \cdot \mathbf{m} \, \mathrm{d}\mathbf{x} & \implies & \mathbf{h}_{\text{eff,ext}} = \mathbf{h}_{\text{ext}}, \\
\mathcal{E}_{\text{DM}}^*(\mathbf{m}) &= \frac{\lambda_{\text{DM}}}{2} \int_{\Omega} (\nabla \times \mathbf{m}) \cdot \mathbf{m} \, \mathrm{d}\mathbf{x} & \implies & \mathbf{h}_{\text{eff,DM}} = -\lambda_{\text{DM}} \nabla \times \mathbf{m}, \\
\mathcal{E}_{\text{stray}}^*(\mathbf{m}) &= \frac{1}{2} \int_{\mathbb{R}^3} |\mathbf{h}_{\text{s}}|^2 \, \mathrm{d}\mathbf{x} & \implies & \mathbf{h}_{\text{eff,stray}} = \mathbf{h}_{\text{s}}, \\
\mathcal{E}_{\text{el}}^*(\mathbf{m}, \mathbf{u}) &= \frac{1}{2} \int_{\Omega} \varepsilon_{\text{el}}(\mathbf{u}, \mathbf{m}) : [\mathbf{C}^* \varepsilon_{\text{el}}(\mathbf{u}, \mathbf{m})] \, \mathrm{d}\mathbf{x} + \dots & \implies & \mathbf{h}_{\text{eff,el}} = 2(\lambda \sigma^*) \mathbf{m}.
\end{aligned}$$

Here, λ_{ex} is the exchange length from (2.22), q is the magnetic hardness parameter from (2.23), $\mathbf{h}_{\text{ext}} = \mathbf{H}_{\text{ext}}/M_{\text{s}}$ is the rescaled applied field, $\lambda_{\text{DM}} = D/K_{\text{s}}$ is a length scale associated with the Dzyaloshinskii–Moriya interaction (in m), \mathbf{h}_{s} solves a rescaled version of the magnetostatic Maxwell equations (2.12), namely

$$\begin{aligned}
\nabla \cdot \mathbf{h}_{\text{s}} &= -\nabla \cdot (\chi_{\Omega} \mathbf{m}) & \text{in } \mathbb{R}^3, \\
\nabla \times \mathbf{h}_{\text{s}} &= \mathbf{0} & \text{in } \mathbb{R}^3.
\end{aligned}$$

Similarly, the nondimensional Oersted field \mathbf{h}_{c} solves a rescaled version of (2.13), namely

$$\begin{aligned}
\nabla \cdot \mathbf{h}_{\text{c}} &= 0 & \text{in } \mathbb{R}^3, \\
\nabla \times \mathbf{h}_{\text{c}} &= \chi_{\Omega} \mathbf{j}_{\text{e}} & \text{in } \mathbb{R}^3,
\end{aligned}$$

where $\mathbf{j}_{\text{e}} = \mathbf{J}_{\text{e}}/M_{\text{s}}$. Correspondingly, we obtain the transmission problem

$$-\Delta u^{\text{int}} = -\nabla \cdot \mathbf{m} \quad \text{in } \Omega, \quad (3.1a)$$

$$-\Delta u^{\text{ext}} = 0 \quad \text{in } \mathbb{R}^3 \setminus \overline{\Omega}, \quad (3.1b)$$

$$u^{\text{ext}} - u^{\text{int}} = 0 \quad \text{on } \Gamma, \quad (3.1c)$$

$$(\nabla u^{\text{ext}} - \nabla u^{\text{int}}) \cdot \mathbf{n} = -\mathbf{m} \cdot \mathbf{n} \quad \text{on } \Gamma, \quad (3.1d)$$

$$u(\mathbf{x}) = \mathcal{O}(1/|\mathbf{x}|) \quad \text{as } |\mathbf{x}| \rightarrow \infty \quad (3.1e)$$

for the rescaled magnetostatic potential and the transmission problem

$$-\Delta \mathbf{h}_{\text{c}}^{\text{int}} = \nabla \times \mathbf{j}_{\text{e}} \quad \text{in } \Omega, \quad (3.2a)$$

$$-\Delta \mathbf{h}_{\text{c}}^{\text{ext}} = \mathbf{0} \quad \text{in } \mathbb{R}^3 \setminus \overline{\Omega}, \quad (3.2b)$$

$$\mathbf{h}_{\text{c}}^{\text{ext}} - \mathbf{h}_{\text{c}}^{\text{int}} = \mathbf{0} \quad \text{on } \Gamma, \quad (3.2c)$$

$$(\nabla \mathbf{h}_{\text{c}}^{\text{ext}} - \nabla \mathbf{h}_{\text{c}}^{\text{int}}) \mathbf{n} = \mathbf{n} \times \mathbf{j}_{\text{e}} \quad \text{on } \Gamma, \quad (3.2d)$$

$$\mathbf{h}_{\text{c}}(\mathbf{x}) = \mathcal{O}(1/|\mathbf{x}|) \quad \text{as } |\mathbf{x}| \rightarrow \infty \quad (3.2e)$$

for the rescaled Oersted field; see (2.14) and (2.16). However, to simplify the notation, we will always omit the *-superscripts from the equations, e.g., we denote the reduced time also by t .

With these substitutions, the nondimensional form of the LLG equation (2.30) becomes

$$\partial_t \mathbf{m} = -\frac{1}{1+\alpha^2} \mathbf{m} \times \mathbf{h}_{\text{eff}} - \frac{\alpha}{1+\alpha^2} \mathbf{m} \times (\mathbf{m} \times \mathbf{h}_{\text{eff}}) \quad \text{in } \Omega.$$

The homogeneous Neumann boundary conditions

$$\partial_{\mathbf{n}} \mathbf{m} = \mathbf{0} \quad \text{on } \Gamma := \partial\Omega$$

associated with the exchange interaction becomes

$$2\lambda_{\text{ex}}^2 \partial_{\mathbf{n}} \mathbf{m} + \lambda_{\text{DM}} \mathbf{m} \times \mathbf{n} = \mathbf{0} \quad \text{on } \Gamma$$

in the presence of the Dzyaloshinskii–Moriya interaction. The same formal computation performed in Section 2.2.2 yields the energy law

$$\frac{d}{dt} \mathcal{E}(\mathbf{m}, \mathbf{h}_{\text{ext}}) = -\alpha \int_{\Omega} |\partial_t \mathbf{m}|^2 d\mathbf{x} - \int_{\Omega} \partial_t \mathbf{h}_{\text{ext}} \cdot \mathbf{m} d\mathbf{x}, \quad (3.3)$$

which reveals the dissipative behavior of the model, when \mathbf{h}_{ext} is constant in time.

In the following proposition, we establish the equivalence of three different reformulations of the LLG equation.

Proposition 3.1.1. *Under the constraint $|\mathbf{m}| = 1$, the following three reformulations of the LLG equation are equivalent:*

- the Landau–Lifshitz form

$$\partial_t \mathbf{m} = -\frac{1}{1 + \alpha^2} \mathbf{m} \times \mathbf{h}_{\text{eff}} - \frac{\alpha}{1 + \alpha^2} \mathbf{m} \times (\mathbf{m} \times \mathbf{h}_{\text{eff}})$$

- the Gilbert form

$$\partial_t \mathbf{m} = -\mathbf{m} \times \mathbf{h}_{\text{eff}} + \alpha \mathbf{m} \times \partial_t \mathbf{m} \quad (3.4)$$

- the so-called ‘alternative form’

$$\alpha \partial_t \mathbf{m} + \mathbf{m} \times \partial_t \mathbf{m} = \mathbf{h}_{\text{eff}} - (\mathbf{h}_{\text{eff}} \cdot \mathbf{m}) \mathbf{m}. \quad (3.5)$$

Proof. The proof follows from straightforward algebraic manipulations. It exploits the triple product expansion formula

$$\mathbf{a} \times (\mathbf{b} \times \mathbf{c}) = (\mathbf{a} \cdot \mathbf{c}) \mathbf{b} - (\mathbf{a} \cdot \mathbf{b}) \mathbf{c} \quad \text{for all } \mathbf{a}, \mathbf{b}, \mathbf{c} \in \mathbb{R}^3$$

from Proposition B.2.1(vi), in combination with the modulus constraint $|\mathbf{m}| = 1$ and the resulting orthogonality property $\partial_t \mathbf{m} \cdot \mathbf{m} = 0$. For the complete argument, we refer the reader to [109, Lemma 1.2.1]. \square

3.1.1 Coupling with the Maxwell equations and magnetostriction

In this section, we denote the micromagnetic Gibbs free energy by $\mathcal{E}_{\text{Gibbs}}$ in order to distinguish it from the energy of the system, which can also depend on quantities associated with the equation(s) coupled to the LLG equation.

For the nondimensionalization of the coupling of the LLG equation with the full Maxwell system (2.34), we consider the substitutions $\mu_0^* = \gamma_0 M_s \mu_0$, $\varepsilon^* = \gamma_0 M_s \varepsilon$, $\mathbf{e} = \mathbf{E}/M_s$, and $\mathbf{h} = \mathbf{H}/M_s$. We obtain the system

$$\partial_t \mathbf{m} = -\mathbf{m} \times (\mathbf{h}_{\text{eff}} + \mathbf{h}) + \alpha \mathbf{m} \times \partial_t \mathbf{m} \quad \text{in } \Omega, \quad (3.6a)$$

$$\mu_0 \partial_t \mathbf{h} = -\nabla \times \mathbf{e} - \mu_0 \chi_{\Omega} \partial_t \mathbf{m} \quad \text{in } \mathbb{R}^3, \quad (3.6b)$$

$$\varepsilon \partial_t \mathbf{e} = \nabla \times \mathbf{h} - \chi_{\Omega} \sigma \mathbf{e} \quad \text{in } \mathbb{R}^3. \quad (3.6c)$$

For the sake of simplicity, we assume the Maxwell equations (3.6b)–(3.6c) to be posed on a bounded cavity $\Omega' \subset \mathbb{R}^3$ with perfectly conducting boundary in which the ferromagnet is embedded, i.e., $\Omega \Subset \Omega'$; see [24, 28]. Moreover, we assume $\Omega' \setminus \bar{\Omega}$ to be vacuum. The resulting system, i.e.,

$$\partial_t \mathbf{m} = -\mathbf{m} \times (\mathbf{h}_{\text{eff}} + \mathbf{h}) + \alpha \mathbf{m} \times \partial_t \mathbf{m} \quad \text{in } \Omega,$$

$$\mu_0 \partial_t \mathbf{h} = -\nabla \times \mathbf{e} - \mu_0 \chi_{\Omega} \partial_t \mathbf{m} \quad \text{in } \Omega',$$

$$\varepsilon \partial_t \mathbf{e} = \nabla \times \mathbf{h} - \chi_{\Omega} \sigma \mathbf{e} \quad \text{in } \Omega',$$

is supplemented with the appropriate boundary conditions on Γ for the LLG equation (which depend on the contributions included into \mathbf{h}_{eff}) as well as the following boundary conditions for the electric field

$$\mathbf{e} \times \mathbf{n} = \mathbf{0} \quad \text{on } \Gamma' = \partial\Omega'.$$

The energy of the system, defined as the sum of the micromagnetic Gibbs free energy and the electromagnetic energy, i.e.,

$$\mathcal{E}(\mathbf{e}, \mathbf{h}, \mathbf{m}) = \mathcal{E}_{\text{Gibbs}}(\mathbf{m}) + \frac{1}{2\mu_0} \int_{\Omega'} \varepsilon |\mathbf{e}|^2 \, d\mathbf{x} + \frac{1}{2} \int_{\Omega'} |\mathbf{h}|^2 \, d\mathbf{x},$$

satisfies the energy law

$$\frac{d}{dt} \mathcal{E}(\mathbf{e}, \mathbf{h}, \mathbf{m}) = -\alpha \int_{\Omega} |\partial_t \mathbf{m}|^2 \, d\mathbf{x} - \int_{\Omega} \partial_t \mathbf{h}_{\text{ext}} \cdot \mathbf{m} \, d\mathbf{x} - \mu_0^{-1} \int_{\Omega} \sigma |\mathbf{e}|^2 \, d\mathbf{x}.$$

For the nondimensionalization of the coupling of the LLG equation with the magnetoquasistatic Maxwell equations (2.33), we perform the same substitutions used for the full Maxwell equations. We obtain the system

$$\begin{aligned} \partial_t \mathbf{m} &= -\mathbf{m} \times (\mathbf{h}_{\text{eff}} + \mathbf{h}) + \alpha \mathbf{m} \times \partial_t \mathbf{m} && \text{in } \Omega, \\ \nabla \cdot (\varepsilon \mathbf{e}) &= \gamma_0 \chi_{\Omega} \rho && \text{in } \mathbb{R}^3, \\ \nabla \cdot \mathbf{h} &= -\nabla \cdot (\chi_{\Omega} \mathbf{m}) && \text{in } \mathbb{R}^3, \\ \nabla \times \mathbf{e} &= -\mu_0 \partial_t \mathbf{h} - \mu_0 \chi_{\Omega} \partial_t \mathbf{m} && \text{in } \mathbb{R}^3, \\ \nabla \times \mathbf{h} &= \chi_{\Omega} \sigma \mathbf{e} && \text{in } \mathbb{R}^3. \end{aligned}$$

Moreover, for the sake of simplicity, we consider the system only on the ferromagnetic domain Ω , which we assume to be a perfectly conducting body; see [142, 141]. Eliminating the electric field yields the system

$$\begin{aligned} \partial_t \mathbf{m} &= -\mathbf{m} \times (\mathbf{h}_{\text{eff}} + \mathbf{h}) + \alpha \mathbf{m} \times \partial_t \mathbf{m} && \text{in } \Omega, \\ \mu_0 \partial_t \mathbf{h} &= -\nabla \times (\sigma^{-1} \nabla \times \mathbf{h}) - \mu_0 \partial_t \mathbf{m} && \text{in } \Omega, \end{aligned}$$

where the LLG equation is coupled with the eddy current equation. The adequate boundary conditions for the magnetization are supplemented with the following boundary conditions for the magnetic field

$$(\nabla \times \mathbf{h}) \times \mathbf{n} = \mathbf{0} \quad \text{on } \Gamma.$$

The energy, defined in this case as the sum of the micromagnetic Gibbs free energy and the magnetic energy, i.e.,

$$\mathcal{E}(\mathbf{h}, \mathbf{m}) = \mathcal{E}_{\text{Gibbs}}(\mathbf{m}) + \frac{1}{2} \int_{\Omega} |\mathbf{h}|^2 \, d\mathbf{x},$$

is driven by the energy law

$$\frac{d}{dt} \mathcal{E}(\mathbf{h}, \mathbf{m}) = -\alpha \int_{\Omega} |\partial_t \mathbf{m}|^2 \, d\mathbf{x} - \int_{\Omega} \partial_t \mathbf{h}_{\text{ext}} \cdot \mathbf{m} \, d\mathbf{x} - \mu_0^{-1} \int_{\Omega} \sigma^{-1} |\nabla \times \mathbf{h}|^2 \, d\mathbf{x}.$$

With the substitutions previously introduced to rescale the elastic energy, the coupling of the LLG equation with the conservation of momentum law takes the form

$$\begin{aligned} \partial_t \mathbf{m} &= -\mathbf{m} \times \mathbf{h}_{\text{eff}} + \alpha \mathbf{m} \times \partial_t \mathbf{m} && \text{in } \Omega, \\ \kappa \partial_{tt} \mathbf{u} &= \nabla \cdot \boldsymbol{\sigma} + \mathbf{f} && \text{in } \Omega, \end{aligned}$$

where $\boldsymbol{\sigma} = \mathbf{C}[\boldsymbol{\varepsilon}(\mathbf{u}) - \boldsymbol{\varepsilon}_m(\mathbf{m})]$ and the effective field, among others, comprises the magnetoelastic contribution $\mathbf{h}_{\text{eff,el}} = 2(\boldsymbol{\lambda} \boldsymbol{\sigma}) \mathbf{m}$. The appropriate boundary conditions for the magnetization are supplemented with the following mixed boundary conditions for the displacement

$$\begin{aligned} \mathbf{u} &= \mathbf{0} && \text{on } \Gamma_D, \\ \boldsymbol{\sigma} \mathbf{n} &= \mathbf{t} && \text{on } \Gamma_N, \end{aligned}$$

for a partition of the boundary $\Gamma = \overline{\Gamma_D} \cup \overline{\Gamma_N}$ into relatively open parts $\Gamma_D, \Gamma_N \subset \Gamma$ such that $\Gamma_D \cap \Gamma_N = \emptyset$ and $|\Gamma_D| > 0$. The energy of the system, given by the micromagnetic Gibbs free energy (which includes the elastic energy), satisfies the law

$$\frac{d}{dt}\mathcal{E}(\mathbf{m}, \mathbf{u}) = \frac{d}{dt}\mathcal{E}_{\text{Gibbs}}(\mathbf{m}, \mathbf{u}) = -\alpha \int_{\Omega} |\partial_t \mathbf{m}|^2 d\mathbf{x} - \int_{\Omega} \partial_t \mathbf{h}_{\text{ext}} \cdot \mathbf{m} d\mathbf{x} - \int_{\Omega} \partial_t \mathbf{f} \cdot \mathbf{u} d\mathbf{x} - \int_{\Gamma_N} \partial_t \mathbf{t} \cdot \mathbf{u} dS.$$

3.1.2 Spintronic extensions of micromagnetics

Finally, we discuss the spintronic extensions of the LLG equation presented in Section 2.3. We recall that they are not characterized by an energy approach. The energy considered throughout this section therefore coincides with the micromagnetic Gibbs free energy.

We start with the LLGS equation (2.38). Rescaling the intensity of the electric current density and the ballistic function (2.37) according to $j_e = J_e/M_s$ and $G^*(\cdot, \cdot) = \hbar/(e\mu_0 M_s)G(\cdot, \cdot)$, we obtain the equation

$$\partial_t \mathbf{m} = -\mathbf{m} \times \mathbf{h}_{\text{eff}} + \alpha \mathbf{m} \times \partial_t \mathbf{m} - \frac{j_e G(\mathbf{m} \cdot \mathbf{p}, P)}{d} \mathbf{m} \times (\mathbf{m} \times \mathbf{p}) \quad \text{in } \Omega \quad (3.7)$$

and the corresponding energy law

$$\frac{d}{dt}\mathcal{E}(\mathbf{m}) = -\alpha \int_{\Omega} |\partial_t \mathbf{m}|^2 d\mathbf{x} - \int_{\Omega} \partial_t \mathbf{h}_{\text{ext}} \cdot \mathbf{m} d\mathbf{x} + d^{-1} \int_{\Omega} j_e G(\mathbf{m} \cdot \mathbf{p}, P) (\mathbf{m} \times \mathbf{p}) \cdot \partial_t \mathbf{m} d\mathbf{x}.$$

Similarly, for the extended LLGS equation (2.39) for general current-perpendicular-to-plane (CPP) injection geometries, we define the quantity $a_P := \hbar P/(2e\mu_0 M_s)$. We obtain the equation

$$\partial_t \mathbf{m} = -\mathbf{m} \times \mathbf{h}_{\text{eff}} + \alpha \mathbf{m} \times \partial_t \mathbf{m} - \frac{a_P j_e}{d} \mathbf{m} \times (\mathbf{m} \times \mathbf{p} + \xi \mathbf{p}) \quad \text{in } \Omega \quad (3.8)$$

as well as the associated energy law

$$\frac{d}{dt}\mathcal{E}(\mathbf{m}) = -\alpha \int_{\Omega} |\partial_t \mathbf{m}|^2 d\mathbf{x} - \int_{\Omega} \partial_t \mathbf{h}_{\text{ext}} \cdot \mathbf{m} d\mathbf{x} + \frac{a_P}{d} \int_{\Omega} j_e (\mathbf{m} \times \mathbf{p} + \xi \mathbf{p}) \cdot \partial_t \mathbf{m} d\mathbf{x}.$$

For the LLG equation (2.51) with Zhang–Li spin transfer torque, we rescale the spin velocity vector according to $\mathbf{v}^* = \mathbf{v}/(\gamma_0 M_s)$. We obtain the equation

$$\partial_t \mathbf{m} = -\mathbf{m} \times \mathbf{h}_{\text{eff}} + \alpha \mathbf{m} \times \partial_t \mathbf{m} - \mathbf{m} \times [\mathbf{m} \times (\mathbf{v} \cdot \nabla) \mathbf{m} + \xi (\mathbf{v} \cdot \nabla) \mathbf{m}] \quad \text{in } \Omega. \quad (3.9)$$

In this case, the evolution of the Gibbs free energy follows the law

$$\frac{d}{dt}\mathcal{E}(\mathbf{m}) = -\alpha \int_{\Omega} |\partial_t \mathbf{m}|^2 d\mathbf{x} - \int_{\Omega} \partial_t \mathbf{h}_{\text{ext}} \cdot \mathbf{m} d\mathbf{x} + \int_{\Omega} [\mathbf{m} \times (\mathbf{v} \cdot \nabla) \mathbf{m} + \xi (\mathbf{v} \cdot \nabla) \mathbf{m}] \cdot \partial_t \mathbf{m} d\mathbf{x}.$$

We conclude this section by considering the spin diffusion model from Section 2.3.2 and the self-consistent model from Section 2.3.4. Let $\Omega' \subset \mathbb{R}^3$ be a bounded domain such that $\Omega \subseteq \Omega'$. We rescale the spin accumulation by $\mathbf{s}^* = \mathbf{s}/M_s$, the spin current density by $\mathbf{j}_s = \mathbf{J}_s/(\gamma_0 M_s^2)$, the diffusion coefficient by $D_0^* = (e/\mu_B)D_0$, the characteristic times by $\tau_{\text{sf}}^* = \gamma_0 M_s \tau_{\text{sf}}$ and $\tau_J^* = \gamma_0 M_s \tau_J$, respectively. Moreover, we recall the scaling of the electric field and the electric current density already introduced for the Maxwell equations, namely $\mathbf{e} = \mathbf{E}/M_s$ and $\mathbf{j}_e = \mathbf{J}_e/M_s$, and define $z := \mu_B/(e\gamma_0 M_s)$. As a result, we obtain the expressions

$$\begin{aligned} \mathbf{j}_e &= \sigma \mathbf{e} - \beta' D_0 \nabla \mathbf{s}^{\top} \mathbf{m}, \\ \mathbf{j}_s/z &= \beta \sigma \mathbf{m} \otimes \mathbf{e} - D_0 \nabla \mathbf{s}. \end{aligned}$$

The spin diffusion model is given by the system

$$\partial_t \mathbf{m} = -\mathbf{m} \times \mathbf{h}_{\text{eff}} + \alpha \mathbf{m} \times \partial_t \mathbf{m} - \tau_J^{-1} \mathbf{m} \times \mathbf{s} \quad \text{in } \Omega, \quad (3.10a)$$

$$\partial_t \mathbf{s} = z \nabla \cdot [D_0 (\mathbf{I}_{3 \times 3} - \beta \beta' \mathbf{m} \otimes \mathbf{m}) \nabla \mathbf{s}] - \tau_{\text{sf}}^{-1} \mathbf{s} - \tau_J^{-1} \mathbf{s} \times \mathbf{m} - z \beta \nabla \cdot (\mathbf{m} \otimes \mathbf{j}_e) \quad \text{in } \Omega'. \quad (3.10b)$$

On $\Gamma' := \partial\Omega'$, either the homogeneous Neumann boundary conditions

$$\partial_{\mathbf{n}} \mathbf{s} = \mathbf{0} \quad \text{on } \Gamma'$$

or the mixed boundary conditions

$$\mathbf{s} = \mathbf{0} \quad \text{on } \Gamma'_D \quad \text{and} \quad \mathbf{j}_s \cdot \mathbf{n} = \mathbf{0} \quad \text{on } \Gamma'_N \quad (3.11)$$

can be considered. In the second case, we consider a partition of the boundary $\Gamma' = \overline{\Gamma'_D} \cup \overline{\Gamma'_N}$ into relatively open disjoint parts $\Gamma'_D, \Gamma'_N \subset \Gamma'$. The Gibbs free energy evolves according to the law

$$\frac{d}{dt} \mathcal{E}(\mathbf{m}) = -\alpha \int_{\Omega} |\partial_t \mathbf{m}|^2 d\mathbf{x} - \int_{\Omega} \partial_t \mathbf{h}_{\text{ext}} \cdot \mathbf{m} d\mathbf{x} + \tau_J^{-1} \int_{\Omega} \mathbf{s} \cdot \partial_t \mathbf{m} d\mathbf{x}. \quad (3.12)$$

For the self-consistent model, we rescale the electric potential by $V^* = V/M_s$ so that $\mathbf{e} = -\nabla V^*$. We obtain the system

$$\begin{aligned} \partial_t \mathbf{m} &= -\mathbf{m} \times (\mathbf{h}_{\text{eff}} + \mathbf{h}_c) + \alpha \mathbf{m} \times \partial_t \mathbf{m} - \tau_J^{-1} \mathbf{m} \times \mathbf{s} && \text{in } \Omega, \\ -c \nabla \cdot (D_0 \nabla V) - \beta' \nabla \cdot (D_0 \nabla \mathbf{s}^\top \mathbf{m}) &= 0 && \text{in } \Omega', \\ -\beta c z \nabla \cdot (D_0 \mathbf{m} \otimes \nabla V) - z \nabla \cdot (D_0 \nabla \mathbf{s}) &= -\tau_{\text{sf}}^{-1} \mathbf{s} - \tau_J^{-1} \mathbf{s} \times \mathbf{m} && \text{in } \Omega'. \end{aligned}$$

The mixed boundary conditions (3.11) for the spin accumulation are supplemented by analogous conditions for the electric potential, namely

$$V = V_D \quad \text{on } \Gamma'_D \quad \text{and} \quad \mathbf{j}_e \cdot \mathbf{n} = \mathbf{0} \quad \text{on } \Gamma'_N.$$

3.2 Notation for Lebesgue/Sobolev/Bochner spaces

We use the standard notation for Lebesgue, Sobolev, and Bochner spaces and norms; see, e.g., [88, Chapter 5]. For $d \geq 1$ integer, let $D \subset \mathbb{R}^d$ be a domain. For $1 \leq p \leq \infty$, we consider the Banach space

$$L^p(D) = \{v : D \rightarrow \mathbb{R} \text{ measurable} : \|v\|_{L^p(D)} < \infty\},$$

endowed with the norm

$$\|v\|_{L^p(D)} = \begin{cases} \left(\int_D |v(\mathbf{x})|^p d\mathbf{x} \right)^{1/p}, & \text{if } 1 \leq p < \infty, \\ \text{ess sup}_{\mathbf{x} \in D} |v(\mathbf{x})|, & \text{if } p = \infty. \end{cases}$$

For $p = 2$, $L^2(D)$ is a Hilbert space with respect to the scalar product

$$\langle u, v \rangle_D = \int_D u(\mathbf{x}) v(\mathbf{x}) d\mathbf{x}.$$

For $k \geq 0$ integer and $1 \leq p \leq \infty$, we consider the Banach space

$$W^{k,p}(D) = \{v \in L^p(D) : D^\alpha v \in L^p(D) \text{ for all } |\alpha| \leq k\}$$

endowed with the norm

$$\|v\|_{W^{k,p}(D)} = \begin{cases} \left(\sum_{0 \leq |\alpha| \leq k} \|D^\alpha v\|_{L^p(D)}^p \right)^{1/p}, & \text{if } 1 \leq p < \infty, \\ \max_{0 \leq |\alpha| \leq k} \|D^\alpha v\|_{L^\infty(D)}, & \text{if } p = \infty. \end{cases}$$

For $k = 0$, we recover the L^p -spaces, i.e., $W^{0,p}(D) = L^p(D)$ for all $1 \leq p \leq \infty$. For $p = 2$, $W^{k,2}(D)$ is a Hilbert space with respect to the scalar product

$$\langle u, v \rangle_{W^{k,2}(D)} = \sum_{0 \leq |\alpha| \leq k} \langle D^\alpha u, D^\alpha v \rangle_D.$$

In this case, we write $H^k(D) = W^{k,2}(D)$ and consider also the seminorm defined by

$$|v|_{H^k(D)}^2 = \sum_{|\alpha|=k} \|D^\alpha v\|_{L^2(D)}^2.$$

To deal with time-dependent evolution equations, we also consider spaces of functions with values in a Banach space. Given $1 \leq p \leq \infty$ and a Banach space B , we consider the Banach space

$$L^p(0, T; B) = \{v : (0, T) \rightarrow B \text{ measurable} : \|v\|_{L^p(0, T; B)} < \infty\}$$

endowed with the norm

$$\|v\|_{L^p(0, T; B)} = \begin{cases} \left(\int_0^T \|v(t)\|_B^p dt \right)^{1/p}, & \text{if } 1 \leq p < \infty, \\ \text{ess sup}_{t \in (0, T)} \|v(t)\|_B, & \text{if } p = \infty. \end{cases}$$

Similarly, for $1 \leq p \leq \infty$, we consider the space

$$W^{1,p}(0, T; B) = \{v \in L^p(0, T; B) : \partial_t v \in L^p(0, T; B)\}$$

endowed with the norm

$$\|v\|_{W^{1,p}(0, T; B)} = \begin{cases} \left(\|v\|_{L^p(0, T; B)}^p + \|\partial_t v\|_{L^p(0, T; B)}^p \right)^{1/p}, & \text{if } 1 \leq p < \infty, \\ \text{ess sup}_{t \in (0, T)} (\|v(t)\|_B + \|\partial_t v(t)\|_B), & \text{if } p = \infty. \end{cases}$$

As before, we write $H^1(0, T; B) = W^{1,2}(0, T; B)$. For $k \geq 0$ integer, we consider the space

$$C^k([0, T]; B) = \{v : [0, T] \rightarrow B \text{ of class } C^k\}$$

endowed with the norm

$$\|v\|_{C^k([0, T]; B)} = \sum_{i=0}^k \left(\max_{t \in [0, T]} \|v^{(i)}(t)\|_B \right).$$

The inclusion $W^{1,p}(0, T; B) \subset C^0([0, T]; B)$ is continuous for all $1 \leq p \leq \infty$; see, e.g., [88, Section 5.9.2, Theorem 2].

Let H be a separable Hilbert space. Let V be a reflexive and separable Banach space such that the inclusion $V \hookrightarrow H$ is continuous and dense. Under these assumptions, it follows that the inclusion $H^* \hookrightarrow V^*$ is continuous, dense, and injective. With the identification $H \simeq H^*$ given by the Riesz theorem, we obtain the chain of continuous and dense inclusions $V \subset H \subset V^*$. The triple (V, H, V^*) is usually referred to as Gelfand triple. The most famous example, in the frame of the analysis of PDEs, is the Gelfand triple $H_0^1(D) \subset L^2(D) \subset H_0^1(D)^* =: H^{-1}(D)$.

Given $1 < p < \infty$, let $1 < q < \infty$ such that $1/p + 1/q = 1$. For a Gelfand triple (V, H, V^*) , we consider the Banach space

$$W^{1,p}(0, T; V, H) = \{v \in L^p(0, T; V) : \partial_t v \in L^q(0, T; V^*)\}$$

endowed with the norm

$$\|v\|_{W^{1,p}(0, T; V, H)} = \|v\|_{L^p(0, T; V)} + \|\partial_t v\|_{L^q(0, T; V^*)}.$$

Then, the inclusion $W^{1,p}(0, T; V, H) \subset C^0([0, T]; H)$ is continuous (see, e.g., [88, Section 5.9.2, Theorem 3] for the case $p = 2$), and $C^1([0, T]; V)$ is dense in $W^{1,p}(0, T; V, H)$.

The above definitions can be naturally extended to measurable vector-valued functions $\mathbf{v} : D \rightarrow \mathbb{R}^d$ and matrix-valued functions $\mathbf{V} : D \rightarrow \mathbb{R}^{d \times d}$. In the case of (spaces of) vector-valued or matrix-valued functions, we use bold letters, e.g., we denote both $L^2(D, \mathbb{R}^d)$ and $L^2(D, \mathbb{R}^{d \times d})$ by $\mathbf{L}^2(D)$ and the corresponding scalar product by

$$\begin{aligned} \langle \mathbf{u}, \mathbf{v} \rangle_D &= \int_D \mathbf{u}(\mathbf{x}) \cdot \mathbf{v}(\mathbf{x}) \, d\mathbf{x} \quad \text{for all } \mathbf{u}, \mathbf{v} \in \mathbf{L}^2(D) = L^2(D, \mathbb{R}^d), \\ \langle \mathbf{U}, \mathbf{V} \rangle_D &= \int_D \mathbf{U}(\mathbf{x}) : \mathbf{V}(\mathbf{x}) \, d\mathbf{x} \quad \text{for all } \mathbf{U}, \mathbf{V} \in \mathbf{L}^2(D) = L^2(D, \mathbb{R}^{d \times d}). \end{aligned}$$

The abuse of notation is resolved by the arguments of the scalar product.

3.3 Time discretization

Let $T > 0$. For the time discretization of a time interval $[0, T]$, we restrict ourselves to the case of a uniform partition into $M \geq 1$ subintervals with time-step size $k = T/M$, i.e., $t_i = ik$ for all $0 \leq i \leq M$.

Let B be a Banach space. Given a sequence $\{\phi^i\}_{0 \leq i \leq M}$ in B , such that any $\phi^i \in B$ is associated with the time-step t_i , for all $0 \leq i \leq M-1$ we define the difference quotient $d_t \phi^{i+1} := (\phi^{i+1} - \phi^i)/k$. We consider the continuous piecewise linear approximation and two piecewise constant (backward and forward) approximations: For $0 \leq i \leq M-1$ and $t \in [t_i, t_{i+1})$, we define

$$\phi_k(t) := \frac{t - t_i}{k} \phi^{i+1} + \frac{t_{i+1} - t}{k} \phi^i, \quad (3.13a)$$

$$\phi_k^-(t) := \phi^i, \quad (3.13b)$$

$$\phi_k^+(t) := \phi^{i+1}. \quad (3.13c)$$

It is straightforward to show that $\phi_k \in H^1(0, T; B)$ and $\phi_k^\pm \in L^2(0, T; B)$ as well as $\partial_t \phi_k(t) = d_t \phi^{i+1}$ for all $t \in [t_i, t_{i+1})$ and $0 \leq i \leq M-1$. Moreover, it holds that

$$\|\phi_k(t) - \phi_k^\pm(t)\|_B \leq \|\phi_k^+(t) - \phi_k^-(t)\|_B = k \|\partial_t \phi_k(t)\|_B \quad \text{for all } t \in (0, T), \quad (3.14)$$

from which it follows that

$$\|\phi_k - \phi_k^\pm\|_{L^2(0, T; B)} \leq \|\phi_k^+ - \phi_k^-\|_{L^2(0, T; B)} = k \|\partial_t \phi_k\|_{L^2(0, T; B)}. \quad (3.15)$$

3.4 Finite element discretization

In this section, we present some definitions and results related to the Finite Element Method (FEM). Classical references for the method are, e.g., the books [68, 170, 51, 53]. Throughout this section, $C > 0$ denotes a generic constant, which is always independent of the discretization parameters, but is not necessarily the same at each occurrence. We also use the notation \lesssim and \gtrsim to denote *smaller or equal* and *larger or equal*, respectively, up to a multiplicative constant, e.g., given two expressions A and B , we write $A \lesssim B$ if there exists a constant $c > 0$, which is independent of the discretization parameters, such that $A \leq cB$. Finally, we abbreviate $A \lesssim B \lesssim A$ by $A \simeq B$.

Let Ω be a bounded Lipschitz domain in \mathbb{R}^3 with polyhedral boundary $\Gamma = \partial\Omega$. We recall the standard definition of a regular triangulation of Ω .

Definition 3.4.1 (regular triangulation). *A finite decomposition \mathcal{T} of Ω is called a regular triangulation provided the following properties are satisfied:*

- $\bar{\Omega} = \bigcup_{K \in \mathcal{T}} K$,
- each $K \in \mathcal{T}$ is a polyhedron with $\text{int}(K) \neq \emptyset$,
- if $F = K_1 \cap K_2 \neq \emptyset$ for some distinct elements $K_1, K_2 \in \mathcal{T}$, then F is either a common face, or a common edge, or a common vertex of K_1 and K_2 .

The adjective ‘regular’, sometimes replaced by ‘conforming’, refers to the last property, which excludes the presence of hanging nodes. For a regular triangulation \mathcal{T} , we denote by $\mathcal{N} = \mathcal{N}(\mathcal{T})$ the set of all of its vertices and by $\mathcal{E} = \mathcal{E}(\mathcal{T})$ the set of all of its faces. The same notation is also used for subsets, e.g., we denote by $\mathcal{N}(K)$ the set of the vertices of an element $K \in \mathcal{T}$.

We restrict ourselves to the case in which any element $K \in \mathcal{T}$ can be obtained as the image of a fixed reference element \hat{K} under an invertible affine mapping T_K , i.e., for all $K \in \mathcal{T}$, there exists $T_K : \hat{K} \rightarrow K$ such that $K = T_K(\hat{K})$. In particular, it holds that $T_K(\hat{\mathbf{x}}) = \mathbf{B}_K \hat{\mathbf{x}} + \mathbf{b}_K$ for all $\hat{\mathbf{x}} \in \hat{K}$, for some nonsingular matrix $\mathbf{B}_K \in \mathbb{R}^{3 \times 3}$ and a vector $\mathbf{b}_K \in \mathbb{R}^3$. We assume that the reference element is the unit 3-simplex, i.e., $\hat{K} = \text{conv} \{\mathbf{e}_i\}_{0 \leq i \leq 3}$, where $\mathbf{e}_0 = \mathbf{0} \in \mathbb{R}^3$ and $\{\mathbf{e}_i\}_{1 \leq i \leq 3}$ denotes the standard basis of \mathbb{R}^3 . As a consequence, any element $K = T_K(\hat{K})$ of \mathcal{T} is a tetrahedron.

Given a tetrahedron $K \in \mathcal{T}$, we consider the quantities

$$h_K = \text{diam}(K) \quad \text{and} \quad \rho_K = \sup \{ \text{diam}(B) : B \text{ is a ball contained in } K \},$$

which satisfy

$$\frac{\pi \rho_K^3}{6} \leq |K| \leq h_K^3.$$

We define the *shape-regularity parameter* by

$$\sigma(\mathcal{T}) = \max_{K \in \mathcal{T}} \frac{h_K}{\rho_K} \geq 1.$$

Let $\gamma > 0$. A triangulation \mathcal{T} is called γ -*shape-regular* if $\sigma(\mathcal{T}) \leq \gamma$. For γ -shape-regular triangulations, the cardinality of the set of neighboring nodes of a given node $\mathbf{z} \in \mathcal{N}$ is uniformly bounded, i.e., there exists a positive constant $C > 0$, which depends only on γ , such that

$$\# \{ \mathbf{y} \in \mathcal{N} : \exists K \in \mathcal{T} \text{ such that } \mathbf{z}, \mathbf{y} \in \mathcal{N}(K) \} \leq C.$$

Moreover, for every element $K \in \mathcal{T}$ of a γ -shape-regular triangulation \mathcal{T} , it holds that $|K| \simeq h_K^3$.

We define as *dihedral angle* each of the six angles between any pair of the four faces of a tetrahedron. Let F_1 and F_2 be two faces of a tetrahedron with outward unit normal vectors \mathbf{n}_1 and \mathbf{n}_2 , respectively. The dihedral angle $\angle(F_1, F_2)$ between F_1 and F_2 is given by $\angle(F_1, F_2) = \pi - \angle(\mathbf{n}_1, \mathbf{n}_2)$, where $\angle(\mathbf{n}_1, \mathbf{n}_2)$ denotes the angle between the normals \mathbf{n}_1 and \mathbf{n}_2 . It is straightforward to show that $\angle(F_1, F_2) \leq \pi/2$ if and only if $\mathbf{n}_1 \cdot \mathbf{n}_2 \leq 0$. A tetrahedron is called *weakly acute* (or *of acute type* or *nonobtuse*) if the measure of any of its dihedral angles is less than or equal to $\pi/2$. A triangulation is called *weakly acute* if all its tetrahedra are weakly acute. The construction of a weakly acute tetrahedral triangulation and the generation of weakly acute (global or local) refinements of a given weakly acute triangulation are not trivial tasks. For a deeper discussion of these issues, we refer the interested reader to [128, 129, 130, 131, 132].

Let \mathcal{T} be a regular triangulation. For all $K \in \mathcal{T}$, we denote by $\mathcal{P}^1(K)$ the space of linear polynomials on K . We consider the space of piecewise linear and globally continuous functions from Ω to \mathbb{R}

$$\mathcal{S}^1(\mathcal{T}) = \{ v_h \in C^0(\bar{\Omega}) : v_h|_K \in \mathcal{P}_1(K) \text{ for all } K \in \mathcal{T} \}.$$

A classical basis for this finite-dimensional linear space is given by the set of the nodal shape functions $\{\varphi_{\mathbf{z}}\}_{\mathbf{z} \in \mathcal{N}}$, usually referred to as *hat functions*, which satisfy $\varphi_{\mathbf{z}}(\mathbf{y}) = \delta_{\mathbf{z}\mathbf{y}}$ for all $\mathbf{z}, \mathbf{y} \in \mathcal{N}$. With our assumptions, for all $K \in \mathcal{T}$ and $\mathbf{z} \in \mathcal{N}(K)$, it holds that $\varphi_{\mathbf{z}}|_K \circ T_K = \hat{\varphi}_i$ for some $0 \leq i \leq 3$, where $\{\hat{\varphi}_i\}_{0 \leq i \leq 3}$ is the set of the hat functions on the reference element, i.e.,

$$\hat{\varphi}_0(\hat{\mathbf{x}}) = 1 - \sum_{i=1}^3 \hat{x}_i, \quad \hat{\varphi}_i(\hat{\mathbf{x}}) = \hat{x}_i \quad (1 \leq i \leq 3) \quad \text{for all } \hat{\mathbf{x}} = (\hat{x}_1, \hat{x}_2, \hat{x}_3) \in \hat{K}.$$

The weak acuteness of a triangulation can be characterized in terms of the hat functions. In order to show this, let $K \in \mathcal{T}$ and $\mathbf{z} \in \mathcal{N}(K)$. The key observation is that the gradient of the hat function $\varphi_{\mathbf{z}}$ is antiparallel to the normal of the face opposite to \mathbf{z} . In particular, a tetrahedron K is weakly acute if and only if $\nabla \varphi_{\mathbf{z}}|_K \cdot \nabla \varphi_{\mathbf{y}}|_K \leq 0$ for all $\mathbf{z} \neq \mathbf{y} \in \mathcal{N}(K)$. It follows that, for weakly acute triangulations, it holds that

$$\langle \nabla \varphi_{\mathbf{z}}, \nabla \varphi_{\mathbf{y}} \rangle_{\Omega} \leq 0 \quad \text{for all distinct nodes } \mathbf{z}, \mathbf{y} \in \mathcal{N}, \quad (3.16)$$

i.e., if and only if the off-diagonal entries of the so-called stiffness matrix are nonpositive.

For a family of triangulations $\{\mathcal{T}_h\}_{h>0}$ parametrized by the mesh size $h = \max_{K \in \mathcal{T}_h} h_K$, we use the shorthand notation $\mathcal{N}_h = \mathcal{N}(\mathcal{T}_h)$ and $N_h = \#\mathcal{N}_h$. In the following definition, we state two useful properties that are usually required for families of triangulations in the analysis of finite element methods.

Definition 3.4.2 (shape-regularity & quasi-uniformity). *Let $\{\mathcal{T}_h\}_{h>0}$ be a family of regular triangulations.*

- $\{\mathcal{T}_h\}_{h>0}$ is called *shape-regular* if there exists $\gamma > 0$, independent of h , such that \mathcal{T}_h is γ -shape-regular for all $h > 0$.
- $\{\mathcal{T}_h\}_{h>0}$ is called *quasi-uniform* if there exists $\gamma > 0$, independent of h , such that $h \leq \gamma \min_{K \in \mathcal{T}_h} \rho_K$ for all $h > 0$.

We will refer to the above properties as γ -shape-regularity and γ -quasi-uniformity when we want to specify the constants which realize the definitions. Note that a γ -quasi-uniform family of regular triangulations is also γ -shape-regular.

We consider the nodal interpolant $\mathcal{I}_h : C^0(\overline{\Omega}) \rightarrow \mathcal{S}^1(\mathcal{T}_h)$ such that $\mathcal{I}_h[v](\mathbf{z}) = v(\mathbf{z})$ for all $\mathbf{z} \in \mathcal{N}_h$ and $v \in C^0(\overline{\Omega})$, i.e.,

$$\mathcal{I}_h[v] = \sum_{\mathbf{z} \in \mathcal{N}_h} v(\mathbf{z}) \varphi_{\mathbf{z}}.$$

It is well known that the nodal interpolant satisfies the following approximation estimate; see, e.g., [53, Theorem 4.4.4 and Theorem 4.4.20].

Proposition 3.4.3 (approximation estimate). *Let $\{\mathcal{T}_h\}_{h>0}$ be a γ -shape-regular family of regular triangulations of Ω . Let $3/2 < p \leq \infty$ so that $W^{2,p}(\Omega) \subset C^0(\overline{\Omega})$ with continuous inclusion. For all integers $0 \leq m \leq 2$, it holds that*

$$|v - \mathcal{I}_h[v]|_{W^{m,p}(\Omega)} \leq Ch^{2-m} |v|_{W^{2,p}(\Omega)} \quad \text{for all } v \in W^{2,p}(\Omega).$$

The constant $C > 0$ depends only on γ and p .

Inverse estimates are typically needed for the analysis of finite element methods when it is required to have estimates for a stronger norm of a discrete function in terms of a weaker norm. The following classical inverse estimate requires the quasi-uniformity of the underlying family of triangulations; see, e.g., [68, Theorem 3.2.6].

Proposition 3.4.4 (inverse estimate). *Let $\{\mathcal{T}_h\}_{h>0}$ be a γ -quasi-uniform family of regular triangulations of Ω and let $1 \leq p \leq \infty$. Then, it holds that*

$$\|\nabla v_h\|_{L^p(\Omega)} \leq Ch^{-1} \|v_h\|_{L^p(\Omega)} \quad \text{for all } v_h \in \mathcal{S}^1(\mathcal{T}_h). \quad (3.17)$$

The constant $C > 0$ depends only on γ and p .

The following result follows from standard scaling arguments. It states that for discrete functions the L^p -norm is equivalent to a weighted ℓ^p -norm of the vector of the nodal values.

Proposition 3.4.5. *Let $\{\mathcal{T}_h\}_{h>0}$ be a γ -quasi-uniform family of regular triangulations of Ω . Given $p \in [1, \infty)$, it holds that*

$$C^{-1} \|v_h\|_{L^p(\Omega)}^p \leq h^3 \sum_{\mathbf{z} \in \mathcal{N}_h} |v_h(\mathbf{z})|^p \leq C \|v_h\|_{L^p(\Omega)}^p \quad \text{for all } v_h \in \mathcal{S}^1(\mathcal{T}_h). \quad (3.18)$$

The constant $C > 0$ depends only on γ and p .

We denote by $\mathcal{P}_h : L^2(\Omega) \rightarrow \mathcal{S}^1(\mathcal{T}_h)$ the L^2 -orthogonal projection, defined by

$$\langle \mathcal{P}_h v, v_h \rangle_\Omega = \langle v, v_h \rangle_\Omega \quad \text{for all } v_h \in \mathcal{S}^1(\mathcal{T}_h).$$

Clearly, considered as a mapping of $L^2(\Omega)$ onto $\mathcal{S}^1(\mathcal{T}_h)$ endowed with the L^2 -norm, \mathcal{P}_h is a bounded operator with norm 1, i.e.,

$$\|\mathcal{P}_h v\|_{L^2(\Omega)} \leq \|v\|_{L^2(\Omega)} \quad \text{for all } v \in L^2(\Omega).$$

Moreover, in the case of a γ -quasi-uniform family of triangulations, it is well known that \mathcal{P}_h is H^1 -stable, i.e., it holds that

$$\|\mathcal{P}_h v\|_{H^1(\Omega)} \leq C \|v\|_{H^1(\Omega)} \quad \text{for all } v \in H^1(\Omega), \quad (3.19)$$

where $C > 0$ depends only on γ . We refer to [52, 123, 32] for more results on the H^1 -stability of the L^2 -projection on locally refined meshes.

For the approximation of vector-valued functions, such as the unknown of the LLG equation, we approximate each component by piecewise linear and globally continuous functions, i.e., we consider the space $\mathcal{S}^1(\mathcal{T}_h)^3$. We consider the corresponding nodal interpolant $\mathcal{I}_h : C^0(\bar{\Omega}) \rightarrow \mathcal{S}^1(\mathcal{T}_h)^3$ such that $\mathcal{I}_h[\phi](\mathbf{z}) = \phi(\mathbf{z})$ for all $\mathbf{z} \in \mathcal{N}_h$ and $\phi \in C^0(\bar{\Omega})$. It is clear that any function $\phi_h \in \mathcal{S}^1(\mathcal{T}_h)^3$ takes the form

$$\phi_h = \sum_{\mathbf{z} \in \mathcal{N}_h} \varphi_{\mathbf{z}} \phi_h(\mathbf{z}).$$

Similarly, we denote by $\mathcal{P}_h : L^2(\Omega) \rightarrow \mathcal{S}^1(\mathcal{T}_h)^3$ the L^2 -projection for vector-valued functions. Moreover, the inequalities from Proposition 3.4.3, Proposition 3.4.4 and Proposition 3.4.5 clearly transfer to the vector-valued case (up to some generic multiplicative factor in the involved constants).

The solution of the LLG equation is characterized by the nonconvex pointwise constraint $|\mathbf{m}| = 1$. Since any discrete function of $\mathcal{S}^1(\mathcal{T}_h)^3$ which satisfies the pointwise constraint everywhere in Ω is constant, it appears necessary to weaken the constraint. A fair compromise is obtained by requiring the discrete solution to realize the pointwise constraint only at the nodes of the triangulation. To this end, we therefore introduce the set

$$\mathcal{M}_h := \{\phi_h \in \mathcal{S}^1(\mathcal{T}_h)^3 : |\phi_h(\mathbf{z})| = 1 \text{ for all } \mathbf{z} \in \mathcal{N}_h\}. \quad (3.20)$$

The following lemma follows from the fact that piecewise linear functions attain their L^∞ -norm in one of the vertices.

Lemma 3.4.6. *For all $\phi_h \in \mathcal{M}_h$, it holds that $\|\phi_h\|_{L^\infty(\Omega)} = 1$.*

Proof. Let $\mathbf{x} \in \Omega$. There exists $\{\mathbf{z}_i\}_{0 \leq i \leq 3} \subset \mathcal{N}_h$ such that $\mathbf{x} \in K = \text{conv}\{\mathbf{z}_i\}_{0 \leq i \leq 3} \in \mathcal{T}_h$. On the simplex K , we can consider the barycentric coordinate system and write $\mathbf{x} = \sum_{i=0}^3 \lambda_i \mathbf{z}_i$ for some coefficients $\lambda_i \geq 0$ such that $\sum_{i=0}^3 \lambda_i = 1$. Since $\phi_h|_K$ is an affine function, for all $\mathbf{y} \in K$ we have $\phi_h(\mathbf{y}) = \mathbf{A}\mathbf{y} + \mathbf{b}$ for some matrix $\mathbf{A} \in \mathbb{R}^{3 \times 3}$ and some vector $\mathbf{b} \in \mathbb{R}^3$. It holds that

$$\phi_h(\mathbf{x}) = \mathbf{A}\mathbf{x} + \mathbf{b} = \mathbf{A} \left(\sum_{i=0}^3 \lambda_i \mathbf{z}_i \right) + \mathbf{b} = \sum_{i=0}^3 \lambda_i (\mathbf{A}\mathbf{z}_i + \mathbf{b}) = \sum_{i=0}^3 \lambda_i \phi_h(\mathbf{z}_i).$$

Since $|\phi_h(\mathbf{z}_i)| = 1$ for all $0 \leq i \leq 3$, it follows that

$$|\phi_h(\mathbf{x})| = \left| \sum_{i=0}^3 \lambda_i \phi_h(\mathbf{z}_i) \right| \leq \sum_{i=0}^3 \lambda_i |\phi_h(\mathbf{z}_i)| = \sum_{i=0}^3 \lambda_i = 1,$$

which concludes the proof. \square

The following proposition shows that satisfying the constraint at the nodes of the triangulation is sufficient to guarantee that the limit of a convergent sequence of elements of \mathbf{M}_h satisfies the constraint almost everywhere; see [36, Proposition 7.1].

Proposition 3.4.7. *Let $\{\mathcal{T}_h\}_{h>0}$ be a γ -quasi-uniform family of regular triangulations of Ω . Let $\{\phi_h\}_{h>0}$ be a sequence in \mathbf{M}_h such that*

- $\{\phi_h\}_{h>0}$ is uniformly bounded in $\mathbf{H}^1(\Omega)$,
- there exists $\phi \in \mathbf{L}^2(\Omega)$ such that $\phi_h \rightarrow \phi$ in $\mathbf{L}^2(\Omega)$ as $h \rightarrow 0$.

Then, it holds that $|\phi| = 1$ a.e. in Ω .

Proof. Since $\phi_h \in \mathbf{M}_h$ it follows that $\mathcal{I}_h[|\phi_h|^2] = 1$. Let $K \in \mathcal{T}_h$. Due to the approximation properties of the nodal interpolant (Proposition 3.4.3), it holds that

$$\| |\phi_h|^2 - 1 \|_{L^2(K)} = \| |\phi_h|^2 - \mathcal{I}_h[|\phi_h|^2] \|_{L^2(K)} \lesssim h_K^2 \| |\phi_h|^2 \|_{H^2(K)}.$$

Since $\nabla \phi_h|_K$ is constant, we obtain that

$$\begin{aligned} \| |\phi_h|^2 \|_{H^2(K)}^2 &= \sum_{1 \leq i \leq j \leq 3} \| \partial_i \partial_j |\phi_h|^2 \|_{L^2(K)}^2 = 4 \sum_{1 \leq i \leq j \leq 3} \| \partial_i \phi_h \cdot \partial_j \phi_h \|_{L^2(K)}^2 \leq 4 \| \nabla \phi_h \|_{L^4(K)}^4 \\ &= 4 |K| \| \nabla \phi_h |_K|^4 = 4 \| \nabla \phi_h \|_{L^\infty(K)}^2 \| \nabla \phi_h \|_{L^2(K)}^2. \end{aligned}$$

Using an inverse estimate and $\| \phi_h \|_{L^\infty(\Omega)} = 1$ (see Lemma 3.4.6), we deduce that

$$\begin{aligned} \| |\phi_h|^2 - 1 \|_{L^2(K)} &\lesssim h_K^2 \| \nabla \phi_h \|_{L^\infty(K)} \| \nabla \phi_h \|_{L^2(K)} \\ &\stackrel{(3.17)}{\lesssim} h_K \| \phi_h \|_{L^\infty(K)} \| \nabla \phi_h \|_{L^2(K)} \\ &= h_K \| \nabla \phi_h \|_{L^2(K)}. \end{aligned}$$

Summing over all elements $K \in \mathcal{T}_h$, we thus obtain

$$\| |\phi_h|^2 - 1 \|_{L^2(\Omega)} \lesssim h \| \nabla \phi_h \|_{L^2(\Omega)}.$$

Since the sequence is uniformly bounded in $\mathbf{H}^1(\Omega)$, we deduce that $|\phi_h|^2 \rightarrow 1$ in $L^2(\Omega)$ as $h \rightarrow 0$. In particular, upon extraction of a subsequence (not relabeled), it holds that $|\phi_h| \rightarrow 1$ a.e. in Ω . Moreover, since $\phi_h \rightarrow \phi$ in $\mathbf{L}^2(\Omega)$ by assumption, it follows that $|\phi_h| \rightarrow |\phi|$ in $L^2(\Omega)$ and thus, upon extraction of a further subsequence (also not relabeled), it holds that $|\phi_h| \rightarrow |\phi|$ a.e. in Ω . We conclude that $|\phi| = 1$ a.e. in Ω . \square

In the following proposition, which generalizes the previous one, we show that the result remains valid even if the nodewise constraint is satisfied by the sequence of discrete functions only in an approximate way; see [36, Lemma 7.2].

Proposition 3.4.8. *Let $\{\mathcal{T}_h\}_{h>0}$ be a γ -shape-regular family of regular triangulations of Ω . Let $\{\phi_h\}_{h>0}$ be a sequence in $\mathcal{S}^1(\mathcal{T}_h)^3$ such that*

- $\| \mathcal{I}_h[|\phi_h|^2] - 1 \|_{L^1(\Omega)} \rightarrow 0$ as $h \rightarrow 0$,

- $\{\phi_h\}_{h>0}$ is uniformly bounded in $\mathbf{H}^1(\Omega)$,
- there exists $\phi \in \mathbf{L}^2(\Omega)$ such that $\phi_h \rightarrow \phi$ in $\mathbf{L}^2(\Omega)$ as $h \rightarrow 0$.

Then, it holds that $|\phi| = 1$ a.e. in Ω .

Proof. From the triangle inequality, it holds that

$$\| |\phi|^2 - 1 \|_{L^1(\Omega)} \leq \| |\phi|^2 - |\phi_h|^2 \|_{L^1(\Omega)} + \| |\phi_h|^2 - \mathcal{I}_h[|\phi_h|^2] \|_{L^1(\Omega)} + \| \mathcal{I}_h[|\phi_h|^2] - 1 \|_{L^1(\Omega)}. \quad (3.21)$$

The first term on the right-hand side can be estimated as

$$\| |\phi|^2 - |\phi_h|^2 \|_{L^1(\Omega)} \leq \| \phi + \phi_h \|_{L^2(\Omega)} \| \phi - \phi_h \|_{L^2(\Omega)} \lesssim \| \phi - \phi_h \|_{L^2(\Omega)}.$$

Since $\phi_h \rightarrow \phi$ in $\mathbf{L}^2(\Omega)$ by assumption, we deduce that $\| |\phi|^2 - |\phi_h|^2 \|_{L^1(\Omega)} \rightarrow 0$. For the second term on the right-hand side of (3.21), we proceed as in the proof of Proposition 3.4.7. For each $K \in \mathcal{T}_h$, it holds that

$$\begin{aligned} \| |\phi_h|^2 - \mathcal{I}_h[|\phi_h|^2] \|_{L^1(K)} &\leq \| 1 \|_{L^2(K)} \| |\phi_h|^2 - \mathcal{I}_h[|\phi_h|^2] \|_{L^2(K)} \\ &\leq |K|^{1/2} h_K^2 \| |\phi_h|^2 \|_{H^2(K)} \\ &\leq 2 |K|^{1/2} h_K^2 \| \nabla \phi_h \|_{L^4(K)}^2 \\ &= 2 |K| h_K^2 \| \nabla \phi_h |_K \|^2 \\ &= 2 h_K^2 \| \nabla \phi_h \|_{L^2(K)}^2. \end{aligned}$$

Summing over all the elements yields

$$\| |\phi_h|^2 - \mathcal{I}_h[|\phi_h|^2] \|_{L^1(\Omega)} \lesssim h^2 \| \nabla \phi_h \|_{L^2(\Omega)}^2.$$

Since the sequence is bounded in $\mathbf{H}^1(\Omega)$, it follows that $\| |\phi_h|^2 - \mathcal{I}_h[|\phi_h|^2] \|_{L^1(\Omega)} \rightarrow 0$. The third term on the right-hand side of (3.21) converges to 0 by assumption. Passing (3.21) to the limit as $h \rightarrow 0$, we conclude that $|\phi| = 1$ a.e. in Ω . \square

The following proposition shows that, at the continuous level, the global normalization of H^1 -functions reduces their Dirichlet energy, defined as the square of the L^2 -norm of the Jacobian; see [11, Proposition 1].

Proposition 3.4.9. *Let $\phi \in \mathbf{H}^1(\Omega)$ such that $|\phi| \geq 1$ a.e. in Ω . Then, $\phi/|\phi|$ belongs to $\mathbf{H}^1(\Omega)$. Moreover, it holds that*

$$\| \nabla (\phi/|\phi|) \|_{L^2(\Omega)} \leq \| \nabla \phi \|_{L^2(\Omega)}.$$

Proof. Let $\phi = (\phi_1, \phi_2, \phi_3) \in \mathbf{C}^\infty(\bar{\Omega})$ such that $|\phi| \geq 1$ in Ω . For $1 \leq i, j \leq 3$, we compute the (i, j) -coefficient of the Jacobian of $\phi/|\phi|$

$$[\nabla(\phi/|\phi|)]_{ij} = \partial_j \left(\frac{\phi_i}{|\phi|} \right) = \frac{\partial_j \phi_i |\phi| - \phi_i \partial_j |\phi|}{|\phi|^2} = \frac{1}{|\phi|} \partial_j \phi_i - \frac{1}{|\phi|^3} \phi_i (\phi \cdot \partial_j \phi).$$

In particular, we get the compact formula

$$\nabla (\phi/|\phi|) = \frac{1}{|\phi|} \left(\mathbf{I}_{3 \times 3} - \frac{\phi \otimes \phi}{|\phi|^2} \right) \nabla \phi$$

from Proposition B.3.1(xii). An explicit computation of the Frobenius norm then yields

$$\begin{aligned}
|\nabla(\phi/|\phi|)|^2 &= \sum_{1 \leq i, j \leq 3} \left[\partial_j \left(\frac{\phi_i}{|\phi|} \right) \right]^2 = \sum_{1 \leq i, j \leq 3} \left[\frac{1}{|\phi|} \partial_j \phi_i - \frac{1}{|\phi|^3} \phi_i (\phi \cdot \partial_j \phi) \right]^2 \\
&= \sum_{1 \leq i, j \leq 3} \left[\frac{1}{|\phi|^2} (\partial_j \phi_i)^2 - \frac{2}{|\phi|^4} \phi_i \partial_j \phi_i (\phi \cdot \partial_j \phi) + \frac{1}{|\phi|^6} \phi_i^2 (\phi \cdot \partial_j \phi)^2 \right] \\
&= \frac{1}{|\phi|^2} \sum_{1 \leq i, j \leq 3} (\partial_j \phi_i)^2 - \frac{2}{|\phi|^4} \sum_{1 \leq i, j \leq 3} \phi_i \partial_j \phi_i (\phi \cdot \partial_j \phi) + \frac{1}{|\phi|^6} \sum_{1 \leq i, j \leq 3} \phi_i^2 (\phi \cdot \partial_j \phi)^2 \\
&= \frac{1}{|\phi|^2} |\nabla \phi|^2 - \frac{2}{|\phi|^4} \sum_{j=1}^3 (\phi \cdot \partial_j \phi)^2 + \frac{1}{|\phi|^4} \sum_{j=1}^3 (\phi \cdot \partial_j \phi)^2 \\
&= \frac{1}{|\phi|^2} |\nabla \phi|^2 - \frac{1}{|\phi|^4} \sum_{j=1}^3 (\phi \cdot \partial_j \phi)^2 = \frac{1}{|\phi|^2} |\nabla \phi|^2 - \frac{1}{|\phi|^4} |\nabla \phi^\top \phi|^2.
\end{aligned}$$

Since $|\phi| \geq 1$, we deduce

$$|\nabla(\phi/|\phi|)|^2 = \frac{1}{|\phi|^2} \left(|\nabla \phi|^2 - \frac{1}{|\phi|^2} |\nabla \phi^\top \phi|^2 \right) \leq \frac{|\nabla \phi|^2}{|\phi|^2} \leq |\nabla \phi|^2.$$

Starting from this pointwise estimate, integration over Ω leads to the result for smooth functions. The assertion then follows by density. \square

The easiest way to transform a discrete function into an element of \mathcal{M}_h is by projecting each nodal value (assumed to be nonzero) onto the sphere. Consider the set

$$\mathcal{U}_h := \{\phi_h \in \mathcal{S}^1(\mathcal{T}_h)^3 : |\phi_h(z)| \geq 1 \text{ for all } z \in \mathcal{N}_h\}.$$

Clearly, it holds that $\mathcal{M}_h \subset \mathcal{U}_h$. For $\phi_h \in \mathcal{U}_h$, we consider the nodal projection mapping $\phi_h \mapsto \mathcal{I}_h[\phi_h/|\phi_h|]$.

We now look for a discrete counterpart of Proposition 3.4.9 for the nodal projection mapping. To start with, we recall that, since the projection onto a nonempty closed convex set is nonexpansive, the mapping $\mathbb{R}^3 \setminus B_1(\mathbf{0}) \rightarrow \mathbb{S}^2$ defined by $\mathbf{x} \mapsto \mathbf{x}/|\mathbf{x}|$ is Lipschitz continuous with Lipschitz constant 1, i.e.,

$$\left| \frac{\mathbf{x}_1}{|\mathbf{x}_1|} - \frac{\mathbf{x}_2}{|\mathbf{x}_2|} \right| \leq |\mathbf{x}_1 - \mathbf{x}_2| \quad \text{for all } \mathbf{x}_1, \mathbf{x}_2 \in \mathbb{R}^3 \setminus B_1(\mathbf{0}). \quad (3.22)$$

In general, the nodal projection of a discrete function does not reduce its Dirichlet energy. However, the Dirichlet energy of the nodal projection of a discrete function is uniformly bounded by the Dirichlet energy of the original discrete function as stated by the following proposition.

Proposition 3.4.10. *Let $\{\mathcal{T}_h\}_{h>0}$ be a γ -shape-regular family of regular triangulations of Ω . It holds that*

$$\|\nabla \mathcal{I}_h[\phi_h/|\phi_h|]\|_{L^2(\Omega)} \leq C \|\nabla \phi_h\|_{L^2(\Omega)} \quad \text{for all } \phi_h \in \mathcal{U}_h, \quad (3.23)$$

where the constant $C > 0$ depends only on γ .

Proof. Let $K \in \mathcal{T}_h$ be an arbitrary tetrahedron. We assume that $K = \text{conv}\{\mathbf{z}_i\}_{0 \leq i \leq 3}$ for some $\{\mathbf{z}_i\}_{0 \leq i \leq 3} \subset \mathcal{N}_h$. We consider the reference element \hat{K} as well as the affine mapping $T_K : \hat{K} \rightarrow K$ such that $T_K(\mathbf{e}_i) = \mathbf{z}_i$ for all $0 \leq i \leq 3$. Given an arbitrary $\phi_h \in \mathcal{U}_h$, set $\hat{\phi}_h = \phi_h \circ T_K$ and $\widehat{\mathcal{I}}_h[\phi_h/|\phi_h|] = \mathcal{I}_h[\phi_h/|\phi_h|] \circ T_K$. For all $\hat{\mathbf{x}} \in \hat{K}$ and $1 \leq i \leq 3$, it holds that

$$\begin{aligned}
\left| \frac{\partial \widehat{\mathcal{I}}_h[\phi_h/|\phi_h|](\hat{\mathbf{x}})}{\partial \hat{x}_i} \right| &= \left| \widehat{\mathcal{I}}_h[\phi_h/|\phi_h|](\mathbf{e}_i) - \widehat{\mathcal{I}}_h[\phi_h/|\phi_h|](\mathbf{0}) \right| = \left| \frac{\phi_h(\mathbf{z}_i)}{|\phi_h(\mathbf{z}_i)|} - \frac{\phi_h(\mathbf{z}_0)}{|\phi_h(\mathbf{z}_0)|} \right| \\
&\stackrel{(3.22)}{\leq} |\phi_h(\mathbf{z}_i) - \phi_h(\mathbf{z}_0)| = |\hat{\phi}_h(\mathbf{e}_i) - \hat{\phi}_h(\mathbf{0})| = \left| \frac{\partial \hat{\phi}_h(\hat{\mathbf{x}})}{\partial \hat{x}_i} \right|,
\end{aligned}$$

from which it follows that

$$\|\widehat{\nabla \mathcal{I}_h}[\phi_h/|\phi_h|]\|_{L^2(\widehat{K})} \leq \|\widehat{\nabla \phi_h}\|_{L^2(\widehat{K})}. \quad (3.24)$$

With this estimate, a standard scaling argument (see, e.g., [170, Propositions 3.4.1 and 3.4.2]) yields

$$\begin{aligned} \|\nabla \mathcal{I}_h[\phi_h/|\phi_h|]\|_{L^2(K)} &\lesssim |\mathbf{B}_K^{-1}| |\det \mathbf{B}_K|^{1/2} \|\widehat{\nabla \mathcal{I}_h}[\phi_h/|\phi_h|]\|_{L^2(\widehat{K})} \\ &\stackrel{(3.24)}{\leq} |\mathbf{B}_K^{-1}| |\det \mathbf{B}_K|^{1/2} \|\widehat{\nabla \phi_h}\|_{L^2(\widehat{K})} \\ &\lesssim |\mathbf{B}_K^{-1}| |\mathbf{B}_K| \|\nabla \phi_h\|_{L^2(K)} \\ &\lesssim \frac{h_K}{\rho_K} \|\nabla \phi_h\|_{L^2(K)}. \end{aligned}$$

To get (3.23), we sum over all elements and take the γ -shape-regularity of the family of triangulations into account. \square

It has been shown by S. BARTELS in 2005 that (3.23) holds with unit constant $C = 1$, provided the triangulation satisfies the angle condition (3.16); see [33, Lemma 3.2].

Proposition 3.4.11. *Let $\{\mathcal{T}_h\}_{h>0}$ be a family of regular triangulations of Ω satisfying the angle condition (3.16). Then, it holds that*

$$\|\nabla \mathcal{I}_h[\phi_h/|\phi_h|]\|_{L^2(\Omega)} \leq \|\nabla \phi_h\|_{L^2(\Omega)} \quad \text{for all } \phi_h \in \mathcal{U}_h, \quad (3.25)$$

i.e., (3.23) holds with unit constant $C = 1$.

Proof. For $\mathbf{z}, \mathbf{y} \in \mathcal{N}_h$, let $K_{\mathbf{zy}} = \langle \nabla \varphi_{\mathbf{z}}, \nabla \varphi_{\mathbf{y}} \rangle_{\Omega}$. From the partition of unity property of the hat functions, i.e., the equality $\sum_{\mathbf{z} \in \mathcal{N}_h} \varphi_{\mathbf{z}} = 1$ in Ω , we deduce that

$$\sum_{\mathbf{y} \in \mathcal{N}_h} K_{\mathbf{zy}} = 0 \quad \text{for all } \mathbf{z} \in \mathcal{N}_h. \quad (3.26)$$

For arbitrary $\boldsymbol{\eta}_h \in \mathcal{S}^1(\mathcal{T}_h)^3$, it holds that

$$\begin{aligned} \|\nabla \boldsymbol{\eta}_h\|_{L^2(\Omega)}^2 &= \langle \nabla \boldsymbol{\eta}_h, \nabla \boldsymbol{\eta}_h \rangle_{\Omega} = \sum_{\mathbf{z}, \mathbf{y} \in \mathcal{N}_h} K_{\mathbf{zy}} \boldsymbol{\eta}_h(\mathbf{z}) \cdot \boldsymbol{\eta}_h(\mathbf{y}) \stackrel{(3.26)}{=} \sum_{\mathbf{z}, \mathbf{y} \in \mathcal{N}_h} K_{\mathbf{zy}} \boldsymbol{\eta}_h(\mathbf{z}) \cdot (\boldsymbol{\eta}_h(\mathbf{y}) - \boldsymbol{\eta}_h(\mathbf{z})) \\ &= \frac{1}{2} \sum_{\mathbf{z}, \mathbf{y} \in \mathcal{N}_h} K_{\mathbf{zy}} \boldsymbol{\eta}_h(\mathbf{z}) \cdot (\boldsymbol{\eta}_h(\mathbf{y}) - \boldsymbol{\eta}_h(\mathbf{z})) + \frac{1}{2} \sum_{\mathbf{z}, \mathbf{y} \in \mathcal{N}_h} K_{\mathbf{zy}} \boldsymbol{\eta}_h(\mathbf{y}) \cdot (\boldsymbol{\eta}_h(\mathbf{z}) - \boldsymbol{\eta}_h(\mathbf{y})) \\ &= -\frac{1}{2} \sum_{\mathbf{z}, \mathbf{y} \in \mathcal{N}_h} K_{\mathbf{zy}} |\boldsymbol{\eta}_h(\mathbf{z}) - \boldsymbol{\eta}_h(\mathbf{y})|^2. \end{aligned}$$

For any $\phi_h \in \mathcal{U}_h$, from the angle condition (3.16) and (3.22), it follows that

$$\begin{aligned} \|\nabla \mathcal{I}_h[\phi_h/|\phi_h|]\|_{L^2(\Omega)}^2 &= -\frac{1}{2} \sum_{\mathbf{z}, \mathbf{y} \in \mathcal{N}_h} K_{\mathbf{zy}} \left| \frac{\phi_h(\mathbf{z})}{|\phi_h(\mathbf{z})|} - \frac{\phi_h(\mathbf{y})}{|\phi_h(\mathbf{y})|} \right|^2 \\ &\leq -\frac{1}{2} \sum_{\mathbf{z}, \mathbf{y} \in \mathcal{N}_h} K_{\mathbf{zy}} |\phi_h(\mathbf{z}) - \phi_h(\mathbf{y})|^2 = \|\nabla \phi_h\|_{L^2(\Omega)}^2, \end{aligned}$$

which yields the desired result. \square

The result is sharp, in the sense that if the triangulation is not weakly acute, then there exists a discrete function for which the nodewise normalization increases the Dirichlet energy; see [33, Example 3.4] or [36, Proposition 7.3] for a two-dimensional counterexample.

The acute type condition is also a key ingredient for establishing the validity of a discrete maximum principle for finite element discretizations of second order elliptic PDEs. The first result in this direction for a scalar-valued linear equation in the two-dimensional case was proved in [70]. The result was extended to the three-dimensional case in [138] and then improved in [133]. Discrete maximum principles for nonlinear problems and generalizations for vector-valued problems were considered in [122] and [81], respectively.

A differentiable function $\phi : \Omega \rightarrow \mathbb{R}^3$ such that $|\phi| = 1$ in Ω satisfies the orthogonality property

$$\partial_i \phi \cdot \phi = 0 \quad \text{for all } 1 \leq i \leq 3.$$

This easily follows by taking the derivative of the pointwise constraint $|\phi|^2 = 1$

$$\partial_i |\phi|^2 = 2\partial_i \phi \cdot \phi = 0 \quad \text{for all } 1 \leq i \leq 3.$$

To mimic this property at a discrete level, as we did for the pointwise constraint, we require this orthogonality to be satisfied only at the nodes of the triangulation. For $\phi_h \in \mathcal{S}^1(\mathcal{T}_h)^3$, we therefore introduce the linear space

$$\mathcal{K}_{\phi_h} := \{\psi_h \in \mathcal{S}^1(\mathcal{T}_h)^3 : \phi_h(z) \cdot \psi_h(z) = 0 \text{ for all } z \in \mathcal{N}_h\}, \quad (3.27)$$

which we call the *discrete tangent space* of ϕ_h .

We conclude this section with an auxiliary result which provides a bound for the H^2 -seminorm of the vector product of a discrete function and a smooth function.

Lemma 3.4.12. *Let $\{\mathcal{T}_h\}_{h>0}$ be a family of regular triangulations of Ω . For all $\phi_h \in \mathcal{S}^1(\mathcal{T}_h)^3$ and $\varphi \in C^\infty(\bar{\Omega})$, it holds that*

$$\sum_{K \in \mathcal{T}_h} |\phi_h \times \varphi|_{\mathbf{H}^2(K)}^2 \leq C \|\phi_h\|_{\mathbf{H}^1(\Omega)}^2 \|\varphi\|_{\mathbf{W}^{2,\infty}(\Omega)}^2, \quad (3.28)$$

where the constant $C > 0$ is generic and, in particular, independent of h .

Proof. Let $\phi_h \in \mathcal{S}^1(\mathcal{T}_h)^3$ and $\varphi \in C^\infty(\bar{\Omega})$. We prove the estimate for every element $K \in \mathcal{T}_h$, which implies (3.28) by summation. Since $\phi_h|_K$ is a linear polynomial, it holds that $\partial_\alpha \phi_h = \mathbf{0}$ for all $|\alpha| > 1$. It follows that

$$\begin{aligned} |\phi_h \times \varphi|_{\mathbf{H}^2(K)}^2 &= \sum_{|\alpha|=2} \|\partial_\alpha(\phi_h \times \varphi)\|_{L^2(K)}^2 = \sum_{1 \leq i \leq j \leq 3} \|\partial_i \partial_j(\phi_h \times \varphi)\|_{L^2(K)}^2 \\ &= \sum_{1 \leq i \leq j \leq 3} \|\partial_j \phi_h \times \partial_i \varphi + \partial_i \phi_h \times \partial_j \varphi + \phi_h \times \partial_i \partial_j \varphi\|_{L^2(K)}^2 \\ &\lesssim \|\phi_h\|_{\mathbf{H}^1(K)}^2 \|\nabla \varphi\|_{\mathbf{W}^{1,\infty}(K)}^2. \end{aligned}$$

This establishes (3.28). □

Chapter 4

Tangent plane integrators

In this chapter, we introduce and analyze two variants of the tangent plane scheme for the numerical approximation of the LLG equation. We show that the methods are (unconditionally) convergent towards a weak solution of the problem. Throughout this chapter, we use the standard notation for Lebesgue/Sobolev/Bochner spaces and norms; see Section 3.2.

4.1 Model problem

Let $\Omega \subset \mathbb{R}^3$ be a bounded Lipschitz domain with polyhedral boundary $\Gamma := \partial\Omega$. Let $T > 0$ be some finite time. We denote the space-time cylinder by $\Omega_T := \Omega \times (0, T)$ and define $\Gamma_T := \Gamma \times (0, T)$. Moreover, we use the notation $\langle \cdot, \cdot \rangle := \langle \cdot, \cdot \rangle_\Omega$ to denote the scalar product in $L^2(\Omega)$ (resp. $\mathbf{L}^2(\Omega)$). This does not lead to ambiguities, since Ω is the unique domain considered throughout the chapter.

We consider the initial boundary value problem

$$\partial_t \mathbf{m} = -\mathbf{m} \times [\mathbf{h}_{\text{eff}}(\mathbf{m}, \mathbf{f}) + \mathbf{\Pi}(\mathbf{m})] + \alpha \mathbf{m} \times \partial_t \mathbf{m} \quad \text{in } \Omega_T, \quad (4.1a)$$

$$\partial_n \mathbf{m} = \mathbf{0} \quad \text{on } \Gamma_T, \quad (4.1b)$$

$$\mathbf{m}(0) = \mathbf{m}^0 \quad \text{in } \Omega. \quad (4.1c)$$

In (4.1a), which is the Gilbert form (3.4) of the nondimensional LLG equation, $\alpha > 0$ is constant and the effective field takes the form

$$\mathbf{h}_{\text{eff}}(\mathbf{m}, \mathbf{f}) = \lambda_{\text{ex}}^2 \Delta \mathbf{m} + \boldsymbol{\pi}(\mathbf{m}) + \mathbf{f}, \quad (4.2)$$

where $\lambda_{\text{ex}} > 0$ is constant, while $\boldsymbol{\pi}(\mathbf{m})$ and \mathbf{f} denote the general \mathbf{m} -dependent and \mathbf{m} -independent effective field contributions, respectively. We assume that $\boldsymbol{\pi} : \mathbf{L}^2(\Omega) \rightarrow \mathbf{L}^2(\Omega)$ is a bounded, linear, and self-adjoint operator, while \mathbf{f} belongs to $H^1(0, T; \mathbf{L}^2(\Omega))$. Under these assumptions, the effective field satisfies

$$\mathbf{h}_{\text{eff}}(\mathbf{m}, \mathbf{f}) = -\frac{\delta \mathcal{E}(\mathbf{m}, \mathbf{f})}{\delta \mathbf{m}}$$

for the energy functional

$$\mathcal{E}(\mathbf{m}, \mathbf{f}) = \frac{\lambda_{\text{ex}}^2}{2} \|\nabla \mathbf{m}\|_{\mathbf{L}^2(\Omega)}^2 - \frac{1}{2} \langle \boldsymbol{\pi}(\mathbf{m}), \mathbf{m} \rangle - \langle \mathbf{f}, \mathbf{m} \rangle. \quad (4.3)$$

We assume $\mathbf{\Pi} : \{\mathbf{m} \in \mathbf{H}^1(\Omega) : |\mathbf{m}| = 1 \text{ a.e. in } \Omega\} \rightarrow \mathbf{L}^2(\Omega)$ to be a bounded operator. For the initial condition in (4.1c), we assume that $\mathbf{m}^0 \in \mathbf{H}^1(\Omega)$ satisfies $|\mathbf{m}^0| = 1$ a.e. in Ω . In the following definition, we introduce the notion of a weak solution of (4.1).

Definition 4.1.1 (weak solution). *A function $\mathbf{m} : \Omega_T \rightarrow \mathbb{R}^3$ is called a weak solution of (4.1) if the following properties (i)–(iv) are satisfied:*

- (i) $\mathbf{m} \in L^\infty(0, T; \mathbf{H}^1(\Omega)) \cap H^1(0, T; \mathbf{L}^2(\Omega))$ and $|\mathbf{m}| = 1$ a.e. in Ω_T ,
- (ii) $\mathbf{m}(0) = \mathbf{m}^0$ in the sense of traces,
- (iii) for all $\boldsymbol{\varphi} \in \mathbf{H}^1(\Omega_T)$, it holds that

$$\begin{aligned}
& \int_0^T \langle \partial_t \mathbf{m}(t), \boldsymbol{\varphi}(t) \rangle dt - \alpha \int_0^T \langle \mathbf{m}(t) \times \partial_t \mathbf{m}(t), \boldsymbol{\varphi}(t) \rangle dt \\
&= \lambda_{\text{ex}}^2 \int_0^T \langle \mathbf{m}(t) \times \nabla \mathbf{m}(t), \nabla \boldsymbol{\varphi}(t) \rangle dt - \int_0^T \langle \mathbf{m}(t) \times \boldsymbol{\pi}(\mathbf{m}(t)), \boldsymbol{\varphi}(t) \rangle dt \\
&\quad - \int_0^T \langle \mathbf{m}(t) \times \mathbf{f}(t), \boldsymbol{\varphi}(t) \rangle dt - \int_0^T \langle \mathbf{m}(t) \times \boldsymbol{\Pi}(\mathbf{m}(t)), \boldsymbol{\varphi}(t) \rangle dt,
\end{aligned} \tag{4.4}$$

- (iv) \mathbf{m} satisfies the energy inequality

$$\begin{aligned}
& \mathcal{E}(\mathbf{m}(\tau), \mathbf{f}(\tau)) + \alpha \int_0^\tau \|\partial_t \mathbf{m}(t)\|_{\mathbf{L}^2(\Omega)}^2 dt + \int_0^\tau \langle \partial_t \mathbf{f}(t), \mathbf{m}(t) \rangle dt \\
& \leq \mathcal{E}(\mathbf{m}^0, \mathbf{f}(0)) + \int_0^\tau \langle \boldsymbol{\Pi}(\mathbf{m}(t)), \partial_t \mathbf{m}(t) \rangle dt
\end{aligned} \tag{4.5}$$

for a.e. $\tau \in (0, T)$.

Definition 4.1.1 extends [17, Definition 1.2], introduced by F. ALOUGES and A. SOYEUR to define the notion of a weak solution for the case in which the effective field comprises only the exchange contribution. After possibly being redefined on a set of measure zero, any solution \mathbf{m} in the sense of Definition 4.1.1 belongs to $C^0([0, T]; \mathbf{L}^2(\Omega))$; see [88, Section 5.9.2, Theorem 2]. For functions in $\mathbf{H}^1(\Omega_T)$, the time evaluation can be defined by density as the limit of the time evaluation for smooth functions. In this sense, for all $t \in [0, T]$, it holds that $\mathbf{m}(t) \in \mathbf{H}^{1/2}(\Omega)$. This concept is implied behind the expression ‘in the sense of traces’ in part (ii) of Definition 4.1.1. The variational formulation (4.4) comes from a weak formulation of (4.1a) in the space-time domain. The boundary conditions (4.1b) are enforced in the variational formulation (4.4) as natural boundary conditions. In particular, using (4.1b), the boundary term, which arises from integrating by parts the exchange contribution, vanishes. The energy inequality (4.5) is a weak counterpart of the energy law (3.3) for (4.1). In (4.4)–(4.5), by $\boldsymbol{\pi}(\mathbf{m})$ and $\boldsymbol{\Pi}(\mathbf{m})$ we mean the functions defined by $t \mapsto \boldsymbol{\pi}(\mathbf{m}(t))$ and $t \mapsto \boldsymbol{\Pi}(\mathbf{m}(t))$ for all $t \in (0, T)$. From the regularity of \mathbf{m} required by the definition and the stability of $\boldsymbol{\pi}$ and $\boldsymbol{\Pi}$, it follows that both $\boldsymbol{\pi}(\mathbf{m})$ and $\boldsymbol{\Pi}(\mathbf{m})$ belong to $\mathbf{L}^2(\Omega_T)$, so that all the integrals involving these functions in (4.4)–(4.5) are well defined.

This abstract framework covers most of the physics introduced in Chapter 2. The first term of the effective field (4.2), which corresponds to the first term of the energy (4.3), clearly refers to the exchange contribution. If the general \mathbf{m} -dependent field contribution comprises, e.g., uniaxial anisotropy and stray field, the corresponding operator takes the form

$$\boldsymbol{\pi}(\mathbf{m}) = q^2(\mathbf{a} \cdot \mathbf{m})\mathbf{a} + \mathbf{h}_s(\mathbf{m}),$$

where $q > 0$ is constant, $\mathbf{a} \in \mathbb{S}^2$ denotes the easy axis, and \mathbf{h}_s is the stray field. In this case, $\boldsymbol{\pi}$ is a linear, bounded and self-adjoint operator $\mathbf{L}^2(\Omega) \rightarrow \mathbf{L}^2(\Omega)$. The \mathbf{m} -independent effective field contribution \mathbf{f} includes the applied external field \mathbf{h}_{ext} and the Oersted field \mathbf{h}_c generated by a given electric current density. Only the Dzyaloshinskii–Moriya interaction and the magnetoelastic contribution cannot be included into this setting; see Remark 4.1.2. The operator $\boldsymbol{\Pi}$ takes the possible presence of nonenergetic (i.e., not belonging to the effective field) torque terms into account. This is the case, for instance, for the spintronic extensions of the LLG equation presented in Section 2.3, for which the application of the present framework will be discussed in details in Chapter 5.

Remark 4.1.2. The magnetoelastic contribution of the effective field takes the form

$$\mathbf{h}_{\text{eff,el}} = 2(\boldsymbol{\lambda}\boldsymbol{\sigma})\mathbf{m},$$

where $\boldsymbol{\lambda} \in \mathbf{L}^\infty(\Omega)$ is a 4th order tensor, while $\boldsymbol{\sigma} \in \mathbf{L}^2(\Omega)$ is the weak solution of the boundary value problem

$$\begin{aligned} \nabla \cdot \boldsymbol{\sigma} + \mathbf{f} &= \mathbf{0} & \text{in } \Omega, \\ C[\boldsymbol{\varepsilon}(\mathbf{u}) - \boldsymbol{\varepsilon}_m(\mathbf{m})] &= \boldsymbol{\sigma} & \text{in } \Omega, \\ \mathbf{u} &= \mathbf{0} & \text{on } \Gamma_D, \\ \boldsymbol{\sigma}\mathbf{n} &= \mathbf{t} & \text{on } \Gamma_N; \end{aligned}$$

see page 16 for the definition of all involved quantities. Clearly, the mapping $\boldsymbol{\pi} : \mathbf{m} \mapsto 2(\boldsymbol{\lambda}\boldsymbol{\sigma})\mathbf{m}$ is not a linear, bounded, and self-adjoint operator $\mathbf{L}^2(\Omega) \rightarrow \mathbf{L}^2(\Omega)$. In particular, $\boldsymbol{\pi}(\mathbf{m})$ belongs to $\mathbf{L}^2(\Omega)$ only if $\mathbf{m} \in \mathbf{L}^\infty(\Omega)$.

In the presence of the Dzyaloshinskii–Moriya interaction, i.e., when the effective field also comprises the term

$$\mathbf{h}_{\text{eff,DM}} = -\lambda_{\text{DM}}\nabla \times \mathbf{m},$$

the homogeneous Neumann boundary conditions (4.1b), which are appropriate whenever the unique component of the effective field involving magnetization derivatives is the exchange contribution, must be replaced by

$$2\lambda_{\text{ex}}^2\partial_{\mathbf{n}}\mathbf{m} + \lambda_{\text{DM}}\mathbf{m} \times \mathbf{n} = \mathbf{0}.$$

This clearly affects the variational formulation (4.4). The analysis of the algorithm introduced in the next section for this situation is currently being investigated, and we refer the interested reader to a forthcoming publication [116].

4.2 Numerical algorithm

In this section, we introduce a numerical method for the approximation of the abstract problem discussed in Section 4.1. The starting point is the alternative form of the LLG equation (3.5), which in this case takes the form

$$\alpha\partial_t\mathbf{m} + \mathbf{m} \times \partial_t\mathbf{m} = \mathbf{h}_{\text{eff}}(\mathbf{m}, \mathbf{f}) + \boldsymbol{\Pi}(\mathbf{m}) - [\mathbf{h}_{\text{eff}}(\mathbf{m}, \mathbf{f}) \cdot \mathbf{m} + \boldsymbol{\Pi}(\mathbf{m}) \cdot \mathbf{m}]\mathbf{m}. \quad (4.6)$$

We recall that, under the constraint $|\mathbf{m}| = 1$, this formulation is equivalent to the Landau–Lifshitz form and to the Gilbert form; see Proposition 3.1.1.

Since (4.6) is linear with respect to the time derivative $\partial_t\mathbf{m}$, we introduce the free variable $\mathbf{v} = \partial_t\mathbf{m}$

$$\alpha\mathbf{v} + \mathbf{m} \times \mathbf{v} = \mathbf{h}_{\text{eff}}(\mathbf{m}, \mathbf{f}) + \boldsymbol{\Pi}(\mathbf{m}) - [\mathbf{h}_{\text{eff}}(\mathbf{m}, \mathbf{f}) \cdot \mathbf{m} + \boldsymbol{\Pi}(\mathbf{m}) \cdot \mathbf{m}]\mathbf{m}. \quad (4.7)$$

From the equality $|\mathbf{m}|^2 = 1$, we deduce the orthogonality $\mathbf{m} \cdot \mathbf{v} = 0$. Hence, for each $t \in (0, T)$, $\mathbf{v}(t) \in \mathbb{R}^3$ belongs to the tangent space of the sphere at $\mathbf{m}(t)$. Taking this orthogonality as well as the expression (4.2) of the effective field into account, we obtain the following variational formulation of (4.7): Find $\mathbf{v}(t) \in \mathbf{L}^2(\Omega)$ with $\mathbf{m}(t) \cdot \mathbf{v}(t) = 0$ a.e. in Ω such that

$$\alpha\langle \mathbf{v}(t), \boldsymbol{\phi} \rangle + \langle \mathbf{m}(t) \times \mathbf{v}(t), \boldsymbol{\phi} \rangle = -\lambda_{\text{ex}}^2\langle \nabla\mathbf{m}(t), \nabla\boldsymbol{\phi} \rangle + \langle \boldsymbol{\pi}(\mathbf{m}(t)), \boldsymbol{\phi} \rangle + \langle \mathbf{f}, \boldsymbol{\phi} \rangle + \langle \boldsymbol{\Pi}(\mathbf{m}(t)), \boldsymbol{\phi} \rangle \quad (4.8)$$

for all $\boldsymbol{\phi} \in \mathbf{H}^1(\Omega)$ satisfying $\mathbf{m}(t) \cdot \boldsymbol{\phi} = 0$ a.e. in Ω . Note that in (4.8) the boundary integral which arises from integrating by parts the exchange contribution vanishes thanks to the boundary conditions (4.1b). Moreover, since the test function $\boldsymbol{\phi}$ belongs to the tangent space of the sphere at $\mathbf{m}(t)$, in (4.8) the term corresponding to the last (strongly nonlinear in \mathbf{m}) term on the right-hand side of (4.7) also vanishes.

For the time discretization, given an integer $M > 0$, we consider a uniform partition of the time interval $(0, T)$ with time-step size $k = T/M$, i.e., $t_i = ik$ for all $0 \leq i \leq M$; see Section 3.3. For the spatial discretization, we consider a γ -quasi-uniform family $\{\mathcal{T}_h\}_{h>0}$ of regular tetrahedral triangulations of Ω ; see Section 3.4.

For each time-step $0 \leq i \leq M-1$, the structure of the numerical scheme is the following: First of all, given an approximation $\mathbf{m}_h^i \in \mathcal{S}^1(\mathcal{T}_h)^3$ of $\mathbf{m}(t_i)$, we compute $\mathbf{v}_h^i \approx \mathbf{v}(t_i)$ from a finite element discretization of (4.8) based on the discrete tangent space introduced in (3.27), i.e.,

$$\mathcal{K}_{\mathbf{m}_h^i} := \{\psi_h \in \mathcal{S}^1(\mathcal{T}_h)^3 : \mathbf{m}_h^i(z) \cdot \psi_h(z) = 0 \text{ for all } z \in \mathcal{N}_h\}.$$

We obtain the following variational problem: Find $\mathbf{v}_h^i \in \mathcal{K}_{\mathbf{m}_h^i}$ such that

$$\begin{aligned} & \alpha \langle \mathbf{v}_h^i, \phi_h \rangle + \langle \mathbf{m}_h^i \times \mathbf{v}_h^i, \phi_h \rangle + \lambda_{\text{ex}}^2 \theta k \langle \nabla \mathbf{v}_h^i, \nabla \phi_h \rangle \\ & = -\lambda_{\text{ex}}^2 \langle \nabla \mathbf{m}_h^i, \nabla \phi_h \rangle + \langle \pi_h(\mathbf{m}_h^i), \phi_h \rangle + \langle \mathbf{f}_h^i, \phi_h \rangle + \langle \Pi_h(\mathbf{m}_h^i), \phi_h \rangle \end{aligned}$$

for all $\phi_h \in \mathcal{K}_{\mathbf{m}_h^i}$. Here, the operators $\pi_h : \mathcal{S}^1(\mathcal{T}_h)^3 \rightarrow \mathbf{L}^2(\Omega)$ and $\Pi_h : \mathcal{S}^1(\mathcal{T}_h)^3 \rightarrow \mathbf{L}^2(\Omega)$ denote discretized versions of π and Π , respectively, while, for all $0 \leq i \leq M-1$, $\mathbf{f}_h^i \in \mathbf{L}^2(\Omega)$ denotes an approximation of $\mathbf{f}(t_i)$. The parameter $0 \leq \theta \leq 1$ modulates the ‘degree of implicitness’ of the method in the treatment of the leading-order term of the effective field (which is the second-order exchange contribution).

The computed $\mathbf{v}_h^i \in \mathcal{K}_{\mathbf{m}_h^i}$ is then used to update the current magnetization $\mathbf{m}_h^i \approx \mathbf{m}(t_i)$ to the new value $\mathbf{m}_h^{i+1} \approx \mathbf{m}(t_{i+1})$ via a 1st order time-stepping. A simple choice is given by the classical linear time-stepping

$$\mathbf{m}_h^{i+1} = \mathbf{m}_h^i + k \mathbf{v}_h^i.$$

In this case, the pointwise constraint $|\mathbf{m}| = 1$ which characterizes the solution of the LLG equation is ignored by the numerical scheme. To have a numerical realization of it, the nodal projection mapping $\phi_h \mapsto \mathcal{I}_h(\phi_h/|\phi_h|)$ can be applied. The resulting time-stepping is then given by

$$\mathbf{m}_h^{i+1} = \mathcal{I}_h \left[\frac{\mathbf{m}_h^i + k \mathbf{v}_h^i}{|\mathbf{m}_h^i + k \mathbf{v}_h^i|} \right].$$

With this choice, for every $0 \leq i \leq M-1$, \mathbf{m}_h^{i+1} belongs to the set \mathcal{M}_h of the discrete functions which satisfy the pointwise constraint at the nodes of the triangulation introduced in (3.20), i.e.,

$$\mathcal{M}_h := \{\phi_h \in \mathcal{S}^1(\mathcal{T}_h)^3 : |\phi_h(z)| = 1 \text{ for all } z \in \mathcal{N}_h\}.$$

We refer to the method which includes the nodal projection as *standard tangent plane scheme (TPS)*. We refer to the method in which the nodal projection is omitted as *projection-free tangent plane scheme (PFTPS)*.

We recall the definition of the set

$$\mathcal{U}_h := \{\phi_h \in \mathcal{S}^1(\mathcal{T}_h)^3 : |\phi_h(z)| \geq 1 \text{ for all } z \in \mathcal{N}_h\} \supset \mathcal{M}_h,$$

which is the domain of the nodal projection mapping, and summarize the proposed numerical schemes in the following algorithm.

Algorithm 4.2.1 (tangent plane scheme). *Input:* Either $\mathbf{m}_h^0 \in \mathcal{M}_h$ (TPS) or $\mathbf{m}_h^0 \in \mathcal{U}_h$ (PFTPS). *Loop:* For all $0 \leq i \leq M-1$, iterate:

- (i) Compute $\pi_h(\mathbf{m}_h^i) \in \mathbf{L}^2(\Omega)$ and $\Pi_h(\mathbf{m}_h^i) \in \mathbf{L}^2(\Omega)$,
- (ii) Compute $\mathbf{v}_h^i \in \mathcal{K}_{\mathbf{m}_h^i}$ such that

$$\begin{aligned} & \alpha \langle \mathbf{v}_h^i, \phi_h \rangle + \langle \mathbf{m}_h^i \times \mathbf{v}_h^i, \phi_h \rangle + \lambda_{\text{ex}}^2 \theta k \langle \nabla \mathbf{v}_h^i, \nabla \phi_h \rangle \\ & = -\lambda_{\text{ex}}^2 \langle \nabla \mathbf{m}_h^i, \nabla \phi_h \rangle + \langle \pi_h(\mathbf{m}_h^i), \phi_h \rangle + \langle \mathbf{f}_h^i, \phi_h \rangle + \langle \Pi_h(\mathbf{m}_h^i), \phi_h \rangle \end{aligned} \tag{4.9}$$

for all $\phi_h \in \mathcal{K}_{\mathbf{m}_h^i}$,

(iii) Either define $\mathbf{m}_h^{i+1} \in \mathcal{U}_h$ by

$$\mathbf{m}_h^{i+1} = \mathbf{m}_h^i + k\mathbf{v}_h^i \quad (\text{PFTPS}) \quad (4.10a)$$

or define $\mathbf{m}_h^{i+1} \in \mathcal{M}_h$ by

$$\mathbf{m}_h^{i+1} = \mathcal{I}_h \left[\frac{\mathbf{m}_h^i + k\mathbf{v}_h^i}{|\mathbf{m}_h^i + k\mathbf{v}_h^i|} \right] \quad (\text{TPS}). \quad (4.10b)$$

Output: Sequence of discrete functions $\{(\mathbf{v}_h^i, \mathbf{m}_h^{i+1})\}_{0 \leq i \leq M-1}$.

In Algorithm 4.2.1, in the same spirit as [56] and unlike [16], the numerical approximation of the lower-order effective field contributions and the additional torque term is considered. Indeed, step (i) can include the solution of a nonlocal problem, e.g., the computation of the stray field for a given configuration of the magnetization. In the case of the standard tangent plane scheme, omitting both the lower-order effective field terms and the additional nonenergetic torque term, and choosing $\theta = 0$, we recover the explicit method of [14]. The idea of removing the nodal projection from the tangent plane scheme goes back to [6] for the LLG equation and has been inspired by [37], where the same principle is applied to a certain class of geometrically constrained partial differential equations, e.g., the harmonic map heat flow.

In Algorithm 4.2.1, the approach for the treatment of the leading-order effective field contribution, introduced in [12], is similar to the classical θ -method for the heat equation: The choice $\theta = 0$ produces an explicit version of the scheme, the choice $\theta = 1/2$ yields a Crank-Nicolson-type scheme, while for $\theta = 1$ we obtain a kind of fully implicit version of the scheme. In analogy with the corresponding result for the heat equation, one may conjecture that the method is unconditionally stable for $\theta > 1/2$, but requires a stability condition, usually referred to as *CFL condition* (Courant–Friedrichs–Lewy condition, named after the mathematicians R. COURANT, K. FRIEDRICHS, and H. LEWY), for $\theta < 1/2$. We will indeed prove a result of that kind in the next section; see Theorem 4.3.2. Note that this approach concerns only the exchange contribution of the effective field, but does not affect the other terms, which are treated explicitly.

Both versions of the scheme are formally 1st order methods in time. In order to show this, for a sufficiently smooth solution and $0 \leq i \leq M-1$, let $\mathbf{m}^i = \mathbf{m}(t_i)$ and $\mathbf{v}^i = \mathbf{v}(t_i) = \partial_t \mathbf{m}(t_i)$. In the case of the projection-free version of the method, the Taylor theorem directly shows

$$|\mathbf{m}^{i+1} - \mathbf{m}^i - k\mathbf{v}^i| = \mathcal{O}(k^2) \quad \text{as } k \rightarrow 0. \quad (4.11)$$

In the case of the standard version of the method, it holds that

$$\mathbf{m}^{i+1} - \frac{\mathbf{m}^i + k\mathbf{v}^i}{|\mathbf{m}^i + k\mathbf{v}^i|} = \mathbf{m}^i + k\mathbf{v}^i + \mathcal{O}(k^2) - \frac{\mathbf{m}^i + k\mathbf{v}^i}{|\mathbf{m}^i + k\mathbf{v}^i|} = (\mathbf{m}^i + k\mathbf{v}^i) \left(1 - \frac{1}{|\mathbf{m}^i + k\mathbf{v}^i|} \right) + \mathcal{O}(k^2).$$

Since $|\mathbf{m}^i| = 1$ and $\mathbf{m}^i \cdot \mathbf{v}^i = 0$, we deduce that

$$|\mathbf{m}^i + k\mathbf{v}^i|^2 = |\mathbf{m}^i|^2 + 2\mathbf{m}^i \cdot \mathbf{v}^i + k^2 |\mathbf{v}^i|^2 = 1 + k^2 |\mathbf{v}^i|^2.$$

The Taylor expansion

$$\frac{1}{\sqrt{1+x}} = 1 - \frac{x}{2} + \mathcal{O}(x^2) \quad \text{as } x \rightarrow 0$$

then reveals

$$\frac{1}{|\mathbf{m}^i + k\mathbf{v}^i|} = 1 - \frac{1}{2}k^2 |\mathbf{v}^i|^2 + \mathcal{O}(k^4) \quad \text{as } k \rightarrow 0.$$

Altogether, we thus obtain

$$\left| \mathbf{m}^{i+1} - \frac{\mathbf{m}^i + k\mathbf{v}^i}{|\mathbf{m}^i + k\mathbf{v}^i|} \right| = \left| (\mathbf{m}^i + k\mathbf{v}^i) \left(\frac{k^2}{2} |\mathbf{v}^i|^2 + \mathcal{O}(k^4) \right) + \mathcal{O}(k^2) \right| = \mathcal{O}(k^2) \quad \text{as } k \rightarrow 0. \quad (4.12)$$

Strategies to improve the convergence order in time of the standard tangent plane scheme are based on similar Taylor expansions and have been proposed in [16, 15].

The following proposition states that Algorithm 4.2.1 is well posed.

Proposition 4.2.2. *For all $0 \leq i \leq M-1$, there exists a unique solution $\mathbf{v}_h^i \in \mathcal{K}_{\mathbf{m}_h^i}$ of (4.9). Moreover, the time-stepping (4.10) is well defined.*

Proof. Let $0 \leq i \leq M-1$. Consider the bilinear form $a(\mathbf{m}_h^i; \cdot, \cdot) : \mathcal{S}^1(\mathcal{T}_h)^3 \times \mathcal{S}^1(\mathcal{T}_h)^3 \rightarrow \mathbb{R}$ defined by

$$a(\mathbf{m}_h^i; \boldsymbol{\eta}_h, \boldsymbol{\phi}_h) := \alpha \langle \boldsymbol{\eta}_h, \boldsymbol{\phi}_h \rangle + \langle \mathbf{m}_h^i \times \boldsymbol{\eta}_h, \boldsymbol{\phi}_h \rangle + \lambda_{\text{ex}}^2 \theta k \langle \nabla \boldsymbol{\eta}_h, \nabla \boldsymbol{\phi}_h \rangle$$

for all $\boldsymbol{\eta}_h, \boldsymbol{\phi}_h \in \mathcal{S}^1(\mathcal{T}_h)^3$, and the linear functional $F(\mathbf{m}_h^i; \cdot) : \mathcal{S}^1(\mathcal{T}_h)^3 \rightarrow \mathbb{R}$ defined by

$$F(\mathbf{m}_h^i; \boldsymbol{\phi}_h) := -\lambda_{\text{ex}}^2 \langle \nabla \mathbf{m}_h^i, \nabla \boldsymbol{\phi}_h \rangle + \langle \boldsymbol{\pi}_h(\mathbf{m}_h^i), \boldsymbol{\phi}_h \rangle + \langle \mathbf{f}_h^i, \boldsymbol{\phi}_h \rangle + \langle \boldsymbol{\Pi}_h(\mathbf{m}_h^i), \boldsymbol{\phi}_h \rangle$$

for all $\boldsymbol{\phi}_h \in \mathcal{S}^1(\mathcal{T}_h)^3$. Then, we can rewrite step (ii) of the algorithm as: Find $\mathbf{v}_h^i \in \mathcal{K}_{\mathbf{m}_h^i}$ such that

$$a(\mathbf{m}_h^i; \mathbf{v}_h^i, \boldsymbol{\phi}_h) = F(\mathbf{m}_h^i; \boldsymbol{\phi}_h) \quad \text{for all } \boldsymbol{\phi}_h \in \mathcal{K}_{\mathbf{m}_h^i}.$$

Since it holds that

$$a(\mathbf{m}_h^i; \boldsymbol{\phi}_h, \boldsymbol{\phi}_h) = \alpha \|\boldsymbol{\phi}_h\|_{L^2(\Omega)}^2 + \lambda_{\text{ex}}^2 \theta k \|\nabla \boldsymbol{\phi}_h\|_{L^2(\Omega)}^2 \quad \text{for all } \boldsymbol{\phi}_h \in \mathcal{S}^1(\mathcal{T}_h)^3,$$

the bilinear form is elliptic (even in the full space $\mathcal{S}^1(\mathcal{T}_h)^3$). Existence and uniqueness of the solution $\mathbf{v}_h^i \in \mathcal{K}_{\mathbf{m}_h^i}$ to (4.9) thus follows from the Lax–Milgram theorem. It remains to show that the time-stepping (4.10) is always well defined. This is straightforward for the projection-free time stepping (4.10a). If the algorithm includes the nodal projection, it holds that $\mathbf{m}_h^i \in \mathcal{M}_h$. Since $\mathbf{v}_h \in \mathcal{K}_{\mathbf{m}_h^i}$, it follows that

$$|\mathbf{m}_h^i(\mathbf{z}) + k\mathbf{v}_h^i(\mathbf{z})|^2 = |\mathbf{m}_h^i(\mathbf{z})|^2 + k^2 |\mathbf{v}_h^i(\mathbf{z})|^2 = 1 + k^2 |\mathbf{v}_h^i(\mathbf{z})|^2 \geq 1,$$

i.e., $\mathbf{m}_h^i + k\mathbf{v}_h^i \in \mathcal{U}_h$. The projection step (4.10b) is therefore also well defined. \square

4.3 Convergence analysis

From Algorithm 4.2.1 we obtain two sequences of discrete functions $\{\mathbf{m}_h^i\}_{0 \leq i \leq M}$ and $\{\mathbf{v}_h^i\}_{0 \leq i \leq M-1}$, which can be used to define the piecewise linear and piecewise constant time reconstructions from (3.13). In particular, we consider the functions defined, for all $t \in [t_i, t_{i+1})$ and $0 \leq i \leq M-1$, by

$$\mathbf{m}_{hk}(t) := \frac{t - t_i}{k} \mathbf{m}_h^{i+1} + \frac{t_{i+1} - t}{k} \mathbf{m}_h^i, \quad \mathbf{m}_{hk}^-(t) := \mathbf{m}_h^i, \quad \mathbf{m}_{hk}^+(t) := \mathbf{m}_h^{i+1}, \quad \text{and} \quad \mathbf{v}_{hk}^-(t) := \mathbf{v}_h^i. \quad (4.13)$$

Similarly, we define the functions $\boldsymbol{\pi}_{hk}^-, \boldsymbol{\Pi}_{hk}^- : [0, T) \rightarrow \mathbf{L}^2(\Omega)$ by

$$\boldsymbol{\pi}_{hk}^-(t) := \boldsymbol{\pi}_h(\mathbf{m}_h^i), \quad \text{and} \quad \boldsymbol{\Pi}_{hk}^-(t) := \boldsymbol{\Pi}_h(\mathbf{m}_h^i), \quad (4.14)$$

for all $t \in [t_i, t_{i+1})$ and $0 \leq i \leq M-1$.

In the following assumption, we collect some of the requirements on the approximation of the initial condition \mathbf{m}_h^0 , on the discrete operators $\boldsymbol{\pi}_h$ and $\boldsymbol{\Pi}_h$, and on the sequence $\{\mathbf{f}_h^i\}_{0 \leq i \leq M-1}$.

Assumption 4.3.1. *The discrete initial condition \mathbf{m}_h^0 belongs to \mathcal{U}_h and satisfies the convergence property*

$$\mathbf{m}_h^0 \rightharpoonup \mathbf{m}^0 \quad \text{in } \mathbf{H}^1(\Omega) \quad \text{as } h \rightarrow 0. \quad (4.15)$$

For the standard tangent plane scheme, we additionally assume that $\mathbf{m}_h^0 \in \mathcal{M}_h$. The discrete operators $\boldsymbol{\pi}_h : \mathcal{U}_h \rightarrow \mathbf{L}^2(\Omega)$ and $\boldsymbol{\Pi}_h : \mathcal{U}_h \rightarrow \mathbf{L}^2(\Omega)$ are stable, in the sense that there exist two positive constants, C_π and C_Π , independent of h , such that

$$\|\boldsymbol{\pi}_h(\boldsymbol{\phi}_h)\|_{\mathbf{L}^2(\Omega)} \leq C_\pi \left(1 + \|\boldsymbol{\phi}_h\|_{\mathbf{H}^1(\Omega)}\right) \quad \text{for all } \boldsymbol{\phi}_h \in \mathcal{U}_h, \quad (4.16a)$$

$$\|\boldsymbol{\Pi}_h(\boldsymbol{\phi}_h)\|_{\mathbf{L}^2(\Omega)} \leq C_\Pi \left(1 + \|\boldsymbol{\phi}_h\|_{\mathbf{H}^1(\Omega)}\right) \quad \text{for all } \boldsymbol{\phi}_h \in \mathcal{U}_h. \quad (4.16b)$$

For the sequence $\{\mathbf{f}_h^i\}_{0 \leq i \leq M-1}$ in $\mathbf{L}^2(\Omega)$, we define the piecewise constant time reconstruction \mathbf{f}_{hk}^- by $\mathbf{f}_{hk}^-(t) := \mathbf{f}_h^i$ for all $t \in [t_i, t_{i+1})$ and $0 \leq i \leq M-1$, and assume that it satisfies the convergence property

$$\mathbf{f}_{hk}^- \rightharpoonup \mathbf{f} \quad \text{in } \mathbf{L}^2(\Omega_T) \quad \text{as } k, h \rightarrow 0. \quad (4.17)$$

Moreover, for the sake of simplicity, we assume that $\mathbf{f} \in C^1([0, T], \mathbf{L}^2(\Omega))$. In particular, the expressions $\mathbf{f}(t)$ and $\partial_t \mathbf{f}(t)$ are meaningful for all $t \in [0, T]$.

The following theorem, which is the main result of this chapter, states that the time reconstructions from (4.13) converge in an appropriate sense towards a weak solution of (4.1) as $k, h \rightarrow 0$.

Theorem 4.3.2. *Let $\{\mathcal{T}_h\}_{h>0}$ be a γ -quasi-uniform family of regular tetrahedral triangulations of Ω .*

(a) *Suppose that Assumption 4.3.1 is satisfied. For the standard tangent plane scheme, assume that*

- *either $1/2 < \theta \leq 1$ and any triangulation \mathcal{T}_h satisfies the angle condition (3.16),*
- *or $\theta = 1/2$, any triangulation \mathcal{T}_h satisfies the angle condition (3.16), and $k = o(h)$ as $k, h \rightarrow 0$,*
- *or $k = o(h^2)$ as $k, h \rightarrow 0$.*

For the projection-free tangent plane scheme, assume that

- *either $1/2 < \theta \leq 1$,*
- *or $\theta = 1/2$ and $k = o(h)$ as $k, h \rightarrow 0$,*
- *or $k = o(h^2)$ as $k, h \rightarrow 0$.*

Then, the sequences of discrete functions $\{\mathbf{m}_{hk}\}$ and $\{\mathbf{m}_{hk}^\pm\}$, constructed from the output of Algorithm 4.2.1 according to (4.13), admit subsequences (not relabeled) which converge towards a function \mathbf{m} satisfying the requirements (i)–(ii) of Definition 4.1.1. More precisely, it holds that $\mathbf{m}_{hk} \rightharpoonup \mathbf{m}$ in $\mathbf{H}^1(\Omega_T)$ and $\mathbf{m}_{hk}, \mathbf{m}_{hk}^\pm \overset{}{\rightharpoonup} \mathbf{m}$ in $L^\infty(0, T; \mathbf{H}^1(\Omega))$ as $k, h \rightarrow 0$.*

(b) *Under the assumptions of part (a), suppose that the discrete operators π_h and Π_h are consistent, in the sense that, given the convergent subsequences of part (a), the corresponding subsequences of discrete functions (4.14) satisfy*

$$\pi_{hk}^- \rightharpoonup \pi(\mathbf{m}) \quad \text{in } \mathbf{L}^2(\Omega_T) \quad \text{as } k, h \rightarrow 0, \quad (4.18a)$$

$$\Pi_{hk}^- \rightharpoonup \Pi(\mathbf{m}) \quad \text{in } \mathbf{L}^2(\Omega_T) \quad \text{as } k, h \rightarrow 0. \quad (4.18b)$$

Then, the limit function \mathbf{m} of part (a) satisfies also the requirement (iii) of Definition 4.1.1.

(c) *Under the assumption of part (b), assume that (4.15), (4.17) and (4.18) hold with strong convergence. In the case of the standard tangent plane scheme, assume the following additional L^4 -regularity on \mathbf{f} and π*

$$\mathbf{f} \in C^0([0, T], \mathbf{L}^4(\Omega)) \quad \text{and} \quad \|\pi(\phi)\|_{\mathbf{L}^4(\Omega)} \leq C \|\phi\|_{\mathbf{L}^4(\Omega)} \quad \text{for all } \phi \in \mathbf{L}^4(\Omega), \quad (4.19)$$

where $C > 0$ is constant. Then, the limit function \mathbf{m} from part (b) satisfies also the requirement (iv) of Definition 4.1.1. In particular, \mathbf{m} is a weak solution of (4.1).

For both versions of the method, for $1/2 < \theta \leq 1$, the convergence is unconditional. The proof of Theorem 4.3.2 is constructive, in the sense that it also establishes the existence of a weak solution of (4.1). The proof will follow the usual energy method for proving existence of solutions of linear second-order parabolic problems; see, e.g., [88, Section 7.1.2]. The main difference is that the construction of approximate solutions is not obtained by applying the Galerkin method based on a set of appropriately normalized eigenfunctions of the Laplacian, but rather by using the discrete solutions of Algorithm 4.2.1.

Remark 4.3.3. For the applicability of Theorem 4.3.2 to effective discretizations of the lower-order effective field terms, we refer the reader to [56, Section 4]. There, it is shown that if the discrete operator π_h is a continuous function of the magnetization (which is the case, e.g., for anisotropy contributions) or the approximate stray field computed with the hybrid FEM-BEM method of D. R. FREDKIN and T. R. KOEHLER [99], then the stability (4.16a) and the consistency assumption (4.18a) are satisfied. In Chapter 5, we will discuss the applicability of Theorem 4.3.2 to the analysis of the tangent plane scheme for the spintronic extensions of the LLG equation presented in Section 2.3, which will provide concrete examples for the discrete operator Π_h .

For the sake of clarity, we divide the proof of Theorem 4.3.2 into several lemmata and propositions. We start with the observation that, for the standard tangent plane scheme, from Lemma 3.4.6 it follows that $\|\mathbf{m}_h^i\|_{L^\infty(\Omega)} = 1$ for all $0 \leq i \leq M$. The following lemma concerns two geometric estimates satisfied by the iterates of Algorithm 4.2.1 in this case.

Lemma 4.3.4. For all $0 \leq i \leq M - 1$ and $\mathbf{z} \in \mathcal{N}_h$, the iterates of the standard tangent plane scheme satisfy

$$|\mathbf{m}_h^{i+1}(\mathbf{z}) - \mathbf{m}_h^i(\mathbf{z}) - k\mathbf{v}_h^i(\mathbf{z})| \leq \frac{1}{2}k^2 |\mathbf{v}_h^i(\mathbf{z})|^2 \quad (4.20)$$

and

$$|\mathbf{m}_h^{i+1}(\mathbf{z}) - \mathbf{m}_h^i(\mathbf{z})| \leq k |\mathbf{v}_h^i(\mathbf{z})|. \quad (4.21)$$

Proof. Let $0 \leq i \leq M - 1$. For $\mathbf{z} \in \mathcal{N}_h$, using the expression (4.10b) of the time-stepping, we obtain that

$$\begin{aligned} & |\mathbf{m}_h^{i+1}(\mathbf{z}) - \mathbf{m}_h^i(\mathbf{z}) - k\mathbf{v}_h^i(\mathbf{z})| \\ &= \left| \frac{\mathbf{m}_h^i(\mathbf{z}) + k\mathbf{v}_h^i(\mathbf{z})}{|\mathbf{m}_h^i(\mathbf{z}) + k\mathbf{v}_h^i(\mathbf{z})|} - \mathbf{m}_h^i(\mathbf{z}) - k\mathbf{v}_h^i(\mathbf{z}) \right| = |\mathbf{m}_h^i(\mathbf{z}) + k\mathbf{v}_h^i(\mathbf{z})| \left| \frac{1}{|\mathbf{m}_h^i(\mathbf{z}) + k\mathbf{v}_h^i(\mathbf{z})|} - 1 \right| \\ &= |\mathbf{m}_h^i(\mathbf{z}) + k\mathbf{v}_h^i(\mathbf{z})| \left(1 - \frac{1}{|\mathbf{m}_h^i(\mathbf{z}) + k\mathbf{v}_h^i(\mathbf{z})|} \right) = |\mathbf{m}_h^i(\mathbf{z}) + k\mathbf{v}_h^i(\mathbf{z})| - 1. \end{aligned}$$

To estimate the right-hand side, we compute

$$\begin{aligned} 0 &\leq (|\mathbf{m}_h^i(\mathbf{z}) + k\mathbf{v}_h^i(\mathbf{z})| - 1)^2 = |\mathbf{m}_h^i(\mathbf{z}) + k\mathbf{v}_h^i(\mathbf{z})|^2 - 2|\mathbf{m}_h^i(\mathbf{z}) + k\mathbf{v}_h^i(\mathbf{z})| + 1 \\ &= |\mathbf{m}_h^i(\mathbf{z})|^2 + k^2 |\mathbf{v}_h^i(\mathbf{z})|^2 - 2|\mathbf{m}_h^i(\mathbf{z}) + k\mathbf{v}_h^i(\mathbf{z})| + 1 = 2 + k^2 |\mathbf{v}_h^i(\mathbf{z})|^2 - 2|\mathbf{m}_h^i(\mathbf{z}) + k\mathbf{v}_h^i(\mathbf{z})|. \end{aligned}$$

Rearranging the terms, we deduce that

$$|\mathbf{m}_h^i(\mathbf{z}) + k\mathbf{v}_h^i(\mathbf{z})| - 1 \leq \frac{1}{2}k^2 |\mathbf{v}_h^i(\mathbf{z})|^2.$$

As a result, we obtain (4.20).

For $\mathbf{z} \in \mathcal{N}_h$, a simple computation reveals

$$\begin{aligned} |\mathbf{m}_h^{i+1}(\mathbf{z}) - \mathbf{m}_h^i(\mathbf{z})|^2 &= |\mathbf{m}_h^{i+1}(\mathbf{z})|^2 - 2\mathbf{m}_h^{i+1}(\mathbf{z}) \cdot \mathbf{m}_h^i(\mathbf{z}) + |\mathbf{m}_h^i(\mathbf{z})|^2 = 2(1 - \mathbf{m}_h^{i+1}(\mathbf{z}) \cdot \mathbf{m}_h^i(\mathbf{z})) \\ &= 2 \left(1 - \frac{\mathbf{m}_h^i(\mathbf{z}) + k\mathbf{v}_h^i(\mathbf{z})}{|\mathbf{m}_h^i(\mathbf{z}) + k\mathbf{v}_h^i(\mathbf{z})|} \cdot \mathbf{m}_h^i(\mathbf{z}) \right) = 2 \left(1 - \frac{1}{|\mathbf{m}_h^i(\mathbf{z}) + k\mathbf{v}_h^i(\mathbf{z})|} \right) \\ &= 2 \frac{|\mathbf{m}_h^i(\mathbf{z}) + k\mathbf{v}_h^i(\mathbf{z})| - 1}{|\mathbf{m}_h^i(\mathbf{z}) + k\mathbf{v}_h^i(\mathbf{z})|} = 2 \frac{|\mathbf{m}_h^i(\mathbf{z}) + k\mathbf{v}_h^i(\mathbf{z})| - |\mathbf{m}_h^{i+1}(\mathbf{z})|}{|\mathbf{m}_h^i(\mathbf{z}) + k\mathbf{v}_h^i(\mathbf{z})|}. \end{aligned}$$

Due to the Lipschitz continuity (with unit constant) of the Euclidean norm, we can estimate the numerator by

$$|\mathbf{m}_h^i(\mathbf{z}) + k\mathbf{v}_h^i(\mathbf{z})| - |\mathbf{m}_h^{i+1}(\mathbf{z})| \leq |\mathbf{m}_h^i(\mathbf{z}) + k\mathbf{v}_h^i(\mathbf{z}) - \mathbf{m}_h^{i+1}(\mathbf{z})| \stackrel{(4.20)}{\leq} \frac{1}{2}k^2 |\mathbf{v}_h^i(\mathbf{z})|^2.$$

For the denominator, it holds that $|\mathbf{m}_h^i(\mathbf{z}) + k\mathbf{v}_h^i(\mathbf{z})| \geq 1$. We deduce

$$|\mathbf{m}_h^{i+1}(\mathbf{z}) - \mathbf{m}_h^i(\mathbf{z})|^2 \leq 2 \frac{|\mathbf{m}_h^i(\mathbf{z}) + k\mathbf{v}_h^i(\mathbf{z})| - |\mathbf{m}_h^{i+1}(\mathbf{z})|}{|\mathbf{m}_h^i(\mathbf{z}) + k\mathbf{v}_h^i(\mathbf{z})|} \leq k^2 |\mathbf{v}_h^i(\mathbf{z})|^2.$$

This yields (4.21). \square

We recall the norm equivalence

$$\|\phi_h\|_{\mathbf{L}^p(\Omega)}^p \simeq h^3 \sum_{\mathbf{z} \in \mathcal{N}_h} |\phi_h(\mathbf{z})|^p \quad \text{for all } \phi_h \in \mathcal{S}^1(\mathcal{T}_h)^3 \text{ and } p \in [1, \infty) \quad (4.22)$$

from Proposition 3.4.5, which holds with an equivalence constant that depends only on the mesh regularity parameter γ . The combination of (4.22) with the geometric estimates from Lemma 4.3.4 leads to the following result.

Corollary 4.3.5. *For all $0 \leq i \leq M-1$, the iterates of the standard tangent plane scheme satisfy*

$$\|\mathbf{m}_h^{i+1} - \mathbf{m}_h^i\|_{\mathbf{L}^2(\Omega)} \leq Ck \|\mathbf{v}_h^i\|_{\mathbf{L}^2(\Omega)}, \quad (4.23a)$$

$$\|\mathbf{m}_h^{i+1} - \mathbf{m}_h^i - k\mathbf{v}_h^i\|_{\mathbf{L}^1(\Omega)} \leq Ck^2 \|\mathbf{v}_h^i\|_{\mathbf{L}^2(\Omega)}^2, \quad (4.23b)$$

$$\|\mathbf{m}_h^{i+1} - \mathbf{m}_h^i - k\mathbf{v}_h^i\|_{\mathbf{L}^{4/3}(\Omega)} \leq Ck^2 \|\mathbf{v}_h^i\|_{\mathbf{L}^{8/3}(\Omega)}^2, \quad (4.23c)$$

where the constant $C > 0$ depends only on γ .

Proof. The estimate (4.23a) follows from (4.21) and a double application of (4.22) ($p = 2$). The estimate (4.23b) follows from (4.20) and a double application of (4.22) (first $p = 1$, then $p = 2$). The estimate (4.23c) follows from (4.20) and a double application of (4.22) (first $p = 4/3$, then $p = 8/3$). \square

If the nodal projection mapping is omitted in Algorithm 4.2.1, thanks to (4.10a), the estimates from Lemma 4.3.4 and Corollary 4.3.5 become trivial. However, in this case, the equality $\|\mathbf{m}_h^i\|_{\mathbf{L}^\infty(\Omega)} = 1$ for all $0 \leq i \leq M$ is not satisfied. In the following lemma, we prove an easy recursive relation.

Lemma 4.3.6. *For all $1 \leq j \leq M$, the iterates of the projection-free tangent plane scheme satisfy*

$$|\mathbf{m}_h^j(\mathbf{z})|^2 = |\mathbf{m}_h^0(\mathbf{z})|^2 + k^2 \sum_{i=0}^{j-1} |\mathbf{v}_h^i(\mathbf{z})|^2 \quad \text{for all } \mathbf{z} \in \mathcal{N}_h. \quad (4.24)$$

Proof. Let $1 \leq j \leq M$. For all $0 \leq i \leq j-1$ and $\mathbf{z} \in \mathcal{N}_h$, since \mathbf{v}_h^i belongs to $\mathcal{K}_{\mathbf{m}_h^i}$, it holds that

$$|\mathbf{m}_h^{i+1}(\mathbf{z})|^2 \stackrel{(4.10a)}{=} |\mathbf{m}_h^i(\mathbf{z}) + k\mathbf{v}_h^i(\mathbf{z})|^2 = |\mathbf{m}_h^i(\mathbf{z})|^2 + k^2 |\mathbf{v}_h^i(\mathbf{z})|^2.$$

Summation over $0 \leq i \leq j-1$ yields (4.24). \square

In the following lemma, we start with the study of the evolution of the discrete energy.

Lemma 4.3.7. *Let $0 \leq i \leq M-1$. For the standard tangent plane scheme, it holds that*

$$\begin{aligned} & \frac{\lambda_{\text{ex}}^2}{2} k d_t \|\nabla \mathbf{m}_h^{i+1}\|_{\mathbf{L}^2(\Omega)}^2 + [\alpha - c(k, h)] k \|\mathbf{v}_h^i\|_{\mathbf{L}^2(\Omega)}^2 + \lambda_{\text{ex}}^2 \left(\theta - \frac{1}{2} \right) k^2 \|\nabla \mathbf{v}_h^i\|_{\mathbf{L}^2(\Omega)}^2 \\ & \leq k \langle \pi_h(\mathbf{m}_h^i), \mathbf{v}_h^i \rangle + k \langle \mathbf{f}_h^i, \mathbf{v}_h^i \rangle + k \langle \Pi_h(\mathbf{m}_h^i), \mathbf{v}_h^i \rangle, \end{aligned} \quad (4.25)$$

with

$$c(k, h) = \begin{cases} 0 & \text{if the triangulation } \mathcal{T}_h \text{ satisfies the angle condition (3.16),} \\ Ckh^{-2} & \text{else.} \end{cases}$$

The constant $C > 0$ depends only on γ and λ_{ex} . In particular, it is independent of k and h . For the projection-free tangent plane scheme, it holds that

$$\begin{aligned} & \frac{\lambda_{\text{ex}}^2}{2} k d_t \|\nabla \mathbf{m}_h^{i+1}\|_{L^2(\Omega)}^2 + \alpha k \|\mathbf{v}_h^i\|_{L^2(\Omega)}^2 + \lambda_{\text{ex}}^2 \left(\theta - \frac{1}{2} \right) k^2 \|\nabla \mathbf{v}_h^i\|_{L^2(\Omega)}^2 \\ & = k \langle \pi_h(\mathbf{m}_h^i), \mathbf{v}_h^i \rangle + k \langle \mathbf{f}_h^i, \mathbf{v}_h^i \rangle + k \langle \Pi_h(\mathbf{m}_h^i), \mathbf{v}_h^i \rangle. \end{aligned} \quad (4.26)$$

Proof. Let $0 \leq i \leq M-1$. We test (4.9) with $\phi_h = \mathbf{v}_h^i \in \mathcal{K}_{\mathbf{m}_h^i}$ and multiply the resulting equation by k :

$$\begin{aligned} & \alpha k \|\mathbf{v}_h^i\|_{L^2(\Omega)}^2 + k \overbrace{\langle \mathbf{m}_h^i \times \mathbf{v}_h^i, \mathbf{v}_h^i \rangle}^{=0} + \lambda_{\text{ex}}^2 \theta k^2 \|\nabla \mathbf{v}_h^i\|_{L^2(\Omega)}^2 \\ & = -\lambda_{\text{ex}}^2 k \langle \nabla \mathbf{m}_h^i, \nabla \mathbf{v}_h^i \rangle + k \langle \pi_h(\mathbf{m}_h^i), \mathbf{v}_h^i \rangle + k \langle \mathbf{f}_h^i, \mathbf{v}_h^i \rangle + k \langle \Pi_h(\mathbf{m}_h^i), \mathbf{v}_h^i \rangle. \end{aligned} \quad (4.27)$$

We apply the vector identity

$$|\mathbf{a}|^2 - |\mathbf{b}|^2 = |\mathbf{a} - \mathbf{b}|^2 + 2(\mathbf{a} - \mathbf{b}) \cdot \mathbf{b} \quad \text{for all } \mathbf{a}, \mathbf{b} \in \mathbb{R}^9$$

with the choices $\mathbf{a} = \nabla \mathbf{m}_h^{i+1}$ and $\mathbf{b} = \nabla \mathbf{m}_h^i$, and multiply the resulting equation by $\lambda_{\text{ex}}^2/2$. We obtain

$$\begin{aligned} & \frac{\lambda_{\text{ex}}^2}{2} \|\nabla \mathbf{m}_h^{i+1}\|_{L^2(\Omega)}^2 - \frac{\lambda_{\text{ex}}^2}{2} \|\nabla \mathbf{m}_h^i\|_{L^2(\Omega)}^2 \\ & = \frac{\lambda_{\text{ex}}^2}{2} \|\nabla \mathbf{m}_h^{i+1} - \nabla \mathbf{m}_h^i\|_{L^2(\Omega)}^2 + \lambda_{\text{ex}}^2 \langle \nabla \mathbf{m}_h^{i+1} - \nabla \mathbf{m}_h^i, \nabla \mathbf{m}_h^i \rangle. \end{aligned}$$

Summation of the latter with (4.27) yields

$$\begin{aligned} & \frac{\lambda_{\text{ex}}^2}{2} \|\nabla \mathbf{m}_h^{i+1}\|_{L^2(\Omega)}^2 - \frac{\lambda_{\text{ex}}^2}{2} \|\nabla \mathbf{m}_h^i\|_{L^2(\Omega)}^2 + \alpha k \|\mathbf{v}_h^i\|_{L^2(\Omega)}^2 + \lambda_{\text{ex}}^2 \theta k^2 \|\nabla \mathbf{v}_h^i\|_{L^2(\Omega)}^2 \\ & = \frac{\lambda_{\text{ex}}^2}{2} \|\nabla \mathbf{m}_h^{i+1} - \nabla \mathbf{m}_h^i\|_{L^2(\Omega)}^2 + \lambda_{\text{ex}}^2 \langle \nabla \mathbf{m}_h^{i+1} - \nabla \mathbf{m}_h^i - k \nabla \mathbf{v}_h^i, \nabla \mathbf{m}_h^i \rangle \\ & \quad + k \langle \pi_h(\mathbf{m}_h^i), \mathbf{v}_h^i \rangle + k \langle \mathbf{f}_h^i, \mathbf{v}_h^i \rangle + k \langle \Pi_h(\mathbf{m}_h^i), \mathbf{v}_h^i \rangle. \end{aligned} \quad (4.28)$$

We first discuss the case of the standard tangent plane scheme. If the triangulation satisfies the angle condition (3.16), we subtract the quantity $\lambda_{\text{ex}}^2 k^2 \|\nabla \mathbf{v}_h^i\|_{L^2(\Omega)}^2 / 2$ from both sides of (4.28). We obtain

$$\begin{aligned} & \frac{\lambda_{\text{ex}}^2}{2} \|\nabla \mathbf{m}_h^{i+1}\|_{L^2(\Omega)}^2 - \frac{\lambda_{\text{ex}}^2}{2} \|\nabla \mathbf{m}_h^i\|_{L^2(\Omega)}^2 + \alpha k \|\mathbf{v}_h^i\|_{L^2(\Omega)}^2 + \lambda_{\text{ex}}^2 \left(\theta - \frac{1}{2} \right) k^2 \|\nabla \mathbf{v}_h^i\|_{L^2(\Omega)}^2 \\ & = \frac{\lambda_{\text{ex}}^2}{2} \|\nabla \mathbf{m}_h^{i+1} - \nabla \mathbf{m}_h^i\|_{L^2(\Omega)}^2 + \lambda_{\text{ex}}^2 \langle \nabla \mathbf{m}_h^{i+1} - \nabla \mathbf{m}_h^i - k \nabla \mathbf{v}_h^i, \nabla \mathbf{m}_h^i \rangle - \frac{\lambda_{\text{ex}}^2}{2} k^2 \|\nabla \mathbf{v}_h^i\|_{L^2(\Omega)}^2 \\ & \quad + k \langle \pi_h(\mathbf{m}_h^i), \mathbf{v}_h^i \rangle + k \langle \mathbf{f}_h^i, \mathbf{v}_h^i \rangle + k \langle \Pi_h(\mathbf{m}_h^i), \mathbf{v}_h^i \rangle. \end{aligned}$$

An explicit computation of the first three terms on the right-hand side, together with Proposition 3.4.11, then reveals

$$\begin{aligned} & \frac{\lambda_{\text{ex}}^2}{2} \|\nabla \mathbf{m}_h^{i+1} - \nabla \mathbf{m}_h^i\|_{L^2(\Omega)}^2 + \lambda_{\text{ex}}^2 \langle \nabla \mathbf{m}_h^{i+1} - \nabla \mathbf{m}_h^i - k \nabla \mathbf{v}_h^i, \nabla \mathbf{m}_h^i \rangle - \frac{\lambda_{\text{ex}}^2}{2} k^2 \|\nabla \mathbf{v}_h^i\|_{L^2(\Omega)}^2 \\ & = \frac{\lambda_{\text{ex}}^2}{2} \|\nabla \mathbf{m}_h^{i+1}\|_{L^2(\Omega)}^2 - \frac{\lambda_{\text{ex}}^2}{2} \|\nabla(\mathbf{m}_h^i + k \mathbf{v}_h^i)\|_{L^2(\Omega)}^2 \stackrel{(3.25)}{\leq} 0. \end{aligned}$$

We conclude that

$$\begin{aligned} & \frac{\lambda_{\text{ex}}^2}{2} \|\nabla \mathbf{m}_h^{i+1}\|_{L^2(\Omega)}^2 + \alpha k \|\mathbf{v}_h^i\|_{L^2(\Omega)}^2 + \lambda_{\text{ex}}^2 \left(\theta - \frac{1}{2} \right) k^2 \|\nabla \mathbf{v}_h^i\|_{L^2(\Omega)}^2 \\ & \leq \frac{\lambda_{\text{ex}}^2}{2} \|\nabla \mathbf{m}_h^i\|_{L^2(\Omega)}^2 + k \langle \pi_h(\mathbf{m}_h^i), \mathbf{v}_h^i \rangle + k \langle \mathbf{f}_h^i, \mathbf{v}_h^i \rangle + k \langle \Pi_h(\mathbf{m}_h^i), \mathbf{v}_h^i \rangle, \end{aligned}$$

which is (4.25) with $c(k, h) = 0$.

If the triangulation does not satisfy the angle condition (3.16), we proceed with the direct estimate of the first two terms on the right-hand side of (4.28). Using an inverse estimate and Corollary 4.3.5, we can estimate the first term as

$$\|\nabla \mathbf{m}_h^{i+1} - \nabla \mathbf{m}_h^i\|_{L^2(\Omega)}^2 \stackrel{(3.17)}{\lesssim} h^{-2} \|\mathbf{m}_h^{i+1} - \mathbf{m}_h^i\|_{L^2(\Omega)}^2 \stackrel{(4.23a)}{\lesssim} k^2 h^{-2} \|\mathbf{v}_h^i\|_{L^2(\Omega)}^2.$$

Using the Hölder inequality, an inverse estimate, the equality $\|\mathbf{m}_h^i\|_{L^\infty(\Omega)} = 1$ and Corollary 4.3.5, we can similarly obtain an estimate for the second term on the right-hand side

$$\begin{aligned} |\langle \nabla \mathbf{m}_h^{i+1} - \nabla \mathbf{m}_h^i - k \nabla \mathbf{v}_h^i, \nabla \mathbf{m}_h^i \rangle| &\leq \|\nabla \mathbf{m}_h^{i+1} - \nabla \mathbf{m}_h^i - k \nabla \mathbf{v}_h^i\|_{L^1(\Omega)} \|\nabla \mathbf{m}_h^i\|_{L^\infty(\Omega)} \\ &\stackrel{(3.17)}{\lesssim} h^{-2} \|\mathbf{m}_h^{i+1} - \mathbf{m}_h^i - k \mathbf{v}_h^i\|_{L^1(\Omega)} \|\mathbf{m}_h^i\|_{L^\infty(\Omega)} \\ &\stackrel{(4.23b)}{\lesssim} k^2 h^{-2} \|\mathbf{v}_h^i\|_{L^2(\Omega)}^2. \end{aligned}$$

We thus obtain

$$\begin{aligned} &\frac{\lambda_{\text{ex}}^2}{2} \|\nabla \mathbf{m}_h^{i+1}\|_{L^2(\Omega)}^2 + [\alpha - Ckh^{-2}]k \|\mathbf{v}_h^i\|_{L^2(\Omega)}^2 + \lambda_{\text{ex}}^2 \left(\theta - \frac{1}{2} \right) k^2 \|\nabla \mathbf{v}_h^i\|_{L^2(\Omega)}^2 \\ &\leq \frac{\lambda_{\text{ex}}^2}{2} \|\nabla \mathbf{m}_h^i\|_{L^2(\Omega)}^2 + k \langle \pi_h(\mathbf{m}_h^i), \mathbf{v}_h^i \rangle + k \langle \mathbf{f}_h^i, \mathbf{v}_h^i \rangle + k \langle \Pi_h(\mathbf{m}_h^i), \mathbf{v}_h^i \rangle, \end{aligned}$$

where $C > 0$ depends only on γ and λ_{ex} . This establishes (4.25) and concludes the proof for the standard tangent plane scheme.

In the case of the projection-free method, thanks to the linear time-stepping (4.10a), (4.28) simplifies to

$$\begin{aligned} &\frac{\lambda_{\text{ex}}^2}{2} \|\nabla \mathbf{m}_h^{i+1}\|_{L^2(\Omega)}^2 - \frac{\lambda_{\text{ex}}^2}{2} \|\nabla \mathbf{m}_h^i\|_{L^2(\Omega)}^2 + \alpha k \|\mathbf{v}_h^i\|_{L^2(\Omega)}^2 + \lambda_{\text{ex}}^2 \theta k^2 \|\nabla \mathbf{v}_h^i\|_{L^2(\Omega)}^2 \\ &= \frac{\lambda_{\text{ex}}^2}{2} k^2 \|\nabla \mathbf{v}_h^i\|_{L^2(\Omega)}^2 + k \langle \pi_h(\mathbf{m}_h^i), \mathbf{v}_h^i \rangle + k \langle \mathbf{f}_h^i, \mathbf{v}_h^i \rangle + k \langle \Pi_h(\mathbf{m}_h^i), \mathbf{v}_h^i \rangle, \end{aligned}$$

which is (4.26). \square

In the following lemma, we establish an energy estimate for the iterates of Algorithm 4.2.1.

Lemma 4.3.8. *Let Assumption 4.3.1 be satisfied.*

(a) *Let $1/2 < \theta \leq 1$. For the standard tangent plane scheme, suppose additionally that either any triangulation \mathcal{T}_h satisfies the angle condition (3.16) or $k = o(h^2)$ as $k, h \rightarrow 0$. If k is sufficiently small, then, for all $1 \leq j \leq M$, it holds that*

$$\|\mathbf{m}_h^j\|_{H^1(\Omega)}^2 + k \sum_{i=0}^{j-1} \|\mathbf{v}_h^i\|_{L^2(\Omega)}^2 + k^2 \sum_{i=0}^{j-1} \|\nabla \mathbf{v}_h^i\|_{L^2(\Omega)}^2 \leq C. \quad (4.29)$$

(b) *Let $0 \leq \theta < 1/2$. Suppose that*

- *either $\theta = 1/2$ and, additionally for the standard tangent plane scheme, that any triangulation \mathcal{T}_h satisfies the angle condition (3.16),*
- *or $k = o(h^2)$ as $k, h \rightarrow 0$.*

If k is sufficiently small, then, for all $1 \leq j \leq M$, it holds that

$$\|\mathbf{m}_h^j\|_{H^1(\Omega)}^2 + k \sum_{i=0}^{j-1} \|\mathbf{v}_h^i\|_{L^2(\Omega)}^2 \leq C. \quad (4.30)$$

In both cases, the constant $C > 0$ depends only on the problem data $(\alpha, C_\pi, C_\Pi, \mathbf{f}, \lambda_{\text{ex}}, \mathbf{m}^0, |\Omega|, T)$ and on the discretization parameters γ and θ . In particular, it is independent of k and h .

Proof. To start with, we recall that, since $\mathbf{m}_h^0 \rightharpoonup \mathbf{m}^0$ in $\mathbf{H}^1(\Omega)$ by assumption (4.15), there exists a positive constant $C = C(\mathbf{m}^0) > 0$ such that $\|\mathbf{m}_h^0\|_{\mathbf{H}^1(\Omega)} \leq C$.

Let $1 \leq j \leq M$. For the standard tangent plane scheme, since $\|\mathbf{m}_h^j\|_{\mathbf{L}^\infty(\Omega)}^2 = 1$, it holds that

$$\|\mathbf{m}_h^j\|_{\mathbf{L}^2(\Omega)}^2 \leq |\Omega|.$$

For the projection-free tangent plane scheme, from the combination of Lemma 4.3.6 and the norm equivalence (4.22), we deduce that

$$\|\mathbf{m}_h^j\|_{\mathbf{L}^2(\Omega)}^2 \leq C \left(\|\mathbf{m}_h^0\|_{\mathbf{L}^2(\Omega)}^2 + k^2 \sum_{i=0}^{j-1} \|\mathbf{v}_h^i\|_{\mathbf{L}^2(\Omega)}^2 \right),$$

for a positive constant $C = C(\gamma) > 0$. We can summarize the preceding estimates by means of the inequality

$$\|\mathbf{m}_h^j\|_{\mathbf{L}^2(\Omega)}^2 \leq C_1 + C_2 k^2 \sum_{i=0}^{j-1} \|\mathbf{v}_h^i\|_{\mathbf{L}^2(\Omega)}^2, \quad (4.31)$$

with $C_1 = C_1(\gamma, \mathbf{m}^0, |\Omega|) > 0$ and $C_2 = C_2(\gamma) > 0$ being constants.

We now apply Lemma 4.3.7. For all $0 \leq i \leq M-1$ and both versions of the tangent plane scheme, it holds that

$$\begin{aligned} & \frac{\lambda_{\text{ex}}^2}{2} k d_t \|\nabla \mathbf{m}_h^{i+1}\|_{\mathbf{L}^2(\Omega)}^2 + (\alpha - C_3 k h^{-2}) k \|\mathbf{v}_h^i\|_{\mathbf{L}^2(\Omega)}^2 + \lambda_{\text{ex}}^2 \left(\theta - \frac{1}{2} \right) k^2 \|\nabla \mathbf{v}_h^i\|_{\mathbf{L}^2(\Omega)}^2 \\ & \leq k \langle \boldsymbol{\pi}_h(\mathbf{m}_h^i), \mathbf{v}_h^i \rangle + k \langle \mathbf{f}_h^i, \mathbf{v}_h^i \rangle + k \langle \boldsymbol{\Pi}_h(\mathbf{m}_h^i), \mathbf{v}_h^i \rangle. \end{aligned}$$

Note that, for the projection-free tangent plane scheme and for the standard tangent plane scheme if any triangulation of the family satisfies the angle condition (3.16), the estimate holds with $C_3 = 0$. Otherwise, it holds that $C_3 = C_3(\gamma, \lambda_{\text{ex}}) > 0$; see (4.25)–(4.26). Summation over all $0 \leq i \leq j-1$ then yields

$$\begin{aligned} & \frac{\lambda_{\text{ex}}^2}{2} \|\nabla \mathbf{m}_h^j\|_{\mathbf{L}^2(\Omega)}^2 + (\alpha - C_3 k h^{-2}) k \sum_{i=0}^{j-1} \|\mathbf{v}_h^i\|_{\mathbf{L}^2(\Omega)}^2 + \lambda_{\text{ex}}^2 \left(\theta - \frac{1}{2} \right) k^2 \sum_{i=0}^{j-1} \|\nabla \mathbf{v}_h^i\|_{\mathbf{L}^2(\Omega)}^2 \\ & \leq \frac{\lambda_{\text{ex}}^2}{2} \|\nabla \mathbf{m}_h^0\|_{\mathbf{L}^2(\Omega)}^2 + k \sum_{i=0}^{j-1} (\langle \boldsymbol{\pi}_h(\mathbf{m}_h^i), \mathbf{v}_h^i \rangle + \langle \mathbf{f}_h^i, \mathbf{v}_h^i \rangle + \langle \boldsymbol{\Pi}_h(\mathbf{m}_h^i), \mathbf{v}_h^i \rangle). \end{aligned} \quad (4.32)$$

The first term on the right-hand side is uniformly bounded by assumption (4.15). For the second term, we use the Cauchy–Schwarz inequality as well as the weighted Young inequality. Let $\delta > 0$ be arbitrary (we will choose it later in a convenient way). It holds that

$$\begin{aligned} & k \sum_{i=0}^{j-1} (\langle \boldsymbol{\pi}_h(\mathbf{m}_h^i), \mathbf{v}_h^i \rangle + \langle \mathbf{f}_h^i, \mathbf{v}_h^i \rangle + \langle \boldsymbol{\Pi}_h(\mathbf{m}_h^i), \mathbf{v}_h^i \rangle) \\ & \leq k \sum_{i=0}^{j-1} \left(\|\boldsymbol{\pi}_h(\mathbf{m}_h^i)\|_{\mathbf{L}^2(\Omega)} + \|\mathbf{f}_h^i\|_{\mathbf{L}^2(\Omega)} + \|\boldsymbol{\Pi}_h(\mathbf{m}_h^i)\|_{\mathbf{L}^2(\Omega)} \right) \|\mathbf{v}_h^i\|_{\mathbf{L}^2(\Omega)} \\ & \leq \frac{3\delta}{2} k \sum_{i=0}^{j-1} \|\mathbf{v}_h^i\|_{\mathbf{L}^2(\Omega)}^2 + \frac{1}{2\delta} k \sum_{i=0}^{j-1} \left(\|\boldsymbol{\pi}_h(\mathbf{m}_h^i)\|_{\mathbf{L}^2(\Omega)}^2 + \|\mathbf{f}_h^i\|_{\mathbf{L}^2(\Omega)}^2 + \|\boldsymbol{\Pi}_h(\mathbf{m}_h^i)\|_{\mathbf{L}^2(\Omega)}^2 \right). \end{aligned}$$

The first term on the right-hand side can be absorbed into the corresponding term on the left-hand side of (4.32). For the term associated with the \mathbf{m} -dependent effective field contribution, it holds that

$$k \sum_{i=0}^{j-1} \|\boldsymbol{\pi}_h(\mathbf{m}_h^i)\|_{\mathbf{L}^2(\Omega)}^2 \stackrel{(4.16a)}{\leq} C_\pi^2 k \sum_{i=0}^{j-1} \left(1 + \|\mathbf{m}_h^i\|_{\mathbf{H}^1(\Omega)} \right)^2 \leq 2C_\pi^2 \left(T + k \sum_{i=0}^{j-1} \|\mathbf{m}_h^i\|_{\mathbf{H}^1(\Omega)}^2 \right).$$

The same holds true for the term associated with the nonenergetic torque term. We obtain

$$k \sum_{i=0}^{j-1} \|\Pi_h(\mathbf{m}_h^i)\|_{L^2(\Omega)}^2 \stackrel{(4.16b)}{\leq} 2C_{\Pi}^2 \left(T + k \sum_{i=0}^{j-1} \|\mathbf{m}_h^i\|_{H^1(\Omega)}^2 \right).$$

Moreover, since $\mathbf{f}_{hk}^- \rightharpoonup \mathbf{f}$ in $L^2(\Omega_T)$ by assumption (4.17), it follows that

$$k \sum_{i=0}^{j-1} \|\mathbf{f}_h^i\|_{L^2(\Omega)}^2 \leq k \sum_{i=0}^{M-1} \|\mathbf{f}_h^i\|_{L^2(\Omega)}^2 = \|\mathbf{f}_{hk}^-\|_{L^2(\Omega)}^2 \leq C,$$

with $C = C(\mathbf{f}) > 0$ being constant. Altogether, we thus obtain that

$$\begin{aligned} & \|\nabla \mathbf{m}_h^j\|_{L^2(\Omega)}^2 + \frac{2}{\lambda_{\text{ex}}^2} \left(\alpha - \frac{3\delta}{2} - C_3 k h^{-2} \right) k \sum_{i=0}^{j-1} \|\mathbf{v}_h^i\|_{L^2(\Omega)}^2 + (2\theta - 1) k^2 \sum_{i=0}^{j-1} \|\nabla \mathbf{v}_h^i\|_{L^2(\Omega)}^2 \\ & \leq C_4 + C_5 k \sum_{i=0}^{j-1} \|\mathbf{m}_h^i\|_{H^1(\Omega)}^2, \end{aligned} \quad (4.33)$$

where $C_4 = C_4(C_{\pi}, C_{\Pi}, \delta, \mathbf{f}, \lambda_{\text{ex}}, \mathbf{m}^0, T) > 0$ and $C_5 = C_5(C_{\pi}, C_{\Pi}, \delta, \lambda_{\text{ex}}) > 0$ are constants. The summation of (4.31) and (4.33) then yields

$$\begin{aligned} & \|\mathbf{m}_h^j\|_{H^1(\Omega)}^2 + \frac{2}{\lambda_{\text{ex}}^2} \left(\alpha - \frac{3\delta}{2} - \frac{C_2 \lambda_{\text{ex}}^2}{2} k - C_3 k h^{-2} \right) k \sum_{i=0}^{j-1} \|\mathbf{v}_h^i\|_{L^2(\Omega)}^2 + (2\theta - 1) k^2 \sum_{i=0}^{j-1} \|\nabla \mathbf{v}_h^i\|_{L^2(\Omega)}^2 \\ & \leq C_1 + C_4 + C_5 k \sum_{i=0}^{j-1} \|\mathbf{m}_h^i\|_{H^1(\Omega)}^2. \end{aligned} \quad (4.34)$$

Under the assumptions of part (a), since $1/2 < \theta \leq 1$, the third term on the left-hand side is nonnegative. We choose $\delta = \alpha/3$. For the projection-free tangent plane scheme, or for the standard tangent plane scheme if any triangulation satisfies the angle condition (3.16), it holds that $C_3 = 0$. Otherwise, for a sufficiently small k it holds that $k h^{-2} < \alpha/(4C_3)$. In both cases, if $k < \alpha/(2C_2 \lambda_{\text{ex}}^2)$, also the second term on the left-hand side of (4.34) is nonnegative. In particular, for a sufficiently small time-step size k , we thus obtain the estimate

$$\|\mathbf{m}_h^j\|_{H^1(\Omega)}^2 + k \sum_{i=0}^{j-1} \|\mathbf{v}_h^i\|_{L^2(\Omega)}^2 + k^2 \sum_{i=0}^{j-1} \|\nabla \mathbf{v}_h^i\|_{L^2(\Omega)}^2 \leq C'_1 + C'_2 k \sum_{i=0}^{j-1} \|\mathbf{m}_h^i\|_{H^1(\Omega)}^2,$$

where the constants $C'_1, C'_2 > 0$ depend only on the problem data $(\alpha, C_{\pi}, C_{\Pi}, \mathbf{f}, \lambda_{\text{ex}}, \mathbf{m}^0, |\Omega|, T)$ and on the discretization parameters γ and θ , but are independent of time-step size k and mesh size h . An application of the discrete Gronwall lemma (see Lemma B.2.4) then yields (4.29) and concludes the proof of part (a).

Under the assumptions of part (b), if $\theta = 1/2$ the third term on the left-hand side of (4.34) vanishes. If $0 \leq \theta < 1/2$, it can be estimated by means of an inverse estimate as

$$0 \leq (1 - 2\theta) k^2 \sum_{i=0}^{j-1} \|\nabla \mathbf{v}_h^i\|_{L^2(\Omega)}^2 \stackrel{(3.17)}{\leq} C(1 - 2\theta) k^2 h^{-2} \sum_{i=0}^{j-1} \|\mathbf{v}_h^i\|_{L^2(\Omega)}^2,$$

where $C = C(\gamma) > 0$. In both cases, we obtain the estimate

$$\begin{aligned} & \|\mathbf{m}_h^j\|_{H^1(\Omega)}^2 + \frac{2}{\lambda_{\text{ex}}^2} \left[\alpha - \frac{3\delta}{2} - \frac{C_2 \lambda_{\text{ex}}^2}{2} k - (C_3 + C_6) k h^{-2} \right] k \sum_{i=0}^{j-1} \|\mathbf{v}_h^i\|_{L^2(\Omega)}^2 \\ & \leq C_1 + C_4 + C_5 k \sum_{i=0}^{j-1} \|\mathbf{m}_h^i\|_{H^1(\Omega)}^2, \end{aligned}$$

where $C_6 = C_6(\gamma, \lambda_{\text{ex}}, \theta) > 0$ is constant.

We choose $\delta = \alpha/3$. If $kh^{-2} < \alpha/[4(C_3 + C_6)]$ (which is true, by assumption, if k is sufficiently small) and $k < \alpha/(2C_2\lambda_{\text{ex}}^2)$, all the terms on the left-hand side are nonnegative. Under our assumptions, for a sufficiently small time-step size k , it thus holds that

$$\|\mathbf{m}_h^j\|_{\mathbf{H}^1(\Omega)}^2 + k \sum_{i=0}^{j-1} \|\mathbf{v}_h^i\|_{\mathbf{L}^2(\Omega)}^2 \leq C_1'' + C_2'' k \sum_{i=0}^{j-1} \|\mathbf{m}_h^i\|_{\mathbf{H}^1(\Omega)}^2,$$

where the constants $C_1'', C_2'' > 0$ depend only on the problem data $(\alpha, C_\pi, C_\Pi, \mathbf{f}, \lambda_{\text{ex}}, \mathbf{m}^0, |\Omega|, T)$ and on the discretization parameters γ and θ , but are independent of the time-step size k and the mesh size h . As before, an application of the discrete Gronwall lemma then yields (4.30). This establishes part (b) of the lemma and concludes the proof. \square

Exploiting Lemma 4.3.8, we are now able to prove that the discrete functions in (4.13) are uniformly bounded.

Proposition 4.3.9. *Suppose that the assumptions of Lemma 4.3.8 are satisfied. Then, if k is sufficiently small, the sequences $\{\mathbf{m}_{hk}\}$, $\{\mathbf{m}_{hk}^\pm\}$ and $\{\mathbf{v}_{hk}^\pm\}$ are uniformly bounded in the sense that*

$$\|\mathbf{m}_{hk}^*\|_{L^\infty(0,T;\mathbf{H}^1(\Omega))} + \|\partial_t \mathbf{m}_{hk}\|_{\mathbf{L}^2(\Omega_T)} + \|\mathbf{v}_{hk}^-\|_{\mathbf{L}^2(\Omega_T)} \leq C, \quad (4.35)$$

for $\mathbf{m}_{hk}^* \in \{\mathbf{m}_{hk}, \mathbf{m}_{hk}^\pm\}$. The constant $C > 0$ depends only on the problem data $(\alpha, C_\pi, C_\Pi, \mathbf{f}, \lambda_{\text{ex}}, \mathbf{m}^0, |\Omega|, T)$ and on the discretization parameters γ and θ . In particular, it is independent of k and h .

Proof. We apply Lemma 4.3.8. Since (4.29) is stronger than (4.30), the latter is always satisfied provided the time-step size k is sufficiently small.

For any $t \in (0, T)$, let $0 \leq i \leq M-1$ such that $t \in [t_i, t_{i+1})$. It holds that

$$\begin{aligned} \|\mathbf{m}_{hk}(t)\|_{\mathbf{H}^1(\Omega)} &= \left\| \frac{t-t_i}{k} \mathbf{m}_h^{i+1} + \frac{t_{i+1}-t}{k} \mathbf{m}_h^i \right\|_{\mathbf{H}^1(\Omega)} \\ &\leq \frac{t-t_i}{k} \|\mathbf{m}_h^{i+1}\|_{\mathbf{H}^1(\Omega)} + \frac{t_{i+1}-t}{k} \|\mathbf{m}_h^i\|_{\mathbf{H}^1(\Omega)} \\ &\leq \|\mathbf{m}_h^{i+1}\|_{\mathbf{H}^1(\Omega)} + \|\mathbf{m}_h^i\|_{\mathbf{H}^1(\Omega)} \stackrel{(4.30)}{\leq} C. \end{aligned}$$

This shows that $\|\mathbf{m}_{hk}\|_{L^\infty(0,T;\mathbf{H}^1(\Omega))} \leq C$. The same proof holds also for \mathbf{m}_{hk}^\pm .

For the time derivative, it holds that

$$\|\partial_t \mathbf{m}_{hk}\|_{\mathbf{L}^2(\Omega_T)}^2 = \int_0^T \|\partial_t \mathbf{m}_{hk}(t)\|_{\mathbf{L}^2(\Omega)}^2 dt = k \sum_{i=0}^{M-1} \|d_t \mathbf{m}_h^{i+1}\|_{\mathbf{L}^2(\Omega)}^2.$$

For the standard tangent plane scheme, it follows from Corollary 4.3.5 that

$$\|d_t \mathbf{m}_h^{i+1}\|_{\mathbf{L}^2(\Omega)} \stackrel{(4.23a)}{\lesssim} \|\mathbf{v}_h^i\|_{\mathbf{L}^2(\Omega)}.$$

For the projection-free tangent plane scheme, it holds that

$$\|d_t \mathbf{m}_h^{i+1}\|_{\mathbf{L}^2(\Omega)} \stackrel{(4.10a)}{=} \|\mathbf{v}_h^i\|_{\mathbf{L}^2(\Omega)}.$$

In both cases, we thus obtain the estimate

$$\|\partial_t \mathbf{m}_{hk}\|_{\mathbf{L}^2(\Omega_T)}^2 \lesssim k \sum_{i=0}^{M-1} \|\mathbf{v}_h^i\|_{\mathbf{L}^2(\Omega)}^2 \stackrel{(4.30)}{\leq} C.$$

Finally, it holds that

$$\|\mathbf{v}_{hk}^-\|_{\mathbf{L}^2(\Omega_T)}^2 = \int_0^T \|\mathbf{v}_{hk}^-(t)\|_{\mathbf{L}^2(\Omega)}^2 dt = k \sum_{i=0}^{M-1} \|\mathbf{v}_h^i\|_{\mathbf{L}^2(\Omega)}^2 \stackrel{(4.30)}{\leq} C,$$

which establishes (4.35) and concludes the proof. \square

In general, the sequence $\{\mathbf{v}_{hk}^-\}$ is not uniformly bounded in $L^2(0, T; \mathbf{H}^1(\Omega))$. Nevertheless, in the following lemma, we show that, under assumptions that are similar to those of Proposition 4.3.9 (slightly stronger only for the case $\theta = 1/2$), the norm $\|\nabla \mathbf{v}_{hk}^-\|_{\mathbf{L}^2(\Omega_T)}$ can be somehow controlled.

Lemma 4.3.10. *Suppose that Assumption 4.3.1 is satisfied. For the standard tangent plane scheme, assume that*

- *either $1/2 < \theta \leq 1$ and any triangulation \mathcal{T}_h satisfies the angle condition (3.16),*
- *or $\theta = 1/2$, any triangulation \mathcal{T}_h satisfies the angle condition (3.16), and $k = o(h)$ as $k, h \rightarrow 0$,*
- *or $k = o(h^2)$ as $k, h \rightarrow 0$.*

For the projection-free tangent plane scheme, assume that

- *either $1/2 < \theta \leq 1$,*
- *or $\theta = 1/2$ and $k = o(h)$ as $k, h \rightarrow 0$,*
- *or $k = o(h^2)$ as $k, h \rightarrow 0$.*

Then, it holds that

$$\lim_{k, h \rightarrow 0} k \|\nabla \mathbf{v}_{hk}^-\|_{\mathbf{L}^2(\Omega_T)} = 0. \quad (4.36)$$

Proof. For $1/2 < \theta \leq 1$, we can apply Lemma 4.3.8(a). It follows that, if k is sufficiently small, it holds that

$$k^2 \|\nabla \mathbf{v}_{hk}^-\|_{\mathbf{L}^2(\Omega_T)}^2 = k^3 \sum_{i=0}^{M-1} \|\nabla \mathbf{v}_h^i\|_{\mathbf{L}^2(\Omega)}^2 \stackrel{(4.29)}{\leq} Ck,$$

where $C > 0$ is independent of k and h . This concludes the proof of (4.36) for $1/2 < \theta \leq 1$.

For $0 \leq \theta \leq 1/2$, using an inverse estimate, we obtain that

$$k^2 \|\nabla \mathbf{v}_{hk}^-\|_{\mathbf{L}^2(\Omega_T)}^2 = k^3 \sum_{i=0}^{M-1} \|\nabla \mathbf{v}_h^i\|_{\mathbf{L}^2(\Omega)}^2 \stackrel{(3.17)}{\lesssim} k^3 h^{-2} \sum_{i=0}^{M-1} \|\mathbf{v}_h^i\|_{\mathbf{L}^2(\Omega)}^2 = k^2 h^{-2} \|\mathbf{v}_{hk}^-\|_{\mathbf{L}^2(\Omega_T)}^2.$$

We now apply Proposition 4.3.9, which ensures that the sequence $\{\mathbf{v}_{hk}^-\}$ is uniformly bounded in $\mathbf{L}^2(\Omega)$ if k is sufficiently small. Since at least $k = o(h)$, it follows that

$$k^2 \|\nabla \mathbf{v}_{hk}^-\|_{\mathbf{L}^2(\Omega_T)}^2 \lesssim k^2 h^{-2} \|\mathbf{v}_{hk}^-\|_{\mathbf{L}^2(\Omega_T)}^2 \stackrel{(4.35)}{\lesssim} k^2 h^{-2} \rightarrow 0.$$

This concludes (4.36). \square

Thanks to the boundedness established in Proposition 4.3.9, we are able to derive the existence of convergent subsequences.

Proposition 4.3.11. *Suppose that the assumptions of part (a) of Theorem 4.3.2 are satisfied. Then, there exists $\mathbf{m} \in L^\infty(0, T; \mathbf{H}^1(\Omega)) \cap H^1(0, T; \mathbf{L}^2(\Omega))$, which satisfies $|\mathbf{m}| = 1$ and $\mathbf{m} \cdot \partial_t \mathbf{m} = 0$ a.e. in Ω_T , such that, upon extraction of a subsequence, it holds that*

$$\mathbf{m}_{hk} \rightharpoonup \mathbf{m} \quad \text{in } \mathbf{H}^1(\Omega_T), \quad (4.37a)$$

$$\mathbf{m}_{hk} \rightarrow \mathbf{m} \quad \text{in } \mathbf{H}^s(\Omega_T) \text{ for all } 0 < s < 1, \quad (4.37b)$$

$$\mathbf{m}_{hk} \rightarrow \mathbf{m} \quad \text{in } L^2(0, T; \mathbf{H}^s(\Omega)) \text{ for all } 0 < s < 1, \quad (4.37c)$$

$$\mathbf{m}_{hk}, \mathbf{m}_{hk}^\pm \rightharpoonup \mathbf{m} \quad \text{in } L^2(0, T; \mathbf{H}^1(\Omega)), \quad (4.37d)$$

$$\mathbf{m}_{hk}, \mathbf{m}_{hk}^\pm \rightarrow \mathbf{m} \quad \text{in } \mathbf{L}^2(\Omega_T), \quad (4.37e)$$

$$\mathbf{m}_{hk}, \mathbf{m}_{hk}^\pm \rightarrow \mathbf{m} \quad \text{pointwise a.e. in } \Omega_T, \quad (4.37f)$$

$$\mathbf{m}_{hk}, \mathbf{m}_{hk}^\pm \xrightarrow{*} \mathbf{m} \quad \text{in } L^\infty(0, T; \mathbf{H}^1(\Omega)), \quad (4.37g)$$

$$\mathbf{v}_{hk}^- \rightharpoonup \partial_t \mathbf{m} \quad \text{in } \mathbf{L}^2(\Omega_T), \quad (4.37h)$$

as $k, h \rightarrow 0$. In particular, all the limits are attained simultaneously for at least one particular subsequence.

Proof. For the sake of clarity, we divide the proof into three steps.

• **Step 1:** Proof of the convergence results (4.37a)–(4.37g).

The uniform boundedness (4.35) from Proposition 4.3.9 allows us to apply the Eberlein–Šmulian theorem to extract weakly convergent subsequences (not relabeled) of $\{\mathbf{m}_{hk}\}$, $\{\mathbf{m}_{hk}^\pm\}$, with possible different limits, and $\{\mathbf{v}_{hk}^-\}$ in $\mathbf{H}^1(\Omega_T)$, $L^2(0, T; \mathbf{H}^1(\Omega))$, and $\mathbf{L}^2(\Omega_T)$, respectively.

Let $\mathbf{m} \in \mathbf{H}^1(\Omega_T)$ be such that $\mathbf{m}_{hk} \rightharpoonup \mathbf{m}$ in $\mathbf{H}^1(\Omega_T)$. The continuous inclusions

$$\mathbf{H}^1(\Omega_T) \subset L^2(0, T; \mathbf{H}^1(\Omega)) \subset \mathbf{L}^2(\Omega_T) \quad (4.38)$$

and the compact embedding $\mathbf{H}^1(\Omega_T) \Subset \mathbf{L}^2(\Omega_T)$ from the Rellich–Kondrashov theorem show that $\mathbf{m}_{hk} \rightharpoonup \mathbf{m}$ in $L^2(0, T; \mathbf{H}^1(\Omega))$ and $\mathbf{m}_{hk} \rightarrow \mathbf{m}$ in $\mathbf{L}^2(\Omega_T)$. Moreover, the strong convergence in $\mathbf{L}^2(\Omega_T)$ guarantees that, upon extraction of a further subsequence, $\mathbf{m}_{hk} \rightarrow \mathbf{m}$ pointwise a.e. in Ω_T .

Let $0 < s < 1$. From the compact embedding $\mathbf{H}^1(\Omega_T) \Subset \mathbf{L}^2(\Omega_T)$ and the well-known interpolation result $[\mathbf{L}^2(\Omega_T), \mathbf{H}^1(\Omega_T)]_s = \mathbf{H}^s(\Omega_T)$ (see, e.g., [45, Theorem 6.4.5]), we obtain the compact embedding $\mathbf{H}^1(\Omega_T) \Subset \mathbf{H}^s(\Omega_T)$; see, e.g., [45, Theorem 3.8.1]. From the continuous inclusions (4.38) and the interpolation result $[\mathbf{L}^2(\Omega_T), L^2(0, T; \mathbf{H}^1(\Omega))]_s = L^2(0, T; \mathbf{H}^s(\Omega))$ (see, e.g., [45, Theorem 5.1.2]), we deduce that the inclusion $\mathbf{H}^s(\Omega_T) \subset L^2(0, T; \mathbf{H}^s(\Omega))$ is continuous. To sum up, it holds that

$$\mathbf{H}^1(\Omega_T) \Subset \mathbf{H}^s(\Omega_T) \subset L^2(0, T; \mathbf{H}^s(\Omega)),$$

from which it follows that $\mathbf{m}_{hk} \rightarrow \mathbf{m}$ in $\mathbf{H}^s(\Omega_T)$ and in $L^2(0, T; \mathbf{H}^s(\Omega))$. This concludes the proof of the convergence results (4.37a)–(4.37f) for the sequence $\{\mathbf{m}_{hk}\}$.

From (3.15), it follows that

$$\|\mathbf{m}_{hk} - \mathbf{m}_{hk}^\pm\|_{\mathbf{L}^2(\Omega_T)} \leq k \|\partial_t \mathbf{m}_{hk}\|_{\mathbf{L}^2(\Omega_T)} \stackrel{(4.35)}{\lesssim} k.$$

In particular, it follows that $\mathbf{m}_{hk}^\pm \rightharpoonup \mathbf{m}$ in $L^2(0, T; \mathbf{H}^1(\Omega))$ as well as $\mathbf{m}_{hk}^\pm \rightarrow \mathbf{m}$ in $\mathbf{L}^2(\Omega_T)$ and pointwise a.e. in Ω_T .

Since the sequences $\{\mathbf{m}_{hk}\}$ and $\{\mathbf{m}_{hk}^\pm\}$ are uniformly bounded in $L^\infty(0, T; \mathbf{H}^1(\Omega))$, from the Banach–Alaoglu theorem, we can extract further weakly-star convergent subsequences (also not relabeled). From the continuous inclusion $L^\infty(0, T; \mathbf{H}^1(\Omega)) \subset L^2(0, T; \mathbf{H}^1(\Omega))$, it follows that the limits coincide with the weak limits in $L^2(0, T; \mathbf{H}^1(\Omega))$, i.e., it holds that $\mathbf{m}_{hk}, \mathbf{m}_{hk}^\pm \xrightarrow{*} \mathbf{m}$ in $L^\infty(0, T; \mathbf{H}^1(\Omega))$.

• **Step 2:** Proof of (4.37h)

Let $\mathbf{v} \in \mathbf{L}^2(\Omega_T)$ such that $\mathbf{v}_{hk}^- \rightharpoonup \mathbf{v}$ in $\mathbf{L}^2(\Omega_T)$. We show that $\mathbf{v} = \partial_t \mathbf{m}$ a.e. in Ω_T . For the standard tangent plane scheme, for all $t \in (0, T)$, let $0 \leq i \leq M-1$ such that $t \in [t_i, t_{i+1})$. From Corollary 4.3.5, it follows that

$$\|\partial_t \mathbf{m}_{hk}(t) - \mathbf{v}_{hk}^-(t)\|_{\mathbf{L}^1(\Omega)} = \|d_t \mathbf{m}_h^{i+1} - \mathbf{v}_h^i\|_{\mathbf{L}^1(\Omega)} \stackrel{(4.23b)}{\lesssim} k \|\mathbf{v}_h^i\|_{\mathbf{L}^2(\Omega)}^2 = k \|\mathbf{v}_{hk}^-(t)\|_{\mathbf{L}^2(\Omega)}^2.$$

Integrating over time, we obtain that

$$\|\partial_t \mathbf{m}_{hk} - \mathbf{v}_{hk}^-\|_{\mathbf{L}^1(\Omega_T)} \lesssim k \|\mathbf{v}_{hk}^-\|_{\mathbf{L}^2(\Omega_T)}^2 \stackrel{(4.35)}{\lesssim} k.$$

Exploiting the sequential weak lower semicontinuity of the L^1 -norm, we deduce that

$$\|\partial_t \mathbf{m} - \mathbf{v}\|_{\mathbf{L}^1(\Omega_T)} \leq \liminf_{k, h \rightarrow 0} \|\partial_t \mathbf{m}_{hk} - \mathbf{v}_{hk}^-\|_{\mathbf{L}^1(\Omega_T)} = 0,$$

which leads to the desired result. For the projection-free tangent plane scheme, the result directly follows from (4.10a), which leads to the equality $d_t \mathbf{m}_h^{i+1} = \mathbf{v}_h^i$ for all $0 \leq i \leq M-1$.

• **Step 3:** The limit function \mathbf{m} satisfies $|\mathbf{m}| = 1$ and $\mathbf{m} \cdot \partial_t \mathbf{m} = 0$ a.e. in Ω_T .

Since $\mathbf{m}_{hk}^- \rightarrow \mathbf{m}$ in $\mathbf{L}^2(\Omega_T)$ by (4.37e) and $\mathbf{v}_{hk}^- \rightharpoonup \partial_t \mathbf{m}$ in $\mathbf{L}^2(\Omega_T)$ by (4.37h), we obtain the convergence $\mathbf{m}_{hk}^- \cdot \mathbf{v}_{hk}^- \rightharpoonup \mathbf{m} \cdot \partial_t \mathbf{m}$ in $L^1(\Omega_T)$. From the sequential weak lower semicontinuity of the L^1 -norm and the fact that $\mathbf{v}_h^i \in \mathcal{K}_{\mathbf{m}_h^i}$ for all $0 \leq i \leq M-1$, it follows that

$$\begin{aligned} & \|\mathbf{m} \cdot \partial_t \mathbf{m}\|_{L^1(\Omega_T)} \\ & \leq \liminf_{k, h \rightarrow 0} \|\mathbf{m}_{hk}^- \cdot \mathbf{v}_{hk}^-\|_{L^1(\Omega_T)} = \liminf_{k, h \rightarrow 0} \int_0^T \|\mathbf{m}_{hk}^-(t) \cdot \mathbf{v}_{hk}^-(t)\|_{L^1(\Omega)} dt \\ & = \liminf_{k, h \rightarrow 0} \sum_{i=0}^{M-1} \int_{t_i}^{t_{i+1}} \|\mathbf{m}_{hk}^-(t) \cdot \mathbf{v}_{hk}^-(t)\|_{L^1(\Omega)} dt = \liminf_{k, h \rightarrow 0} \left(k \sum_{i=0}^{M-1} \|\mathbf{m}_h^i \cdot \mathbf{v}_h^i\|_{L^1(\Omega)} \right) = 0. \end{aligned}$$

This shows that $\mathbf{m} \cdot \partial_t \mathbf{m} = 0$ a.e. in Ω_T .

It remains to show that $|\mathbf{m}| = 1$ a.e. in Ω_T . For the standard tangent plane scheme, we argue as in the proof of Proposition 3.4.7. With the same argument, one can prove that

$$\| |\mathbf{m}_{hk}^-(t)|^2 - 1 \|_{L^2(\Omega)} \lesssim h \|\nabla \mathbf{m}_{hk}^-(t)\|_{\mathbf{L}^2(\Omega)} \quad \text{for all } t \in (0, T).$$

Integrating over time, it follows that

$$\| |\mathbf{m}_{hk}^-|^2 - 1 \|_{L^2(\Omega_T)} \lesssim h \|\nabla \mathbf{m}_{hk}^-\|_{\mathbf{L}^2(\Omega_T)} \stackrel{(4.35)}{\lesssim} h,$$

which yields the convergence $|\mathbf{m}_{hk}^-|^2 \rightarrow 1$ in $L^2(\Omega_T)$. Since $\mathbf{m}_{hk}^- \rightarrow \mathbf{m}$ pointwise a.e. in Ω_T by (4.37f), we deduce that $|\mathbf{m}| = 1$ a.e. in Ω_T .

For the projection-free tangent plane scheme, we argue as in the proof of Proposition 3.4.8. From the triangle inequality, it follows that

$$\begin{aligned} & \| |\mathbf{m}|^2 - 1 \|_{L^1(\Omega_T)} \\ & \leq \| |\mathbf{m}|^2 - |\mathbf{m}_{hk}^+|^2 \|_{L^1(\Omega_T)} + \| |\mathbf{m}_{hk}^+|^2 - \mathcal{I}_h[|\mathbf{m}_{hk}^+|^2] \|_{L^1(\Omega_T)} + \| \mathcal{I}_h[|\mathbf{m}_{hk}^+|^2] - 1 \|_{L^1(\Omega_T)} \end{aligned}$$

Since

$$\| |\mathbf{m}|^2 - |\mathbf{m}_{hk}^+|^2 \|_{L^1(\Omega_T)} \leq \| \mathbf{m} + \mathbf{m}_{hk}^+ \|_{\mathbf{L}^2(\Omega_T)} \| \mathbf{m} - \mathbf{m}_{hk}^+ \|_{\mathbf{L}^2(\Omega_T)} \lesssim \| \mathbf{m} - \mathbf{m}_{hk}^+ \|_{\mathbf{L}^2(\Omega_T)}$$

and $\mathbf{m}_{hk}^+ \rightarrow \mathbf{m}$ in $\mathbf{L}^2(\Omega_T)$ by (4.37e), the first term on the right-hand side converges to 0. An argument similar to the one used in the proof of Proposition 3.4.8 shows that

$$\| |\mathbf{m}_{hk}^+|^2 - \mathcal{I}_h[|\mathbf{m}_{hk}^+|^2] \|_{L^1(\Omega_T)} \lesssim h^2 \|\nabla \mathbf{m}_{hk}^+\|_{\mathbf{L}^2(\Omega_T)}^2 \stackrel{(4.35)}{\lesssim} h^2.$$

The second term on the right-hand side thus also converges to 0. It remains to show that

$$\| \mathcal{I}_h[|\mathbf{m}_{hk}^+|^2] - 1 \|_{L^1(\Omega_T)} \rightarrow 0. \quad (4.39)$$

For all $t \in (0, T)$, let $0 \leq i \leq M-1$ such that $t \in [t_i, t_{i+1})$. From the triangle inequality, it follows that

$$\begin{aligned} & \| \mathcal{I}_h[|\mathbf{m}_{hk}^+(t)|^2] - 1 \|_{L^1(\Omega)} \\ &= \| \mathcal{I}_h[|\mathbf{m}_h^{i+1}|^2] - 1 \|_{L^1(\Omega)} \\ &\leq \| \mathcal{I}_h[|\mathbf{m}_h^{i+1}|^2] - \mathcal{I}_h[|\mathbf{m}_h^0|^2] \|_{L^1(\Omega)} + \| \mathcal{I}_h[|\mathbf{m}_h^0|^2] - |\mathbf{m}_h^0|^2 \|_{L^1(\Omega)} + \| |\mathbf{m}_h^0|^2 - 1 \|_{L^1(\Omega)}. \end{aligned}$$

Using the norm equivalence (4.22) and applying Lemma 4.3.6, it follows that

$$\begin{aligned} & \| \mathcal{I}_h[|\mathbf{m}_h^{i+1}|^2] - \mathcal{I}_h[|\mathbf{m}_h^0|^2] \|_{L^1(\Omega)} \simeq h^3 \sum_{\mathbf{z} \in \mathcal{N}_h} \left| |\mathbf{m}_h^{i+1}(\mathbf{z})|^2 - |\mathbf{m}_h^0(\mathbf{z})|^2 \right| \\ & \stackrel{(4.24)}{=} h^3 \sum_{\mathbf{z} \in \mathcal{N}_h} k^2 \sum_{\ell=0}^i |\mathbf{v}_h^\ell(\mathbf{z})|^2 \\ & \simeq k^2 \sum_{\ell=0}^i \|\mathbf{v}_h^\ell\|_{\mathbf{L}^2(\Omega)}^2 \lesssim k \|\mathbf{v}_{hk}^-\|_{\mathbf{L}^2(\Omega_T)}^2 \stackrel{(4.35)}{\lesssim} k. \end{aligned}$$

For all $K \in \mathcal{T}_h$, using the approximation properties of the nodal interpolant (see Proposition 3.4.3), we deduce that

$$\begin{aligned} & \| \mathcal{I}_h[|\mathbf{m}_h^0|^2] - |\mathbf{m}_h^0|^2 \|_{L^1(K)} \leq |K|^{1/2} \| \mathcal{I}_h[|\mathbf{m}_h^0|^2] - |\mathbf{m}_h^0|^2 \|_{L^2(K)} \lesssim |K|^{1/2} h_K^2 \| |\mathbf{m}_h^0|^2 \|_{H^2(K)} \\ & \leq 2 |K|^{1/2} h_K^2 \|\nabla \mathbf{m}_h^0\|_{\mathbf{L}^4(K)}^2 = 2 |K| h_K^2 \|\nabla \mathbf{m}_h^0\|_K^2 \\ & = 2 h_K^2 \|\nabla \mathbf{m}_h^0\|_{\mathbf{L}^2(K)}^2. \end{aligned}$$

It follows that

$$\| \mathcal{I}_h[|\mathbf{m}_h^0|^2] - |\mathbf{m}_h^0|^2 \|_{L^1(\Omega)} \lesssim h^2 \|\nabla \mathbf{m}_h^0\|_{\mathbf{L}^2(\Omega)}^2 \lesssim h^2.$$

Finally, since $|\mathbf{m}^0| = 1$ a.e. in Ω , it holds that

$$\begin{aligned} & \| |\mathbf{m}_h^0|^2 - 1 \|_{L^1(\Omega)} = \| |\mathbf{m}_h^0|^2 - |\mathbf{m}^0|^2 \|_{L^1(\Omega)} \leq \| \mathbf{m}_h^0 + \mathbf{m}^0 \|_{\mathbf{L}^2(\Omega)} \| \mathbf{m}_h^0 - \mathbf{m}^0 \|_{\mathbf{L}^2(\Omega)} \\ & \lesssim \| \mathbf{m}_h^0 - \mathbf{m}^0 \|_{\mathbf{L}^2(\Omega)}, \end{aligned}$$

which, thanks to (4.15), yields the convergence $|\mathbf{m}_h^0|^2 \rightarrow 1$ in $L^1(\Omega)$. This shows (4.39). We conclude that, also for the limit of the output obtained from the projection-free tangent plane scheme, it holds that $|\mathbf{m}| = 1$ a.e. in Ω_T . \square

We aim to discuss the convergence of the sequences in $\mathbf{L}^\infty(\Omega_T)$. To that end, we define the ‘normalized iterate’ by

$$\widehat{\mathbf{m}}_h^i := \mathcal{I}_h[\mathbf{m}_h^i / |\mathbf{m}_h^i|] \quad \text{for all } 0 \leq i \leq M, \quad (4.40)$$

and consider the corresponding time reconstructions from (3.13), i.e., the functions defined, for all $0 \leq i \leq M-1$ and $t \in [t_i, t_{i+1})$, by

$$\widehat{\mathbf{m}}_{hk}(t) := \frac{t - t_i}{k} \widehat{\mathbf{m}}_h^{i+1} + \frac{t_{i+1} - t}{k} \widehat{\mathbf{m}}_h^i, \quad \widehat{\mathbf{m}}_{hk}^-(t) := \widehat{\mathbf{m}}_h^i, \quad \text{and} \quad \widehat{\mathbf{m}}_{hk}^+(t) := \widehat{\mathbf{m}}_h^{i+1}. \quad (4.41)$$

Note that, in the case of the standard tangent plane scheme, which already includes the nodal projection mapping in the time-stepping, we have the equality $\widehat{\mathbf{m}}_h^i = \mathbf{m}_h^i$ for all $0 \leq i \leq M$, from which it follows that $\widehat{\mathbf{m}}_{hk} = \mathbf{m}_{hk}$ and $\widehat{\mathbf{m}}_{hk}^\pm = \mathbf{m}_{hk}^\pm$. In the following proposition, we discuss the convergence properties, also in $\mathbf{L}^\infty(\Omega_T)$, of the functions (4.41). This result will be useful in Chapter 5.

Proposition 4.3.12. *Suppose that the assumptions of part (a) of Theorem 4.3.2 are satisfied. For the subsequences which satisfy the convergence properties (4.37) of Proposition 4.3.11, upon extraction of a further subsequence, it holds that*

$$\widehat{\mathbf{m}}_{hk}, \widehat{\mathbf{m}}_{hk}^\pm \rightharpoonup \mathbf{m} \quad \text{in } L^2(0, T; \mathbf{H}^1(\Omega)), \quad (4.42a)$$

$$\widehat{\mathbf{m}}_{hk}, \widehat{\mathbf{m}}_{hk}^\pm \rightarrow \mathbf{m} \quad \text{in } \mathbf{L}^2(\Omega_T), \quad (4.42b)$$

$$\widehat{\mathbf{m}}_{hk}, \widehat{\mathbf{m}}_{hk}^\pm \rightarrow \mathbf{m} \quad \text{pointwise a.e. in } \Omega_T, \quad (4.42c)$$

$$\widehat{\mathbf{m}}_{hk}, \widehat{\mathbf{m}}_{hk}^\pm \xrightarrow{*} \mathbf{m} \quad \text{in } L^\infty(0, T; \mathbf{H}^1(\Omega)), \quad (4.42d)$$

$$\widehat{\mathbf{m}}_{hk}, \widehat{\mathbf{m}}_{hk}^\pm \xrightarrow{*} \mathbf{m} \quad \text{in } \mathbf{L}^\infty(\Omega_T) \quad (4.42e)$$

as $k, h \rightarrow 0$. In particular, there exists a subsequence for which the convergence properties (4.37) and (4.42) are simultaneously valid.

Proof. For the standard tangent plane scheme, since $\widehat{\mathbf{m}}_{hk} = \mathbf{m}_{hk}$ and $\widehat{\mathbf{m}}_{hk}^\pm = \mathbf{m}_{hk}^\pm$, the convergence results (4.42a)–(4.42d) already follow from Proposition 4.3.11. To show (4.42e), since $\|\widehat{\mathbf{m}}_{hk}\|_{\mathbf{L}^\infty(\Omega_T)} = 1$, thanks to the Banach–Alaoglu theorem, we can extract a weakly-star convergent subsequence (not relabeled) which converges towards some $\widetilde{\mathbf{m}}$ in $\mathbf{L}^\infty(\Omega_T)$. In particular, $\widehat{\mathbf{m}}_{hk} \rightharpoonup \widetilde{\mathbf{m}}$ in $\mathbf{L}^p(\Omega_T)$ for all $1 \leq p < \infty$. Since we already know that $\widehat{\mathbf{m}}_{hk} \rightarrow \mathbf{m}$ in $\mathbf{L}^2(\Omega_T)$ by (4.42b), it follows that $\widetilde{\mathbf{m}} = \mathbf{m}$. The same result holds for the sequences $\{\widehat{\mathbf{m}}_{hk}^\pm\}$, which leads to (4.42e) and concludes the proof of (4.42).

For the projection-free tangent plane scheme, we start with the observation that, for all $\mathbf{x} \in \mathbb{R}^3$ such that $|\mathbf{x}| \geq 1$, it holds that

$$\left| \mathbf{x} - \frac{\mathbf{x}}{|\mathbf{x}|} \right| = |\mathbf{x}| - 1 = \frac{|\mathbf{x}|^2 - 1}{|\mathbf{x}| + 1} \leq \frac{1}{2} (|\mathbf{x}|^2 - 1). \quad (4.43)$$

It follows that

$$|\mathbf{m}_h^0(\mathbf{z}) - \widehat{\mathbf{m}}_h^0(\mathbf{z})| \stackrel{(4.43)}{\leq} \frac{1}{2} (|\mathbf{m}_h^0(\mathbf{z})|^2 - 1)$$

as well as, for $1 \leq j \leq M$,

$$\begin{aligned} |\mathbf{m}_h^j(\mathbf{z}) - \widehat{\mathbf{m}}_h^j(\mathbf{z})| &\stackrel{(4.43)}{\leq} \frac{1}{2} (|\mathbf{m}_h^j(\mathbf{z})|^2 - 1) \\ &= \frac{1}{2} (|\mathbf{m}_h^j(\mathbf{z})|^2 - |\mathbf{m}_h^0(\mathbf{z})|^2) + \frac{1}{2} (|\mathbf{m}_h^0(\mathbf{z})|^2 - 1) \\ &\stackrel{(4.24)}{\leq} \frac{1}{2} k^2 \sum_{i=0}^{j-1} |\mathbf{v}_h^i(\mathbf{z})|^2 + \frac{1}{2} (|\mathbf{m}_h^0(\mathbf{z})|^2 - 1), \end{aligned}$$

where in the second inequality we have used Lemma 4.3.6. Exploiting the norm equivalence (4.22), we deduce that

$$\|\mathbf{m}_h^j - \widehat{\mathbf{m}}_h^j\|_{\mathbf{L}^1(\Omega)} \lesssim k^2 \sum_{i=0}^{j-1} \|\mathbf{v}_h^i\|_{\mathbf{L}^2(\Omega)}^2 + \|\mathcal{I}_h[|\mathbf{m}_h^0|^2] - 1\|_{\mathbf{L}^1(\Omega)} \quad \text{for all } 0 \leq j \leq M,$$

where the sum on the right-hand side vanishes if $j = 0$. Since

$$\|\mathcal{I}_h[|\mathbf{m}_h^0|^2] - 1\|_{\mathbf{L}^1(\Omega)} \lesssim h^2 + \|\mathbf{m}_h^0 - \mathbf{m}^0\|_{\mathbf{L}^2(\Omega)}$$

(see the last part of Step 3 of the proof of Proposition 4.3.11 on page 64), it follows that

$$\|\mathbf{m}_{hk} - \widehat{\mathbf{m}}_{hk}\|_{\mathbf{L}^1(\Omega_T)} + \|\mathbf{m}_{hk}^\pm - \widehat{\mathbf{m}}_{hk}^\pm\|_{\mathbf{L}^1(\Omega_T)} \lesssim k \|\mathbf{v}_{hk}^-\|_{\mathbf{L}^2(\Omega_T)}^2 + h^2 + \|\mathbf{m}_h^0 - \mathbf{m}^0\|_{\mathbf{L}^2(\Omega)}.$$

Since $\mathbf{m}_{hk}, \mathbf{m}_{hk}^\pm \rightarrow \mathbf{m}$ in $\mathbf{L}^2(\Omega_T)$ by (4.37e), and thus also in $\mathbf{L}^1(\Omega_T)$, we infer that $\widehat{\mathbf{m}}_{hk}, \widehat{\mathbf{m}}_{hk}^\pm \rightarrow \mathbf{m}$ in $\mathbf{L}^1(\Omega_T)$.

Since $\|\widehat{\mathbf{m}}_{hk}\|_{\mathbf{L}^\infty(\Omega_T)} = \|\widehat{\mathbf{m}}_{hk}^\pm\|_{\mathbf{L}^\infty(\Omega_T)} = 1$, we can extract weakly-star convergent subsequences in $\mathbf{L}^\infty(\Omega_T)$ and identify their limits with \mathbf{m} . This yields (4.42e). The convergence results (4.42a)–(4.42d) can be proved with the same argument based on the Eberlein–Šmulian theorem and the Banach–Alaoglu theorem of Proposition 4.3.11. The uniform boundedness of the norms, necessary to extract weakly(-star) convergent subsequences, follows from the identity $\|\widehat{\mathbf{m}}_h^i\|_{\mathbf{L}^\infty(\Omega)} = 1$ and the estimate

$$\|\nabla \widehat{\mathbf{m}}_h^i\|_{\mathbf{L}^2(\Omega)} \stackrel{(3.23)}{\lesssim} \|\nabla \mathbf{m}_h^i\|_{\mathbf{L}^2(\Omega)} \stackrel{(4.30)}{\leq} C,$$

which hold for all $0 \leq i \leq M$. \square

Remark 4.3.13. In Assumption 4.3.1, for the projection-free tangent plane scheme, we assumed the approximate initial condition \mathbf{m}_h^0 to belong to \mathcal{U}_h only to guarantee that the ‘normalized iterate’ (4.40) is always well defined.

In the following lemma, we establish two convergence results that will be exploited in the proof of Theorem 4.3.2.

Lemma 4.3.14. Suppose that the assumptions of Proposition 4.3.11 are satisfied. For the standard tangent plane scheme, it holds that

$$\mathbf{m}_{hk}^- \times \mathbf{v}_{hk}^- \rightharpoonup \mathbf{m} \times \partial_t \mathbf{m} \quad \text{in } \mathbf{L}^2(\Omega_T) \quad (4.44)$$

as $k, h \rightarrow 0$. For the projection-free tangent plane scheme, it holds that

$$\mathbf{m}_{hk}^\pm \rightarrow \mathbf{m} \quad \text{in } L^2(0, T; \mathbf{H}^s(\Omega)) \text{ for all } 0 < s < 1 \quad (4.45)$$

as $k, h \rightarrow 0$.

Proof. We start with the proof of (4.44). Since $\mathbf{m}_{hk}^- \rightarrow \mathbf{m}$ in $\mathbf{L}^2(\Omega_T)$ by (4.37e) and $\mathbf{v}_{hk}^- \rightharpoonup \partial_t \mathbf{m}$ in $\mathbf{L}^2(\Omega_T)$ by (4.37h), it follows that

$$\mathbf{m}_{hk}^- \times \mathbf{v}_{hk}^- \rightharpoonup \mathbf{m} \times \partial_t \mathbf{m} \quad \text{in } \mathbf{L}^1(\Omega_T).$$

For the standard tangent plane scheme, since $\|\mathbf{m}_{hk}^-\|_{\mathbf{L}^\infty(\Omega_T)} = 1$, the sequence $\{\mathbf{m}_{hk}^- \times \mathbf{v}_{hk}^-\}$ is uniformly bounded in $\mathbf{L}^2(\Omega_T)$ and we can extract a weakly convergent subsequence. From the continuous inclusion $\mathbf{L}^2(\Omega_T) \subset \mathbf{L}^1(\Omega_T)$, it follows that the limit in $\mathbf{L}^2(\Omega_T)$ coincides with the limit in $\mathbf{L}^1(\Omega_T)$.

In order to prove (4.45) for the projection-free tangent plane scheme, we show that, for all $0 < s < 1$, it holds that

$$\|\mathbf{m}_{hk} - \mathbf{m}_{hk}^\pm\|_{L^2(0, T; \mathbf{H}^s(\Omega))} \rightarrow 0 \quad \text{as } k, h \rightarrow 0.$$

Since $\mathbf{m}_{hk} \rightarrow \mathbf{m}$ in $L^2(0, T; \mathbf{H}^s(\Omega))$ by (4.37c), this leads to the desired result. Let $0 < s < 1$. It holds that

$$\begin{aligned} \|\mathbf{m}_{hk} - \mathbf{m}_{hk}^\pm\|_{L^2(0, T; \mathbf{H}^s(\Omega))}^2 &= \int_0^T \|\mathbf{m}_{hk}(t) - \mathbf{m}_{hk}^\pm(t)\|_{\mathbf{H}^s(\Omega)}^2 dt \stackrel{(3.14)}{\leq} k^2 \int_0^T \|\partial_t \mathbf{m}_{hk}(t)\|_{\mathbf{H}^s(\Omega)}^2 dt \\ &= k^2 \sum_{i=0}^{M-1} \int_{t_i}^{t_{i+1}} \|\partial_t \mathbf{m}_{hk}(t)\|_{\mathbf{H}^s(\Omega)}^2 dt = k^3 \sum_{i=0}^{M-1} \|d_t \mathbf{m}_h^{i+1}\|_{\mathbf{H}^s(\Omega)}^2 \\ &\stackrel{(4.10a)}{=} k^3 \sum_{i=0}^{M-1} \|\mathbf{v}_h^i\|_{\mathbf{H}^s(\Omega)}^2 \lesssim k^3 \sum_{i=0}^{M-1} \|\mathbf{v}_h^i\|_{\mathbf{H}^1(\Omega)}^2 \\ &= k^2 \|\mathbf{v}_{hk}^-\|_{\mathbf{L}^2(\Omega_T)}^2 + k^2 \|\nabla \mathbf{v}_{hk}^-\|_{\mathbf{L}^2(\Omega_T)}^2. \end{aligned}$$

The result follows from Proposition 4.3.11 and Lemma 4.3.10. \square

We are ready for the proof of Theorem 4.3.2.

Proof of Theorem 4.3.2. For the sake of clarity, we divide the proof into five steps.

• **Step 1:** Proof of part (a) of the theorem.

Proposition 4.3.11 yields the desired convergences towards a function $\mathbf{m} \in L^\infty(0, T; \mathbf{H}^1(\Omega)) \cap H^1(0, T; \mathbf{L}^2(\Omega))$ such that $|\mathbf{m}| = 1$ a.e. in Ω_T . Since $\mathbf{m}_{hk} \rightharpoonup \mathbf{m}$ in $\mathbf{H}^1(\Omega_T)$, we also have the weak convergence of the traces, i.e., $\mathbf{m}_{hk}(0) \rightharpoonup \mathbf{m}(0)$ in $\mathbf{H}^{1/2}(\Omega)$. By assumption (4.15), it holds that $\mathbf{m}_{hk}(0) = \mathbf{m}_h^0 \rightharpoonup \mathbf{m}^0$ in $\mathbf{H}^1(\Omega)$. It follows that $\mathbf{m}(0) = \mathbf{m}^0$ in the sense of traces, which verifies Definition 4.1.1(ii) and thus concludes the proof.

• **Step 2:** Set up and auxiliary results for the verification of Definition 4.1.1(iii).

Let $\varphi \in C^\infty(\overline{\Omega_T})$ be an arbitrary test function. Let $\zeta_h : [0, T] \rightarrow \mathcal{S}^1(\mathcal{T}_h)^3$ be defined by

$$\zeta_h(t) = \mathcal{I}_h[\mathbf{m}_{hk}^-(t) \times \varphi(t)] \quad \text{for all } t \in [0, T].$$

Let $0 \leq i \leq M-1$. For all $t \in [t_i, t_{i+1})$ and $\mathbf{z} \in \mathcal{N}_h$, it holds that

$$\begin{aligned} \zeta_h(t)(\mathbf{z}) \cdot \mathbf{m}_h^i(\mathbf{z}) &= \mathcal{I}_h[\mathbf{m}_{hk}^-(t) \times \varphi(t)](\mathbf{z}) \cdot \mathbf{m}_h^i(\mathbf{z}) \\ &= \mathcal{I}_h[\mathbf{m}_h^i \times \varphi(t)](\mathbf{z}) \cdot \mathbf{m}_h^i(\mathbf{z}) \\ &= [\mathbf{m}_h^i(\mathbf{z}) \times \varphi(\mathbf{z}, t)] \cdot \mathbf{m}_h^i(\mathbf{z}) = 0. \end{aligned}$$

This shows that, for all $0 \leq i \leq M-1$ and $t \in [t_i, t_{i+1})$, $\zeta_h(t)$ belongs to $\mathcal{K}_{\mathbf{m}_h^i}$. Therefore, for each $0 \leq i \leq M-1$, in (4.9) we can choose the test function $\phi_h = \zeta_h(t) \in \mathcal{K}_{\mathbf{m}_h^i}$ for all $t \in (t_i, t_{i+1})$. Then, integrating over time, we obtain the identity

$$\begin{aligned} &\alpha \int_0^T \langle \mathbf{v}_{hk}^-(t), \zeta_h(t) \rangle dt + \int_0^T \langle \mathbf{m}_{hk}^-(t) \times \mathbf{v}_{hk}^-(t), \zeta_h(t) \rangle dt + \lambda_{\text{ex}}^2 \theta k \int_0^T \langle \nabla \mathbf{v}_{hk}^-(t), \nabla \zeta_h(t) \rangle dt \\ &= -\lambda_{\text{ex}}^2 \int_0^T \langle \nabla \mathbf{m}_{hk}^-(t), \nabla \zeta_h(t) \rangle dt + \int_0^T \langle \pi_{hk}^-(t) + \mathbf{f}_{hk}^-(t) + \Pi_{hk}^-(t), \zeta_h(t) \rangle dt. \end{aligned} \quad (4.46)$$

Since $\mathbf{m}_{hk}^- \rightarrow \mathbf{m}$ in $\mathbf{L}^2(\Omega_T)$ by (4.37e), it is straightforward to show that

$$\mathbf{m}_{hk}^- \times \varphi \rightarrow \mathbf{m} \times \varphi \quad \text{in } \mathbf{L}^2(\Omega_T), \quad (4.47a)$$

$$\mathbf{m}_{hk}^- \times \nabla \varphi \rightarrow \mathbf{m} \times \nabla \varphi \quad \text{in } \mathbf{L}^2(\Omega_T). \quad (4.47b)$$

From the approximation properties of the nodal interpolant (Proposition 3.4.3) and Lemma 3.4.12, we deduce that, for all $t \in (0, T)$, it holds that

$$\begin{aligned} \|(\text{Id} - \mathcal{I}_h)[\mathbf{m}_{hk}^-(t) \times \varphi(t)]\|_{\mathbf{H}^1(\Omega)}^2 &= \sum_{K \in \mathcal{T}_h} \|(\text{Id} - \mathcal{I}_h)[\mathbf{m}_{hk}^-(t) \times \varphi(t)]\|_{\mathbf{H}^1(K)}^2 \\ &\lesssim h^2 \sum_{K \in \mathcal{T}_h} |\mathbf{m}_{hk}^-(t) \times \varphi(t)|_{\mathbf{H}^2(K)}^2 \\ &\stackrel{(3.28)}{\lesssim} h^2 \|\mathbf{m}_{hk}^-(t)\|_{\mathbf{H}^1(\Omega)}^2 \|\varphi(t)\|_{\mathbf{W}^{2,\infty}(\Omega)}^2. \end{aligned}$$

In particular, it follows that

$$\|(\text{Id} - \mathcal{I}_h)[\mathbf{m}_{hk}^- \times \varphi]\|_{L^\infty(0,T;\mathbf{H}^1(\Omega))} \lesssim h \|\mathbf{m}_{hk}^-\|_{L^\infty(0,T;\mathbf{H}^1(\Omega))} \|\varphi\|_{\mathbf{W}^{2,\infty}(\Omega_T)} \lesssim h. \quad (4.48)$$

Finally, we recall the convergence results

$$\begin{aligned} \pi_{hk}^- &\rightharpoonup \pi(\mathbf{m}) \quad \text{in } \mathbf{L}^2(\Omega_T), \\ \mathbf{f}_{hk}^- &\rightharpoonup \mathbf{f} \quad \text{in } \mathbf{L}^2(\Omega_T), \\ \Pi_{hk}^- &\rightharpoonup \Pi(\mathbf{m}) \quad \text{in } \mathbf{L}^2(\Omega_T), \end{aligned}$$

which hold thanks to assumptions (4.17)–(4.18).

• **Step 3:** We show that

$$\begin{aligned}
& \alpha \int_0^T \langle \mathbf{v}_{hk}^-(t), \mathbf{m}_{hk}^-(t) \times \boldsymbol{\varphi}(t) \rangle dt + \int_0^T \langle \mathbf{m}_{hk}^-(t) \times \mathbf{v}_{hk}^-(t), \mathbf{m}_{hk}^-(t) \times \boldsymbol{\varphi}(t) \rangle dt \\
& + \lambda_{\text{ex}}^2 \int_0^T \langle \nabla \mathbf{m}_{hk}^-(t), \nabla (\mathbf{m}_{hk}^-(t) \times \boldsymbol{\varphi}(t)) \rangle dt + \lambda_{\text{ex}}^2 \theta k \int_0^T \langle \nabla \mathbf{v}_{hk}^-(t), \nabla (\mathbf{m}_{hk}^-(t) \times \boldsymbol{\varphi}(t)) \rangle dt \\
& - \int_0^T \langle \boldsymbol{\pi}_{hk}^-(t) + \mathbf{f}_{hk}^-(t) + \boldsymbol{\Pi}_{hk}^-(t), \mathbf{m}_{hk}^-(t) \times \boldsymbol{\varphi}(t) \rangle dt = \mathcal{O}(h) \quad \text{as } k, h \rightarrow 0.
\end{aligned} \tag{4.49}$$

First, comparing (4.46) to (4.49), we note that (4.49) is equivalent to the identity

$$\begin{aligned}
& \alpha \int_0^T \langle \mathbf{v}_{hk}^-(t), (\mathcal{I}_h - \mathbf{Id})[\mathbf{m}_{hk}^-(t) \times \boldsymbol{\varphi}(t)] \rangle dt + \int_0^T \langle \mathbf{m}_{hk}^-(t) \times \mathbf{v}_{hk}^-(t), (\mathcal{I}_h - \mathbf{Id})[\mathbf{m}_{hk}^-(t) \times \boldsymbol{\varphi}(t)] \rangle dt \\
& + \lambda_{\text{ex}}^2 \int_0^T \langle \nabla \mathbf{m}_{hk}^-(t), \nabla (\mathcal{I}_h - \mathbf{Id})[\mathbf{m}_{hk}^-(t) \times \boldsymbol{\varphi}(t)] \rangle dt \\
& + \lambda_{\text{ex}}^2 \theta k \int_0^T \langle \nabla \mathbf{v}_{hk}^-(t), \nabla (\mathcal{I}_h - \mathbf{Id})[\mathbf{m}_{hk}^-(t) \times \boldsymbol{\varphi}(t)] \rangle dt \\
& - \int_0^T \langle \boldsymbol{\pi}_{hk}^-(t) + \mathbf{f}_{hk}^-(t) + \boldsymbol{\Pi}_{hk}^-(t), (\mathcal{I}_h - \mathbf{Id})[\mathbf{m}_{hk}^-(t) \times \boldsymbol{\varphi}(t)] \rangle dt = \mathcal{O}(h) \quad \text{as } k, h \rightarrow 0.
\end{aligned} \tag{4.50}$$

To show (4.50), we prove that each term which appears on the left-hand side is essentially bounded by the mesh size h . For the first term and the third term, we deduce from Proposition 4.3.9 that

$$\begin{aligned}
\left| \int_0^T \langle \mathbf{v}_{hk}^-(t), (\mathcal{I}_h - \mathbf{Id})[\mathbf{m}_{hk}^-(t) \times \boldsymbol{\varphi}(t)] \rangle dt \right| & \leq \| \mathbf{v}_{hk}^- \|_{L^2(\Omega_T)} \| (\mathcal{I}_h - \mathbf{Id})[\mathbf{m}_{hk}^- \times \boldsymbol{\varphi}] \|_{L^2(\Omega_T)} \\
& \stackrel{(4.35)}{\lesssim} \| (\mathcal{I}_h - \mathbf{Id})[\mathbf{m}_{hk}^- \times \boldsymbol{\varphi}] \|_{L^2(\Omega_T)} \stackrel{(4.48)}{\lesssim} h
\end{aligned}$$

and

$$\begin{aligned}
& \left| \int_0^T \langle \nabla \mathbf{m}_{hk}^-(t), \nabla (\mathcal{I}_h - \mathbf{Id})[\mathbf{m}_{hk}^-(t) \times \boldsymbol{\varphi}(t)] \rangle dt \right| \\
& \leq \| \nabla \mathbf{m}_{hk}^- \|_{L^2(\Omega_T)} \| \nabla (\mathcal{I}_h - \mathbf{Id})[\mathbf{m}_{hk}^- \times \boldsymbol{\varphi}] \|_{L^2(\Omega_T)} \\
& \stackrel{(4.35)}{\lesssim} \| \nabla (\mathcal{I}_h - \mathbf{Id})[\mathbf{m}_{hk}^- \times \boldsymbol{\varphi}] \|_{L^2(\Omega_T)} \stackrel{(4.48)}{\lesssim} h,
\end{aligned}$$

respectively. For the second term, we apply the generalized Hölder inequality and Proposition 4.3.9, and we exploit the Sobolev embedding $\mathbf{H}^1(\Omega) \subset \mathbf{L}^4(\Omega)$; see, e.g., [106, Theorem 7.26]. It follows that

$$\begin{aligned}
& \left| \int_0^T \langle \mathbf{m}_{hk}^-(t) \times \mathbf{v}_{hk}^-(t), (\mathcal{I}_h - \mathbf{Id})[\mathbf{m}_{hk}^-(t) \times \boldsymbol{\varphi}(t)] \rangle dt \right| \\
& \leq \int_0^T \| \mathbf{m}_{hk}^-(t) \|_{L^4(\Omega)} \| \mathbf{v}_{hk}^-(t) \|_{L^2(\Omega)} \| (\mathcal{I}_h - \mathbf{Id})[\mathbf{m}_{hk}^-(t) \times \boldsymbol{\varphi}(t)] \|_{L^4(\Omega)} dt \\
& \lesssim \int_0^T \| \mathbf{m}_{hk}^-(t) \|_{\mathbf{H}^1(\Omega)} \| \mathbf{v}_{hk}^-(t) \|_{L^2(\Omega)} \| (\mathcal{I}_h - \mathbf{Id})[\mathbf{m}_{hk}^-(t) \times \boldsymbol{\varphi}(t)] \|_{\mathbf{H}^1(\Omega)} dt \\
& \leq \| \mathbf{m}_{hk}^- \|_{L^\infty(0,T;\mathbf{H}^1(\Omega))} \| \mathbf{v}_{hk}^- \|_{L^2(0,T;\mathbf{H}^1(\Omega))} \| (\mathcal{I}_h - \mathbf{Id})[\mathbf{m}_{hk}^- \times \boldsymbol{\varphi}] \|_{L^2(0,T;\mathbf{H}^1(\Omega))} \\
& \stackrel{(4.35)}{\lesssim} \| (\mathcal{I}_h - \mathbf{Id})[\mathbf{m}_{hk}^- \times \boldsymbol{\varphi}] \|_{L^2(0,T;\mathbf{H}^1(\Omega))} \stackrel{(4.48)}{\lesssim} h.
\end{aligned}$$

For the fourth term, since $k \|\nabla \mathbf{v}_{hk}^-\|_{\mathbf{L}^2(\Omega_T)} \rightarrow 0$ by Lemma 4.3.10, we obtain

$$\begin{aligned} & k \left| \int_0^T \langle \nabla \mathbf{v}_{hk}^-(t), \nabla(\mathcal{I}_h - \mathbf{Id})[\mathbf{m}_{hk}^-(t) \times \boldsymbol{\varphi}(t)] \rangle dt \right| \\ & \leq k \|\nabla \mathbf{v}_{hk}^-\|_{\mathbf{L}^2(\Omega_T)} \|\nabla(\mathcal{I}_h - \mathbf{Id})[\mathbf{m}_{hk}^- \times \boldsymbol{\varphi}]\|_{\mathbf{L}^2(\Omega_T)} \\ & \stackrel{(4.36)}{\lesssim} \|\nabla(\mathcal{I}_h - \mathbf{Id})[\mathbf{m}_{hk}^- \times \boldsymbol{\varphi}]\|_{\mathbf{L}^2(\Omega_T)} \stackrel{(4.48)}{\lesssim} h. \end{aligned}$$

For the last term on the left-hand side of (4.50), we proceed in a similar way and obtain the estimate

$$\begin{aligned} & \left| \int_0^T \langle \boldsymbol{\pi}_{hk}^-(t) + \mathbf{f}_{hk}^-(t) + \boldsymbol{\Pi}_{hk}^-(t), (\mathcal{I}_h - \mathbf{Id})[\mathbf{m}_{hk}^-(t) \times \boldsymbol{\varphi}(t)] \rangle dt \right| \\ & \leq \left(\|\boldsymbol{\pi}_{hk}^-\|_{\mathbf{L}^2(\Omega_T)} + \|\mathbf{f}_{hk}^-\|_{\mathbf{L}^2(\Omega_T)} + \|\boldsymbol{\Pi}_{hk}^-\|_{\mathbf{L}^2(\Omega_T)} \right) \|(\mathcal{I}_h - \mathbf{Id})[\mathbf{m}_{hk}^- \times \boldsymbol{\varphi}]\|_{\mathbf{L}^2(\Omega_T)} \\ & \lesssim \|(\mathcal{I}_h - \mathbf{Id})[\mathbf{m}_{hk}^- \times \boldsymbol{\varphi}]\|_{\mathbf{L}^2(\Omega_T)} \stackrel{(4.48)}{\lesssim} h. \end{aligned}$$

This concludes the proof of (4.50) and thus yields (4.49).

- **Step 4:** We consider each of the five terms on the left-hand side of (4.49) and show that, as $k, h \rightarrow 0$, the fourth integral vanishes, while the remaining four terms converge towards the corresponding terms in the variational formulation (4.4).

We will repeatedly use the fact that, in a Hilbert space, the sequence of scalar products of a weakly and a strongly convergent sequence converges towards the scalar product of the limits of both the sequences.

For the first term on the left-hand side of (4.49), thanks to (4.47a) and the weak convergence $\mathbf{v}_{hk} \rightharpoonup \partial_t \mathbf{m}$ in $\mathbf{L}^2(\Omega_T)$ by (4.37h), we obtain that

$$\int_0^T \langle \mathbf{v}_{hk}^-(t), \mathbf{m}_{hk}^-(t) \times \boldsymbol{\varphi}(t) \rangle dt \rightarrow \int_0^T \langle \partial_t \mathbf{m}(t), \mathbf{m}(t) \times \boldsymbol{\varphi}(t) \rangle dt = - \int_0^T \langle \mathbf{m}(t) \times \partial_t \mathbf{m}(t), \boldsymbol{\varphi}(t) \rangle dt.$$

To treat the second term on the left-hand side of (4.49), we first recall the so-called Lagrange identity

$$(\mathbf{a} \times \mathbf{b}) \cdot (\mathbf{c} \times \mathbf{d}) = (\mathbf{a} \cdot \mathbf{c})(\mathbf{b} \cdot \mathbf{d}) - (\mathbf{a} \cdot \mathbf{d})(\mathbf{b} \cdot \mathbf{c}) \quad \text{for all } \mathbf{a}, \mathbf{b}, \mathbf{c}, \mathbf{d} \in \mathbb{R}^3; \quad (4.51)$$

see Proposition B.2.1(vii). On the one hand, in the case of the standard tangent plane scheme, from Lemma 4.3.14, we obtain the weak convergence

$$\mathbf{m}_{hk}^- \times \mathbf{v}_{hk}^- \rightharpoonup \mathbf{m} \times \partial_t \mathbf{m} \quad \text{in } \mathbf{L}^2(\Omega_T).$$

Using (4.47a), it follows that

$$\begin{aligned} \int_0^T \langle \mathbf{m}_{hk}^-(t) \times \mathbf{v}_{hk}^-(t), \mathbf{m}_{hk}^-(t) \times \boldsymbol{\varphi}(t) \rangle dt & \rightarrow \int_0^T \langle \mathbf{m}(t) \times \partial_t \mathbf{m}(t), \mathbf{m}(t) \times \boldsymbol{\varphi}(t) \rangle dt \\ & = \int_0^T \langle \partial_t \mathbf{m}(t), \boldsymbol{\varphi}(t) \rangle dt. \end{aligned}$$

The latter equality follows from (4.51), together with $|\mathbf{m}| = 1$ and $\mathbf{m} \cdot \partial_t \mathbf{m} = 0$, which hold a.e. in Ω_T . On the other hand, to show the convergence of the integral in the case of the projection-free tangent plane scheme, we first recall the continuous embedding $\mathbf{H}^s(\Omega) \subset \mathbf{L}^4(\Omega)$, which holds for all $s \geq 3/4$, and note that, thanks to Lemma 4.3.14, we have the strong convergence

$$\mathbf{m}_{hk}^- \rightarrow \mathbf{m} \quad \text{in } L^2(0, T; \mathbf{H}^s(\Omega)) \text{ for all } 0 < s < 1.$$

Choosing an arbitrary $3/4 \leq s < 1$, we obtain the estimate

$$\begin{aligned}
\| |\mathbf{m}_{hk}^-|^2 - 1 \|_{L^2(\Omega_T)}^2 &= \| |\mathbf{m}_{hk}^-|^2 - |\mathbf{m}|^2 \|_{L^2(\Omega_T)}^2 \\
&= \int_0^T \| |\mathbf{m}_{hk}^-(t)|^2 - |\mathbf{m}(t)|^2 \|_{L^2(\Omega)}^2 dt \\
&= \int_0^T \| [\mathbf{m}_{hk}^-(t) + \mathbf{m}(t)] \cdot [\mathbf{m}_{hk}^-(t) - \mathbf{m}(t)] \|_{L^2(\Omega)}^2 dt \\
&\leq \int_0^T \| \mathbf{m}_{hk}^-(t) + \mathbf{m}(t) \|_{L^4(\Omega)}^2 \| \mathbf{m}_{hk}^-(t) - \mathbf{m}(t) \|_{L^4(\Omega)}^2 dt \\
&\leq \int_0^T \| \mathbf{m}_{hk}^-(t) + \mathbf{m}(t) \|_{H^1(\Omega)}^2 \| \mathbf{m}_{hk}^-(t) - \mathbf{m}(t) \|_{H^s(\Omega)}^2 dt \\
&\leq \| \mathbf{m}_{hk}^- + \mathbf{m} \|_{L^\infty(0,T;H^1(\Omega))}^2 \| \mathbf{m}_{hk}^- - \mathbf{m} \|_{L^2(0,T;H^s(\Omega))}^2 \\
&\lesssim \| \mathbf{m}_{hk}^- - \mathbf{m} \|_{L^2(0,T;H^s(\Omega))}^2 \rightarrow 0,
\end{aligned}$$

i.e., it holds that $|\mathbf{m}_{hk}^-|^2 \rightarrow 1$ in $L^2(\Omega_T)$. Together with the weak convergence $\mathbf{v}_{hk}^- \cdot \boldsymbol{\varphi} \rightharpoonup \partial_t \mathbf{m} \cdot \boldsymbol{\varphi}$ in $L^2(\Omega_T)$, it follows that

$$\begin{aligned}
&\int_0^T \langle \mathbf{m}_{hk}^-(t) \times \mathbf{v}_{hk}^-(t), \mathbf{m}_{hk}^-(t) \times \boldsymbol{\varphi}(t) \rangle dt \\
&\stackrel{(4.51)}{=} \int_0^T \langle |\mathbf{m}_{hk}^-(t)|^2, \mathbf{v}_{hk}^-(t) \cdot \boldsymbol{\varphi}(t) \rangle dt \rightarrow \int_0^T \langle \partial_t \mathbf{m}(t), \boldsymbol{\varphi}(t) \rangle dt,
\end{aligned}$$

which is the desired result.

For the third term on the left-hand side of (4.49), from the weak convergence $\nabla \mathbf{m}_{hk}^- \rightharpoonup \nabla \mathbf{m}$ in $L^2(\Omega_T)$ and (4.47b), we deduce that

$$\begin{aligned}
&\int_0^T \langle \nabla \mathbf{m}_{hk}^-(t), \nabla [\mathbf{m}_{hk}^-(t) \times \boldsymbol{\varphi}(t)] \rangle dt = \int_0^T \langle \nabla \mathbf{m}_{hk}^-(t), \mathbf{m}_{hk}^-(t) \times \nabla \boldsymbol{\varphi}(t) \rangle dt \\
&\rightarrow \int_0^T \langle \nabla \mathbf{m}(t), \mathbf{m}(t) \times \nabla \boldsymbol{\varphi}(t) \rangle dt = - \int_0^T \langle \mathbf{m}(t) \times \nabla \mathbf{m}(t), \nabla \boldsymbol{\varphi}(t) \rangle dt.
\end{aligned}$$

Similarly, for the last term on the left-hand side of (4.49), thanks to (4.17)–(4.18) and (4.47a), it follows that

$$\begin{aligned}
&\int_0^T \langle \boldsymbol{\pi}_{hk}^-(t), \mathbf{m}_{hk}^-(t) \times \boldsymbol{\varphi}(t) \rangle dt \rightarrow \int_0^T \langle \boldsymbol{\pi}(\mathbf{m}(t)), \mathbf{m}(t) \times \boldsymbol{\varphi}(t) \rangle dt = - \int_0^T \langle \mathbf{m}(t) \times \boldsymbol{\pi}(\mathbf{m}(t)), \boldsymbol{\varphi}(t) \rangle dt, \\
&\int_0^T \langle \mathbf{f}_{hk}^-(t), \mathbf{m}_{hk}^-(t) \times \boldsymbol{\varphi}(t) \rangle dt \rightarrow \int_0^T \langle \mathbf{f}(t), \mathbf{m}(t) \times \boldsymbol{\varphi}(t) \rangle dt = - \int_0^T \langle \mathbf{m}(t) \times \mathbf{f}(t), \boldsymbol{\varphi}(t) \rangle dt,
\end{aligned}$$

and

$$\int_0^T \langle \boldsymbol{\Pi}_{hk}^-(t), \mathbf{m}_{hk}^-(t) \times \boldsymbol{\varphi}(t) \rangle dt \rightarrow \int_0^T \langle \boldsymbol{\Pi}(\mathbf{m}(t)), \mathbf{m}(t) \times \boldsymbol{\varphi}(t) \rangle dt = - \int_0^T \langle \mathbf{m}(t) \times \boldsymbol{\Pi}(\mathbf{m}(t)), \boldsymbol{\varphi}(t) \rangle dt.$$

We conclude this step of the proof by considering the fourth term on the left-hand side of (4.49). It holds that

$$\begin{aligned}
k \left| \int_0^T \langle \nabla \mathbf{v}_{hk}^-(t), \nabla (\mathbf{m}_{hk}^-(t) \times \boldsymbol{\varphi}(t)) \rangle dt \right| &\leq k \| \nabla \mathbf{v}_{hk}^- \|_{L^2(\Omega_T)} \| \nabla \mathbf{m}_{hk}^- \|_{L^2(\Omega_T)} \| \boldsymbol{\varphi} \|_{\mathbf{W}^{1,\infty}(\Omega_T)} \\
&\lesssim k \| \nabla \mathbf{v}_{hk}^- \|_{L^2(\Omega_T)}.
\end{aligned}$$

From the convergence $k \|\nabla \mathbf{v}_{hk}^-\|_{L^2(\Omega_T)} \rightarrow 0$ ensured by Lemma 4.3.10, it follows that

$$k \int_0^T \langle \nabla \mathbf{v}_{hk}^-(t), \nabla(\mathbf{m}_{hk}^-(t) \times \boldsymbol{\varphi}(t)) \rangle dt \rightarrow 0.$$

This shows that \mathbf{m} satisfies the variational formulation (4.4) for all $\boldsymbol{\varphi} \in \mathbf{C}^\infty(\overline{\Omega_T})$. By density, the result also holds for all $\boldsymbol{\varphi} \in \mathbf{H}^1(\Omega_T)$, which verifies Definition 4.1.1(iii) and concludes the proof of part (b) of the theorem.

• **Step 5:** Proof of part (c) of the theorem.

We aim to verify Definition 4.1.1(iv), i.e., to show that \mathbf{m} satisfies the energy inequality (4.5).

For all $0 \leq i \leq M$, we use the notation $\mathbf{f}^i := \mathbf{f}(t_i)$. We recall that, in the case of the standard tangent plane scheme, by assumption (4.19) it holds that $\mathbf{f}^i \in \mathbf{L}^4(\Omega)$ for all $0 \leq i \leq M$. Moreover, we consider the continuous piecewise linear time-approximation \mathbf{f}_k and the two piecewise constant time-approximations \mathbf{f}_k^- and \mathbf{f}_k^+ from (3.13), defined by

$$\mathbf{f}_k(t) := \frac{t - t_i}{k} \mathbf{f}^{i+1} + \frac{t_{i+1} - t}{k} \mathbf{f}^i, \quad \mathbf{f}_k^-(t) := \mathbf{f}^i, \quad \text{and} \quad \mathbf{f}_k^+(t) := \mathbf{f}^{i+1}$$

for all $t \in [t_i, t_{i+1})$ and $0 \leq i \leq M - 1$. Note that, since $\mathbf{f} \in C^1([0, T], \mathbf{L}^2(\Omega))$, it holds that $\mathbf{f}_k, \mathbf{f}_k^\pm \rightarrow \mathbf{f}$ in $\mathbf{L}^2(\Omega_T)$ and $\partial_t \mathbf{f}_k \rightarrow \partial_t \mathbf{f}$ in $\mathbf{L}^2(\Omega_T)$ as $k \rightarrow 0$.

Given an arbitrary time $\tau \in [0, T)$, let $1 \leq j \leq M$ such that $\tau \in [t_{j-1}, t_j)$. Let $0 \leq i \leq j - 1$. From Lemma 4.3.7, we deduce that

$$\begin{aligned} & \mathcal{E}(\mathbf{m}_h^{i+1}, \mathbf{f}^{i+1}) - \mathcal{E}(\mathbf{m}_h^i, \mathbf{f}^i) \\ &= \frac{\lambda_{\text{ex}}^2}{2} k d_t \|\nabla \mathbf{m}_h^{i+1}\|_{L^2(\Omega)}^2 - \frac{1}{2} \langle \boldsymbol{\pi}(\mathbf{m}_h^{i+1}), \mathbf{m}_h^{i+1} \rangle + \frac{1}{2} \langle \boldsymbol{\pi}(\mathbf{m}_h^i), \mathbf{m}_h^i \rangle - \langle \mathbf{f}^{i+1}, \mathbf{m}_h^{i+1} \rangle + \langle \mathbf{f}^i, \mathbf{m}_h^i \rangle \\ &\leq -[\alpha - c(k, h)] k \|\mathbf{v}_h^i\|_{L^2(\Omega)}^2 - \lambda_{\text{ex}}^2 \left(\theta - \frac{1}{2} \right) k^2 \|\nabla \mathbf{v}_h^i\|_{L^2(\Omega)}^2 \\ &\quad - \underbrace{\langle \mathbf{f}^{i+1}, \mathbf{m}_h^{i+1} \rangle + \langle \mathbf{f}^i, \mathbf{m}_h^i \rangle + k \langle \mathbf{f}_h^i, \mathbf{v}_h^i \rangle}_{T_{\mathbf{f}} :=} \\ &\quad - \underbrace{\frac{1}{2} \langle \boldsymbol{\pi}(\mathbf{m}_h^{i+1}), \mathbf{m}_h^{i+1} \rangle + \frac{1}{2} \langle \boldsymbol{\pi}(\mathbf{m}_h^i), \mathbf{m}_h^i \rangle + k \langle \boldsymbol{\pi}_h(\mathbf{m}_h^i), \mathbf{v}_h^i \rangle + k \langle \boldsymbol{\Pi}_h(\mathbf{m}_h^i), \mathbf{v}_h^i \rangle}_{T_{\boldsymbol{\pi}} :=}. \end{aligned}$$

On the one hand, for the standard tangent plane scheme, it holds that $c(k, h) = 0$ if the triangulation \mathcal{T}_h satisfies the angle condition (3.16) and $c(k, h) = Ckh^{-2}$ otherwise, with $C > 0$ being a constant which depends only on γ and λ_{ex} ; see (4.25). On the other hand, for the projection-free tangent plane scheme, it holds that $c(k, h) = 0$ and the inequality actually turns out to be an equality; see (4.26). In $T_{\boldsymbol{\pi}}$ and $T_{\mathbf{f}}$, we have collected the terms related to $\boldsymbol{\pi}$ and \mathbf{f} , respectively.

We now perform some algebraic manipulations. We can rewrite $T_{\boldsymbol{\pi}}$ as

$$\begin{aligned} T_{\boldsymbol{\pi}} &= -\frac{1}{2} \langle \boldsymbol{\pi}(\mathbf{m}_h^{i+1}), \mathbf{m}_h^{i+1} \rangle + \frac{1}{2} \langle \boldsymbol{\pi}(\mathbf{m}_h^i), \mathbf{m}_h^i \rangle + k \langle \boldsymbol{\pi}_h(\mathbf{m}_h^i), \mathbf{v}_h^i \rangle \\ &= -k \langle \boldsymbol{\pi}(\mathbf{m}_h^i) - \boldsymbol{\pi}_h(\mathbf{m}_h^i), \mathbf{v}_h^i \rangle + k \langle \boldsymbol{\pi}(\mathbf{m}_h^i), \mathbf{v}_h^i \rangle - \frac{1}{2} \langle \boldsymbol{\pi}(\mathbf{m}_h^{i+1}), \mathbf{m}_h^{i+1} \rangle + \frac{1}{2} \langle \boldsymbol{\pi}(\mathbf{m}_h^i), \mathbf{m}_h^i \rangle \\ &= -k \langle \boldsymbol{\pi}(\mathbf{m}_h^i) - \boldsymbol{\pi}_h(\mathbf{m}_h^i), \mathbf{v}_h^i \rangle - \frac{k}{2} \langle \boldsymbol{\pi}(\mathbf{m}_h^{i+1}) - \boldsymbol{\pi}(\mathbf{m}_h^i), \mathbf{v}_h^i \rangle + \frac{k}{2} \langle \boldsymbol{\pi}(\mathbf{m}_h^{i+1}) + \boldsymbol{\pi}(\mathbf{m}_h^i), \mathbf{v}_h^i \rangle \\ &\quad - \frac{1}{2} \langle \boldsymbol{\pi}(\mathbf{m}_h^{i+1}), \mathbf{m}_h^{i+1} \rangle + \frac{1}{2} \langle \boldsymbol{\pi}(\mathbf{m}_h^i), \mathbf{m}_h^i \rangle, \end{aligned}$$

where in the second equality we have just added and subtracted the quantity $k \langle \boldsymbol{\pi}(\mathbf{m}_h^i), \mathbf{v}_h^i \rangle$, while in the third equality we have just added and subtracted the quantity $\frac{k}{2} \langle \boldsymbol{\pi}(\mathbf{m}_h^{i+1}), \mathbf{v}_h^i \rangle$. Since $\boldsymbol{\pi}$ is self-adjoint, it holds that

$$\langle \boldsymbol{\pi}(\mathbf{m}_h^{i+1}), \mathbf{m}_h^{i+1} \rangle - \langle \boldsymbol{\pi}(\mathbf{m}_h^i), \mathbf{m}_h^i \rangle = \langle \boldsymbol{\pi}(\mathbf{m}_h^{i+1}) + \boldsymbol{\pi}(\mathbf{m}_h^i), \mathbf{m}_h^{i+1} - \mathbf{m}_h^i \rangle.$$

Finally, using the linearity of π , it follows that

$$T\pi = -k\langle \pi(\mathbf{m}_h^i) - \pi_h(\mathbf{m}_h^i), \mathbf{v}_h^i \rangle - \frac{k}{2}\langle \pi(\mathbf{m}_h^{i+1} - \mathbf{m}_h^i), \mathbf{v}_h^i \rangle - \frac{1}{2}\langle \pi(\mathbf{m}_h^{i+1} + \mathbf{m}_h^i), \mathbf{m}_h^{i+1} - \mathbf{m}_h^i - k\mathbf{v}_h^i \rangle.$$

For T_f , we proceed similarly. Rearranging the terms, we can rewrite T_f as

$$\begin{aligned} T_f &= -\langle \mathbf{f}^{i+1}, \mathbf{m}_h^{i+1} \rangle + \langle \mathbf{f}^i, \mathbf{m}_h^i \rangle + k\langle \mathbf{f}_h^i, \mathbf{v}_h^i \rangle \\ &= -\langle \mathbf{f}^{i+1} - \mathbf{f}^i, \mathbf{m}_h^{i+1} \rangle - \langle \mathbf{f}^i, \mathbf{m}_h^{i+1} - \mathbf{m}_h^i \rangle + k\langle \mathbf{f}_h^i, \mathbf{v}_h^i \rangle \\ &= -k\langle d_t \mathbf{f}^{i+1}, \mathbf{m}_h^{i+1} \rangle - \langle \mathbf{f}^i, \mathbf{m}_h^{i+1} - \mathbf{m}_h^i - k\mathbf{v}_h^i \rangle - k\langle \mathbf{f}^i - \mathbf{f}_h^i, \mathbf{v}_h^i \rangle, \end{aligned}$$

where in the second equality we have just added and subtracted the quantity $\langle \mathbf{f}^i, \mathbf{m}_h^{i+1} \rangle$, while in the third equality we have just added and subtracted the quantity $k\langle \mathbf{f}^i, \mathbf{v}_h^i \rangle$.

Altogether, after these algebraic manipulations, we have thus obtained the inequality

$$\begin{aligned} &\mathcal{E}(\mathbf{m}_h^{i+1}, \mathbf{f}^{i+1}) - \mathcal{E}(\mathbf{m}_h^i, \mathbf{f}^i) + [\alpha - c(k, h)]k \|\mathbf{v}_h^i\|_{L^2(\Omega)}^2 + k\langle d_t \mathbf{f}^{i+1}, \mathbf{m}_h^{i+1} \rangle - k\langle \Pi_h(\mathbf{m}_h^i), \mathbf{v}_h^i \rangle \\ &+ \lambda_{\text{ex}}^2 \left(\theta - \frac{1}{2} \right) k^2 \|\nabla \mathbf{v}_h^i\|_{L^2(\Omega)}^2 + k\langle \pi(\mathbf{m}_h^i) - \pi_h(\mathbf{m}_h^i), \mathbf{v}_h^i \rangle + k\langle \mathbf{f}^i - \mathbf{f}_h^i, \mathbf{v}_h^i \rangle \\ &\leq -\frac{k}{2}\langle \pi(\mathbf{m}_h^{i+1} - \mathbf{m}_h^i), \mathbf{v}_h^i \rangle - \frac{1}{2}\langle \pi(\mathbf{m}_h^{i+1} + \mathbf{m}_h^i), \mathbf{m}_h^{i+1} - \mathbf{m}_h^i - k\mathbf{v}_h^i \rangle \\ &\quad - \langle \mathbf{f}^i, \mathbf{m}_h^{i+1} - \mathbf{m}_h^i - k\mathbf{v}_h^i \rangle. \end{aligned} \tag{4.52}$$

We now analyze the three terms which constitute the right-hand side. We start with the case of the standard tangent plane scheme. First of all, using the well-known interpolation result $\mathbf{L}^{8/3}(\Omega) = [\mathbf{L}^2(\Omega), \mathbf{L}^4(\Omega)]_{1/2}$ (see, e.g., [45, Theorem 5.1.1]) together with the Sobolev embedding $\mathbf{H}^1(\Omega) \subset \mathbf{L}^4(\Omega)$, we obtain the inequality

$$\|\mathbf{v}_h^i\|_{\mathbf{L}^{8/3}(\Omega)}^2 \leq \|\mathbf{v}_h^i\|_{L^2(\Omega)} \|\mathbf{v}_h^i\|_{L^4(\Omega)} \lesssim \|\mathbf{v}_h^i\|_{L^2(\Omega)} \|\mathbf{v}_h^i\|_{\mathbf{H}^1(\Omega)}. \tag{4.53}$$

For the first term on the right-hand side of (4.52), we apply the Cauchy–Schwarz inequality and exploit the boundedness of π in $\mathbf{L}^2(\Omega)$ as well as Corollary 4.3.5. We obtain that

$$\begin{aligned} \frac{k}{2} |\langle \pi(\mathbf{m}_h^{i+1} - \mathbf{m}_h^i), \mathbf{v}_h^i \rangle| &\leq \frac{k}{2} \|\pi(\mathbf{m}_h^{i+1} - \mathbf{m}_h^i)\|_{L^2(\Omega)} \|\mathbf{v}_h^i\|_{L^2(\Omega)} \\ &\lesssim k \|\mathbf{m}_h^{i+1} - \mathbf{m}_h^i\|_{L^2(\Omega)} \|\mathbf{v}_h^i\|_{L^2(\Omega)} \\ &\stackrel{(4.23a)}{\lesssim} k^2 \|\mathbf{v}_h^i\|_{L^2(\Omega)}^2. \end{aligned}$$

Using the Hölder inequality, the boundedness of π in $\mathbf{L}^4(\Omega)$ by assumption (4.19), the identity $\|\mathbf{m}_h^i\|_{L^\infty(\Omega)} = 1$ for all $0 \leq i \leq M$, and Corollary 4.3.5, we can estimate the second term by

$$\begin{aligned} \frac{1}{2} |\langle \pi(\mathbf{m}_h^{i+1} + \mathbf{m}_h^i), \mathbf{m}_h^{i+1} - \mathbf{m}_h^i - k\mathbf{v}_h^i \rangle| &\leq \frac{1}{2} \|\pi(\mathbf{m}_h^{i+1} + \mathbf{m}_h^i)\|_{L^4(\Omega)} \|\mathbf{m}_h^{i+1} - \mathbf{m}_h^i - k\mathbf{v}_h^i\|_{L^{4/3}(\Omega)} \\ &\lesssim \|\mathbf{m}_h^{i+1} + \mathbf{m}_h^i\|_{L^4(\Omega)} \|\mathbf{m}_h^{i+1} - \mathbf{m}_h^i - k\mathbf{v}_h^i\|_{L^{4/3}(\Omega)} \\ &\stackrel{(4.23c)}{\lesssim} k^2 \|\mathbf{v}_h^i\|_{L^{8/3}(\Omega)}^2 \\ &\stackrel{(4.53)}{\lesssim} k^2 \|\mathbf{v}_h^i\|_{L^2(\Omega)} \|\mathbf{v}_h^i\|_{\mathbf{H}^1(\Omega)}. \end{aligned}$$

As for the third term, using the Hölder inequality, the uniform boundedness of $\|\mathbf{f}^i\|_{L^4(\Omega)}$ by

assumption (4.19), and Corollary 4.3.5, we obtain the estimate

$$\begin{aligned}
|\langle \mathbf{f}^i, \mathbf{m}_h^{i+1} - \mathbf{m}_h^i - k\mathbf{v}_h^i \rangle| &\leq \|\mathbf{f}^i\|_{L^4(\Omega)} \|\mathbf{m}_h^{i+1} - \mathbf{m}_h^i - k\mathbf{v}_h^i\|_{L^{4/3}(\Omega)} \\
&\stackrel{(4.23c)}{\lesssim} k^2 \|\mathbf{v}_h^i\|_{L^{8/3}(\Omega)}^2 \\
&\stackrel{(4.53)}{\lesssim} k^2 \|\mathbf{v}_h^i\|_{L^2(\Omega)} \|\mathbf{v}_h^i\|_{H^1(\Omega)}.
\end{aligned}$$

In the case of the projection-free tangent plane scheme, we estimate the first term on the right-hand side of (4.52) in the same way and observe that, thanks to (4.10a), the second term and the third term vanish. In both cases, we thus obtain the following inequality

$$\begin{aligned}
&\mathcal{E}(\mathbf{m}_h^{i+1}, \mathbf{f}^{i+1}) - \mathcal{E}(\mathbf{m}_h^i, \mathbf{f}^i) + [\alpha - c(k, h)]k \|\mathbf{v}_h^i\|_{L^2(\Omega)}^2 + k \langle d_t \mathbf{f}^{i+1}, \mathbf{m}_h^{i+1} \rangle - k \langle \Pi_h(\mathbf{m}_h^i), \mathbf{v}_h^i \rangle \\
&+ \lambda_{\text{ex}}^2 \left(\theta - \frac{1}{2} \right) k^2 \|\nabla \mathbf{v}_h^i\|_{L^2(\Omega)}^2 + k \langle \pi(\mathbf{m}_h^i) - \pi_h(\mathbf{m}_h^i), \mathbf{v}_h^i \rangle + k \langle \mathbf{f}^i - \mathbf{f}_h^i, \mathbf{v}_h^i \rangle \\
&\lesssim k^2 \left(\|\mathbf{v}_h^i\|_{L^2(\Omega)}^2 + \|\mathbf{v}_h^i\|_{L^2(\Omega)} \|\nabla \mathbf{v}_h^i\|_{L^2(\Omega)} \right).
\end{aligned}$$

If $1/2 \leq \theta \leq 1$, the sixth term on the left-hand side is nonnegative. If $0 \leq \theta < 1/2$, we can argue as in the proof of Lemma 4.3.8 and use an inverse estimate to absorb it into the third term. In both cases, summing over $0 \leq i \leq j-1$, we obtain that

$$\begin{aligned}
&\mathcal{E}(\mathbf{m}_h^j, \mathbf{f}^j) - \mathcal{E}(\mathbf{m}_h^0, \mathbf{f}^0) + [\alpha - C(k, h, \theta)]k \sum_{i=0}^{j-1} \|\mathbf{v}_h^i\|_{L^2(\Omega)}^2 + k \sum_{i=0}^{j-1} \langle d_t \mathbf{f}^{i+1}, \mathbf{m}_h^{i+1} \rangle \\
&- k \sum_{i=0}^{j-1} \langle \Pi_h(\mathbf{m}_h^i), \mathbf{v}_h^i \rangle + k \sum_{i=0}^{j-1} \langle \pi(\mathbf{m}_h^i) - \pi_h(\mathbf{m}_h^i), \mathbf{v}_h^i \rangle + k \sum_{i=0}^{j-1} \langle \mathbf{f}^i - \mathbf{f}_h^i, \mathbf{v}_h^i \rangle \\
&\lesssim k^2 \sum_{i=0}^{j-1} \left(\|\mathbf{v}_h^i\|_{L^2(\Omega)}^2 + \|\mathbf{v}_h^i\|_{L^2(\Omega)} \|\nabla \mathbf{v}_h^i\|_{L^2(\Omega)} \right),
\end{aligned}$$

which can be equivalently rewritten as

$$\begin{aligned}
&\mathcal{E}(\mathbf{m}_{hk}^+(\tau), \mathbf{f}_k^+(\tau)) - \mathcal{E}(\mathbf{m}_{hk}^-(0), \mathbf{f}(0)) + [\alpha - C(k, h, \theta)] \int_0^{t_j} \|\mathbf{v}_{hk}^-(t)\|_{L^2(\Omega)}^2 dt \\
&+ \int_0^{t_j} \langle \partial_t \mathbf{f}_k(t), \mathbf{m}_{hk}^+(t) \rangle dt - \int_0^{t_j} \langle \Pi_{hk}^-(t), \mathbf{v}_{hk}^-(t) \rangle dt + \int_0^{t_j} \langle \pi(\mathbf{m}_{hk}^-(t)) - \pi_{hk}^-(t), \mathbf{v}_{hk}^-(t) \rangle dt \\
&+ \int_0^{t_j} \langle \mathbf{f}_k^-(t) - \mathbf{f}_{hk}^-(t), \mathbf{v}_{hk}^-(t) \rangle dt \\
&\lesssim k \left(\|\mathbf{v}_{hk}^-\|_{L^2(\Omega \times (0, t_j))}^2 + \|\mathbf{v}_{hk}^-\|_{L^2(\Omega \times (0, t_j))} \|\nabla \mathbf{v}_{hk}^-\|_{L^2(\Omega \times (0, t_j))} \right).
\end{aligned}$$

With our assumptions, for all $0 \leq \theta \leq 1$, it holds that $C(k, h, \theta) \rightarrow 0$ as $k, h \rightarrow 0$. In particular, it follows that

$$\begin{aligned}
&\mathcal{E}(\mathbf{m}_{hk}^+(\tau), \mathbf{f}_k^+(\tau)) - \mathcal{E}(\mathbf{m}_{hk}^-(0), \mathbf{f}(0)) + [\alpha - C(k, h, \theta)] \int_0^\tau \|\mathbf{v}_{hk}^-(t)\|_{L^2(\Omega)}^2 dt \\
&+ \int_0^\tau \langle \partial_t \mathbf{f}_k(t), \mathbf{m}_{hk}^+(t) \rangle dt - \int_0^\tau \langle \Pi_{hk}^-(t), \mathbf{v}_{hk}^-(t) \rangle dt \\
&+ \int_\tau^{t_j} \langle \partial_t \mathbf{f}_k(t), \mathbf{m}_{hk}^+(t) \rangle dt - \int_\tau^{t_j} \langle \Pi_{hk}^-(t), \mathbf{v}_{hk}^-(t) \rangle dt \\
&+ \int_0^{t_j} \langle \pi(\mathbf{m}_{hk}^-(t)) - \pi_{hk}^-(t), \mathbf{v}_{hk}^-(t) \rangle dt + \int_0^{t_j} \langle \mathbf{f}_k^-(t) - \mathbf{f}_{hk}^-(t), \mathbf{v}_{hk}^-(t) \rangle dt \\
&\lesssim k \left(\|\mathbf{v}_{hk}^-\|_{L^2(\Omega \times (0, t_j))}^2 + \|\mathbf{v}_{hk}^-\|_{L^2(\Omega \times (0, t_j))} \|\nabla \mathbf{v}_{hk}^-\|_{L^2(\Omega \times (0, t_j))} \right).
\end{aligned} \tag{4.54}$$

We now consider the limit as $k, h \rightarrow 0$ for each term of (4.54). Since $\mathbf{m}_{hk}^+ \rightarrow \mathbf{m}$ in $L^2(0, T; \mathbf{H}^1(\Omega))$ by (4.37d) and $\mathbf{f}_k^+ \rightarrow \mathbf{f}$ in $\mathbf{L}^2(\Omega_T)$, it holds that

$$\mathcal{E}(\mathbf{m}(\tau), \mathbf{f}(\tau)) \leq \liminf_{k, h \rightarrow 0} \mathcal{E}(\mathbf{m}_{hk}^+(\tau), \mathbf{f}_k^+(\tau)).$$

Since $\mathbf{m}_h^0 \rightarrow \mathbf{m}^0$ in $\mathbf{H}^1(\Omega)$ by assumption (4.15) (with strong convergence), it holds that

$$\liminf_{k, h \rightarrow 0} \mathcal{E}(\mathbf{m}_{hk}^-(0), \mathbf{f}(0)) = \lim_{k, h \rightarrow 0} \mathcal{E}(\mathbf{m}_{hk}^-(0), \mathbf{f}(0)) = \mathcal{E}(\mathbf{m}^0, \mathbf{f}(0)).$$

From the convergence $\mathbf{v}_{hk}^- \rightarrow \partial_t \mathbf{m}$ in $\mathbf{L}^2(\Omega_T)$ by (4.37h), it follows that

$$\int_0^\tau \|\partial_t \mathbf{m}(t)\|_{\mathbf{L}^2(\Omega)}^2 dt \leq \liminf_{k, h \rightarrow 0} \int_0^\tau \|\mathbf{v}_{hk}^-(t)\|_{\mathbf{L}^2(\Omega)}^2 dt.$$

Since $\partial_t \mathbf{f}_k \rightarrow \partial_t \mathbf{f}$ in $\mathbf{L}^2(\Omega_T)$ and $\mathbf{m}_{hk}^+ \rightarrow \mathbf{m}$ in $\mathbf{L}^2(\Omega_T)$ by (4.37e), it holds that

$$\int_0^\tau \langle \partial_t \mathbf{f}_k(t), \mathbf{m}_{hk}^+(t) \rangle dt \rightarrow \int_0^\tau \langle \partial_t \mathbf{f}(t), \mathbf{m}(t) \rangle dt.$$

Similarly, since $\Pi_{hk}^- \rightarrow \Pi(\mathbf{m})$ in $\mathbf{L}^2(\Omega_T)$ by (4.18b) (with strong convergence) and $\mathbf{v}_{hk}^- \rightarrow \partial_t \mathbf{m}$ in $\mathbf{L}^2(\Omega_T)$ by (4.37h), it holds that

$$\int_0^\tau \langle \Pi_{hk}^-(t), \mathbf{v}_{hk}^-(t) \rangle dt \rightarrow \int_0^\tau \langle \Pi(\mathbf{m}(t)), \partial_t \mathbf{m}(t) \rangle dt.$$

By no-concentration of Lebesgue functions (note that $\tau \leq t_j \leq \tau + k$), the sixth and the seventh terms on the left-hand side of (4.54) vanish, i.e., it holds that

$$\int_\tau^{t_j} \langle \partial_t \mathbf{f}_k(t), \mathbf{m}_{hk}^+(t) \rangle dt \rightarrow 0$$

and

$$\int_\tau^{t_j} \langle \Pi_{hk}^-(t), \mathbf{v}_{hk}^-(t) \rangle dt \rightarrow 0.$$

From the fact that $\pi : \mathbf{L}^2(\Omega) \rightarrow \mathbf{L}^2(\Omega)$ is a linear and bounded operator, together with the convergence $\mathbf{m}_{hk}^- \rightarrow \mathbf{m}$ in $\mathbf{L}^2(\Omega_T)$ given by (4.37e), we obtain the strong convergence in $\mathbf{L}^2(\Omega_T)$ of the function $\pi(\mathbf{m}_{hk})$, defined by $t \mapsto \pi(\mathbf{m}_{hk}(t))$ for all $t \in (0, T)$, towards $\pi(\mathbf{m}) \in \mathbf{L}^2(\Omega_T)$. Since $\pi_{hk}^- \rightarrow \pi(\mathbf{m})$ in $\mathbf{L}^2(\Omega_T)$ by assumption (4.18a) (with strong convergence), it follows that

$$\int_0^{t_j} \langle \pi(\mathbf{m}_{hk}^-(t)) - \pi_{hk}^-(t), \mathbf{v}_{hk}^-(t) \rangle dt \rightarrow 0.$$

Similarly, since $\mathbf{f}_k^-, \mathbf{f}_{hk}^- \rightarrow \mathbf{f}$ in $\mathbf{L}^2(\Omega_T)$, we obtain

$$\int_0^{t_j} \langle \mathbf{f}_k^-(t) - \mathbf{f}_{hk}^-(t), \mathbf{v}_{hk}^-(t) \rangle dt \rightarrow 0.$$

From the uniform boundedness of the sequence $\{\mathbf{v}_{hk}^-\}$ in $\mathbf{L}^2(\Omega_T)$ by Proposition 4.3.9 and the convergence of Lemma 4.3.10, it follows that the right-hand side of (4.54) vanishes as $k, h \rightarrow 0$.

Hence, for every measurable set $I \subseteq [0, T]$, it holds that

$$\begin{aligned}
& \int_I \left[\mathcal{E}(\mathbf{m}(\tau), \mathbf{f}(\tau)) + \int_0^\tau \|\partial_t \mathbf{m}(t)\|_{\mathbf{L}^2(\Omega)}^2 dt \right] d\tau \\
& \leq \liminf_{k, h \rightarrow 0} \int_I \left[\mathcal{E}(\mathbf{m}_{hk}^+(\tau), \mathbf{f}_k^+(\tau)) + \int_0^\tau \|\mathbf{v}_{hk}^-(t)\|_{\mathbf{L}^2(\Omega)}^2 dt \right] d\tau \\
& \stackrel{(4.54)}{\leq} \liminf_{k, h \rightarrow 0} \int_I \left[\mathcal{E}(\mathbf{m}_{hk}^-(0), \mathbf{f}(0)) + C(k, h, \theta) \int_0^\tau \|\mathbf{v}_{hk}^-(t)\|_{\mathbf{L}^2(\Omega)}^2 dt \right. \\
& \quad - \int_0^\tau \langle \partial_t \mathbf{f}_k(t), \mathbf{m}_{hk}^+(t) \rangle dt + \int_0^\tau \langle \mathbf{\Pi}_{hk}^-(t), \mathbf{v}_{hk}^-(t) \rangle dt - \int_\tau^{t_j} \langle \partial_t \mathbf{f}_k(t), \mathbf{m}_{hk}^+(t) \rangle dt \\
& \quad + \int_\tau^{t_j} \langle \mathbf{\Pi}_{hk}^-(t), \mathbf{v}_{hk}^-(t) \rangle dt - \int_0^{t_j} \langle \boldsymbol{\pi}(\mathbf{m}_{hk}^-(t)) - \boldsymbol{\pi}_{hk}^-(t), \mathbf{v}_{hk}^-(t) \rangle dt \\
& \quad - \int_0^{t_j} \langle \mathbf{f}_k^-(t) - \mathbf{f}_{hk}^-(t), \mathbf{v}_{hk}^-(t) \rangle dt \\
& \quad \left. + Ck \left(\|\mathbf{v}_{hk}^-\|_{\mathbf{L}^2(\Omega \times (0, t_j))}^2 + \|\mathbf{v}_{hk}^-\|_{\mathbf{L}^2(\Omega \times (0, t_j))} \|\nabla \mathbf{v}_{hk}^-\|_{\mathbf{L}^2(\Omega \times (0, t_j))} \right) \right] d\tau \\
& = \int_I \left[\mathcal{E}(\mathbf{m}^0, \mathbf{f}(0)) - \int_0^\tau \langle \partial_t \mathbf{f}(t), \mathbf{m}(t) \rangle dt + \int_0^\tau \langle \mathbf{\Pi}(\mathbf{m}(t)), \partial_t \mathbf{m}(t) \rangle dt \right] d\tau.
\end{aligned}$$

Since $I \subseteq [0, T]$ was an arbitrary measurable subset, we deduce that the integrand satisfies the inequality a.e. in $(0, T)$, i.e., it holds that

$$\begin{aligned}
& \mathcal{E}(\mathbf{m}(\tau), \mathbf{f}(\tau)) + \alpha \int_0^\tau \|\partial_t \mathbf{m}(t)\|_{\mathbf{L}^2(\Omega)}^2 dt + \int_0^\tau \langle \partial_t \mathbf{f}(t), \mathbf{m}(t) \rangle dt \\
& \leq \mathcal{E}(\mathbf{m}^0, \mathbf{f}(0)) + \int_0^\tau \langle \mathbf{\Pi}(\mathbf{m}(t)), \partial_t \mathbf{m}(t) \rangle dt
\end{aligned}$$

for a.e. $\tau \in (0, T)$, which is (4.5). This verifies the validity of the energy inequality of Definition 4.1.1(iv) and thus concludes the proof. \square

Remark 4.3.15. Retracing the proof of Theorem 4.3.2, it comes to light that many assumptions can be weakened if one gives up the proof of the energy inequality (4.5). In Definition 4.1.1(iv), if one settles for the inequality

$$\|\nabla \mathbf{m}(\tau)\|_{\mathbf{L}^2(\Omega)}^2 + \int_0^\tau \|\partial_t \mathbf{m}(t)\|_{\mathbf{L}^2(\Omega)}^2 dt \leq C \quad \text{for a.e. } \tau \in (0, T),$$

where $C > 0$ is a constant which depends only on the problem data, the assumptions of part (b) of Theorem 4.3.2 are sufficient; see, e.g., [56]. In particular, the strong convergence in (4.15), (4.17), and (4.18) is not needed. Moreover, the linearity and self-adjointness of $\boldsymbol{\pi}$ as well as assuming that $\mathbf{f} \in C^1([0, T], \mathbf{L}^2(\Omega))$ can be avoided.

Chapter 5

Application to metal spintronics

In this chapter, we discuss the numerical approximation of the spintronic models introduced in Section 2.3. The discretization of the LLG equation is based on the tangent plane scheme analyzed in Chapter 4.

5.1 Spin diffusion model

In this section, we introduce an algorithm for the discretization of the spin diffusion model introduced in Section 2.3.2 and rescaled in nondimensional form in (3.10). For ease of presentation, we assume that the micromagnetic energy comprises only the exchange contribution. Lower-order terms can be included into the analysis using the approach discussed in Chapter 4.

5.1.1 Setting

Let Ω and Ω' be two bounded Lipschitz domains in \mathbb{R}^3 with polyhedral boundaries $\Gamma := \partial\Omega$ and $\Gamma' := \partial\Omega'$, such that $\Omega \subseteq \Omega'$. Given $T > 0$, we denote the space-time cylinders by $\Omega_T := \Omega \times (0, T)$ and $\Omega'_T := \Omega' \times (0, T)$. We define $\Gamma_T := \Gamma \times (0, T)$ and $\Gamma'_T := \Gamma' \times (0, T)$. We consider the coupling of the LLG equation for the normalized magnetization \mathbf{m} with a diffusion equation for the spin accumulation \mathbf{s} , i.e.,

$$\partial_t \mathbf{m} = -\mathbf{m} \times \mathbf{h}_{\text{eff}} + \alpha \mathbf{m} \times \partial_t \mathbf{m} - \tau_J^{-1} \mathbf{m} \times \mathbf{s} \quad \text{in } \Omega_T, \quad (5.1a)$$

$$\partial_t \mathbf{s} = z \nabla \cdot [D_0 (\mathbf{I}_{3 \times 3} - \beta \beta' \mathbf{m} \otimes \mathbf{m}) \nabla \mathbf{s}] - \tau_{\text{sf}}^{-1} \mathbf{s} - \tau_J^{-1} \mathbf{s} \times \mathbf{m} - \beta z \nabla \cdot (\mathbf{m} \otimes \mathbf{j}) \quad \text{in } \Omega'_T. \quad (5.1b)$$

In (5.1a), the effective field is given by $\mathbf{h}_{\text{eff}} = \lambda_{\text{ex}}^2 \Delta \mathbf{m}$, while α , λ_{ex} , and τ_J are positive constants. In (5.1b) the quantities $z > 0$, $\tau_{\text{sf}} > 0$, and $0 < \beta, \beta' < 1$ are constant, the function¹ \mathbf{j} belongs to $C^0([0, T]; \mathbf{H}^1(\Omega')) \cap \mathbf{L}^\infty(\Omega')$, while $D_0 \in L^\infty(\Omega')$ is positive and bounded away from zero, i.e., there exists a constant $D_* > 0$ such that $D_0 \geq D_*$ a.e. in Ω' . The system is supplemented with homogeneous Neumann boundary conditions

$$\partial_{\mathbf{n}} \mathbf{m} = \mathbf{0} \quad \text{on } \Gamma_T \quad \text{and} \quad \partial_{\mathbf{n}} \mathbf{s} = \mathbf{0} \quad \text{on } \Gamma'_T \quad (5.1c)$$

and initial conditions

$$\mathbf{m} = \mathbf{m}^0 \quad \text{in } \Omega \quad \text{and} \quad \mathbf{s} = \mathbf{s}^0 \quad \text{in } \Omega', \quad (5.1d)$$

where $\mathbf{m}^0 \in \mathbf{H}^1(\Omega)$ satisfies $|\mathbf{m}| = 1$ a.e. in Ω , and $\mathbf{s}^0 \in \mathbf{H}^1(\Omega')$. The energy of the system is given by the functional

$$\mathcal{E}(\mathbf{m}) = \frac{\lambda_{\text{ex}}^2}{2} \|\nabla \mathbf{m}\|_{L^2(\Omega)}^2.$$

¹Here, to simplify the notation, we denote the rescaled electric current density by \mathbf{j} . In (3.10) it was denoted by \mathbf{j}_e .

The system is a nonlinearly coupled system of the nonlinear LLG equation (5.1a) and a linear diffusion equation (5.1b). As it happens for the Maxwell equations (both the full system and the eddy current approximation) and the conservation of momentum (magnetostriction), the quantity governed by the coupled equation (in this case, the spin accumulation) affects the LLG equation as an additional source of torque added to the effective field. However, differently from those cases, here the magnetization affects not only the right-hand side of the coupled equation, but also the main part of the involved differential operator.

For $\mathbf{m} \in \mathbf{L}^\infty(\Omega)$ satisfying $|\mathbf{m}| = 1$ a.e. in Ω , we consider the bilinear form $a(\mathbf{m}; \cdot, \cdot) : \mathbf{H}^1(\Omega') \times \mathbf{H}^1(\Omega') \rightarrow \mathbb{R}$ defined, for all $\boldsymbol{\zeta}_1, \boldsymbol{\zeta}_2 \in \mathbf{H}^1(\Omega')$, by

$$a(\mathbf{m}; \boldsymbol{\zeta}_1, \boldsymbol{\zeta}_2) = z \langle D_0 \nabla \boldsymbol{\zeta}_1, \nabla \boldsymbol{\zeta}_2 \rangle_{\Omega'} - z \beta \beta' \langle D_0(\mathbf{m} \otimes \mathbf{m}) \nabla \boldsymbol{\zeta}_1, \nabla \boldsymbol{\zeta}_2 \rangle_{\Omega'} + \tau_{\text{sf}}^{-1} \langle \boldsymbol{\zeta}_1, \boldsymbol{\zeta}_2 \rangle_{\Omega'} + \tau_{\text{J}}^{-1} \langle \boldsymbol{\zeta}_1 \times \mathbf{m}, \boldsymbol{\zeta}_2 \rangle_{\Omega}. \quad (5.2)$$

In the following lemma we show that the bilinear form (5.2) is elliptic. This highlights the parabolic nature of (5.1b).

Lemma 5.1.1. *For any $\mathbf{m} \in \mathbf{L}^\infty(\Omega)$ satisfying $|\mathbf{m}| = 1$ a.e. in Ω , the bilinear form $a(\mathbf{m}; \cdot, \cdot)$ is continuous and elliptic.*

Proof. For all $\boldsymbol{\zeta}_1, \boldsymbol{\zeta}_2 \in \mathbf{H}^1(\Omega')$, it holds that

$$a(\mathbf{m}; \boldsymbol{\zeta}_1, \boldsymbol{\zeta}_2) \leq z(1 + \beta \beta') \|D_0\|_{L^\infty(\Omega')} \|\nabla \boldsymbol{\zeta}_1\|_{L^2(\Omega')} \|\nabla \boldsymbol{\zeta}_2\|_{L^2(\Omega')} + (\tau_{\text{sf}}^{-1} + \tau_{\text{J}}^{-1}) \|\boldsymbol{\zeta}_1\|_{L^2(\Omega')} \|\boldsymbol{\zeta}_2\|_{L^2(\Omega')}.$$

This shows that the bilinear form is continuous. As for the positive definiteness, it holds that

$$\begin{aligned} a(\mathbf{m}; \boldsymbol{\zeta}, \boldsymbol{\zeta}) &= z \langle D_0 \nabla \boldsymbol{\zeta}, \nabla \boldsymbol{\zeta} \rangle_{\Omega'} - z \beta \beta' \langle D_0(\mathbf{m} \otimes \mathbf{m}) \nabla \boldsymbol{\zeta}, \nabla \boldsymbol{\zeta} \rangle_{\Omega'} + \tau_{\text{sf}}^{-1} \|\boldsymbol{\zeta}\|_{L^2(\Omega')}^2 \\ &\geq z(1 - \beta \beta') D_* \|\nabla \boldsymbol{\zeta}\|_{L^2(\Omega')}^2 + \tau_{\text{sf}}^{-1} \|\boldsymbol{\zeta}\|_{L^2(\Omega')}^2 \end{aligned}$$

for all $\boldsymbol{\zeta} \in \mathbf{H}^1(\Omega')$. □

Let us denote by $\widetilde{\mathbf{H}}^{-1}(\Omega') = \mathbf{H}^1(\Omega')^*$ the dual space of $\mathbf{H}^1(\Omega')$. Let $\langle \cdot, \cdot \rangle_{H^{-1} \leftrightarrow H^1}$ be the corresponding duality pairing, to be understood in the sense of the Gelfand triple $\mathbf{H}^1(\Omega') \subset \mathbf{L}^2(\Omega') \subset \widetilde{\mathbf{H}}^{-1}(\Omega')$. In the following definition, we introduce the notion of a weak solution of (5.1), which is similar to those considered in [103, 6].

Definition 5.1.2. *The pair (\mathbf{m}, \mathbf{s}) , with $\mathbf{m} : \Omega_T \rightarrow \mathbb{R}^3$ and $\mathbf{s} : \Omega'_T \rightarrow \mathbb{R}^3$, is called a weak solution of (5.1) if the following properties (i)–(v) are satisfied:*

- (i) \mathbf{m} belongs to $L^\infty(0, T; \mathbf{H}^1(\Omega)) \cap H^1(0, T; \mathbf{L}^2(\Omega))$ and satisfies $|\mathbf{m}| = 1$ a.e. in Ω_T , \mathbf{s} belongs to $L^2(0, T; \mathbf{H}^1(\Omega'), \mathbf{L}^2(\Omega')) \cap L^\infty(0, T; \mathbf{L}^2(\Omega'))$,
- (ii) $\mathbf{m}(0) = \mathbf{m}^0$ in the sense of traces and $\mathbf{s}(0) = \mathbf{s}^0$ in $\mathbf{L}^2(\Omega')$,
- (iii) For all $\boldsymbol{\varphi} \in \mathbf{H}^1(\Omega_T)$, it holds that

$$\begin{aligned} &\int_0^T \langle \partial_t \mathbf{m}(t), \boldsymbol{\varphi}(t) \rangle_{\Omega} dt - \alpha \int_0^T \langle \mathbf{m}(t) \times \partial_t \mathbf{m}(t), \boldsymbol{\varphi}(t) \rangle_{\Omega} dt \\ &= \lambda_{\text{ex}}^2 \int_0^T \langle \mathbf{m}(t) \times \nabla \mathbf{m}(t), \nabla \boldsymbol{\varphi}(t) \rangle_{\Omega} dt - \tau_{\text{J}}^{-1} \int_0^T \langle \mathbf{m}(t) \times \mathbf{s}(t), \boldsymbol{\varphi}(t) \rangle_{\Omega} dt, \end{aligned} \quad (5.3)$$

- (iv) For a.e. $t \in (0, T)$ and all $\boldsymbol{\zeta} \in \mathbf{H}^1(\Omega')$, it holds that

$$\langle \partial_t \mathbf{s}(t), \boldsymbol{\zeta} \rangle_{H^{-1} \leftrightarrow H^1} + a(\mathbf{m}(t); \mathbf{s}(t), \boldsymbol{\zeta}) = z \beta \langle \mathbf{m}(t) \otimes \mathbf{j}(t), \nabla \boldsymbol{\zeta} \rangle_{\Omega} - z \beta \langle \mathbf{j}(t) \cdot \mathbf{n}, \mathbf{m}(t) \cdot \boldsymbol{\zeta} \rangle_{\Gamma' \cap \Gamma}, \quad (5.4)$$

- (v) (\mathbf{m}, \mathbf{s}) satisfies the energy inequality

$$\mathcal{E}(\mathbf{m}(\tau)) + \alpha \int_0^\tau \|\partial_t \mathbf{m}(t)\|_{L^2(\Omega)}^2 dt \leq \mathcal{E}(\mathbf{m}^0) + \tau_{\text{J}}^{-1} \int_0^\tau \langle \mathbf{s}(t), \partial_t \mathbf{m}(t) \rangle_{\Omega} dt \quad (5.5)$$

for a.e. $\tau \in (0, T)$.

Definition 5.1.2 extends Definition 4.1.1 to the present situation. The variational formulation (5.4) of (5.1b) considered in part (iv) follows the classical approach for linear second-order parabolic problems; see, e.g., [88, Section 7.1.1]. In particular, since $\mathbf{s} \in C^0([0, T]; \mathbf{L}^2(\Omega'))$ by [88, Section 5.9.2, Theorem 3], the equality $\mathbf{s}(0) = \mathbf{s}^0$ in $\mathbf{L}^2(\Omega')$ of part (ii) is meaningful. The energy inequality (5.5) is a weak counterpart of the energy law (3.12).

Remark 5.1.3. In [103], the boundary integral of (5.4), which arises from integrating by parts the last term on the right-hand side of (5.1b) and using the homogeneous Neumann boundary conditions for the spin accumulation, was wrongly omitted. This mistake was noticed and corrected in [6] so that the overall existence result of [103] remains valid; see [104].

5.1.2 Decoupled algorithm

For the time discretization, we consider a uniform partition of the time interval $(0, T)$ into $M > 0$ subintervals, i.e., $t_i = ik$ for all $0 \leq i \leq M$, where $k = T/M$ denotes the time-step size; see Section 3.3. For the spatial discretization, we consider a γ -quasi-uniform family $\{\mathcal{T}_h\}_{h>0}$ of regular tetrahedral triangulations of Ω' ; see Section 3.4. We assume that Ω is resolved, i.e., the restriction $\mathcal{T}_h := \mathcal{T}_h|_{\Omega}$ provides a regular triangulation of Ω . We recall the definitions of the sets \mathcal{M}_h and \mathcal{U}_h , i.e.,

$$\begin{aligned}\mathcal{M}_h &= \{\phi_h \in \mathcal{S}^1(\mathcal{T}_h)^3 : |\phi_h(\mathbf{z})| = 1 \text{ for all } \mathbf{z} \in \mathcal{N}_h\} \quad \text{and} \\ \mathcal{U}_h &= \{\phi_h \in \mathcal{S}^1(\mathcal{T}_h)^3 : |\phi_h(\mathbf{z})| \geq 1 \text{ for all } \mathbf{z} \in \mathcal{N}_h\}\end{aligned}$$

as well as the one of the discrete tangent space, i.e.,

$$\mathcal{K}_{\phi_h} := \{\psi_h \in \mathcal{S}^1(\mathcal{T}_h)^3 : \phi_h(\mathbf{z}) \cdot \psi_h(\mathbf{z}) = 0 \text{ for all } \mathbf{z} \in \mathcal{N}_h\} \quad \text{for all } \phi_h \in \mathcal{S}^1(\mathcal{T}_h)^3.$$

For all $0 \leq i \leq M$, we consider the approximations $\mathbf{m}_h^i \approx \mathbf{m}(t_i)$, $\mathbf{v}_h^i \approx \partial_t \mathbf{m}(t_i)$, $\mathbf{s}_h^i \approx \mathbf{s}(t_i)$, and abbreviate $\mathbf{j}^i = \mathbf{j}(t_i)$. For the discretization of (5.1), we propose the following decoupled algorithm.

Algorithm 5.1.4. *Input:* Either $\mathbf{m}_h^0 \in \mathcal{M}_h$ (TPS) or $\mathbf{m}_h^0 \in \mathcal{U}_h$ (PFTPS), $\mathbf{s}_h^0 \in \mathcal{S}^1(\mathcal{T}_h')^3$.
Loop: For all $0 \leq i \leq M-1$, iterate:

(i) Compute $\mathbf{v}_h^i \in \mathcal{K}_{\mathbf{m}_h^i}$ such that

$$\alpha \langle \mathbf{v}_h^i, \phi_h \rangle_{\Omega} + \langle \mathbf{m}_h^i \times \mathbf{v}_h^i, \phi_h \rangle_{\Omega} + \lambda_{\text{ex}}^2 \theta k \langle \nabla \mathbf{v}_h^i, \nabla \phi_h \rangle_{\Omega} = -\lambda_{\text{ex}}^2 \langle \nabla \mathbf{m}_h^i, \nabla \phi_h \rangle_{\Omega} + \tau_j^{-1} \langle \mathbf{s}_h^i, \phi_h \rangle_{\Omega} \quad (5.6)$$

for all $\phi_h \in \mathcal{K}_{\mathbf{m}_h^i}$.

(ii) Either define $\mathbf{m}_h^{i+1} \in \mathcal{U}_h$ by

$$\mathbf{m}_h^{i+1} = \mathbf{m}_h^i + k \mathbf{v}_h^i \quad (\text{PFTPS}) \quad (5.7a)$$

or define $\mathbf{m}_h^{i+1} \in \mathcal{M}_h$ by

$$\mathbf{m}_h^{i+1} = \mathcal{I}_h \left[\frac{\mathbf{m}_h^i + k \mathbf{v}_h^i}{|\mathbf{m}_h^i + k \mathbf{v}_h^i|} \right] \quad (\text{TPS}). \quad (5.7b)$$

(iii) Compute $\mathbf{s}_h^{i+1} \in \mathcal{S}^1(\mathcal{T}_h')^3$ such that

$$\langle d_t \mathbf{s}_h^{i+1}, \boldsymbol{\zeta}_h \rangle_{\Omega'} + a(\widehat{\mathbf{m}}_h^{i+1}; \mathbf{s}_h^{i+1}, \boldsymbol{\zeta}_h) = z\beta \langle \widehat{\mathbf{m}}_h^{i+1} \otimes \mathbf{j}^{i+1}, \nabla \boldsymbol{\zeta}_h \rangle_{\Omega} - z\beta \langle \mathbf{j}^{i+1} \cdot \mathbf{n}, \widehat{\mathbf{m}}_h^{i+1} \cdot \boldsymbol{\zeta}_h \rangle_{\Gamma' \cap \Gamma} \quad (5.8)$$

for all $\boldsymbol{\zeta}_h \in \mathcal{S}^1(\mathcal{T}_h')^3$.

Output: Sequence of discrete functions $\{(\mathbf{v}_h^i, \mathbf{m}_h^{i+1}, \mathbf{s}_h^{i+1})\}_{0 \leq i \leq M-1}$.

Steps (i)–(ii) contain the tangent plane scheme for the discretization of the extended LLG equation (5.1a). The additional torque term given by the spin accumulation is treated explicitly, i.e., it only contributes to the right-hand side of (5.6). Step (iii), in which we discretize (5.1b), consists of a Galerkin approximation of the variational formulation (5.4). For the time discretization, we employ the implicit Euler method. To approximate the magnetization \mathbf{m} , which enters both the bilinear form and the right-hand side of (5.4), we exploit the approximate magnetization \mathbf{m}_h^{i+1} available from step (ii). More precisely, we use the ‘normalized iterate’ introduced in (4.40), namely

$$\widehat{\mathbf{m}}_h^i := \mathcal{I}_h[\mathbf{m}_h^i / |\mathbf{m}_h^i|] \quad \text{for all } 0 \leq i \leq M.$$

Clearly, for the standard tangent plane scheme, it holds that $\widehat{\mathbf{m}}_h^i = \mathbf{m}_h^i$ for all $0 \leq i \leq M$. Although (5.1) is a nonlinearly coupled system of the nonlinear LLG equation and a linear diffusion equation, Algorithm 5.1.4 only requires the solution of two linear systems per time-step.

The following proposition establishes the well-posedness of Algorithm 5.1.4.

Proposition 5.1.5. *For all $0 \leq i \leq M - 1$, there exist unique solutions $\mathbf{v}_h^i \in \mathcal{K}_{\mathbf{m}_h^i}$ of (5.6) and $\mathbf{s}_h^{i+1} \in \mathcal{S}^1(\mathcal{T}_h)^3$ of (5.8). The time-stepping (5.7) is well defined.*

Proof. The well-posedness of the tangent plane scheme of steps (i)–(ii) follows from Proposition 4.2.2, as the presence of the spin accumulation contributes only to the right-hand side of (5.6) and, in particular, does not affect the ellipticity of the bilinear form. Since $\widehat{\mathbf{m}}_h^{i+1} \in \mathcal{M}_h$ for all $0 \leq i \leq M - 1$, from Lemma 5.1.1 we deduce that $a(\widehat{\mathbf{m}}_h^{i+1}; \cdot, \cdot)$ is elliptic. It follows that the bilinear form of the discrete variational problem (5.8), i.e., $a(\widehat{\mathbf{m}}_h^{i+1}; \cdot, \cdot) + \langle \cdot, \cdot \rangle_{\Omega'}$, is also elliptic. Unique solvability thus follows from linearity and finite space dimension. \square

5.1.3 Convergence result

The output of Algorithm 5.1.4 is used to define the piecewise linear and piecewise constant time reconstructions (3.13). In particular, we consider the functions defined, for all $0 \leq i \leq M - 1$ and $t \in [t_i, t_{i+1})$, by

$$\mathbf{m}_{hk}(t) := \frac{t - t_i}{k} \mathbf{m}_h^{i+1} + \frac{t_{i+1} - t}{k} \mathbf{m}_h^i, \quad \mathbf{m}_{hk}^-(t) := \mathbf{m}_h^i, \quad \mathbf{m}_{hk}^+(t) := \mathbf{m}_h^{i+1}, \quad \mathbf{v}_{hk}^-(t) := \mathbf{v}_h^i, \quad (5.9a)$$

$$\widehat{\mathbf{m}}_{hk}(t) := \frac{t - t_i}{k} \widehat{\mathbf{m}}_h^{i+1} + \frac{t_{i+1} - t}{k} \widehat{\mathbf{m}}_h^i, \quad \widehat{\mathbf{m}}_{hk}^-(t) := \widehat{\mathbf{m}}_h^i, \quad \widehat{\mathbf{m}}_{hk}^+(t) := \widehat{\mathbf{m}}_h^{i+1}, \quad (5.9b)$$

$$\mathbf{s}_{hk}(t) := \frac{t - t_i}{k} \mathbf{s}_h^{i+1} + \frac{t_{i+1} - t}{k} \mathbf{s}_h^i, \quad \mathbf{s}_{hk}^-(t) := \mathbf{s}_h^i, \quad \mathbf{s}_{hk}^+(t) := \mathbf{s}_h^{i+1}, \quad (5.9c)$$

Similarly, we define the piecewise constant time approximation \mathbf{j}_k^+ defined by $\mathbf{j}_k^+(t) := \mathbf{j}^{i+1}$ for all $0 \leq i \leq M - 1$ and $t \in [t_i, t_{i+1})$. Since \mathbf{j} belongs to $C^0([0, T]; \mathbf{H}^1(\Omega'))$, it holds that

$$\mathbf{j}_k^+ \rightarrow \mathbf{j} \quad \text{in } L^2(0, T; \mathbf{H}^1(\Omega')) \quad \text{as } k \rightarrow 0. \quad (5.10)$$

The following theorem extends Theorem 4.3.2 to the present situation.

Theorem 5.1.6. *Let $\{\mathcal{T}_h'\}_{h>0}$ be a γ -quasi-uniform family of regular tetrahedral triangulations of Ω' which resolve Ω . Let the discrete initial conditions $\mathbf{m}_h^0 \in \mathcal{U}_h$ and $\mathbf{s}_h^0 \in \mathcal{S}^1(\mathcal{T}_h')^3$ satisfy the convergence properties*

$$\mathbf{m}_h^0 \rightarrow \mathbf{m}^0 \quad \text{in } \mathbf{H}^1(\Omega) \quad \text{as } h \rightarrow 0, \quad (5.11a)$$

$$\mathbf{s}_h^0 \rightharpoonup \mathbf{s}^0 \quad \text{in } \mathbf{H}^1(\Omega') \quad \text{as } h \rightarrow 0. \quad (5.11b)$$

For the standard tangent plane scheme, assume that $\mathbf{m}_h^0 \in \mathcal{M}_h$ and that

- either $1/2 < \theta \leq 1$ and any triangulation \mathcal{T}_h satisfies the angle condition (3.16),

- or $\theta = 1/2$, any triangulation \mathcal{T}_h satisfies the angle condition (3.16), and $k = o(h)$ as $k, h \rightarrow 0$,
- or $k = o(h^2)$ as $k, h \rightarrow 0$.

For the projection-free tangent plane scheme, assume that

- either $1/2 < \theta \leq 1$,
- or $\theta = 1/2$ and $k = o(h)$ as $k, h \rightarrow 0$,
- or $k = o(h^2)$ as $k, h \rightarrow 0$.

Then, there exist $\mathbf{m} \in L^\infty(0, T; \mathbf{H}^1(\Omega)) \cap H^1(0, T; \mathbf{L}^2(\Omega))$ and $\mathbf{s} \in L^2(0, T; \mathbf{H}^1(\Omega'), \mathbf{L}^2(\Omega')) \cap L^\infty(0, T; \mathbf{L}^2(\Omega'))$ such that, for the discrete functions (5.9) constructed using the output of Algorithm 5.1.4, up to extraction of a subsequence, it holds that $\mathbf{m}_{hk} \rightharpoonup \mathbf{m}$ in $\mathbf{H}^1(\Omega_T)$ and $\mathbf{s}_{hk} \rightharpoonup \mathbf{s}$ in $L^2(0, T; \mathbf{H}^1(\Omega'), \mathbf{L}^2(\Omega'))$ as $k, h \rightarrow 0$. In particular, (\mathbf{m}, \mathbf{s}) is a weak solution of (5.1) in the sense of Definition 5.1.2.

With the following lemma, we start with the proof of Theorem 5.1.6. The proof is identical to the one of Lemma 4.3.7, therefore we omit it.

Lemma 5.1.7. *Let $0 \leq i \leq M - 1$. For the standard tangent plane scheme, it holds that*

$$\frac{\lambda_{\text{ex}}^2}{2} k d_t \|\nabla \mathbf{m}_h^{i+1}\|_{\mathbf{L}^2(\Omega)}^2 + [\alpha - c(k, h)] k \|\mathbf{v}_h^i\|_{\mathbf{L}^2(\Omega)}^2 + \lambda_{\text{ex}}^2 \left(\theta - \frac{1}{2} \right) k^2 \|\nabla \mathbf{v}_h^i\|_{\mathbf{L}^2(\Omega)}^2 \leq \tau_J^{-1} k \langle \mathbf{s}_h^i, \mathbf{v}_h^i \rangle_\Omega, \quad (5.12)$$

with

$$c(k, h) = \begin{cases} 0 & \text{if the triangulation } \mathcal{T}_h \text{ satisfies the angle condition (3.16),} \\ Ckh^{-2} & \text{else.} \end{cases}$$

The constant $C > 0$ depends only on γ and λ_{ex} . In particular, it is independent of k and h . For the projection-free tangent plane scheme, it holds that

$$\frac{\lambda_{\text{ex}}^2}{2} k d_t \|\nabla \mathbf{m}_h^{i+1}\|_{\mathbf{L}^2(\Omega)}^2 + \alpha k \|\mathbf{v}_h^i\|_{\mathbf{L}^2(\Omega)}^2 + \lambda_{\text{ex}}^2 \left(\theta - \frac{1}{2} \right) k^2 \|\nabla \mathbf{v}_h^i\|_{\mathbf{L}^2(\Omega)}^2 = \tau_J^{-1} k \langle \mathbf{s}_h^i, \mathbf{v}_h^i \rangle_\Omega. \quad (5.13)$$

In the following two lemmata, we establish two energy estimates for the iterates of Algorithm 5.1.4.

Lemma 5.1.8. *For all $1 \leq j \leq M$, it holds that*

$$\|\mathbf{s}_h^j\|_{\mathbf{L}^2(\Omega')}^2 + \sum_{i=0}^{j-1} \|\mathbf{s}_h^{i+1} - \mathbf{s}_h^i\|_{\mathbf{L}^2(\Omega')}^2 + k \sum_{i=0}^{j-1} \|\mathbf{s}_h^{i+1}\|_{\mathbf{H}^1(\Omega')}^2 \leq C. \quad (5.14)$$

The constant $C > 0$ depends only on the problem data $(\beta, \beta', D_*, \mathbf{j}, \Omega, \mathbf{s}^0, \tau_{\text{sf}}, z)$. In particular, it is independent of the discretization parameters k and h .

Proof. In (5.8), we choose the test function $\boldsymbol{\zeta}_h = \mathbf{s}_h^{i+1}$ to obtain

$$\langle d_t \mathbf{s}_h^{i+1}, \mathbf{s}_h^{i+1} \rangle_{\Omega'} + a(\mathbf{m}_h^{i+1}; \mathbf{s}_h^{i+1}, \mathbf{s}_h^{i+1}) = z\beta \langle \mathbf{m}_h^{i+1} \otimes \mathbf{j}^{i+1}, \nabla \mathbf{s}_h^{i+1} \rangle_\Omega - z\beta \langle \mathbf{j}^{i+1} \cdot \mathbf{n}, \mathbf{m}_h^{i+1} \cdot \mathbf{s}_h^{i+1} \rangle_{\Gamma' \cap \Gamma}.$$

Using the ellipticity of the bilinear form (see the proof of Lemma 5.1.1) and multiplying the resulting equation by the time-step size k yields the inequality

$$\begin{aligned} & \langle \mathbf{s}_h^{i+1} - \mathbf{s}_h^i, \mathbf{s}_h^{i+1} \rangle_{\Omega'} + zD_*(1 - \beta\beta')k \|\nabla \mathbf{s}_h^{i+1}\|_{\mathbf{L}^2(\Omega')}^2 + \tau_{\text{sf}}^{-1}k \|\mathbf{s}_h^{i+1}\|_{\mathbf{L}^2(\Omega')}^2 \\ & \leq z\beta k \langle \mathbf{m}_h^{i+1} \otimes \mathbf{j}^{i+1}, \nabla \mathbf{s}_h^{i+1} \rangle_\Omega - z\beta k \langle \mathbf{j}^{i+1} \cdot \mathbf{n}, \mathbf{m}_h^{i+1} \cdot \mathbf{s}_h^{i+1} \rangle_{\Gamma' \cap \Gamma}. \end{aligned}$$

Summing over $0 \leq i \leq j-1$ and using the identity

$$\sum_{i=0}^{j-1} \langle \mathbf{s}_h^{i+1} - \mathbf{s}_h^i, \mathbf{s}_h^{i+1} \rangle_{\Omega'} = \frac{1}{2} \|\mathbf{s}_h^j\|_{L^2(\Omega')}^2 - \frac{1}{2} \|\mathbf{s}_h^0\|_{L^2(\Omega')}^2 + \frac{1}{2} \sum_{i=0}^{j-1} \|\mathbf{s}_h^{i+1} - \mathbf{s}_h^i\|_{L^2(\Omega')}^2$$

(Abel's summation by parts, see Lemma B.2.3), we obtain

$$\begin{aligned} & \frac{1}{2} \|\mathbf{s}_h^j\|_{L^2(\Omega')}^2 + \frac{1}{2} \sum_{i=0}^{j-1} \|\mathbf{s}_h^{i+1} - \mathbf{s}_h^i\|_{L^2(\Omega')}^2 + zD_*(1 - \beta\beta')k \sum_{i=0}^{j-1} \|\nabla \mathbf{s}_h^{i+1}\|_{L^2(\Omega')}^2 \\ & + \tau_{\text{sf}}^{-1}k \sum_{i=0}^{j-1} \|\mathbf{s}_h^{i+1}\|_{L^2(\Omega')}^2 \\ & \leq \frac{1}{2} \|\mathbf{s}_h^0\|_{L^2(\Omega')}^2 + z\beta k \sum_{i=0}^{j-1} (\langle \widehat{\mathbf{m}}_h^{i+1} \otimes \mathbf{j}^{i+1}, \nabla \mathbf{s}_h^{i+1} \rangle_{\Omega} - \langle \mathbf{j}^{i+1} \cdot \mathbf{n}, \widehat{\mathbf{m}}_h^{i+1} \cdot \mathbf{s}_h^{i+1} \rangle_{\Gamma' \cap \Gamma}). \end{aligned}$$

Let $\delta > 0$ be arbitrary. Since $\|\widehat{\mathbf{m}}_h^{i+1}\|_{L^\infty(\Omega)} = 1$, for the last term on the right-hand side, it holds that

$$\begin{aligned} & \sum_{i=0}^{j-1} \langle \mathbf{m}_h^{i+1} \otimes \mathbf{j}^{i+1}, \nabla \mathbf{s}_h^{i+1} \rangle_{\Omega} - \sum_{i=0}^{j-1} \langle \mathbf{j}^{i+1} \cdot \mathbf{n}, \mathbf{m}_h^{i+1} \cdot \mathbf{s}_h^{i+1} \rangle_{\Gamma' \cap \Gamma} \\ & \leq \sum_{i=0}^{j-1} \left(\|\mathbf{j}^{i+1}\|_{L^2(\Omega')} \|\nabla \mathbf{s}_h^{i+1}\|_{L^2(\Omega')} + \|\mathbf{j}^{i+1}\|_{L^2(\Gamma')} \|\mathbf{s}_h^{i+1}\|_{L^2(\Gamma')} \right) \\ & \leq (1 + C_1) \sum_{i=0}^{j-1} \|\mathbf{j}^{i+1}\|_{H^1(\Omega')} \|\mathbf{s}_h^{i+1}\|_{H^1(\Omega')} \\ & \leq \frac{1 + C_1}{2\delta} \sum_{i=0}^{j-1} \|\mathbf{j}^{i+1}\|_{H^1(\Omega')}^2 + \frac{\delta(1 + C_1)}{2} \sum_{i=0}^{j-1} \|\mathbf{s}_h^{i+1}\|_{H^1(\Omega')}^2, \end{aligned}$$

where $C_1 = C_1(\Omega')$ is the continuity constant of the trace operator. It follows that

$$\begin{aligned} & \|\mathbf{s}_h^j\|_{L^2(\Omega')}^2 + \sum_{i=0}^{j-1} \|\mathbf{s}_h^{i+1} - \mathbf{s}_h^i\|_{L^2(\Omega')}^2 + [2C_2 - \delta z\beta(1 + C_1)]k \sum_{i=0}^{j-1} \|\mathbf{s}_h^{i+1}\|_{H^1(\Omega')}^2 \\ & \leq \|\mathbf{s}_h^0\|_{L^2(\Omega')}^2 + \frac{z\beta(1 + C_1)}{\delta}k \sum_{i=0}^{j-1} \|\mathbf{j}^{i+1}\|_{H^1(\Omega')}^2, \end{aligned}$$

where $C_2 = \min\{zD_*(1 - \beta\beta'), \tau_{\text{sf}}^{-1}\}$. We choose $\delta < 2C_2/(z\beta(1 + C_1))$ so that all the terms on the left-hand side are nonnegative. Thanks to the convergences (5.10) and (5.11b) the right-hand side is uniformly bounded. This leads to (5.14). The involved constant $C > 0$ depends on β , C_1 , C_2 , \mathbf{j} , \mathbf{s}^0 , and z . In particular, it is independent of k and h . \square

Lemma 5.1.9. (a) Let $1/2 < \theta \leq 1$. For the standard tangent plane scheme, suppose that either any triangulation \mathcal{T}_h satisfies the angle condition (3.16) or $k = o(h^2)$ as $k, h \rightarrow 0$. If k is sufficiently small, then, for all $1 \leq j \leq M$, it holds that

$$\|\mathbf{m}_h^j\|_{H^1(\Omega)}^2 + k \sum_{i=0}^{j-1} \|\mathbf{v}_h^i\|_{L^2(\Omega)}^2 + k^2 \sum_{i=0}^{j-1} \|\nabla \mathbf{v}_h^i\|_{L^2(\Omega)}^2 \leq C. \quad (5.15)$$

(b) Let $0 \leq \theta \leq 1/2$. Suppose that

- either $\theta = 1/2$ and, only for the standard tangent plane scheme, that any triangulation \mathcal{T}_h satisfies the angle condition (3.16),

- or $k = o(h^2)$ as $k, h \rightarrow 0$.

If k is sufficiently small, then, for all $1 \leq j \leq M$, it holds that

$$\|\mathbf{m}_h^j\|_{\mathbf{H}^1(\Omega)}^2 + k \sum_{i=0}^{j-1} \|\mathbf{v}_h^i\|_{\mathbf{L}^2(\Omega)}^2 \leq C. \quad (5.16)$$

In both cases, the constant $C > 0$ depends only on the problem data $(\alpha, \beta, \beta', D_*, \mathbf{j}, \lambda_{\text{ex}}, \mathbf{m}^0, \Omega, \mathbf{s}^0, \tau_{\text{sf}}, \tau_J, z)$ and on the discretization parameters γ and θ . In particular, it is independent of k and h .

Proof. The proof follows the lines of the one of Lemma 4.3.8, therefore we only sketch it. Let $1 \leq j \leq M$. First of all, note that (4.31), namely

$$\|\mathbf{m}_h^j\|_{\mathbf{L}^2(\Omega)}^2 \leq C_1 + C_2 k^2 \sum_{i=0}^{j-1} \|\mathbf{v}_h^i\|_{\mathbf{L}^2(\Omega)}^2,$$

with $C_1 = C_1(\gamma, \mathbf{m}^0, |\Omega|) > 0$ and $C_2 = C_2(\gamma) > 0$ being constants, remains valid also for the present situation.

We now apply Lemma 5.1.7. Owing to (5.12)–(5.13) and taking the sum over $0 \leq i \leq j-1$, it follows that

$$\begin{aligned} & \frac{\lambda_{\text{ex}}^2}{2} \|\nabla \mathbf{m}_h^j\|_{\mathbf{L}^2(\Omega)}^2 + [\alpha - C_3 k h^{-2}] k \sum_{i=0}^{j-1} \|\mathbf{v}_h^i\|_{\mathbf{L}^2(\Omega)}^2 + \lambda_{\text{ex}}^2 \left(\theta - \frac{1}{2} \right) k^2 \sum_{i=0}^{j-1} \|\nabla \mathbf{v}_h^i\|_{\mathbf{L}^2(\Omega)}^2 \\ & \leq \frac{\lambda_{\text{ex}}^2}{2} \|\nabla \mathbf{m}_h^0\|_{\mathbf{L}^2(\Omega)}^2 + \tau_J^{-1} k \sum_{i=0}^{j-1} \langle \mathbf{s}_h^i, \mathbf{v}_h^i \rangle_\Omega, \end{aligned} \quad (5.17)$$

where, for the projection-free tangent plane scheme and for the standard tangent plane scheme if any triangulation of the family satisfies the angle condition (3.16), the estimate holds with $C_3 = 0$. Otherwise, it holds that $C_3 = C_3(\gamma, \lambda_{\text{ex}}, |\Omega|) > 0$. The first term on the right-hand side is uniformly bounded by assumption (5.11a). For the second term, we use the Cauchy–Schwarz inequality as well as the weighted Young inequality:

$$\sum_{i=0}^{j-1} \langle \mathbf{s}_h^i, \mathbf{v}_h^i \rangle_\Omega \leq \sum_{i=0}^{j-1} \|\mathbf{s}_h^i\|_{\mathbf{L}^2(\Omega)} \|\mathbf{v}_h^i\|_{\mathbf{L}^2(\Omega)} \leq \frac{\delta}{2} \sum_{i=0}^{j-1} \|\mathbf{v}_h^i\|_{\mathbf{L}^2(\Omega)}^2 + \frac{1}{2\delta} \sum_{i=0}^{j-1} \|\mathbf{s}_h^i\|_{\mathbf{L}^2(\Omega)}^2,$$

where $\delta > 0$ is arbitrary. The first term on the right-hand side can be absorbed into the corresponding term on the left-hand side of (5.17). The second term is uniformly bounded by Lemma 5.1.8; see (5.14). Altogether, we thus obtain that

$$\begin{aligned} & \|\mathbf{m}_h^j\|_{\mathbf{H}^1(\Omega)}^2 + \frac{2}{\lambda_{\text{ex}}^2} \left(\alpha - \frac{\delta}{2\tau_J} - \frac{C_2 \lambda_{\text{ex}}^2}{2} k - C_3 k h^{-2} \right) k \sum_{i=0}^{j-1} \|\mathbf{v}_h^i\|_{\mathbf{L}^2(\Omega)}^2 \\ & + (2\theta - 1) k^2 \sum_{i=0}^{j-1} \|\nabla \mathbf{v}_h^i\|_{\mathbf{L}^2(\Omega)}^2 \leq C_4, \end{aligned}$$

where $C_4 = C_4(C, \delta, \gamma, \lambda_{\text{ex}}, \mathbf{m}^0, \Omega) > 0$ with $C > 0$ being the constant in (5.14). With this estimate, both the inequalities (5.15)–(5.16) easily follow by choosing a sufficiently small δ , e.g., $\delta = \alpha\tau_J$, and a sufficiently small time-step size k (in the case of (5.16) also an inverse estimate is needed). \square

Using the energy estimates proved in Lemma 5.1.9, the result of Lemma 4.3.10, i.e., the convergence

$$k \|\nabla \mathbf{v}_{hk}^-\|_{\mathbf{L}^2(\Omega_T)} \rightarrow 0 \quad \text{as } k, h \rightarrow 0, \quad (5.18)$$

remains valid under the same assumptions on the discretization parameters k , h , and θ . In the following proposition, we establish the uniform boundedness of the discrete functions (5.9).

Proposition 5.1.10. *Suppose that the assumptions of Theorem 5.1.6 are satisfied. Then, if k is sufficiently small, the sequences $\{\mathbf{m}_{hk}\}$, $\{\mathbf{m}_{hk}^\pm\}$, $\{\widehat{\mathbf{m}}_{hk}\}$, $\{\widehat{\mathbf{m}}_{hk}^\pm\}$, $\{\mathbf{v}_{hk}^-\}$, $\{\mathbf{s}_{hk}\}$, and $\{\mathbf{s}_{hk}^\pm\}$ are uniformly bounded in the sense that*

$$\|\mathbf{m}_{hk}^*\|_{L^\infty(0,T;\mathbf{H}^1(\Omega))} + \|\partial_t \mathbf{m}_{hk}\|_{L^2(\Omega_T)} + \|\mathbf{v}_{hk}^-\|_{L^2(\Omega_T)} \leq C, \quad (5.19a)$$

$$\|\widehat{\mathbf{m}}_{hk}^*\|_{L^\infty(0,T;\mathbf{H}^1(\Omega))} + \|\widehat{\mathbf{m}}_{hk}^*\|_{L^\infty(\Omega_T)} \leq C, \quad (5.19b)$$

$$\|\mathbf{s}_{hk}\|_{L^2(0,T;\mathbf{H}^1(\Omega'),L^2(\Omega'))} + \|\mathbf{s}_{hk}^*\|_{L^\infty(0,T;L^2(\Omega'))} + \|\mathbf{s}_{hk}^\pm\|_{L^2(0,T;\mathbf{H}^1(\Omega'))} \leq C, \quad (5.19c)$$

for $\mathbf{m}_{hk}^* = \mathbf{m}_{hk}$, $\mathbf{m}_{hk}^\pm = \widehat{\mathbf{m}}_{hk}^\pm$, $\widehat{\mathbf{m}}_{hk}^* = \widehat{\mathbf{m}}_{hk}$, $\widehat{\mathbf{m}}_{hk}^\pm = \widehat{\mathbf{m}}_{hk}^\pm$, and $\mathbf{s}_{hk}^* = \mathbf{s}_{hk}$, $\mathbf{s}_{hk}^\pm = \mathbf{s}_{hk}^\pm$. The constant $C > 0$ depends only on the problem data $(\alpha, \beta, \beta', D_*, \mathbf{j}, \lambda_{\text{ex}}, \mathbf{m}^0, \Omega, \mathbf{s}^0, \tau_J, \tau_{\text{sf}}, \text{ and } z)$ and on the discretization parameters γ and θ . In particular, it is independent of k and h .

Proof. The estimates (5.19a)–(5.19b) for the magnetization-related functions can be obtained with the same argument of Proposition 4.3.9 and Proposition 4.3.12. For the sake of clarity, we divide the proof of (5.19c) into two steps.

- **Step 1** Proof of the boundedness $\|\mathbf{s}_{hk}^*\|_{L^\infty(0,T;L^2(\Omega'))} + \|\mathbf{s}_{hk}^*\|_{L^2(0,T;\mathbf{H}^1(\Omega'))} \leq C$ for $\mathbf{s}_{hk}^* = \mathbf{s}_{hk}, \mathbf{s}_{hk}^\pm$.

We apply Lemma 5.1.8. For any $t \in (0, T)$, let $0 \leq i \leq M-1$ such that $t \in [t_i, t_{i+1})$. It holds that

$$\begin{aligned} \|\mathbf{s}_{hk}(t)\|_{L^2(\Omega')} &= \left\| \frac{t-t_i}{k} \mathbf{s}_h^{i+1} + \frac{t_{i+1}-t}{k} \mathbf{s}_h^i \right\|_{L^2(\Omega')} \\ &\leq \frac{t-t_i}{k} \|\mathbf{s}_h^{i+1}\|_{L^2(\Omega')} + \frac{t_{i+1}-t}{k} \|\mathbf{s}_h^i\|_{L^2(\Omega')} \\ &\leq \|\mathbf{s}_h^{i+1}\|_{L^2(\Omega')} + \|\mathbf{s}_h^i\|_{L^2(\Omega')} \stackrel{(5.14)}{\leq} C, \end{aligned}$$

which shows that $\|\mathbf{s}_{hk}\|_{L^\infty(0,T;L^2(\Omega'))} \leq C$. Similarly, it holds that

$$\begin{aligned} \|\mathbf{s}_{hk}\|_{L^2(0,T;\mathbf{H}^1(\Omega'))}^2 &= \int_0^T \|\mathbf{s}_{hk}(t)\|_{\mathbf{H}^1(\Omega')}^2 dt \\ &= \sum_{i=0}^{M-1} \int_{t_i}^{t_{i+1}} \left\| \frac{t-t_i}{k} \mathbf{s}_h^{i+1} + \frac{t_{i+1}-t}{k} \mathbf{s}_h^i \right\|_{\mathbf{H}^1(\Omega')}^2 dt \\ &\leq 2 \sum_{i=0}^{M-1} \int_{t_i}^{t_{i+1}} \frac{(t-t_i)^2}{k^2} \|\mathbf{s}_h^{i+1}\|_{\mathbf{H}^1(\Omega')}^2 + \frac{(t_{i+1}-t)^2}{k^2} \|\mathbf{s}_h^i\|_{\mathbf{H}^1(\Omega')}^2 dt \\ &= \frac{2}{3} k \sum_{i=0}^{M-1} \left(\|\mathbf{s}_h^{i+1}\|_{\mathbf{H}^1(\Omega')}^2 + \|\mathbf{s}_h^i\|_{\mathbf{H}^1(\Omega')}^2 \right) \stackrel{(5.14)}{\leq} C, \end{aligned}$$

which shows that $\|\mathbf{s}_{hk}\|_{L^2(0,T;\mathbf{H}^1(\Omega'))} \leq C$. The same proof holds also for \mathbf{s}_{hk}^\pm .

- **Step 2** Proof of the boundedness $\|\mathbf{s}_{hk}\|_{L^2(0,T;\mathbf{H}^1(\Omega'),L^2(\Omega'))} \leq C$.

It remains to show that $\|\partial_t \mathbf{s}_{hk}\|_{L^2(0,T;\widetilde{\mathbf{H}}^{-1}(\Omega))} \leq C$. To that end, let $\mathcal{P}_h : L^2(\Omega') \rightarrow \mathcal{S}^1(\mathcal{T}_h)^3$ be the L^2 -orthogonal projection. Recall that, since we are dealing with a γ -quasi-uniform family of regular triangulations, \mathcal{P}_h is H^1 -stable; see (3.19). Let $\boldsymbol{\zeta} \in \mathbf{H}^1(\Omega') \setminus \{\mathbf{0}\}$ and $0 \leq i \leq M-1$ be

arbitrary. For all $t \in [t_i, t_{i+1})$, it holds that

$$\begin{aligned}
& \langle \partial_t \mathbf{s}_{hk}(t), \boldsymbol{\zeta} \rangle_{H^{-1} \leftrightarrow H^1} \\
&= \langle \partial_t \mathbf{s}_{hk}(t), \boldsymbol{\zeta} \rangle_{\Omega'} = \langle d_t \mathbf{s}_h^{i+1}, \boldsymbol{\zeta} \rangle_{\Omega'} = \langle d_t \mathbf{s}_h^{i+1}, \mathcal{P}_h \boldsymbol{\zeta} \rangle_{\Omega'} \\
&= z\beta \langle \widehat{\mathbf{m}}_h^{i+1} \otimes \mathbf{j}^{i+1}, \nabla \mathcal{P}_h \boldsymbol{\zeta} \rangle_{\Omega} - z\beta \langle \mathbf{j}^{i+1} \cdot \mathbf{n}, \widehat{\mathbf{m}}_h^{i+1} \cdot \mathcal{P}_h \boldsymbol{\zeta} \rangle_{\Gamma' \cap \Gamma} - a(\widehat{\mathbf{m}}_h^{i+1}; \mathbf{s}_h^{i+1}, \mathcal{P}_h \boldsymbol{\zeta}) \\
&\leq z\beta \|\mathbf{j}^{i+1}\|_{L^2(\Omega')} \|\nabla \mathcal{P}_h \boldsymbol{\zeta}\|_{L^2(\Omega')} + z\beta \|\mathbf{j}^{i+1}\|_{L^2(\Gamma')} \|\mathcal{P}_h \boldsymbol{\zeta}\|_{L^2(\Gamma')} + C \|\mathbf{s}_h^{i+1}\|_{\mathbf{H}^1(\Omega')} \|\mathcal{P}_h \boldsymbol{\zeta}\|_{\mathbf{H}^1(\Omega')} \\
&\lesssim \left(\|\mathbf{j}^{i+1}\|_{\mathbf{H}^1(\Omega')} + \|\mathbf{s}_h^{i+1}\|_{\mathbf{H}^1(\Omega')} \right) \|\mathcal{P}_h \boldsymbol{\zeta}\|_{\mathbf{H}^1(\Omega')} \\
&\lesssim \left(\|\mathbf{j}^{i+1}\|_{\mathbf{H}^1(\Omega')} + \|\mathbf{s}_h^{i+1}\|_{\mathbf{H}^1(\Omega')} \right) \|\boldsymbol{\zeta}\|_{\mathbf{H}^1(\Omega')}.
\end{aligned}$$

Here, we have used the continuity of both the bilinear form $a(\widehat{\mathbf{m}}_h^{i+1}; \cdot, \cdot)$ and the trace operator $\mathbf{H}^1(\Omega') \rightarrow L^2(\Gamma')$ as well as the H^1 -stability of the L^2 -projection. Dividing by $\|\boldsymbol{\zeta}\|_{\mathbf{H}^1(\Omega')}$ and taking the supremum with respect to $\boldsymbol{\zeta} \in \mathbf{H}^1(\Omega') \setminus \{\mathbf{0}\}$, it follows that

$$\|\partial_t \mathbf{s}_{hk}(t)\|_{\widetilde{\mathbf{H}}^{-1}(\Omega')} \lesssim \|\mathbf{j}^{i+1}\|_{\mathbf{H}^1(\Omega')} + \|\mathbf{s}_h^{i+1}\|_{\mathbf{H}^1(\Omega')}.$$

Integrating in time over $(0, T)$, we obtain

$$\|\partial_t \mathbf{s}_{hk}\|_{L^2(0, T; \widetilde{\mathbf{H}}^{-1}(\Omega'))} \lesssim \|\mathbf{j}_k^+\|_{L^2(0, T; \mathbf{H}^1(\Omega'))} + \|\mathbf{s}_{hk}^+\|_{L^2(0, T; \mathbf{H}^1(\Omega'))}.$$

Thanks to step 1 and (5.10), the right-hand side is uniformly bounded, which concludes the proof. \square

In the following proposition, we proceed with the extraction of weakly convergent subsequences.

Proposition 5.1.11. *Suppose that the assumptions of Theorem 5.1.6 are satisfied. Then, there exist $\mathbf{m} \in L^\infty(0, T; \mathbf{H}^1(\Omega)) \cap H^1(0, T; L^2(\Omega))$, which satisfies $|\mathbf{m}| = 1$ and $\mathbf{m} \cdot \partial_t \mathbf{m} = 0$ a.e. in Ω_T , and $\mathbf{s} \in L^2(0, T; \mathbf{H}^1(\Omega'), L^2(\Omega')) \cap L^\infty(0, T; L^2(\Omega'))$ such that, upon extraction of a subsequence, it holds that*

$$\mathbf{m}_{hk} \rightharpoonup \mathbf{m} \quad \text{in } \mathbf{H}^1(\Omega_T), \quad (5.20a)$$

$$\mathbf{m}_{hk}, \mathbf{m}_{hk}^\pm, \widehat{\mathbf{m}}_{hk}, \widehat{\mathbf{m}}_{hk}^\pm \rightharpoonup \mathbf{m} \quad \text{in } L^2(0, T; \mathbf{H}^1(\Omega)), \quad (5.20b)$$

$$\mathbf{m}_{hk} \rightarrow \mathbf{m} \quad \text{in } \mathbf{H}^s(\Omega_T) \text{ for all } 0 < s < 1, \quad (5.20c)$$

$$\mathbf{m}_{hk} \rightarrow \mathbf{m} \quad \text{in } L^2(0, T; \mathbf{H}^s(\Omega)) \text{ for all } 0 < s < 1, \quad (5.20d)$$

$$\mathbf{m}_{hk}, \mathbf{m}_{hk}^\pm, \widehat{\mathbf{m}}_{hk}, \widehat{\mathbf{m}}_{hk}^\pm \rightarrow \mathbf{m} \quad \text{in } L^2(\Omega_T), \quad (5.20e)$$

$$\mathbf{m}_{hk}, \mathbf{m}_{hk}^\pm, \widehat{\mathbf{m}}_{hk}, \widehat{\mathbf{m}}_{hk}^\pm \rightarrow \mathbf{m} \quad \text{pointwise a.e. in } \Omega_T, \quad (5.20f)$$

$$\mathbf{m}_{hk}, \mathbf{m}_{hk}^\pm, \widehat{\mathbf{m}}_{hk}, \widehat{\mathbf{m}}_{hk}^\pm \xrightarrow{*} \mathbf{m} \quad \text{in } L^\infty(0, T; \mathbf{H}^1(\Omega)), \quad (5.20g)$$

$$\widehat{\mathbf{m}}_{hk}, \widehat{\mathbf{m}}_{hk}^\pm \xrightarrow{*} \mathbf{m} \quad \text{in } L^\infty(\Omega_T) \quad (5.20h)$$

$$\mathbf{v}_{hk}^- \rightharpoonup \partial_t \mathbf{m} \quad \text{in } L^2(\Omega_T), \quad (5.20i)$$

$$\mathbf{s}_{hk} \rightharpoonup \mathbf{s} \quad \text{in } L^2(0, T; \mathbf{H}^1(\Omega'), L^2(\Omega')), \quad (5.20j)$$

$$\mathbf{s}_{hk}^\pm \rightharpoonup \mathbf{s} \quad \text{in } L^2(0, T; \mathbf{H}^1(\Omega')), \quad (5.20k)$$

$$\mathbf{s}_{hk}, \mathbf{s}_{hk}^\pm \rightarrow \mathbf{s} \quad \text{in } L^2(\Omega'_T), \quad (5.20l)$$

$$\mathbf{s}_{hk}, \mathbf{s}_{hk}^\pm \rightarrow \mathbf{s} \quad \text{pointwise a.e. in } \Omega'_T, \quad (5.20m)$$

$$\mathbf{s}_{hk}, \mathbf{s}_{hk}^\pm \xrightarrow{*} \mathbf{s} \quad \text{in } L^\infty(0, T; L^2(\Omega')) \quad (5.20n)$$

as $k, h \rightarrow 0$. In particular, all the limits are attained simultaneously for at least one particular subsequence.

Proof. We omit the proof of the results for the magnetization-related discrete functions, as it follows the lines of those of Proposition 4.3.11 and Proposition 4.3.12. It remains to show the existence of $\mathbf{s} \in L^2(0, T; \mathbf{H}^1(\Omega'), \mathbf{L}^2(\Omega')) \cap L^\infty(0, T; \mathbf{L}^2(\Omega'))$ such that the convergence results (5.20j)–(5.20n) hold. Thanks to the uniform boundedness (5.19c) established in Proposition 5.1.10, we can apply the Eberlein–Šmulian theorem and extract weakly convergent subsequences (not relabeled) of $\{\mathbf{s}_{hk}\}$, $\{\mathbf{s}_{hk}^\pm\}$, with possible different limits, in $L^2(0, T; \mathbf{H}^1(\Omega'), \mathbf{L}^2(\Omega'))$ and $L^2(0, T; \mathbf{H}^1(\Omega'))$, respectively. Let $\mathbf{s} \in L^2(0, T; \mathbf{H}^1(\Omega'), \mathbf{L}^2(\Omega'))$ such that $\mathbf{s}_{hk} \rightharpoonup \mathbf{s}$ in $L^2(0, T; \mathbf{H}^1(\Omega'), \mathbf{L}^2(\Omega'))$. From the compact embedding $L^2(0, T; \mathbf{H}^1(\Omega'), \mathbf{L}^2(\Omega')) \Subset \mathbf{L}^2(\Omega'_T)$ guaranteed by the Aubin–Lions lemma, it follows that $\mathbf{s}_{hk} \rightarrow \mathbf{s}$ in $\mathbf{L}^2(\Omega'_T)$. Upon extraction of a further subsequence, it also holds that $\mathbf{s}_{hk} \rightarrow \mathbf{s}$ pointwise a.e. in Ω'_T . From Lemma 5.1.8, it follows that

$$\|\mathbf{s}_{hk} - \mathbf{s}_{hk}^\pm\|_{\mathbf{L}^2(\Omega'_T)}^2 \stackrel{(3.15)}{\leq} \|\mathbf{s}_{hk}^+ - \mathbf{s}_{hk}^-\|_{\mathbf{L}^2(\Omega'_T)}^2 = k \sum_{i=0}^{M-1} \|\mathbf{s}_h^{i+1} - \mathbf{s}_h^i\|_{\mathbf{L}^2(\Omega')}^2 \stackrel{(5.14)}{\lesssim} k.$$

In particular, it follows that $\mathbf{s}_{hk}^\pm \rightharpoonup \mathbf{s}$ in $L^2(0, T; \mathbf{H}^1(\Omega'))$ as well as $\mathbf{s}_{hk}^\pm \rightarrow \mathbf{s}$ in $\mathbf{L}^2(\Omega'_T)$ and pointwise a.e. in Ω'_T .

Finally, since the sequences $\{\mathbf{s}_{hk}\}$ and $\{\mathbf{s}_{hk}^\pm\}$ are uniformly bounded in $L^\infty(0, T; \mathbf{L}^2(\Omega'))$, applying the Banach–Alaoglu theorem, we can extract further weakly-star convergent subsequences (also not relabeled). From the continuous inclusion $L^\infty(0, T; \mathbf{L}^2(\Omega')) \subset \mathbf{L}^2(\Omega'_T)$, it follows that the weak-star limits coincide with the strong limits in $\mathbf{L}^2(\Omega'_T)$, i.e., it holds that $\mathbf{s}_{hk}, \mathbf{s}_{hk}^\pm \xrightarrow{*} \mathbf{s}$ in $L^\infty(0, T; \mathbf{L}^2(\Omega'))$. \square

In the following lemma, we establish two convergence results that are preparatory for the proof of Theorem 5.1.6.

Lemma 5.1.12. *Suppose that the assumptions of Theorem 5.1.6 are satisfied. Then, it holds that*

$$\widehat{\mathbf{m}}_{hk}^+ \otimes \mathbf{j}_k^+ \rightarrow \mathbf{m} \otimes \mathbf{j} \quad \text{in } \mathbf{L}^2(\Omega_T), \quad (5.21a)$$

$$\widehat{\mathbf{m}}_{hk}^+ \otimes \widehat{\mathbf{m}}_{hk}^+ \rightarrow \mathbf{m} \otimes \mathbf{m} \quad \text{in } \mathbf{L}^2(\Omega_T) \quad (5.21b)$$

as $k, h \rightarrow 0$.

Proof. An application of the triangle inequality yields the estimate

$$\begin{aligned} \|\widehat{\mathbf{m}}_{hk}^+ \otimes \mathbf{j}_k^+ - \mathbf{m} \otimes \mathbf{j}\|_{\mathbf{L}^2(\Omega_T)} &\leq \|\widehat{\mathbf{m}}_{hk}^+ \otimes (\mathbf{j}_k^+ - \mathbf{j})\|_{\mathbf{L}^2(\Omega_T)} + \|(\widehat{\mathbf{m}}_{hk}^+ - \mathbf{m}) \otimes \mathbf{j}\|_{\mathbf{L}^2(\Omega_T)} \\ &\leq \|\mathbf{j}_k^+ - \mathbf{j}\|_{\mathbf{L}^2(\Omega_T)} + \|\mathbf{j}\|_{\mathbf{L}^\infty(\Omega_T)} \|\widehat{\mathbf{m}}_{hk}^+ - \mathbf{m}\|_{\mathbf{L}^2(\Omega_T)}. \end{aligned}$$

The convergence (5.21a) then follows from (5.10) and (5.20e). The same proof also leads to (5.21b). \square

We are ready for the proof of Theorem 5.1.6.

Proof of Theorem 5.1.6. From Proposition 5.1.11, we obtain the desired convergence properties towards some functions $\mathbf{m} \in L^\infty(0, T; \mathbf{H}^1(\Omega)) \cap H^1(0, T; \mathbf{L}^2(\Omega))$, satisfying $|\mathbf{m}| = 1$ a.e. in Ω , and $\mathbf{s} \in L^2(0, T; \mathbf{H}^1(\Omega'), \mathbf{L}^2(\Omega')) \cap L^\infty(0, T; \mathbf{L}^2(\Omega'))$. It remains to show that (\mathbf{m}, \mathbf{s}) is a weak solution of (5.1) in the sense of Definition 5.1.2. For the sake of clarity, we divide the proof into four steps.

• **Step 1:** Verification of Definition 4.1.1(iii).

The proof of (5.3) coincides with the one of (4.4), therefore we only sketch it; see steps 2–4 of the proof of Theorem 4.3.2.

Let $\varphi \in C^\infty(\overline{\Omega_T})$ be an arbitrary test function. For all $0 \leq i \leq M-1$ and $t \in (t_i, t_{i+1})$, we can choose the test function $\phi_h = \mathcal{I}_h[\mathbf{m}_{hk}^-(t) \times \varphi(t)] \in \mathcal{K}_{\mathbf{m}_h^i}$ in (5.6). Integrating in time over $(0, T)$

yields the identity

$$\begin{aligned}
& \alpha \int_0^T \langle \mathbf{v}_{hk}^-(t), \mathcal{I}_h[\mathbf{m}_{hk}^-(t) \times \boldsymbol{\varphi}(t)] \rangle_\Omega dt + \int_0^T \langle \mathbf{m}_{hk}^-(t) \times \mathbf{v}_{hk}^-(t), \mathcal{I}_h[\mathbf{m}_{hk}^-(t) \times \boldsymbol{\varphi}(t)] \rangle_\Omega dt \\
& + \lambda_{\text{ex}}^2 \theta k \int_0^T \langle \nabla \mathbf{v}_{hk}^-(t), \nabla \mathcal{I}_h[\mathbf{m}_{hk}^-(t) \times \boldsymbol{\varphi}(t)] \rangle_\Omega dt \\
& = -\lambda_{\text{ex}}^2 \int_0^T \langle \nabla \mathbf{m}_{hk}^-(t), \nabla \mathcal{I}_h[\mathbf{m}_{hk}^-(t) \times \boldsymbol{\varphi}(t)] \rangle_\Omega dt + \int_0^T \langle \mathbf{s}_{hk}^-(t), \mathcal{I}_h[\mathbf{m}_{hk}^-(t) \times \boldsymbol{\varphi}(t)] \rangle_\Omega dt.
\end{aligned}$$

With the same argument employed in step 3 of the proof of Theorem 4.3.2, we deduce that

$$\begin{aligned}
& \alpha \int_0^T \langle \mathbf{v}_{hk}^-(t), \mathbf{m}_{hk}^-(t) \times \boldsymbol{\varphi}(t) \rangle_\Omega dt + \int_0^T \langle \mathbf{m}_{hk}^-(t) \times \mathbf{v}_{hk}^-(t), \mathbf{m}_{hk}^-(t) \times \boldsymbol{\varphi}(t) \rangle_\Omega dt \\
& + \lambda_{\text{ex}}^2 \int_0^T \langle \nabla \mathbf{m}_{hk}^-(t), \nabla (\mathbf{m}_{hk}^-(t) \times \boldsymbol{\varphi}(t)) \rangle_\Omega dt + \lambda_{\text{ex}}^2 \theta k \int_0^T \langle \nabla \mathbf{v}_{hk}^-(t), \nabla (\mathbf{m}_{hk}^-(t) \times \boldsymbol{\varphi}(t)) \rangle_\Omega dt \\
& - \int_0^T \langle \mathbf{s}_{hk}^-(t), \mathbf{m}_{hk}^-(t) \times \boldsymbol{\varphi}(t) \rangle_\Omega dt = \mathcal{O}(h) \quad \text{as } k, h \rightarrow 0.
\end{aligned}$$

Passing to the limit as $k, h \rightarrow 0$, we obtain (5.3). The fact that each of the first three terms on the left-hand side converge towards the corresponding one of (5.3) and that the fourth one, thanks to (5.18), vanishes as $k, h \rightarrow 0$ was already shown in step 4 of the proof of Theorem 4.3.2. As for the fifth one, since $\mathbf{s}_{hk}^- \rightarrow \mathbf{s}$ in $\mathbf{L}^2(\Omega_T) \subseteq \mathbf{L}^2(\Omega'_T)$ by (5.20l) and $\mathbf{m}_{hk}^- \times \boldsymbol{\varphi} \rightarrow \mathbf{m} \times \boldsymbol{\varphi}$ in $\mathbf{L}^2(\Omega_T)$ by (4.47a), it holds that

$$\int_0^T \langle \mathbf{s}_{hk}^-(t), \mathbf{m}_{hk}^-(t) \times \boldsymbol{\varphi}(t) \rangle_\Omega dt \rightarrow \int_0^T \langle \mathbf{s}(t), \mathbf{m}(t) \times \boldsymbol{\varphi}(t) \rangle_\Omega dt = - \int_0^T \langle \mathbf{m}(t) \times \mathbf{s}(t), \boldsymbol{\varphi}(t) \rangle_\Omega dt,$$

which concludes the verification of Definition 4.1.1(iii).

• **Step 2:** Verification of Definition 4.1.1(iv).

Let $\boldsymbol{\eta} \in C^1([0, T]; \mathbf{C}^\infty(\Omega'))$. Let $\boldsymbol{\eta}_h : [0, T] \rightarrow \mathcal{S}^1(\mathcal{T}'_h)^3$ be defined by $\boldsymbol{\eta}_h(t) = \mathcal{I}_h[\boldsymbol{\eta}(t)]$ for all $t \in [0, T]$. Owing to the approximation properties of the nodal interpolant (see Proposition 3.4.3), we infer that

$$\boldsymbol{\eta}_h \rightarrow \boldsymbol{\eta} \quad \text{in } L^\infty(0, T; \mathbf{W}^{1,p}(\Omega')) \quad \text{for all } 3/2 < p < \infty. \quad (5.22)$$

For all $0 \leq i \leq M-1$ and $t \in (t_i, t_{i+1})$, we can choose the test function $\boldsymbol{\zeta}_h = \boldsymbol{\eta}_h(t) \in \mathcal{S}^1(\mathcal{T}'_h)^3$ in (5.8). Integrating in time over $(0, T)$, we obtain

$$\begin{aligned}
& \int_0^T \langle \partial_t \mathbf{s}_{hk}(t), \boldsymbol{\eta}_h(t) \rangle_{\Omega'} dt + \int_0^T a(\widehat{\mathbf{m}}_{hk}^+(t); \mathbf{s}_{hk}^+(t), \boldsymbol{\eta}_h(t)) dt \\
& = z\beta \int_0^T \langle \widehat{\mathbf{m}}_{hk}^+(t) \otimes \mathbf{j}_k^+(t), \nabla \boldsymbol{\eta}_h(t) \rangle_\Omega dt - z\beta \int_0^T \langle \mathbf{j}_k^+(t) \cdot \mathbf{n}, \widehat{\mathbf{m}}_{hk}^+(t) \cdot \boldsymbol{\eta}_h(t) \rangle_{\Gamma' \cap \Gamma} dt.
\end{aligned} \quad (5.23)$$

We now study the limit of (5.23) as $k, h \rightarrow 0$. For the first term on the left-hand side, since $\partial_t \mathbf{s}_{hk} \rightharpoonup \partial_t \mathbf{s}$ in $L^2(0, T; \widehat{\mathbf{H}}^{-1}(\Omega'))$ by (5.20j) and $\boldsymbol{\eta}_h \rightarrow \boldsymbol{\eta}$ in $L^2(0, T; \mathbf{H}^1(\Omega'))$ by (5.22), it holds that

$$\int_0^T \langle \partial_t \mathbf{s}_{hk}(t), \boldsymbol{\eta}_h(t) \rangle_{\Omega'} dt = \int_0^T \langle \partial_t \mathbf{s}_{hk}(t), \boldsymbol{\eta}_h(t) \rangle_{H^{-1} \leftrightarrow H^1} dt \rightarrow \int_0^T \langle \partial_t \mathbf{s}(t), \boldsymbol{\eta}(t) \rangle_{H^{-1} \leftrightarrow H^1} dt.$$

For the first term on the right-hand side of (5.23), thanks to the convergence (5.21a), which follows from Lemma 5.1.12, and (5.22), we obtain that

$$\int_0^T \langle \widehat{\mathbf{m}}_{hk}^+(t) \otimes \mathbf{j}_k^+(t), \nabla \boldsymbol{\eta}_h(t) \rangle_\Omega dt \rightarrow \int_0^T \langle \mathbf{m}(t) \otimes \mathbf{j}(t), \nabla \boldsymbol{\eta}(t) \rangle_\Omega dt.$$

For the second term on the right-hand side of (5.23), since $\mathbf{j}_k^+ \rightarrow \mathbf{j}$ in $L^2(0, T; \mathbf{H}^1(\Omega'))$ by (5.10), $\widehat{\mathbf{m}}_{hk}^+ \rightharpoonup \mathbf{m}$ in $L^2(0, T; \mathbf{H}^1(\Omega))$ by (5.20b), and $\boldsymbol{\eta}_h \rightarrow \boldsymbol{\eta}$ in $L^2(0, T; \mathbf{H}^1(\Omega'))$ by (5.22) (together with the resulting convergence of the corresponding traces), it holds that

$$\int_0^T \langle \mathbf{j}_k^+(t) \cdot \mathbf{n}, \widehat{\mathbf{m}}_{hk}^+(t) \cdot \boldsymbol{\eta}_h(t) \rangle_{\Gamma' \cap \Gamma} dt \rightarrow \int_0^T \langle \mathbf{j}(t) \cdot \mathbf{n}, \mathbf{m}(t) \cdot \boldsymbol{\eta}(t) \rangle_{\Gamma' \cap \Gamma} dt.$$

We now analyze the second term on the left-hand side of (5.23). From the convergences $\mathbf{s}_{hk}^+ \rightharpoonup \mathbf{s}$ in $L^2(0, T; \mathbf{H}^1(\Omega'))$ by (5.20k) and (5.22), we deduce that

$$\int_0^T \langle D_0 \nabla \mathbf{s}_{hk}^+(t), \nabla \boldsymbol{\eta}_h(t) \rangle_{\Omega'} dt \rightarrow \int_0^T \langle D_0 \nabla \mathbf{s}(t), \nabla \boldsymbol{\eta}(t) \rangle_{\Omega'} dt.$$

Thanks to (5.20k) and the convergence $(\widehat{\mathbf{m}}_{hk}^+ \otimes \widehat{\mathbf{m}}_{hk}^+) \nabla \boldsymbol{\eta}_h^\top \rightarrow (\mathbf{m} \otimes \mathbf{m}) \nabla \boldsymbol{\eta}^\top$ in $\mathbf{L}^2(\Omega_T)$, which in turn follows from (5.21b) and (5.22), we obtain that

$$\begin{aligned} & \int_0^T \langle D_0 [\widehat{\mathbf{m}}_{hk}^+(t) \otimes \widehat{\mathbf{m}}_{hk}^+(t)] \nabla \mathbf{s}_{hk}^+(t), \nabla \boldsymbol{\eta}_h(t) \rangle_{\Omega'} dt \\ &= \int_0^T \langle D_0 \nabla \mathbf{s}_{hk}^+(t), [\widehat{\mathbf{m}}_{hk}^+(t) \otimes \widehat{\mathbf{m}}_{hk}^+(t)] \nabla \boldsymbol{\eta}_h^\top(t) \rangle_{\Omega'} dt \\ &\rightarrow \int_0^T \langle D_0 \nabla \mathbf{s}(t), [\mathbf{m}(t) \otimes \mathbf{m}(t)] \nabla \boldsymbol{\eta}^\top(t) \rangle_{\Omega'} dt = \int_0^T \langle D_0 [\mathbf{m}(t) \otimes \mathbf{m}(t)] \nabla \mathbf{s}(t), \nabla \boldsymbol{\eta}(t) \rangle_{\Omega'} dt. \end{aligned}$$

Since $\mathbf{s}_{hk}^+ \rightarrow \mathbf{s}$ in $\mathbf{L}^2(\Omega'_T)$ by (5.20l) and (5.22), it follows that

$$\int_0^T \langle \mathbf{s}_{hk}^+(t), \boldsymbol{\eta}_h(t) \rangle_{\Omega'} dt \rightarrow \int_0^T \langle \mathbf{s}(t), \boldsymbol{\eta}(t) \rangle_{\Omega'} dt.$$

Finally, thanks to (5.20l), (5.20e) and (5.22), we obtain that

$$\int_0^T \langle \mathbf{s}_{hk}^+(t) \times \widehat{\mathbf{m}}_{hk}^+(t), \boldsymbol{\eta}_h(t) \rangle_{\Omega} dt \rightarrow \int_0^T \langle \mathbf{s}(t) \times \mathbf{m}(t), \boldsymbol{\eta}(t) \rangle_{\Omega} dt.$$

We conclude that

$$\int_0^T a(\widehat{\mathbf{m}}_{hk}^+(t); \mathbf{s}_{hk}^+(t), \boldsymbol{\eta}_h(t)) dt \rightarrow \int_0^T a(\mathbf{m}(t); \mathbf{s}(t), \boldsymbol{\eta}(t)) dt.$$

Altogether, passing (5.23) to the limit as $k, h \rightarrow 0$, we obtain

$$\begin{aligned} & \int_0^T \langle \partial_t \mathbf{s}(t), \boldsymbol{\eta}(t) \rangle_{H^{-1} \leftrightarrow H^1} dt + \int_0^T a(\mathbf{m}(t); \mathbf{s}(t), \boldsymbol{\eta}(t)) dt \\ &= z\beta \int_0^T \langle \mathbf{m}(t) \otimes \mathbf{j}(t), \nabla \boldsymbol{\eta}(t) \rangle_{\Omega} dt - z\beta \int_0^T \langle \mathbf{j}(t) \cdot \mathbf{n}, \mathbf{m}(t) \cdot \boldsymbol{\eta}(t) \rangle_{\Gamma' \cap \Gamma} dt \end{aligned} \tag{5.24}$$

for all $\boldsymbol{\eta} \in C^1([0, T]; \mathbf{C}^\infty(\Omega'))$. By density, the equality then holds for all $\boldsymbol{\eta} \in L^2(0, T; \mathbf{H}^1(\Omega'))$. In particular, for a.e. $t \in (0, T)$ and $\boldsymbol{\zeta} \in \mathbf{H}^1(\Omega')$ it holds that

$$\langle \partial_t \mathbf{s}(t), \boldsymbol{\zeta} \rangle_{H^{-1} \leftrightarrow H^1} + a(\mathbf{m}(t); \mathbf{s}(t), \boldsymbol{\zeta}) = z\beta \langle \mathbf{m}(t) \otimes \mathbf{j}(t), \nabla \boldsymbol{\zeta} \rangle_{\Omega} - z\beta \langle \mathbf{j}(t) \cdot \mathbf{n}, \mathbf{m}(t) \cdot \boldsymbol{\zeta} \rangle_{\Gamma' \cap \Gamma},$$

which is (5.4).

- **Step 3:** Verification of Definition 5.1.2(ii).

With the same argument used in Step 1 of the proof of Theorem 4.3.2, one can show that $\mathbf{m}(0) = \mathbf{m}^0$ in the sense of traces. In order to prove that $\mathbf{s}(0) = \mathbf{s}^0$ in $\mathbf{L}^2(\Omega')$, we start by integrating by parts in time (5.24). We deduce that

$$\begin{aligned} & - \int_0^T \langle \partial_t \boldsymbol{\eta}(t), \mathbf{s}(t) \rangle_{H^{-1} \leftrightarrow H^1} dt + \int_0^T a(\mathbf{m}(t); \mathbf{s}(t), \boldsymbol{\eta}(t)) dt \\ & = \langle \mathbf{s}(0), \boldsymbol{\eta}(0) \rangle_{\Omega'} + z\beta \int_0^T \langle \mathbf{m}(t) \otimes \mathbf{j}(t), \nabla \boldsymbol{\eta}(t) \rangle_{\Omega} dt - z\beta \int_0^T \langle \mathbf{j}(t) \cdot \mathbf{n}, \mathbf{m}(t) \cdot \boldsymbol{\eta}(t) \rangle_{\Gamma' \cap \Gamma} dt \end{aligned} \quad (5.25)$$

for all $\boldsymbol{\eta} \in C^1([0, T]; \mathbf{H}^1(\Omega'))$ with $\boldsymbol{\eta}(T) = \mathbf{0}$. Similarly, from (5.23) we deduce that

$$\begin{aligned} & - \int_0^T \langle \partial_t \boldsymbol{\eta}_h(t), \mathbf{s}_{hk}(t) \rangle_{H^{-1} \leftrightarrow H^1} dt + \int_0^T a(\widehat{\mathbf{m}}_{hk}^+(t); \mathbf{s}_{hk}^+(t), \boldsymbol{\eta}_h(t)) dt \\ & = \langle \mathbf{s}_{hk}(0), \boldsymbol{\eta}_h(0) \rangle_{\Omega'} + z\beta \int_0^T \langle \widehat{\mathbf{m}}_{hk}^+(t) \otimes \mathbf{j}_k^+(t), \nabla \boldsymbol{\eta}_h(t) \rangle_{\Omega} dt \\ & \quad - z\beta \int_0^T \langle \mathbf{j}_k^+(t) \cdot \mathbf{n}, \widehat{\mathbf{m}}_{hk}^+(t) \cdot \boldsymbol{\eta}_h(t) \rangle_{\Gamma' \cap \Gamma} dt \\ & = \langle \mathbf{s}_h^0, \boldsymbol{\eta}_h(0) \rangle_{\Omega'} + z\beta \int_0^T \langle \widehat{\mathbf{m}}_{hk}^+(t) \otimes \mathbf{j}_k^+(t), \nabla \boldsymbol{\eta}_h(t) \rangle_{\Omega} dt \\ & \quad - z\beta \int_0^T \langle \mathbf{j}_k^+(t) \cdot \mathbf{n}, \widehat{\mathbf{m}}_{hk}^+(t) \cdot \boldsymbol{\eta}_h(t) \rangle_{\Gamma' \cap \Gamma} dt. \end{aligned}$$

With the same argument used in Step 2 of the proof, we can pass this equality to the limit as $k, h \rightarrow 0$. As $\mathbf{s}_h^0 \rightarrow \mathbf{s}^0$ in $\mathbf{L}^2(\Omega')$ by (5.11b), it follows that

$$\begin{aligned} & - \int_0^T \langle \partial_t \boldsymbol{\eta}(t), \mathbf{s}(t) \rangle_{H^{-1} \leftrightarrow H^1} dt + \int_0^T a(\mathbf{m}(t); \mathbf{s}(t), \boldsymbol{\eta}(t)) dt \\ & = \langle \mathbf{s}^0, \boldsymbol{\eta}(0) \rangle_{\Omega'} + z\beta \int_0^T \langle \mathbf{m}(t) \otimes \mathbf{j}(t), \nabla \boldsymbol{\eta}(t) \rangle_{\Omega} dt - z\beta \int_0^T \langle \mathbf{j}(t) \cdot \mathbf{n}, \mathbf{m}(t) \cdot \boldsymbol{\eta}(t) \rangle_{\Gamma' \cap \Gamma} dt \end{aligned} \quad (5.26)$$

for all $\boldsymbol{\eta} \in C^1([0, T]; \mathbf{H}^1(\Omega'))$ with $\boldsymbol{\eta}(T) = \mathbf{0}$. Comparing (5.25) and (5.26), it follows that

$$\langle \mathbf{s}(0), \boldsymbol{\eta}(0) \rangle_{\Omega'} = \langle \mathbf{s}^0, \boldsymbol{\eta}(0) \rangle_{\Omega'}.$$

Since the function $\boldsymbol{\eta} \in C^1([0, T]; \mathbf{H}^1(\Omega'))$ satisfying $\boldsymbol{\eta}(T) = \mathbf{0}$ is arbitrary, we deduce that $\mathbf{s}(0) = \mathbf{s}^0$ in $\mathbf{L}^2(\Omega')$, which concludes the verification of Definition 5.1.2(ii).

• **Step 4:** Verification of Definition 5.1.2(v).

For the proof of (5.5), we follow the lines of the one of (4.5) developed in step 5 of the proof of Theorem 4.3.2. Given $\tau \in [0, T]$, let $1 \leq j \leq M$ such that $\tau \in [t_{j-1}, t_j]$. Let $0 \leq i \leq j-1$. From Lemma 5.1.7, we deduce that

$$\mathcal{E}(\mathbf{m}_h^{i+1}) + [\alpha - c(k, h)]k \|\mathbf{v}_h^i\|_{\mathbf{L}^2(\Omega)}^2 + \lambda_{\text{ex}}^2 \left(\theta - \frac{1}{2} \right) k^2 \|\nabla \mathbf{v}_h^i\|_{\mathbf{L}^2(\Omega)}^2 \leq \mathcal{E}(\mathbf{m}_h^i) + \tau_J^{-1} k \langle \mathbf{s}_h^i, \mathbf{v}_h^i \rangle_{\Omega},$$

where, for the standard tangent plane scheme, it holds that $c(k, h) = 0$ if the triangulation \mathcal{T}_h satisfies the angle condition (3.16) and $c(k, h) = Ckh^{-2}$ otherwise (with $C > 0$ being a constant which depends only on γ and λ_{ex}), while, for the projection-free tangent plane scheme, it holds that $c(k, h) = 0$; see (5.12)–(5.13). If $1/2 \leq \theta \leq 1$, the third term on the left-hand side is nonnegative and the inequality remains valid even if we omit it. If $0 \leq \theta < 1/2$, we can exploit an inverse estimate to absorb it into the second term. In both cases, summing over $0 \leq i \leq j-1$, we obtain that

$$\mathcal{E}(\mathbf{m}_{hk}^+(\tau)) + [\alpha - C(k, h, \theta)] \int_0^\tau \|\mathbf{v}_{hk}^-(t)\|_{\mathbf{L}^2(\Omega)}^2 dt \leq \mathcal{E}(\mathbf{m}_{hk}^-(0)) + \tau_J^{-1} \int_0^{t_j} \langle \mathbf{s}_{hk}^-(t), \mathbf{v}_{hk}^-(t) \rangle dt,$$

where, for all $0 \leq \theta \leq 1$, it holds that $C(k, h, \theta) \rightarrow 0$ as $k, h \rightarrow 0$. The latter is equivalent to the inequality

$$\begin{aligned} & \mathcal{E}(\mathbf{m}_{hk}^+(\tau)) - \mathcal{E}(\mathbf{m}_{hk}^-(0)) + [\alpha - C(k, h, \theta)] \int_0^\tau \|\mathbf{v}_{hk}^-(t)\|_{\mathbf{L}^2(\Omega)}^2 dt - \tau_J^{-1} \int_0^\tau \langle \mathbf{s}_{hk}^-(t), \mathbf{v}_{hk}^-(t) \rangle dt \\ & \leq \tau_J^{-1} \int_\tau^{t_j} \langle \mathbf{s}_{hk}^-(t), \mathbf{v}_{hk}^-(t) \rangle dt, \end{aligned}$$

for which we now consider the limit as $k, h \rightarrow 0$. Since $\mathbf{m}_{hk}^+ \rightharpoonup \mathbf{m}$ in $L^2(0, T; \mathbf{H}^1(\Omega))$ by (5.20b), it holds that

$$\mathcal{E}(\mathbf{m}(\tau)) \leq \liminf_{k, h \rightarrow 0} \mathcal{E}(\mathbf{m}_{hk}^+(\tau)).$$

Since $\mathbf{m}_h^0 \rightarrow \mathbf{m}^0$ in $\mathbf{H}^1(\Omega)$ by assumption (5.11a), it holds that

$$\lim_{k, h \rightarrow 0} \mathcal{E}(\mathbf{m}_{hk}^-(0)) = \mathcal{E}(\mathbf{m}^0).$$

From the convergence $\mathbf{v}_{hk}^- \rightharpoonup \partial_t \mathbf{m}$ in $\mathbf{L}^2(\Omega_T)$ by (5.20i), it follows that

$$\int_0^\tau \|\partial_t \mathbf{m}(t)\|_{\mathbf{L}^2(\Omega)}^2 dt \leq \liminf_{k, h \rightarrow 0} \int_0^\tau \|\mathbf{v}_{hk}^-(t)\|_{\mathbf{L}^2(\Omega)}^2 dt.$$

Since $\mathbf{s}_{hk}^- \rightarrow \mathbf{s}$ in $\mathbf{L}^2(\Omega'_T)$ by (5.20l) and $\mathbf{v}_{hk}^- \rightharpoonup \partial_t \mathbf{m}$ in $\mathbf{L}^2(\Omega_T)$ by (5.20i), it holds that

$$\int_0^\tau \langle \mathbf{s}_{hk}^-(t), \mathbf{v}_{hk}^-(t) \rangle dt \rightarrow \int_0^\tau \langle \mathbf{s}(t), \partial_t \mathbf{m}(t) \rangle dt.$$

Finally, since $\tau \leq t_j \leq \tau + k$, it holds that

$$\int_\tau^{t_j} \langle \mathbf{s}_{hk}^-(t), \mathbf{v}_{hk}^-(t) \rangle dt \rightarrow 0.$$

Hence, for every measurable set $I \subseteq [0, T]$, it holds that

$$\begin{aligned} & \int_I \left(\mathcal{E}(\mathbf{m}(\tau)) + \int_0^\tau \|\partial_t \mathbf{m}(t)\|_{\mathbf{L}^2(\Omega)}^2 dt \right) d\tau \\ & \leq \liminf_{k, h \rightarrow 0} \int_I \left(\mathcal{E}(\mathbf{m}_{hk}^+(\tau)) + \int_0^\tau \|\mathbf{v}_{hk}^-(t)\|_{\mathbf{L}^2(\Omega)}^2 dt \right) d\tau \\ & \leq \liminf_{k, h \rightarrow 0} \int_I \left[\mathcal{E}(\mathbf{m}_{hk}^-(0)) + C(k, h, \theta) \int_0^\tau \|\mathbf{v}_{hk}^-(t)\|_{\mathbf{L}^2(\Omega)}^2 dt \right. \\ & \quad \left. + \tau_J^{-1} \int_0^\tau \langle \mathbf{s}_{hk}^-(t), \mathbf{v}_{hk}^-(t) \rangle dt + \tau_J^{-1} \int_\tau^{t_j} \langle \mathbf{s}_{hk}^-(t), \mathbf{v}_{hk}^-(t) \rangle dt \right] d\tau \\ & = \int_I \left(\mathcal{E}(\mathbf{m}^0) + \tau_J^{-1} \int_0^\tau \langle \mathbf{s}(t), \partial_t \mathbf{m}(t) \rangle dt \right) d\tau. \end{aligned}$$

As $I \subseteq [0, T]$ is arbitrary, the integrand satisfies the inequality a.e. in $(0, T)$, i.e., it holds that

$$\mathcal{E}(\mathbf{m}(\tau)) + \alpha \int_0^\tau \|\partial_t \mathbf{m}(t)\|_{\mathbf{L}^2(\Omega)}^2 dt \leq \mathcal{E}(\mathbf{m}^0) + \tau_J^{-1} \int_0^\tau \langle \mathbf{s}(t), \partial_t \mathbf{m}(t) \rangle dt$$

for a.e. $\tau \in (0, T)$, which is (5.5). This establishes the energy inequality from Definition 5.1.2(v) and thus concludes the proof of the theorem. \square

5.2 Spintronic extensions of the LLG equation

In this section, we consider the models introduced in Section 2.3, in which the LLG equation is supplemented with (possibly nonlocal) additional spin transfer torque terms. Throughout this section, we denote by $\Omega \subset \mathbb{R}^3$ a bounded Lipschitz domain with polyhedral boundary $\Gamma := \partial\Omega$, in which we aim at solving the extended LLG equation

$$\partial_t \mathbf{m} = -\mathbf{m} \times [\mathbf{h}_{\text{eff}} + \mathbf{\Pi}(\mathbf{m})] + \alpha \mathbf{m} \times \partial_t \mathbf{m} \quad (5.27)$$

introduced in Section 4.1. For the analysis, we apply the framework of Theorem 4.3.2.

5.2.1 Slonczewski models

We discuss the extensions of the LLG equation for current-perpendicular-to-plane (CPP) injection geometries. We start with the LLGS equation, introduced in Section 2.3.1 and rescaled in nondimensional form in (3.7), namely

$$\partial_t \mathbf{m} = -\mathbf{m} \times \mathbf{h}_{\text{eff}} + \alpha \mathbf{m} \times \partial_t \mathbf{m} - \frac{j_e G(\mathbf{m} \cdot \mathbf{p}, P)}{d} \mathbf{m} \times (\mathbf{m} \times \mathbf{p}),$$

where $d > 0$, $0 < P < 1$, and $\mathbf{p} \in \mathbb{S}^2$ are constant, while $j_e \in L^\infty(\Omega)$ and $G(\cdot, P) \in C^1[-1, 1]$ for all $0 < P < 1$. If we define the operator $\mathbf{\Pi} : \mathbf{L}^\infty(\Omega) \rightarrow \mathbf{L}^2(\Omega)$ by

$$\mathbf{\Pi}(\mathbf{m}) = \frac{j_e G(\mathbf{m} \cdot \mathbf{p}, P)}{d} \mathbf{m} \times \mathbf{p} \quad \text{for all } \mathbf{m} \in \mathbf{L}^\infty(\Omega),$$

we recover (5.27). To approximate $\mathbf{\Pi}$, we consider the discrete operator defined by

$$\mathbf{\Pi}_h(\mathbf{m}_h) = \frac{j_e G(\mathcal{I}_h[\mathbf{m}_h/|\mathbf{m}_h|] \cdot \mathbf{p}, P)}{d} \mathcal{I}_h[\mathbf{m}_h/|\mathbf{m}_h|] \times \mathbf{p} \quad \text{for all } \mathbf{m}_h \in \mathcal{U}_h.$$

The inclusion of the nodal projection mapping $\mathbf{m}_h \mapsto \mathcal{I}_h[\mathbf{m}_h/|\mathbf{m}_h|]$ in the definition of the discrete operator ensures that the product $\mathcal{I}_h[\mathbf{m}_h/|\mathbf{m}_h|] \cdot \mathbf{p}$ belongs to $[-1, 1]$, which is the domain of the ballistic function G . For all $\mathbf{m}_h \in \mathcal{U}_h$, it holds that

$$\|\mathbf{\Pi}_h(\mathbf{m}_h)\|_{\mathbf{L}^2(\Omega)} \leq \frac{\|j_e\|_{L^\infty(\Omega)} \|G(\cdot, P)\|_{L^\infty[-1, 1]} |\Omega|^{1/2}}{d},$$

which shows that the stability requirement (4.16b) is satisfied. It remains to verify that $\mathbf{\Pi}_h$ fulfills also the consistency assumption (4.18b). Let $\widehat{\mathbf{m}}_{hk}^-$ be the piecewise constant time reconstruction (4.41) obtained from the output of Algorithm 4.2.1 using the ‘normalized iterate’ (4.40). Let $\mathbf{\Pi}_{hk}^-$ be defined by (4.14). It holds that

$$\begin{aligned} & \|\mathbf{\Pi}_{hk}^- - \mathbf{\Pi}(\mathbf{m})\|_{\mathbf{L}^2(\Omega_T)} \\ &= \|[j_e G(\widehat{\mathbf{m}}_{hk}^- \cdot \mathbf{p}, P)/d](\widehat{\mathbf{m}}_{hk}^- \times \mathbf{p}) - [j_e G(\mathbf{m} \cdot \mathbf{p}, P)/d](\mathbf{m} \times \mathbf{p})\|_{\mathbf{L}^2(\Omega_T)} \\ &\leq \frac{\|j_e\|_{L^\infty(\Omega)}}{d} \|G(\widehat{\mathbf{m}}_{hk}^- \cdot \mathbf{p}, P)(\widehat{\mathbf{m}}_{hk}^- \times \mathbf{p}) - G(\mathbf{m} \cdot \mathbf{p}, P)(\mathbf{m} \times \mathbf{p})\|_{\mathbf{L}^2(\Omega_T)} \\ &\leq \frac{\|j_e\|_{L^\infty(\Omega)}}{d} \left(\| [G(\widehat{\mathbf{m}}_{hk}^- \cdot \mathbf{p}, P) - G(\mathbf{m} \cdot \mathbf{p}, P)] (\widehat{\mathbf{m}}_{hk}^- \times \mathbf{p}) \|_{\mathbf{L}^2(\Omega_T)} \right. \\ &\quad \left. + \| G(\mathbf{m} \cdot \mathbf{p}, P) (\widehat{\mathbf{m}}_{hk}^- - \mathbf{m}) \times \mathbf{p} \|_{\mathbf{L}^2(\Omega_T)} \right) \\ &\leq \frac{\|j_e\|_{L^\infty(\Omega)}}{d} \left(L \|\widehat{\mathbf{m}}_{hk}^- - \mathbf{m}\|_{\mathbf{L}^2(\Omega_T)} + \|G(\cdot, P)\|_{L^\infty[-1, 1]} \|\widehat{\mathbf{m}}_{hk}^- - \mathbf{m}\|_{\mathbf{L}^2(\Omega_T)} \right), \end{aligned}$$

where $L > 0$ denotes the Lipschitz continuity constant of G . Since $\widehat{\mathbf{m}}_{hk}^- \rightarrow \mathbf{m}$ in $\mathbf{L}^2(\Omega_T)$ by (4.42b), we obtain (4.18b) with strong convergence. The framework of part (c) of Theorem 4.3.2 is therefore

satisfied, which guarantees the convergence of the approximate solutions towards a weak solution of the LLGS equation.

Next, we consider the extended LLGS equation (3.8)

$$\partial_t \mathbf{m} = -\mathbf{m} \times \mathbf{h}_{\text{eff}} + \alpha \mathbf{m} \times \partial_t \mathbf{m} - \frac{a_P j_e}{d} \mathbf{m} \times (\mathbf{m} \times \mathbf{p} + \xi \mathbf{p}),$$

where $a_P > 0$, $d > 0$, $\xi > 0$, and $\mathbf{p} \in \mathbb{S}^2$ are constant, whereas the scalar function j_e belongs to $L^\infty(\Omega)$. In order to see that also this model fits into the setting of the general LLG equation (5.27), we define the operator $\mathbf{\Pi} : \mathbf{L}^2(\Omega) \rightarrow \mathbf{L}^2(\Omega)$ by

$$\mathbf{\Pi}(\mathbf{m}) = \frac{a_P j_e}{d} (\mathbf{m} \times \mathbf{p} + \xi \mathbf{p}) \quad \text{for all } \mathbf{m} \in \mathbf{L}^2(\Omega).$$

Correspondingly, we consider the discrete operator $\mathbf{\Pi}_h$ defined by

$$\mathbf{\Pi}_h(\mathbf{m}_h) = \frac{a_P j_e}{d} (\mathbf{m}_h \times \mathbf{p} + \xi \mathbf{p}) \quad \text{for all } \mathbf{m}_h \in \mathcal{S}^1(\mathcal{T}_h)^3.$$

Since, for all $\mathbf{m}_h \in \mathcal{S}^1(\mathcal{T}_h)^3$, it holds that

$$\|\mathbf{\Pi}_h(\phi_h)\|_{\mathbf{L}^2(\Omega)} \leq \frac{a_P \|j_e\|_{L^\infty(\Omega)}}{d} \left(\xi |\Omega|^{1/2} + \|\mathbf{m}_h\|_{\mathbf{L}^2(\Omega)} \right),$$

the stability condition (4.16b) is satisfied. It is straightforward to verify that, since $\mathbf{m}_{hk}^- \rightarrow \mathbf{m}$ in $\mathbf{L}^2(\Omega_T)$ by (4.37e), also the consistency condition (4.18b) with strong convergence is satisfied. It follows that the framework of part (c) of Theorem 4.3.2 fully applies also in this case.

5.2.2 Zhang–Li model

In this section, we discuss the numerical approximation of the Zhang–Li model presented in Section 2.3.3 and nondimensionalized in (3.9). We consider the extended LLG equation

$$\partial_t \mathbf{m} = -\mathbf{m} \times \mathbf{h}_{\text{eff}} + \alpha \mathbf{m} \times \partial_t \mathbf{m} - \mathbf{m} \times [\mathbf{m} \times (\mathbf{v} \cdot \nabla) \mathbf{m} + \xi (\mathbf{v} \cdot \nabla) \mathbf{m}],$$

where $\xi > 0$ is constant and \mathbf{v} belongs to $\mathbf{L}^\infty(\Omega)$. To recover (5.27), we consider the operator $\mathbf{\Pi} : \mathbf{H}^1(\Omega) \cap \mathbf{L}^\infty(\Omega) \rightarrow \mathbf{L}^2(\Omega)$ defined by

$$\mathbf{\Pi}(\mathbf{m}) = \mathbf{m} \times (\mathbf{v} \cdot \nabla) \mathbf{m} + \xi (\mathbf{v} \cdot \nabla) \mathbf{m} \quad \text{for all } \mathbf{m} \in \mathbf{H}^1(\Omega) \cap \mathbf{L}^\infty(\Omega).$$

To approximate $\mathbf{\Pi}$ we introduce the discrete operator $\mathbf{\Pi}_h$ defined by

$$\mathbf{\Pi}_h(\mathbf{m}_h) = \mathcal{I}_h[\mathbf{m}_h / |\mathbf{m}_h|] \times (\mathbf{v} \cdot \nabla) \mathbf{m}_h + \xi (\mathbf{v} \cdot \nabla) \mathbf{m}_h \quad \text{for all } \mathbf{m}_h \in \mathcal{U}_h.$$

For all $\mathbf{m}_h \in \mathcal{U}_h$, it holds that

$$\begin{aligned} \|\mathbf{\Pi}_h(\mathbf{m}_h)\|_{\mathbf{L}^2(\Omega)} &= \|\mathcal{I}_h[\mathbf{m}_h / |\mathbf{m}_h|] \times (\mathbf{v} \cdot \nabla) \mathbf{m}_h + \xi (\mathbf{v} \cdot \nabla) \mathbf{m}_h\|_{\mathbf{L}^2(\Omega)} \\ &\leq (1 + \xi) \|\mathbf{v}\|_{\mathbf{L}^\infty(\Omega)} \|\nabla \mathbf{m}_h\|_{\mathbf{L}^2(\Omega)}. \end{aligned}$$

In particular, the stability condition (4.16b) is satisfied. As for the consistency condition (4.18b), let $\varphi \in \mathbf{L}^2(\Omega_T)$ be arbitrary. Let \mathbf{m}_{hk}^- and $\widehat{\mathbf{m}}_{hk}^-$ be the piecewise constant time approximations constructed from the output of Algorithm 4.2.1 and let $\mathbf{\Pi}_{hk}^-$ be defined by (4.14). Note that $\mathbf{m}_{hk}^- \rightharpoonup \mathbf{m}$ in $L^2(0, T; \mathbf{H}^1(\Omega))$ by (4.37d) and $\widehat{\mathbf{m}}_{hk}^- \rightarrow \mathbf{m}$ in $\mathbf{L}^2(\Omega_T)$ by (4.42b), from which it

follows that $(\mathbf{v} \cdot \nabla) \mathbf{m}_{hk}^- \rightharpoonup (\mathbf{v} \cdot \nabla) \mathbf{m}$ and $\widehat{\mathbf{m}}_{hk}^- \times \boldsymbol{\varphi} \rightarrow \mathbf{m} \times \boldsymbol{\varphi}$ in $\mathbf{L}^2(\Omega_T)$. It holds that

$$\begin{aligned}
& \int_0^T \langle \Pi_{hk}^-(t), \boldsymbol{\varphi}(t) \rangle_\Omega dt \\
&= \int_0^T \langle \widehat{\mathbf{m}}_{hk}^-(t) \times (\mathbf{v} \cdot \nabla) \mathbf{m}_{hk}^-(t) + \xi(\mathbf{v} \cdot \nabla) \mathbf{m}_{hk}^-(t), \boldsymbol{\varphi}(t) \rangle_\Omega dt \\
&= - \int_0^T \langle (\mathbf{v} \cdot \nabla) \mathbf{m}_{hk}^-(t), \widehat{\mathbf{m}}_{hk}^-(t) \times \boldsymbol{\varphi}(t) \rangle_\Omega dt + \xi \int_0^T \langle (\mathbf{v} \cdot \nabla) \mathbf{m}_{hk}^-(t), \boldsymbol{\varphi}(t) \rangle_\Omega dt \\
&\rightarrow - \int_0^T \langle (\mathbf{v} \cdot \nabla) \mathbf{m}, \mathbf{m}(t) \times \boldsymbol{\varphi}(t) \rangle_\Omega dt + \xi \int_0^T \langle (\mathbf{v} \cdot \nabla) \mathbf{m}, \boldsymbol{\varphi}(t) \rangle_\Omega dt \\
&= \int_0^T \langle \mathbf{m}(t) \times (\mathbf{v} \cdot \nabla) \mathbf{m}(t) + \xi(\mathbf{v} \cdot \nabla) \mathbf{m}(t), \boldsymbol{\varphi}(t) \rangle_\Omega dt = \int_0^T \langle \Pi(\mathbf{m}(t)), \boldsymbol{\varphi}(t) \rangle_\Omega dt,
\end{aligned}$$

which shows that $\Pi_{hk}^- \rightharpoonup \Pi(\mathbf{m})$ in $\mathbf{L}^2(\Omega_T)$, i.e., the consistency requirement (4.18b) is fulfilled. Therefore, we can apply part (b) of Theorem 4.3.2 and deduce the existence of a function $\mathbf{m} \in L^\infty(0, T; \mathbf{H}^1(\Omega)) \cap H^1(0, T; \mathbf{L}^2(\Omega))$ which satisfies the requirements (i)–(iii) of Definition 4.1.1. Because of the lack of strong convergence in (4.18b), the framework of part (c) of Theorem 4.3.2 does not apply and we are not able to establish the energy inequality (4.5) of Definition 4.1.1 (iv).

5.2.3 Stationary spin diffusion model

Let $\Omega' \subset \mathbb{R}^3$ be a bounded Lipschitz domain with polyhedral boundaries $\Gamma' := \partial\Omega'$ such that $\Omega \subseteq \Omega'$. In Ω , we consider the extended LLG equation

$$\partial_t \mathbf{m} = -\mathbf{m} \times \mathbf{h}_{\text{eff}} + \alpha \mathbf{m} \times \partial_t \mathbf{m} - \tau_J^{-1} \mathbf{m} \times \mathbf{s}$$

where $\tau_J > 0$ is constant, while $\mathbf{s} : \Omega' \rightarrow \mathbb{R}^3$ solves the boundary value problem

$$\begin{aligned}
z \nabla \cdot [D_0(\mathbf{I}_{3 \times 3} - \beta \beta' \mathbf{m} \otimes \mathbf{m}) \nabla \mathbf{s}] - \tau_{\text{sf}}^{-1} \mathbf{s} - \tau_J^{-1} \mathbf{s} \times \mathbf{m} &= \beta z \nabla \cdot (\mathbf{m} \otimes \mathbf{j}) & \text{in } \Omega', \\
\partial_n \mathbf{s} &= \mathbf{0} & \text{on } \Gamma'.
\end{aligned}$$

Here, the quantities $z > 0$, $\tau_{\text{sf}} > 0$, and $0 < \beta, \beta' < 1$ are constant, \mathbf{j} belongs to $\mathbf{H}^1(\Omega') \cap \mathbf{L}^\infty(\Omega')$, while $D_0 \in L^\infty(\Omega')$ is positive and bounded away from zero, i.e., there exists a constant $D_* > 0$ such that $D_0 \geq D_*$ a.e. in Ω' . To recover (5.27), we define the operator $\Pi : \{\mathbf{m} \in \mathbf{L}^\infty(\Omega) : |\mathbf{m}| = 1 \text{ a.e. in } \Omega\} \rightarrow \mathbf{L}^2(\Omega)$ as the mapping $\mathbf{m} \mapsto \tau_J^{-1} \mathbf{s}|_\Omega$, where $\mathbf{s} \in \mathbf{H}^1(\Omega')$ is the solution of the following variational problem: Find $\mathbf{s} \in \mathbf{H}^1(\Omega')$ such that

$$a(\mathbf{m}; \mathbf{s}, \boldsymbol{\zeta}) = F(\mathbf{m}; \boldsymbol{\zeta}) \quad \text{for all } \boldsymbol{\zeta} \in \mathbf{H}^1(\Omega').$$

Here, for $\mathbf{m} \in \mathbf{L}^\infty(\Omega)$ satisfying $|\mathbf{m}| = 1$ a.e. in Ω , $a(\mathbf{m}; \cdot, \cdot)$ is the bilinear form (5.2), while $F(\mathbf{m}; \cdot) \in \mathbf{H}^1(\Omega')^*$ is defined by

$$F(\mathbf{m}; \boldsymbol{\zeta}) = z\beta \langle \mathbf{m} \otimes \mathbf{j}, \nabla \boldsymbol{\zeta} \rangle_\Omega - z\beta \langle \mathbf{j} \cdot \mathbf{n}, \mathbf{m} \cdot \boldsymbol{\zeta} \rangle_{\Gamma' \cap \Gamma} \quad \text{for all } \mathbf{H}^1(\Omega').$$

Since the bilinear form is continuous and elliptic by Lemma 5.1.1, the variational problem is well posed. In particular, the operator Π is well defined.

Let $\{\mathcal{T}_h'\}_{h>0}$ be a γ -quasi-uniform family of regular tetrahedral triangulations of Ω' which resolve Ω , i.e., the restriction $\mathcal{T}_h := \mathcal{T}_h'|_\Omega$ provides a regular triangulation of Ω . To discretize Π , we define the discrete operator $\Pi_h : \mathcal{U}_h \rightarrow \mathcal{S}^1(\mathcal{T}_h)^3$ as the mapping $\mathbf{m}_h \mapsto \tau_J^{-1} \mathbf{s}_h|_\Omega$, where $\mathbf{s}_h \in \mathcal{S}^1(\mathcal{T}_h')^3$ is the solution of the following discrete variational problem: Find $\mathbf{s}_h \in \mathcal{S}^1(\mathcal{T}_h')^3$ such that

$$a[\mathcal{I}_h[\mathbf{m}_h/|\mathbf{m}_h|]](\mathbf{s}_h, \boldsymbol{\zeta}_h) = F[\mathcal{I}_h[\mathbf{m}_h/|\mathbf{m}_h|]](\boldsymbol{\zeta}_h) \quad \text{for all } \boldsymbol{\zeta}_h \in \mathcal{S}^1(\mathcal{T}_h')^3.$$

The application of the nodal projection $\mathbf{m}_h \mapsto \mathcal{I}_h[\mathbf{m}_h/|\mathbf{m}_h|]$ guarantees that $a[\mathcal{I}_h[\mathbf{m}_h/|\mathbf{m}_h|]](\cdot, \cdot)$ is elliptic; see Lemma 5.1.1. In particular, the Lax–Milgram theorem ensures that also the discrete variational problem is well posed and that its unique solution $\mathbf{s}_h \in \mathcal{S}^1(\mathcal{T}'_h)^3$ satisfies

$$\|\mathbf{s}_h\|_{\mathbf{H}^1(\Omega')} \leq \frac{\|F\|_{\mathbf{H}^1(\Omega')^*}}{C} \leq \frac{z\beta\|\mathbf{j}\|_{\mathbf{H}^1(\Omega')}}{C}, \quad (5.28)$$

where $C = \min\{z(1 - \beta\beta')D_*, \tau_{\text{sf}}^{-1}\}$. In particular, the discrete operator $\mathbf{\Pi}_h$ is well defined and fulfills

$$\|\mathbf{\Pi}_h(\mathbf{m}_h)\|_{\mathbf{L}^2(\Omega)} = \frac{\|\mathbf{s}_h\|_{\mathbf{L}^2(\Omega)}}{\tau_J} \leq \frac{\|\mathbf{s}_h\|_{\mathbf{H}^1(\Omega')}}{\tau_J} \leq \frac{z\beta\|\mathbf{j}\|_{\mathbf{H}^1(\Omega')}}{C\tau_J} \quad \text{for all } \mathbf{m}_h \in \mathcal{U}_h,$$

which shows that the stability condition (4.16b) is satisfied. Differently from the previous cases, here the operator $\mathbf{\Pi}$ is a nonlocal operator. Indeed, here the computation of $\mathbf{\Pi}_h(\mathbf{m}_h^i)$ included in step (i) of Algorithm 4.2.1 requires the approximate solution of a boundary value problem.

As for the consistency condition (4.18b), $\widehat{\mathbf{m}}_{hk}^-$ be the piecewise constant time reconstruction defined by (4.41) and let $\mathbf{m} \in L^\infty(0, T; \mathbf{H}^1(\Omega)) \cap H^1(0, T; \mathbf{L}^2(\Omega))$ with $|\mathbf{m}| = 1$ a.e. in Ω such that the convergence results (4.42) are satisfied. Moreover, let $\mathbf{s} \in L^\infty(0, T; \mathbf{H}^1(\Omega'))$ be defined by

$$a(\mathbf{m}(t); \mathbf{s}(t), \boldsymbol{\zeta}) = F(\mathbf{m}(t); \boldsymbol{\zeta}) \quad \text{for all } \boldsymbol{\zeta} \in \mathbf{H}^1(\Omega') \text{ and a.e. } t \in (0, T).$$

Similarly, let $\mathbf{s}_{hk}^- : [0, T] \rightarrow \mathcal{S}^1(\mathcal{T}'_h)^3$ be defined by $\mathbf{s}_{hk}^-(t) := \mathbf{s}_h^i$ for all $0 \leq i \leq M - 1$ such that $t \in [t_i, t_{i+1})$, where $\mathbf{s}_h^i \in \mathcal{S}^1(\mathcal{T}'_h)^3$ satisfies

$$a(\widehat{\mathbf{m}}_h^i; \mathbf{s}_h^i, \boldsymbol{\zeta}_h) = F(\widehat{\mathbf{m}}_h^i; \boldsymbol{\zeta}_h) \quad \text{for all } \boldsymbol{\zeta}_h \in \mathcal{S}^1(\mathcal{T}'_h)^3 \text{ and } 0 \leq i \leq M - 1. \quad (5.29)$$

We aim to show that $\mathbf{s}_{hk}^- \rightharpoonup \mathbf{s}$ in $L^2(0, T; \mathbf{H}^1(\Omega'))$. Since, with the notation of Theorem 4.3.2, it holds that $\mathbf{\Pi}_{hk}^- = \tau_J^{-1} \mathbf{s}_{hk}^-$ and $\mathbf{\Pi}(\mathbf{m}) = \tau_J^{-1} \mathbf{s}$, this implies (4.18b).

From (5.28) it follows that $\{\mathbf{s}_{hk}^-\}$ is uniformly bounded in $L^2(0, T; \mathbf{H}^1(\Omega'))$. We can apply the Eberlein–Šmulian theorem and extract a weakly convergent subsequence (not relabeled) which converges towards some function $\widetilde{\mathbf{s}} \in L^2(0, T; \mathbf{H}^1(\Omega'))$. Now we follow the argument of Step 2 of the proof of Theorem 5.1.6. Let $\boldsymbol{\eta} \in C^1([0, T]; \mathcal{C}^\infty(\Omega'))$ and define $\boldsymbol{\eta}_h : [0, T] \rightarrow \mathcal{S}^1(\mathcal{T}'_h)^3$ by $\boldsymbol{\eta}_h(t) = \mathcal{I}_h[\boldsymbol{\eta}(t)]$ for all $t \in [0, T]$. From (5.29), we deduce that, for every measurable set $I \subseteq [0, T]$, it holds that

$$\int_I a(\widehat{\mathbf{m}}_{hk}^-(t); \mathbf{s}_{hk}^-(t), \boldsymbol{\eta}_h(t)) dt = \int_I F(\widehat{\mathbf{m}}_{hk}^-(t); \boldsymbol{\eta}_h(t)) dt.$$

Passing this identity to the limit as $k, h \rightarrow 0$, thanks to the available convergence results, we obtain that

$$\int_I a(\mathbf{m}(t); \widetilde{\mathbf{s}}(t), \boldsymbol{\eta}(t)) dt = \int_I F(\mathbf{m}(t); \boldsymbol{\eta}(t)) dt$$

(for more details, see Step 2 of the proof of Theorem 5.1.6 on page 87). By density, since $I \subseteq [0, T]$ is arbitrary, it follows that

$$a(\mathbf{m}(t); \widetilde{\mathbf{s}}(t), \boldsymbol{\zeta}) = F(\mathbf{m}(t); \boldsymbol{\zeta}) \quad \text{for all } \boldsymbol{\zeta} \in \mathbf{H}^1(\Omega') \text{ and a.e. } t \in (0, T).$$

This shows that $\mathbf{s} = \widetilde{\mathbf{s}}$, so that the convergence $\mathbf{s}_{hk}^- \rightharpoonup \mathbf{s}$ in $L^2(0, T; \mathbf{H}^1(\Omega'))$ is established. We conclude that the consistency condition (4.18b) is satisfied and the framework of part (b) of Theorem 4.3.2 therefore applies.

5.2.4 Self-consistent model

We conclude this chapter by discussing the numerical discretization of the self-consistent model introduced in Section 2.3.4.

5.2.4.1 Setting

Let $\Omega' \subset \mathbb{R}^3$ be a bounded Lipschitz domain with polyhedral boundaries $\Gamma' := \partial\Omega'$ such that $\Omega \subseteq \Omega'$. Let $\Gamma' = \overline{\Gamma'_D} \cup \overline{\Gamma'_N}$ be a partition of the boundary into relatively open parts $\Gamma'_D, \Gamma'_N \subset \Gamma'$ such that $\Gamma'_D \cap \Gamma'_N = \emptyset$. In Ω , we consider the extended LLG equation

$$\partial_t \mathbf{m} = -\mathbf{m} \times (\mathbf{h}_{\text{eff}} + \mathbf{h}_c) + \alpha \mathbf{m} \times \partial_t \mathbf{m} - \tau_J^{-1} \mathbf{m} \times \mathbf{s},$$

where $\tau_J > 0$ is constant, the Oersted field $\mathbf{h}_c : \mathbb{R}^3 \rightarrow \mathbb{R}^3$ solves the transmission problem (3.2), i.e.,

$$-\Delta \mathbf{h}_c^{\text{int}} = \nabla \times \mathbf{j}_e \quad \text{in } \Omega', \quad (5.30a)$$

$$-\Delta \mathbf{h}_c^{\text{ext}} = \mathbf{0} \quad \text{in } \mathbb{R}^3 \setminus \overline{\Omega'}, \quad (5.30b)$$

$$\mathbf{h}_c^{\text{ext}} - \mathbf{h}_c^{\text{int}} = \mathbf{0} \quad \text{on } \Gamma', \quad (5.30c)$$

$$(\nabla \mathbf{h}_c^{\text{ext}} - \nabla \mathbf{h}_c^{\text{int}}) \mathbf{n} = \mathbf{n} \times \mathbf{j}_e \quad \text{on } \Gamma', \quad (5.30d)$$

$$\mathbf{h}_c(\mathbf{x}) = \mathcal{O}(1/|\mathbf{x}|) \quad \text{as } |\mathbf{x}| \rightarrow \infty, \quad (5.30e)$$

while $\mathbf{s} : \Omega' \rightarrow \mathbb{R}^3$, together with $V : \Omega' \rightarrow \mathbb{R}$, is a solution of the system

$$\nabla \cdot \mathbf{j}_e = 0 \quad \text{in } \Omega', \quad (5.31a)$$

$$\nabla \cdot \mathbf{j}_s = -\tau_{\text{sf}}^{-1} \mathbf{s} - \tau_J^{-1} \mathbf{s} \times \mathbf{m} \quad \text{in } \Omega', \quad (5.31b)$$

$$V = V_D \quad \text{on } \Gamma'_D, \quad (5.31c)$$

$$\mathbf{s} = \mathbf{0} \quad \text{on } \Gamma'_D, \quad (5.31d)$$

$$\mathbf{j}_e \cdot \mathbf{n} = \mathbf{0} \quad \text{on } \Gamma'_N, \quad (5.31e)$$

$$\mathbf{j}_s \cdot \mathbf{n} = \mathbf{0} \quad \text{on } \Gamma'_N, \quad (5.31f)$$

where

$$\mathbf{j}_e = -c D_0 \nabla V - \beta' D_0 \nabla \mathbf{s}^\top \mathbf{m}, \quad (5.31g)$$

$$\mathbf{j}_s / z = -\beta c D_0 \mathbf{m} \otimes \nabla V - D_0 \nabla \mathbf{s}. \quad (5.31h)$$

Here, $0 < \beta, \beta' < 1$ and $c, \tau_{\text{sf}}, z > 0$ are constant, $V_D \in H^{1/2}(\Gamma'_D)$, while $D_0 \in L^\infty(\Omega')$ is positive and bounded away from zero, i.e., there exists a constant $D_* > 0$ such that $D_0 \geq D_*$ a.e. in Ω' .

5.2.4.2 Analysis of the system

In view of the application of Theorem 4.3.2, we discuss the system (5.30)–(5.31) for the spin accumulation \mathbf{s} , the electric potential V , and the Oersted field \mathbf{h}_c , for a given time-independent magnetization \mathbf{m} .

Given $\mathbf{m} \in \mathbf{L}^\infty(\Omega)$ satisfying $|\mathbf{m}| = 1$ a.e. in Ω , the variational formulation of (5.31) reads as follows: Find $\mathbf{s} \in \mathbf{H}_D^1(\Omega')$ and $V \in H^1(\Omega')$ with $V = V_D$ on Γ'_D such that, for all $\psi \in H_D^1(\Omega')$ and $\zeta \in \mathbf{H}_D^1(\Omega')$, it holds that

$$\begin{aligned} c \langle D_0 \nabla V, \nabla \psi \rangle_{\Omega'} + \beta' \langle D_0 \nabla \mathbf{s}^\top \mathbf{m}, \nabla \psi \rangle_{\Omega'} &= 0 \\ \beta c z \langle D_0 \mathbf{m} \otimes \nabla V, \nabla \zeta \rangle_{\Omega'} + z \langle D_0 \nabla \mathbf{s}, \nabla \zeta \rangle_{\Omega'} + \tau_{\text{sf}}^{-1} \langle \mathbf{s}, \zeta \rangle_{\Omega'} + \tau_J^{-1} \langle \mathbf{s} \times \mathbf{m}, \zeta \rangle_{\Omega'} &= 0. \end{aligned}$$

For all $(\zeta_1, \psi_1), (\zeta_2, \psi_2) \in \mathbf{H}^1(\Omega') \times H^1(\Omega')$, we define the bilinear form $b(\mathbf{m}; \cdot, \cdot)$ by

$$\begin{aligned} b(\mathbf{m}; (\zeta_1, \psi_1), (\zeta_2, \psi_2)) &= z \langle D_0 \nabla \mathbf{s}, \nabla \zeta \rangle_{\Omega'} + c^2 z \langle D_0 \nabla V, \nabla \psi \rangle_{\Omega'} + \beta c z \langle D_0 \mathbf{m} \otimes \nabla V, \nabla \zeta \rangle_{\Omega'} \\ &\quad + \beta' c z \langle D_0 \nabla \mathbf{s}^\top \mathbf{m}, \nabla \psi \rangle_{\Omega'} + \tau_{\text{sf}}^{-1} \langle \mathbf{s}, \zeta \rangle_{\Omega'} + \tau_J^{-1} \langle \mathbf{s} \times \mathbf{m}, \zeta \rangle_{\Omega'}. \end{aligned}$$

With this definition, the above variational problem can be rewritten in a more compact form: Find $\mathbf{s} \in \mathbf{H}_D^1(\Omega')$ and $V \in H^1(\Omega')$ with $V = V_D$ on Γ'_D such that

$$b(\mathbf{m}; (\mathbf{s}, V), (\zeta, \psi)) = 0 \quad \text{for all } (\zeta, \psi) \in \mathbf{H}_D^1(\Omega') \times H_D^1(\Omega') \quad (5.32)$$

The well-posedness of (5.32) is established in the following proposition.

Proposition 5.2.1. *For any $\mathbf{m} \in \mathbf{L}^\infty(\Omega)$ satisfying $|\mathbf{m}| = 1$ a.e. in Ω , there exist unique $\mathbf{s} \in \mathbf{H}_D^1(\Omega')$ and $V \in H^1(\Omega')$ with $V = V_D$ on Γ_D' which satisfy the variational problem (5.32). Moreover, there exists a constant $C > 0$ such that*

$$\|\mathbf{s}\|_{\mathbf{H}^1(\Omega')} + \|V\|_{H^1(\Omega')} \leq C. \quad (5.33)$$

The constant C depends only on the problem data $(\beta, \beta', c, D_0, \tau_{\text{sf}}, V_D, z)$.

Proof. Consider the Hilbert space $\mathcal{X} := \mathbf{H}_D^1(\Omega') \times H_D^1(\Omega')$ endowed with the norm

$$\|(\boldsymbol{\zeta}, \psi)\|_{\mathcal{X}}^2 = z\|D_0^{1/2}\nabla\boldsymbol{\zeta}\|_{\mathbf{L}^2(\Omega')}^2 + c^2z\|D_0^{1/2}\nabla\psi\|_{\mathbf{L}^2(\Omega')}^2 + \tau_{\text{sf}}^{-1}\|\boldsymbol{\zeta}\|_{\mathbf{L}^2(\Omega')}^2 \quad \text{for all } (\boldsymbol{\zeta}, \psi) \in \mathcal{X}.$$

We show that the bilinear form $b(\mathbf{m}; \cdot, \cdot) : \mathcal{X} \times \mathcal{X} \rightarrow \mathbb{R}$ is elliptic. To that end, we consider an arbitrary $(\boldsymbol{\zeta}, \psi) \in \mathcal{X}$ and note the pointwise identity $(\mathbf{m} \otimes \nabla\psi) : \nabla\boldsymbol{\zeta} = (\nabla\boldsymbol{\zeta}^\top \mathbf{m}) \cdot \nabla\psi$. Since $\|\mathbf{m}\|_{\mathbf{L}^\infty(\Omega')} = 1$ and $0 < \beta, \beta' < 1$, it holds that

$$\begin{aligned} b(\mathbf{m}; (\boldsymbol{\zeta}, \psi), (\boldsymbol{\zeta}, \psi)) &= z\|D_0^{1/2}\nabla\boldsymbol{\zeta}\|_{\mathbf{L}^2(\Omega')}^2 + c^2z\|D_0^{1/2}\nabla\psi\|_{\mathbf{L}^2(\Omega')}^2 + \tau_{\text{sf}}^{-1}\|\boldsymbol{\zeta}\|_{\mathbf{L}^2(\Omega')}^2 \\ &\quad + cz(\beta + \beta')\langle D_0\mathbf{m} \otimes \nabla\psi, \nabla\boldsymbol{\zeta} \rangle_{\Omega'} \\ &\geq z\|D_0^{1/2}\nabla\boldsymbol{\zeta}\|_{\mathbf{L}^2(\Omega')}^2 + c^2z\|D_0^{1/2}\nabla\psi\|_{\mathbf{L}^2(\Omega')}^2 + \tau_{\text{sf}}^{-1}\|\boldsymbol{\zeta}\|_{\mathbf{L}^2(\Omega')}^2 \\ &\quad - cz(\beta + \beta')\|D_0^{1/2}\nabla\boldsymbol{\zeta}\|_{\mathbf{L}^2(\Omega')}\|D_0^{1/2}\nabla\psi\|_{\mathbf{L}^2(\Omega')} \\ &\geq z\left(1 - \frac{\beta + \beta'}{2}\right)\|D_0^{1/2}\nabla\boldsymbol{\zeta}\|_{\mathbf{L}^2(\Omega')}^2 + c^2z\left(1 - \frac{\beta + \beta'}{2}\right)\|D_0^{1/2}\nabla\psi\|_{\mathbf{L}^2(\Omega')}^2 \\ &\quad + \tau_{\text{sf}}^{-1}\|\boldsymbol{\zeta}\|_{\mathbf{L}^2(\Omega')}^2 \\ &\geq z\left(1 - \frac{\beta + \beta'}{2}\right)\|(\boldsymbol{\zeta}, \psi)\|_{\mathcal{X}}^2. \end{aligned}$$

The result then follows from the Lax–Milgram theorem. \square

As for the Oersted field, we first introduce the Beppo Levi space

$$BL^1(\mathbb{R}^3) = \{\phi \in H_{\text{loc}}^1(\mathbb{R}^3) : \nabla\phi \in \mathbf{L}^2(\mathbb{R}^3)\} / \mathbb{R},$$

endowed with the norm defined by $\|\phi\|_{BL^1(\mathbb{R}^3)} = \|\nabla\phi\|_{\mathbf{L}^2(\mathbb{R}^3)}$ for all $\phi \in BL^1(\mathbb{R}^3)$. Given $\mathbf{j}_e \in \mathbf{L}^2(\Omega')$, the variational formulation of (5.30) reads as follows: Find $\mathbf{h}_c \in BL^1(\mathbb{R}^3)^3$ such that

$$\langle \nabla\mathbf{h}_c, \nabla\phi \rangle_{\mathbb{R}^3} = \langle \mathbf{j}_e, \nabla \times \phi \rangle_{\Omega'} \quad \text{for all } \phi \in BL^1(\mathbb{R}^3)^3. \quad (5.34)$$

From the Riesz representation theorem, it follows that (5.34) admits a unique solution $\mathbf{h}_c \in BL^1(\mathbb{R}^3)^3$ such that $\|\mathbf{h}_c\|_{BL^1(\mathbb{R}^3)^3} \leq \|\mathbf{j}_e\|_{\mathbf{L}^2(\Omega')}$. Moreover, since the inclusion $H^1(\mathbb{R}^3) \hookrightarrow BL^1(\mathbb{R}^3)$ is continuous and injective, the problem has at most one solution in $\mathbf{H}^1(\mathbb{R}^3)$. Indeed, for the three-dimensional case, it can be proved that the solution $\mathbf{h}_c \in BL^1(\mathbb{R}^3)^3$ belongs to $\mathbf{H}^1(\mathbb{R}^3)$ and the solution operator $\mathbf{j}_e \mapsto \mathbf{h}_c$ is a bounded operator $\mathbf{L}^2(\Omega') \rightarrow \mathbf{H}^1(\mathbb{R}^3)$. For more details, we refer the reader to [166], where the theory is developed for the analysis of the transmission problem (3.1) for the magnetostatic potential. Note that (3.1) and (3.2) have the same structure so that the results of [166] transfer to the present situation. We conclude that $\mathbf{h}_c \in \mathbf{H}^1(\mathbb{R}^3)$ satisfies the stability estimate

$$\|\mathbf{h}_c\|_{\mathbf{H}^1(\mathbb{R}^3)} \leq C\|\mathbf{j}_e\|_{\mathbf{L}^2(\Omega')}, \quad (5.35)$$

where $C = C(|\Omega'|)$ is constant. For $\mathbf{m} \in \mathbf{L}^\infty(\Omega')$ satisfying $\|\mathbf{m}\|_{\mathbf{L}^\infty(\Omega')} \leq 1$, applying Proposition 5.2.1 and taking the expression (5.31g) of the electric current into account, we obtain that

$$\|\mathbf{h}_c\|_{\mathbf{H}^1(\mathbb{R}^3)} \stackrel{(5.35)}{\lesssim} \|\mathbf{j}_e\|_{\mathbf{L}^2(\Omega')} \stackrel{(5.31g)}{\lesssim} \|\nabla\mathbf{s}\|_{\mathbf{L}^2(\Omega')} + \|\nabla V\|_{\mathbf{L}^2(\Omega')} \stackrel{(5.33)}{\leq} C.$$

To recover (5.27), we define the operator $\mathbf{\Pi} : \{\mathbf{m} \in \mathbf{L}^\infty(\Omega) : |\mathbf{m}| = 1 \text{ a.e. in } \Omega\} \rightarrow \mathbf{L}^2(\Omega)$ as the mapping $\mathbf{m} \mapsto \mathbf{h}_c|_\Omega + \tau_j^{-1} \mathbf{s}|_\Omega$. From the above discussion, it follows that

$$\|\mathbf{\Pi}(\mathbf{m})\|_{\mathbf{L}^2(\Omega)} \leq C \quad \text{for all } \mathbf{m} \in \mathbf{L}^\infty(\Omega) \text{ such that } |\mathbf{m}| = 1 \text{ a.e. in } \Omega,$$

where the constant $C > 0$ depends only on the data of the problem.

5.2.4.3 Numerical discretization

To define the discrete operator $\mathbf{\Pi}_h$ which approximates $\mathbf{\Pi}$ and apply the framework of Theorem 4.3.2, we need two effective numerical methods to discretize (5.30) and (5.31). To that end, let \mathcal{T}'_h be a γ -quasi-uniform regular tetrahedral triangulation of Ω' . Let $\mathcal{E}'_h := \mathcal{T}'_h|_{\Gamma'}$. We assume that Ω and the partition of Γ' into Γ'_D and Γ'_N are resolved, i.e., the restrictions $\mathcal{T}_h := \mathcal{T}'_h|_{\Omega'}$, $\mathcal{E}'_{D,h} := \mathcal{T}'_h|_{\Gamma'_D}$ and $\mathcal{E}'_{N,h} := \mathcal{T}'_h|_{\Gamma'_N}$ provide regular triangulations of Ω , Γ_D , and Γ_N , respectively. Let $H_*^1(\Omega') = \{\phi \in H^1(\Omega') : \int_{\Omega'} \phi(\mathbf{x}) d\mathbf{x} = 0\}$. We consider the discrete spaces $\mathcal{S}_*^1(\mathcal{T}'_h) = \mathcal{S}^1(\mathcal{T}'_h) \cap H_*^1(\Omega')$, $\mathcal{S}_D^1(\mathcal{T}'_h) = \mathcal{S}^1(\mathcal{T}'_h) \cap H_D^1(\Omega')$, $\mathcal{S}_0^1(\mathcal{T}'_h) = \mathcal{S}^1(\mathcal{T}'_h) \cap H_0^1(\Omega')$, and $\mathcal{S}^1(\mathcal{E}'_{D,h}) = \{v_h|_{\Gamma_D} : v_h \in \mathcal{S}_D^1(\mathcal{T}'_h)\}$.

To approximate (5.31), we consider a finite element discretization of (5.32). Let $\mathbf{m}_h \in \mathcal{U}_h$ be the approximate magnetization. Let $V_{D,h} = \mathcal{P}_h V_D$ be a discretization of the Dirichlet data obtained by applying the L^2 -orthogonal projection $\mathcal{P}_h : L^2(\Gamma'_D) \rightarrow \mathcal{S}^1(\mathcal{E}'_{D,h})$. Since \mathcal{P}_h is H^1 -stable, it is also $H^{1/2}$ -stable by standard interpolation results. We consider the following discrete variational formulation: Find $\mathbf{s}_h \in \mathcal{S}_D^1(\mathcal{T}'_h)^3$ and $V_h \in \mathcal{S}^1(\mathcal{T}'_h)$, with $V_h = V_{D,h}$ on Γ'_D , such that

$$b(\mathcal{I}_h[\mathbf{m}_h/|\mathbf{m}_h|]; (\mathbf{s}_h, V_h), (\boldsymbol{\zeta}_h, \psi_h)) = 0 \quad \text{for all } (\boldsymbol{\zeta}_h, \psi_h) \in \mathcal{S}_D^1(\mathcal{T}'_h)^3 \times \mathcal{S}_D^1(\mathcal{T}'_h). \quad (5.36)$$

Since $\|\mathcal{I}_h[\mathbf{m}_h/|\mathbf{m}_h|]\|_{\mathbf{L}^\infty(\Omega)} = 1$, the bilinear form $b(\mathcal{I}_h[\mathbf{m}_h/|\mathbf{m}_h|]; \cdot, \cdot)$ is uniformly elliptic on $\mathcal{S}_D^1(\mathcal{T}'_h)^3 \times \mathcal{S}_D^1(\mathcal{T}'_h)$. Taking the $H^{1/2}$ -stability of \mathcal{P}_h into account, it follows from Proposition 5.2.1 that (5.36) is well posed. Moreover, the unique solutions $\mathbf{s}_h \in \mathcal{S}_D^1(\mathcal{T}'_h)^3$ and $V_h \in \mathcal{S}^1(\mathcal{T}'_h)$ satisfy

$$\|\mathbf{s}_h\|_{\mathbf{H}^1(\Omega')} + \|V_h\|_{H^1(\Omega')} \leq C, \quad (5.37)$$

where the constant $C > 0$ depends on the problem data and on γ , but it is independent of the mesh size h .

To approximate (5.30), we apply the hybrid FEM-BEM method for stray field computations of [99]; see also [56, Section 4.4.1] and [109, Section 4.3]. The starting point is the decomposition $\mathbf{h}_c|_{\Omega'} = \mathbf{h}_1 + \mathbf{h}_2$, where $\mathbf{h}_1 \in \mathbf{H}_*^1(\Omega')$ and $\mathbf{h}_2 \in \mathbf{H}^1(\Omega')$ are the unique weak solutions of the boundary value problems

$$-\Delta \mathbf{h}_1 = \nabla \times \mathbf{j}_e \quad \text{in } \Omega', \quad (5.38a)$$

$$\partial_n \mathbf{h}_1 = -\mathbf{n} \times \mathbf{j}_e \quad \text{on } \Gamma', \quad (5.38b)$$

and

$$-\Delta \mathbf{h}_2 = \mathbf{0} \quad \text{in } \Omega', \quad (5.38c)$$

$$\mathbf{h}_2 = (\mathcal{K} - \mathbf{1}/2)[\mathbf{h}_1|_{\Gamma'}] \quad \text{on } \Gamma', \quad (5.38d)$$

respectively. In (5.38d), we denote by $\mathcal{K} : \mathbf{H}^{1/2}(\Gamma') \rightarrow \mathbf{H}^{1/2}(\Gamma')$ the (vector-valued) double layer integral operator associated with the Laplace problem, which is formally defined by

$$\mathcal{K}[\phi](\mathbf{x}) = \frac{1}{4\pi} \int_{\Gamma'} \frac{(\mathbf{x} - \mathbf{y}) \cdot \mathbf{n}(\mathbf{y})}{|\mathbf{x} - \mathbf{y}|^3} \phi(\mathbf{y}) dS(\mathbf{y}) \quad \text{for all } \phi \in \mathbf{H}^{1/2}(\Gamma');$$

see, e.g., [186, Section 3.1] or [147, Chapter 7]. Let $\mathbf{j}_{e,h} \in \mathcal{S}^1(\mathcal{T}'_h)^3$ denote a given approximation of $\mathbf{j}_e \in \mathbf{L}^2(\Omega')$. Taking the characterization (5.38) into account, an effective approximation of $\mathbf{h}_c|_{\Omega'}$ can be obtained by means of the following algorithm.

Algorithm 5.2.2 (Hybrid FEM-BEM method for Oersted field computations). *Input:* $\mathbf{j}_{e,h} \in \mathcal{S}^1(\mathcal{T}'_h)^3$.

(i) Compute $\mathbf{h}_{1,h} \in \mathcal{S}_*^1(\mathcal{T}'_h)^3$ such that

$$\langle \nabla \mathbf{h}_{1,h}, \nabla \phi_h \rangle_{\Omega'} = \langle \mathbf{j}_{e,h}, \nabla \times \phi_h \rangle_{\Omega'} \quad \text{for all } \phi_h \in \mathcal{S}_*^1(\mathcal{T}'_h)^3.$$

(ii) Define $\mathbf{g}_h := \mathcal{P}_h(\mathcal{K} - \mathbf{1}/2)[\mathbf{h}_{1,h}|_{\Gamma'}] \in \mathcal{S}^1(\mathcal{E}'_h)^3$, i.e., it holds that

$$\langle \mathbf{g}_h, \phi_h \rangle_{\Gamma'} = \langle (\mathcal{K} - \mathbf{1}/2)[\mathbf{h}_{1,h}|_{\Gamma'}], \phi_h \rangle_{\Gamma'} \quad \text{for all } \phi_h \in \mathcal{S}^1(\mathcal{E}'_h)^3.$$

(iii) Compute $\mathbf{h}_{2,h} \in \mathcal{S}^1(\mathcal{T}'_h)^3$ such that $\mathbf{h}_{2,h}|_{\Gamma'} = \mathbf{g}_h$ and

$$\langle \nabla \mathbf{h}_{1,h}, \nabla \phi_h \rangle_{\Omega'} = 0 \quad \text{for all } \phi_h \in \mathcal{S}_0^1(\mathcal{T}'_h)^3.$$

(iv) Define $\mathbf{h}_{c,h} := \mathbf{h}_{1,h} + \mathbf{h}_{2,h} \in \mathcal{S}^1(\mathcal{T}'_h)^3$.

Output: $\mathbf{h}_{c,h} \in \mathcal{S}^1(\mathcal{T}'_h)^3$.

We have collected all ingredients to define the discrete operator $\mathbf{\Pi}_h : \mathcal{U}_h \rightarrow \mathbf{L}^2(\Omega)$. For any $\mathbf{m}_h \in \mathcal{U}_h$, we first compute the unique solutions $\mathbf{s}_h \in \mathcal{S}_D^1(\mathcal{T}'_h)^3$ and $V_h \in \mathcal{S}^1(\mathcal{T}'_h)$ of (5.36). Then, motivated by (5.31g), we define $\mathbf{j}_{e,h} = -cD_0 \nabla V_h - \beta' D_0 \nabla \mathbf{s}_h^\top \mathcal{I}_h[\mathbf{m}_h / |\mathbf{m}_h|] \in \mathcal{S}^1(\mathcal{T}'_h)^3$. Finally, this function is used as input for the computation of $\mathbf{h}_{c,h} \in \mathcal{S}^1(\mathcal{T}'_h)^3$ by Algorithm 5.2.2. The discrete operator $\mathbf{\Pi}_h$ is then defined as the mapping $\mathbf{m}_h \mapsto \mathbf{h}_{c,h}|_{\Omega} + \tau_J^{-1} \mathbf{s}_h|_{\Omega}$.

In the remainder of this section, we prove that $\mathbf{\Pi}_h$ satisfies the assumptions (4.16b) and (4.18b) of Theorem 4.3.2. Owing to (5.37), it holds that $\|\mathbf{s}_h\|_{\mathbf{L}^2(\Omega')} \leq C$. As for the Oersted field part, stability and consistency follow from [56, Lemma 4.1 and Proposition 4.2]; see also [109, Section 4.3]. It remains to show that the spin accumulation contribution to $\mathbf{\Pi}_h$ satisfies the consistency condition (4.18b). The proof follows the lines of the analogous result for the stationary spin diffusion model considered in the previous section.

Let $\widehat{\mathbf{m}}_{hk}^-$ be the piecewise constant time reconstruction defined by (4.41) using the ‘normalized iterate’ (4.40). We denote by $\mathbf{m} \in L^\infty(0, T; \mathbf{H}^1(\Omega)) \cap H^1(0, T; \mathbf{L}^2(\Omega))$ the function such that the convergence results (4.42) are satisfied. Let $\mathbf{s} \in L^\infty(0, T; \mathbf{H}_D^1(\Omega'))$ and $V \in L^\infty(0, T; H^1(\Omega'))$ with $V(t)|_{\Gamma_D} = V_D$ for a.e. $t \in (0, T)$ be defined by

$$b(\mathbf{m}(t); (\mathbf{s}(t), V(t)), (\zeta, \psi)) = 0 \quad \text{for all } (\zeta, \psi) \in \mathbf{H}_D^1(\Omega') \times H_D^1(\Omega') \text{ and a.e. } t \in (0, T).$$

Similarly, we define $\mathbf{s}_{hk}^- : [0, T] \rightarrow \mathcal{S}^1(\mathcal{T}'_h)^3$ and $V_{hk}^- : [0, T] \rightarrow \mathcal{S}^1(\mathcal{T}'_h)$ by $\mathbf{s}_{hk}^-(t) := \mathbf{s}_{hk}^i$ and $V_{hk}^-(t) := V_h^i$ for all $0 \leq i \leq M-1$ such that $t \in [t_i, t_{i+1})$, where $\mathbf{s}_h^i \in \mathcal{S}_D^1(\mathcal{T}'_h)^3$ and $V_h^i \in \mathcal{S}^1(\mathcal{T}'_h)$ with $V_h^i|_{\Gamma_D} = V_{D,h}$ satisfy

$$b(\widehat{\mathbf{m}}_h^i; (\mathbf{s}_h^i, V_h^i), (\zeta_h, \psi_h)) = 0 \quad \text{for all } \zeta_h \in \mathcal{S}_D^1(\mathcal{T}'_h)^3, \psi_h \in \mathcal{S}_D^1(\mathcal{T}'_h), \text{ and } 0 \leq i \leq M-1. \quad (5.39)$$

We aim to show that $(\mathbf{s}_{hk}^-, V_{hk}^-) \rightharpoonup (\mathbf{s}, V)$ in $L^2(0, T; \mathbf{H}_D^1(\Omega')) \times L^2(0, T; H^1(\Omega'))$.

Thanks to (5.37), $\{(\mathbf{s}_{hk}^-, V_{hk}^-)\}$ is uniformly bounded in $L^2(0, T; \mathbf{H}_D^1(\Omega')) \times L^2(0, T; H^1(\Omega'))$. Hence, by the Eberlein–Smulian theorem, we can extract a weakly convergent subsequence (not relabeled) which converges towards some $(\tilde{\mathbf{s}}, \tilde{V}) \in L^2(0, T; \mathbf{H}_D^1(\Omega')) \times L^2(0, T; H^1(\Omega'))$. Let $\boldsymbol{\eta} \in C^1([0, T]; \mathbf{C}^\infty(\Omega') \cap \mathbf{H}_D^1(\Omega'))$ and $\phi \in C^1([0, T]; C^\infty(\Omega') \cap H_D^1(\Omega'))$ be arbitrary. Define $\boldsymbol{\eta}_h : [0, T] \rightarrow \mathcal{S}^1(\mathcal{T}'_h)^3$ and $\phi_h : [0, T] \rightarrow \mathcal{S}^1(\mathcal{T}'_h)$ by $\boldsymbol{\eta}_h(t) = \mathcal{I}_h[\boldsymbol{\eta}(t)]$ and $\phi_h(t) = \mathcal{I}_h[\phi(t)]$ for all $t \in [0, T]$, respectively. From (5.39), we deduce that, for every measurable set $I \subseteq [0, T]$, it holds that

$$\int_I b(\widehat{\mathbf{m}}_{hk}^-(t); (\mathbf{s}_{hk}^-(t), V_{hk}^-(t)), (\boldsymbol{\eta}_h(t), \phi_h(t))) dt = 0.$$

Passing this identity to the limit as $k, h \rightarrow 0$, thanks to the available convergence results, we obtain that

$$\int_I b(\mathbf{m}(t); (\tilde{\mathbf{s}}(t), \tilde{V}(t)), (\boldsymbol{\eta}(t), \phi(t))) dt = 0.$$

By density, since $I \subseteq [0, T]$ was arbitrary, we obtain that

$$b(\mathbf{m}(t); (\tilde{\mathbf{s}}(t), \tilde{V}(t)), (\boldsymbol{\zeta}, \psi)) = 0 \quad \text{for all } (\boldsymbol{\zeta}, \psi) \in \mathbf{H}_D^1(\Omega') \times H_D^1(\Omega') \text{ and a.e. } t \in (0, T).$$

Moreover, using the approximation properties of the L^2 -projection, we deduce that $\tilde{V}(t)|_{\Gamma'_D} = V_D$ for a.e. $t \in (0, T)$. This shows that $\mathbf{s} = \tilde{\mathbf{s}}$ and $V = \tilde{V}$, so that the desired convergence $(\mathbf{s}_{hk}^-, V_{hk}^-) \rightharpoonup (\mathbf{s}, V)$ in $L^2(0, T; \mathbf{H}_D^1(\Omega')) \times L^2(0, T; H^1(\Omega'))$. We conclude that $\boldsymbol{\Pi}_h$ satisfies the consistency requirement (4.18b) so that the framework of part (b) of Theorem 4.3.2 applies.

Remark 5.2.3. *In step (ii) of Algorithm 5.2.2, the original reference [99] employs the nodal interpolant (instead of the L^2 -orthogonal projection onto $\mathcal{S}^1(\mathcal{E}'_h)^3$) to obtain the discrete Dirichlet data for step (iii). However, since the nodal interpolant is not well defined for $H^{1/2}$ -functions, this choice is not suitable for the rigorous numerical analysis of the algorithm. Unlike [56, Section 4.4.1], where the Scott–Zhang projection from [187] is considered, we use the L^2 -orthogonal projection onto $\mathcal{S}^1(\mathcal{E}'_h)^3$. This choice is motivated by the fact that, in our numerical experiments, the use of the L^2 -projection led to qualitative better results for coarse meshes. Since, on quasi-uniform meshes, the L^2 -orthogonal projection is H^1 -stable and satisfies a first-order approximation property, the result of [56, Lemma 4.1 and Proposition 4.2] remains valid; see also [109, Section 4.3].*

Chapter 6

Numerical results

To support our theoretical findings, this chapter presents some preliminary numerical results, which investigate the performance of the tangent plane integrator discussed in Chapter 4. For deeper numerical experiments, in particular concerning the spintronic extensions of the LLG equation presented in Section 2.3 and analyzed in Chapter 5, we refer to our papers [7, 174, 8]. The numerical results of those papers were obtained using the implementation of the tangent plane scheme included in MAGNUM.fe, a C++/Python code mainly developed by C. ABERT at the Christian Doppler Laboratory of Advanced Magnetic Sensing and Materials of TU Wien [5].

6.1 Solution of the system

In this section, we discuss effective strategies for the solution of the linear system which arises discretizing the LLG equation with the tangent plane scheme (Algorithm 4.2.1). We start by recalling the notation introduced in the proof of Proposition 4.2.2. Given $\mathbf{m}_h \in \mathcal{U}_h$, we denote the discrete tangent space by

$$\mathcal{K}_{\mathbf{m}_h} := \{ \phi_h \in \mathcal{S}^1(\mathcal{T}_h)^3 : \mathbf{m}_h(\mathbf{z}) \cdot \phi_h(\mathbf{z}) = 0 \text{ for all } \mathbf{z} \in \mathcal{N}_h \}.$$

We consider the bilinear form $a(\mathbf{m}_h; \cdot, \cdot) : \mathcal{S}^1(\mathcal{T}_h)^3 \times \mathcal{S}^1(\mathcal{T}_h)^3 \rightarrow \mathbb{R}$ defined by

$$a(\mathbf{m}_h; \boldsymbol{\eta}_h, \phi_h) := \alpha \langle \boldsymbol{\eta}_h, \phi_h \rangle + \langle \mathbf{m}_h \times \boldsymbol{\eta}_h, \phi_h \rangle + \lambda_{\text{ex}}^2 \theta k \langle \nabla \boldsymbol{\eta}_h, \nabla \phi_h \rangle$$

for all $\boldsymbol{\eta}_h, \phi_h \in \mathcal{S}^1(\mathcal{T}_h)^3$, and the linear functional $F(\mathbf{m}_h; \cdot) : \mathcal{S}^1(\mathcal{T}_h)^3 \rightarrow \mathbb{R}$ defined by

$$F(\mathbf{m}_h; \phi_h) := -\lambda_{\text{ex}}^2 \langle \nabla \mathbf{m}_h, \nabla \phi_h \rangle + \langle \boldsymbol{\pi}_h(\mathbf{m}_h), \phi_h \rangle + \langle \mathbf{f}_h, \phi_h \rangle + \langle \boldsymbol{\Pi}_h(\mathbf{m}_h), \phi_h \rangle$$

for all $\phi_h \in \mathcal{S}^1(\mathcal{T}_h)^3$. The tangent plane scheme analyzed in Chapter 4 requires, for every time-step, the solution of the following discrete variational problem (see (4.9) in step (ii) of Algorithm 4.2.1):

$$\text{Find } \mathbf{v}_h \in \mathcal{K}_{\mathbf{m}_h} \text{ such that } a(\mathbf{m}_h; \mathbf{v}_h, \phi_h) = F(\mathbf{m}_h; \phi_h) \text{ for all } \phi_h \in \mathcal{K}_{\mathbf{m}_h}. \quad (6.1)$$

Here, to simplify the notation, we have omitted the superscript i associated with the time-step.

Our approach is based on standard linear algebra arguments; see [50, Chapter 3]. Let $\{\mathbf{e}_p\}_{1 \leq p \leq 3}$ be the standard basis of \mathbb{R}^3 . Here and in the sequel, all vectors are understood as column vectors. We start by enumerating the nodes of the triangulation, i.e., $\mathcal{N}_h = \{\mathbf{z}_n\}_{1 \leq n \leq N}$, which induces an ordering on the set of the hat functions, i.e., $\varphi_n = \varphi_{\mathbf{z}_n}$ for all $1 \leq n \leq N$. The set $\{\boldsymbol{\varphi}_i\}_{1 \leq i \leq 3N}$, where

$$\boldsymbol{\varphi}_{3(n-1)+p} := \varphi_n \mathbf{e}_p \quad \text{for all } 1 \leq n \leq N \text{ and } 1 \leq p \leq 3,$$

then constitutes a basis of $\mathcal{S}^1(\mathcal{T}_h)^3$. With respect to this basis, we define

- the symmetric and positive definite mass matrix $\mathbf{M} \in \mathbb{R}^{3N \times 3N}$, defined by $M_{ij} = \langle \boldsymbol{\varphi}_j, \boldsymbol{\varphi}_i \rangle$ for all $1 \leq i, j \leq 3N$,

- the symmetric and positive semidefinite stiffness matrix $\mathbf{L} \in \mathbb{R}^{3N \times 3N}$, defined by $L_{ij} = \langle \nabla \varphi_j, \nabla \varphi_i \rangle$ for all $1 \leq i, j \leq 3N$,
- the skew-symmetric matrix $\mathbf{S} \in \mathbb{R}^{3N \times 3N}$, defined by $S_{ij} = \langle \mathbf{m}_h \times \varphi_j, \varphi_i \rangle$ for all $1 \leq i, j \leq 3N$,
- the matrix $\mathbf{A} \in \mathbb{R}^{3N \times 3N}$, defined by $\mathbf{A} = \alpha \mathbf{M} + \lambda_{\text{ex}}^2 \theta k \mathbf{L} + \mathbf{S}$,
- the matrix $\mathbf{B} \in \mathbb{R}^{N \times 3N}$, whose transpose is defined by

$$\mathbf{B}^\top = \begin{pmatrix} \frac{\mathbf{m}_h(\mathbf{z}_1)}{|\mathbf{m}_h(\mathbf{z}_1)|} & \mathbf{0} & \cdots & \mathbf{0} \\ \mathbf{0} & \frac{\mathbf{m}_h(\mathbf{z}_2)}{|\mathbf{m}_h(\mathbf{z}_2)|} & \ddots & \mathbf{0} \\ \mathbf{0} & \ddots & \ddots & \mathbf{0} \\ \mathbf{0} & \cdots & \mathbf{0} & \frac{\mathbf{m}_h(\mathbf{z}_N)}{|\mathbf{m}_h(\mathbf{z}_N)|} \end{pmatrix} \in \mathbb{R}^{3N \times N}, \quad (6.2)$$

- the right-hand side vector $\mathbf{r} \in \mathbb{R}^{3N}$, defined by $r_i = F(\mathbf{m}_h; \varphi_i)$ for all $1 \leq i \leq 3N$.

The matrix \mathbf{A} , which represents the bilinear form $a(\mathbf{m}_h^i; \cdot, \cdot)$, is positive definite (and hence regular) and is made of a symmetric and positive definite part $\mathbf{A}_s = \alpha \mathbf{M} + \lambda_{\text{ex}}^2 \theta k \mathbf{L}$ and a skew-symmetric part $\mathbf{A}_{ss} = \mathbf{S}$.

The columns of the matrix \mathbf{B}^\top are orthonormal, i.e., $\mathbf{B}\mathbf{B}^\top = \mathbf{I}_{N \times N}$. In particular, it holds that $\text{rk } \mathbf{B} = \text{rk } \mathbf{B}^\top = N$. The matrix $\mathbf{B}^\top \mathbf{B} \in \mathbb{R}^{3N \times 3N}$ is the matrix associated with the orthogonal projection onto $\text{Im } \mathbf{B}^\top = (\ker \mathbf{B})^\perp$, from which it follows that the matrix $\mathbf{P} = \mathbf{I}_{3N \times 3N} - \mathbf{B}^\top \mathbf{B} \in \mathbb{R}^{3N \times 3N}$ is the matrix associated with the orthogonal projection onto $\ker \mathbf{B}$.

For $\mathbf{w}_h = \sum_{i=1}^{3N} w_i \varphi_i \in \mathcal{S}^1(\mathcal{T}_h)^3$, let $\mathbf{w} \in \mathbb{R}^{3N}$ be the corresponding coordinate vector with respect to the basis $\{\varphi_i\}_{1 \leq i \leq 3N}$. By construction, for all $1 \leq n \leq N$, it holds that

$$(\mathbf{B}\mathbf{w})_n = \sum_{j=1}^{3N} B_{nj} w_j = \frac{\mathbf{m}_h(\mathbf{z}_n)}{|\mathbf{m}_h(\mathbf{z}_n)|} \cdot \mathbf{w}_h(\mathbf{z}_n).$$

We deduce that $\mathbf{w}_h \in \mathcal{S}^1(\mathcal{T}_h)^3$ belongs to $\mathcal{K}_{\mathbf{m}_h}$ if and only if $\mathbf{w} \in \mathbb{R}^{3N}$ satisfies $\mathbf{B}\mathbf{w} = \mathbf{0}$. In particular, $\ker \mathbf{B}$ is isomorphic to $\mathcal{K}_{\mathbf{m}_h}$ so that $\dim(\mathcal{K}_{\mathbf{m}_h}) = \dim(\ker \mathbf{B}) = 3N - \text{rk } \mathbf{B} = 2N$. Moreover, the matrix $\mathbf{P} \in \mathbb{R}^{3N \times 3N}$ is nothing but the transformation matrix associated with the orthogonal projection $\mathcal{S}^1(\mathcal{T}_h)^3 \rightarrow \mathcal{K}_{\mathbf{m}_h}$.

In the remainder of this section, we describe three possible strategies to compute the unique solution $\mathbf{v}_h \in \mathcal{K}_{\mathbf{m}_h}$ of (6.1). For a numerical comparison of them as well as for the analysis of solvers and preconditioning strategies for the resulting linear systems, we refer the interested reader to a forthcoming publication [168].

6.1.1 Saddle point formulation

We introduce the Lagrange multiplier associated with the orthogonality constraint and consider the saddle point problem

$$\begin{pmatrix} \mathbf{A} & \mathbf{B}^\top \\ \mathbf{B} & \mathbf{0} \end{pmatrix} \begin{pmatrix} \mathbf{v} \\ \boldsymbol{\lambda} \end{pmatrix} = \begin{pmatrix} \mathbf{r} \\ \mathbf{0} \end{pmatrix}. \quad (6.3)$$

In the following proposition, we establish the equivalence of (6.1) with the linear system (6.3).

Proposition 6.1.1. *There exists a unique solution $(\mathbf{v}, \boldsymbol{\lambda}) \in \mathbb{R}^{3N} \times \mathbb{R}^N$ of (6.3). The variational problem (6.1) and the linear system (6.3) are equivalent in the sense that $\mathbf{v}_h = \sum_{i=1}^{3N} v_i \varphi_i$ solves (6.1) if and only if $\mathbf{v} \in \mathbb{R}^{3N}$, together with some $\boldsymbol{\lambda} \in \mathbb{R}^N$, constitutes a solution $(\mathbf{v}, \boldsymbol{\lambda})$ of (6.3).*

Proof. Since \mathbf{A} is positive definite and \mathbf{B} is surjective, the matrix of the system (6.3) is regular; see, e.g., [50, Corollary 3.2.2]. Therefore, a solution $(\mathbf{v}, \boldsymbol{\lambda}) \in \mathbb{R}^{3N} \times \mathbb{R}^N$ of (6.3) exists and is unique.

To prove the second part of the statement, let $(\mathbf{v}, \boldsymbol{\lambda}) \in \mathbb{R}^{3N} \times \mathbb{R}^N$ be the unique solution of (6.3). It holds that $\mathbf{A}\mathbf{v} + \mathbf{B}^\top \boldsymbol{\lambda} = \mathbf{r}$ and $\mathbf{B}\mathbf{v} = \mathbf{0}$. In particular, since $\mathbf{v} \in \ker \mathbf{B}$, $\mathbf{v}_h = \sum_{i=1}^{3N} v_i \boldsymbol{\varphi}_i$ belongs to $\mathcal{K}_{\mathbf{m}_h}$. Let $\mathbf{w}_h = \sum_{i=1}^{3N} w_i \boldsymbol{\varphi}_i \in \mathcal{K}_{\mathbf{m}_h}$ be arbitrary. Then, the coordinate vector $\mathbf{w} \in \mathbb{R}^{3N}$ satisfies $\mathbf{B}\mathbf{w} = \mathbf{0}$. It holds that

$$a(\mathbf{m}_h; \mathbf{v}_h, \mathbf{w}_h) = \sum_{i,j=1}^{3N} a(\mathbf{m}_h; \boldsymbol{\varphi}_j, \boldsymbol{\varphi}_i) v_j w_i = \mathbf{A}\mathbf{v} \cdot \mathbf{w} = (\mathbf{A}\mathbf{v} + \mathbf{B}^\top \boldsymbol{\lambda}) \cdot \mathbf{w} = \mathbf{r} \cdot \mathbf{w} = F(\mathbf{m}_h; \mathbf{w}_h).$$

Since $\mathbf{w}_h \in \mathcal{K}_{\mathbf{m}_h}$ was arbitrary, this shows that $\mathbf{v}_h \in \mathcal{K}_{\mathbf{m}_h}$ solves (6.1) and concludes the proof. \square

6.1.2 Reduced constrained problem

The numerical solution of saddle point problems is a well-understood mathematical problem; see, e.g., [43]. However, we notice at least two disadvantages in using this approach for the computation of the solution of (6.1): On the one hand, the resulting linear system is indefinite, despite the positive definiteness of the original variational problem; on the other hand, although the number of actual unknowns of (6.1) is $2N$ (as $\dim(\mathcal{K}_{\mathbf{m}_h}) = \dim(\ker \mathbf{B}) = 2N$), we end up with a system of $4N$ unknowns. Using a geometric approach, we aim to construct a basis of the discrete tangent space so that the computation of the solution $\mathbf{v}_h \in \mathcal{K}_{\mathbf{m}_h}$ of (6.1) will require to solve a linear system of $2N$ equations for $2N$ unknowns.

For the sake of illustration, we start by considering a single node $\mathbf{z} \in \mathcal{N}_h$ of the triangulation, for which we define $\mathbf{m}_z = \mathbf{m}_h(\mathbf{z})/|\mathbf{m}_h(\mathbf{z})| \in \mathbb{S}^2$. Suppose that we are given an orthogonal matrix $\mathbf{R}_z \in \mathbb{R}^{3 \times 3}$ which satisfies either $\mathbf{R}_z^\top \mathbf{e}_3 = \mathbf{m}_z$ or $\mathbf{R}_z^\top \mathbf{e}_3 = -\mathbf{m}_z$. Since \mathbf{R}_z is orthogonal, $\{\mathbf{R}_z^\top \mathbf{e}_p\}_{1 \leq p \leq 3}$ is an orthonormal basis of \mathbb{R}^3 . Using standard linear algebra arguments, it is easy to check that, for any $\mathbf{w} \in \mathbb{R}^3$, the coordinate vector $\mathbf{x} \in \mathbb{R}^3$ with respect to the basis $\{\mathbf{e}_p\}_{1 \leq p \leq 3}$, i.e., $\mathbf{w} = \sum_{p=1}^3 x_p \mathbf{e}_p$, and the coordinate vector $\mathbf{y} \in \mathbb{R}^3$ with respect to the basis $\{\mathbf{R}_z^\top \mathbf{e}_p\}_{1 \leq p \leq 3}$, i.e., $\mathbf{w} = \sum_{p=1}^3 y_p \mathbf{R}_z^\top \mathbf{e}_p$, are related to each other via $\mathbf{y} = \mathbf{R}_z \mathbf{x}$. Moreover, since $\mathbf{R}_z^\top \mathbf{e}_3 \in \{\pm \mathbf{m}_z\}$ by assumption, $\{\mathbf{R}_z^\top \mathbf{e}_p\}_{1 \leq p \leq 2}$ is an orthonormal basis of the subspace $K_z = \text{span}(\mathbf{m}_z)^\perp = \{\mathbf{u} \in \mathbb{R}^3 : \mathbf{u} \cdot \mathbf{m}_z = 0\}$ of \mathbb{R}^3 . In particular, $\mathbf{w} \in K_z$ if and only if the coordinate vector $\mathbf{x} \in \mathbb{R}^3$ with respect to the basis $\{\mathbf{e}_p\}_{1 \leq p \leq 3}$ satisfies $(\mathbf{R}_z \mathbf{x})_3 = 0$.

In the following lemma, we state two possible geometric ways to construct a matrix satisfying the desired properties.

Lemma 6.1.2. *Let $\mathbf{m} \in \mathbb{S}^2$. Let $\mathbf{R} \in \mathbb{R}^{3 \times 3}$ be the matrix constructed according to either of the following two strategies:*

- (i) Define $\sigma = \text{sign}(\mathbf{m} \cdot \mathbf{e}_3)$, with the convention that $\text{sign}(0) = -1$. If $\mathbf{m} = \sigma \mathbf{e}_3$, define

$$\mathbf{R} = \begin{pmatrix} 1 & 0 & 0 \\ 0 & 1 & 0 \\ 0 & 0 & -1 \end{pmatrix},$$

otherwise define the Householder matrix

$$\mathbf{R} = \mathbf{I}_{3 \times 3} - 2\mathbf{w} \otimes \mathbf{w}, \quad \text{where } \mathbf{w} = \frac{\mathbf{m} + \sigma \mathbf{e}_3}{|\mathbf{m} + \sigma \mathbf{e}_3|} \in \mathbb{S}^2.$$

- (ii) Define

$$\mathbf{R} = \mathbf{I}_{3 \times 3} - [\mathbf{e}_3 \times \mathbf{m}]_\times + \frac{1}{1 + \mathbf{m} \cdot \mathbf{e}_3} [\mathbf{e}_3 \times \mathbf{m}]_\times^2$$

where $[\cdot]_\times$ denote the skew-symmetric cross product matrix defined by

$$[\mathbf{u}]_\times = \begin{pmatrix} 0 & -u_3 & u_2 \\ u_3 & 0 & -u_1 \\ -u_2 & u_1 & 0 \end{pmatrix} \quad \text{for all } \mathbf{u} \in \mathbb{R}^3,$$

which satisfies $[\mathbf{u}]_{\times} \mathbf{w} = \mathbf{u} \times \mathbf{w}$ for all $\mathbf{w} \in \mathbb{R}^3$.

Then, in both cases, \mathbf{R} is orthogonal. The matrix \mathbf{R} defined by (i) is symmetric and satisfies $\mathbf{m} = -\sigma \mathbf{R} \mathbf{e}_3 = -\sigma \mathbf{R}^{\top} \mathbf{e}_3$. For the matrix \mathbf{R} defined by (ii), it holds that $\mathbf{m} = \mathbf{R}^{\top} \mathbf{e}_3$.

Proof. The matrix \mathbf{R} of part (i) is the transformation matrix of a reflection. It is symmetric, orthogonal, and therefore also involutory, i.e., $\mathbf{R}^2 = \mathbf{I}_{3 \times 3}$. If $\mathbf{m} = \sigma \mathbf{e}_3$, the reflection is with respect to the plane $\{x_3 = 0\}$. In particular, it holds that $\mathbf{m} = \sigma \mathbf{e}_3 = -\sigma \mathbf{R} \mathbf{e}_3$. Otherwise, it is a reflection with respect to the plane passing through the origin and orthogonal to the vector $\mathbf{w} \in \mathbb{S}^2$. Since

$$|\mathbf{m} + \sigma \mathbf{e}_3|^2 = 2(1 + \sigma \mathbf{m} \cdot \mathbf{e}_3), \quad (6.4)$$

it follows that

$$\mathbf{R} \mathbf{m} = \mathbf{m} - 2(\mathbf{w} \otimes \mathbf{w}) \mathbf{m} = \mathbf{m} - 2(\mathbf{w} \cdot \mathbf{m}) \mathbf{w} = \mathbf{m} - 2 \left(\frac{\mathbf{m} + \sigma \mathbf{e}_3}{|\mathbf{m} + \sigma \mathbf{e}_3|} \cdot \mathbf{m} \right) \frac{\mathbf{m} + \sigma \mathbf{e}_3}{|\mathbf{m} + \sigma \mathbf{e}_3|} \stackrel{(6.4)}{=} -\sigma \mathbf{e}_3.$$

Since \mathbf{R} is involutory, we conclude that $\mathbf{m} = \mathbf{R}^2 \mathbf{m} = -\sigma \mathbf{R} \mathbf{e}_3 = -\sigma \mathbf{R}^{\top} \mathbf{e}_3$.

The matrix \mathbf{R} of part (ii) is the transformation matrix of the rotation around the axis $\mathbf{m} \times \mathbf{e}_3$ by an angle γ such that $\cos \gamma = \mathbf{m} \cdot \mathbf{e}_3$ and $\sin \gamma = |\mathbf{m} \times \mathbf{e}_3|$. In particular, it is orthogonal and satisfies $\mathbf{R} \mathbf{m} = \mathbf{e}_3$ by construction. \square

For all $1 \leq n \leq N$, we denote by $\mathbf{R}_n = \mathbf{R}_{\mathbf{z}_n}$ the orthogonal matrix associated with the vertex \mathbf{z}_n , i.e., it holds that $\mathbf{R}_n^{\top} \mathbf{e}_3 \in \{\pm \mathbf{m}(\mathbf{z}_n) / |\mathbf{m}(\mathbf{z}_n)|\}$. Let $\mathbf{R} \in \mathbb{R}^{3N \times 3N}$ be the orthogonal block diagonal matrix defined by

$$\mathbf{R} = \begin{pmatrix} \mathbf{R}_1 & \mathbf{0} & \cdots & \mathbf{0} \\ \mathbf{0} & \mathbf{R}_2 & \ddots & \mathbf{0} \\ \mathbf{0} & \ddots & \ddots & \mathbf{0} \\ \mathbf{0} & \cdots & \mathbf{0} & \mathbf{R}_N \end{pmatrix} \in \mathbb{R}^{3N \times 3N}.$$

By construction, the set $\{\boldsymbol{\psi}_i\}_{1 \leq i \leq 3N}$, where

$$\boldsymbol{\psi}_{3(n-1)+p} := \varphi_n \mathbf{R}_n^{\top} \mathbf{e}_p \quad \text{for all } 1 \leq n \leq N \text{ and } 1 \leq p \leq 3,$$

provides another basis of $\mathcal{S}^1(\mathcal{T}_h)^3$. Given an arbitrary $\mathbf{w}_h \in \mathcal{S}^1(\mathcal{T}_h)^3$, let $\mathbf{x} \in \mathbb{R}^{3N}$ and $\mathbf{y} \in \mathbb{R}^{3N}$ be the coordinate vectors with respect to the bases $\{\boldsymbol{\varphi}_i\}_{1 \leq i \leq 3N}$ and $\{\boldsymbol{\psi}_i\}_{1 \leq i \leq 3N}$, respectively. It holds that

$$\begin{aligned} \mathbf{w}_h &= \sum_{i=1}^{3N} y_i \boldsymbol{\psi}_i = \sum_{n=1}^N \sum_{p=1}^3 y_{3(n-1)+p} \boldsymbol{\psi}_{3(n-1)+p} = \sum_{n=1}^N \sum_{p=1}^3 y_{3(n-1)+p} \varphi_n \mathbf{R}_n^{\top} \mathbf{e}_p \\ &= \sum_{n=1}^N \varphi_n \sum_{p=1}^3 y_{3(n-1)+p} \left(\sum_{q=1}^3 (\mathbf{R}_n^{\top})_{qp} \mathbf{e}_q \right) = \sum_{n=1}^N \sum_{q=1}^3 \left(\sum_{p=1}^3 (\mathbf{R}_n^{\top})_{qp} y_{3(n-1)+p} \right) \varphi_n \mathbf{e}_q \\ &= \sum_{n=1}^N \sum_{q=1}^3 \left(\sum_{p=1}^3 (\mathbf{R}_n^{\top})_{qp} y_{3(n-1)+p} \right) \varphi_{3(n-1)+q}, \end{aligned}$$

from which it follows that

$$x_{3(n-1)+q} = \sum_{p=1}^3 (\mathbf{R}_n^{\top})_{qp} y_{3(n-1)+p} \quad \text{for all } 1 \leq n \leq N \text{ and } 1 \leq q \leq 3.$$

Owing to the block diagonal structure of \mathbf{R} , this shows that $\mathbf{x} = \mathbf{R}^{\top} \mathbf{y}$, i.e., $\mathbf{y} = \mathbf{R} \mathbf{x}$ by orthogonality. Since $\mathbf{R}_n^{\top} \mathbf{e}_3 \in \{\pm \mathbf{m}_h(\mathbf{z}_n) / |\mathbf{m}_h(\mathbf{z}_n)|\}$, by construction it holds that $\mathbf{w}_h \in \mathcal{S}^1(\mathcal{T}_h)^3$ belongs

to $\mathcal{K}_{\mathbf{m}_h}$ if and only if its coordinate vector $\mathbf{w} \in \mathbb{R}^{3N}$ with respect to the basis $\{\boldsymbol{\varphi}_i\}_{1 \leq i \leq 3N}$ satisfies $(\mathbf{R}\mathbf{w})_{3n} = 0$ for all $1 \leq n \leq N$. In particular, the subset $\{\boldsymbol{\psi}_{3(n-1)+p}\}_{1 \leq n \leq N, 1 \leq p \leq 2}$ is a basis of $\mathcal{K}_{\mathbf{m}_h}$.

Let $\mathbf{Q} \in \mathbb{R}^{2N \times 3N}$ be the matrix such that \mathbf{Q}^\top is the matrix obtained from \mathbf{R}^\top by crossing out the columns whose index is a multiple of 3, i.e.,

$$\mathbf{Q} = \begin{pmatrix} \mathbf{Q}_1 & \mathbf{0} & \cdots & \mathbf{0} \\ \mathbf{0} & \mathbf{Q}_2 & \ddots & \mathbf{0} \\ \mathbf{0} & \ddots & \ddots & \mathbf{0} \\ \mathbf{0} & \cdots & \mathbf{0} & \mathbf{Q}_N \end{pmatrix} \in \mathbb{R}^{2N \times 3N},$$

with $\mathbf{Q}_n^\top = (\mathbf{R}_n^\top \mathbf{e}_1, \mathbf{R}_n^\top \mathbf{e}_2) \in \mathbb{R}^{3 \times 2}$. By construction, the columns of \mathbf{Q}^\top are orthonormal, i.e., $\mathbf{Q}\mathbf{Q}^\top = \mathbf{I}_{2N \times 2N}$. Moreover, it holds that

$$\text{Im } \mathbf{Q}^\top = \left\{ \mathbf{x} \in \mathbb{R}^{3N} : \sum_{i=1}^{3N} x_i \boldsymbol{\varphi}_i \in \mathcal{K}_{\mathbf{m}_h} \right\}. \quad (6.5)$$

Since the matrix \mathbf{Q}_n^\top are obtained from \mathbf{R}_n^\top by crossing out the third column $\mathbf{R}_n^\top \mathbf{e}_3$, for which it holds that $\mathbf{R}_n^\top \mathbf{e}_3 \in \{\pm \mathbf{m}_h(\mathbf{z}_n)/|\mathbf{m}_h(\mathbf{z}_n)|\}$, we deduce that the matrix \mathbf{Q} and the matrix \mathbf{B} , introduced in (6.2) and used in the saddle point formulation, are related to each other by $(\text{Im } \mathbf{Q}^\top)^\perp = \text{Im } \mathbf{B}^\top$. In particular, it follows that $\text{Im } \mathbf{Q}^\top = (\text{Im } \mathbf{B}^\top)^\perp = \ker \mathbf{B}$ as well as the matrix identities

$$\mathbf{B}^\top \mathbf{B} + \mathbf{Q}^\top \mathbf{Q} = \mathbf{I}_{3N \times 3N} \quad \text{and} \quad \mathbf{B}\mathbf{Q}^\top = \mathbf{0}.$$

We deduce the matrix identity $\mathbf{P} = \mathbf{I}_{3N \times 3N} - \mathbf{B}^\top \mathbf{B} = \mathbf{Q}^\top \mathbf{Q}$.

With this geometric argument, we have constructed a basis of the discrete tangent plane, which can be used to obtain an alternative matrix formulation of (6.1). To that end, we consider the linear system

$$(\mathbf{Q}\mathbf{A}\mathbf{Q}^\top)\mathbf{u} = \mathbf{Q}\mathbf{r}. \quad (6.6)$$

In the following proposition, we establish the equivalence of (6.1) with (6.6).

Proposition 6.1.3. *There exists a unique solution $\mathbf{u} \in \mathbb{R}^{2N}$ of (6.6). The variational problem (6.1) and the linear system (6.6) are equivalent in the sense that $\mathbf{v}_h = \sum_{i=1}^{3N} v_i \boldsymbol{\varphi}_i$ solves (6.1) if and only if it holds that $\mathbf{v} = \mathbf{Q}^\top \mathbf{u}$, with $\mathbf{u} \in \mathbb{R}^{2N}$ being the unique solution of (6.6).*

Proof. Since the matrix \mathbf{A} is positive definite, it holds that

$$(\mathbf{Q}\mathbf{A}\mathbf{Q}^\top \mathbf{z}) \cdot \mathbf{z} = (\mathbf{A}\mathbf{Q}^\top \mathbf{z}) \cdot (\mathbf{Q}^\top \mathbf{z}) > 0 \quad \text{for all } \mathbf{z} \in \mathbb{R}^{2N}.$$

We deduce that also the matrix $\mathbf{Q}\mathbf{A}\mathbf{Q}^\top$ is positive definite and the linear system (6.6) thus admits a unique solution $\mathbf{u} \in \mathbb{R}^{2N}$.

To prove the second part of the statement, let $\mathbf{u} \in \mathbb{R}^{2N}$ be the unique solution of (6.6). Define $\mathbf{v} = \mathbf{Q}^\top \mathbf{u} \in \mathbb{R}^{3N}$. By (6.5), we obtain that $\mathbf{v}_h = \sum_{i=1}^{3N} v_i \boldsymbol{\varphi}_i$ belongs to $\mathcal{K}_{\mathbf{m}_h}$. Let $\mathbf{w}_h = \sum_{i=1}^{3N} w_i \boldsymbol{\varphi}_i \in \mathcal{K}_{\mathbf{m}_h}$ be arbitrary. Using again (6.5), there exists $\mathbf{z} \in \mathbb{R}^{2N}$ such that $\mathbf{w} = \mathbf{Q}^\top \mathbf{z}$. It holds that

$$\begin{aligned} a(\mathbf{m}_h; \mathbf{v}_h, \mathbf{w}_h) &= \mathbf{A}\mathbf{v} \cdot \mathbf{w} = (\mathbf{A}\mathbf{Q}^\top \mathbf{u}) \cdot (\mathbf{Q}^\top \mathbf{z}) = (\mathbf{Q}\mathbf{A}\mathbf{Q}^\top \mathbf{u}) \cdot \mathbf{z} \\ &\stackrel{(6.6)}{=} (\mathbf{Q}\mathbf{r}) \cdot \mathbf{z} = \mathbf{r} \cdot (\mathbf{Q}^\top \mathbf{z}) = \mathbf{r} \cdot \mathbf{w} = F(\mathbf{m}_h; \mathbf{w}_h). \end{aligned}$$

We conclude that $\mathbf{v}_h \in \mathcal{K}_{\mathbf{m}_h}$ solves (6.1). This concludes the proof. \square

6.1.3 Projected unconstrained formulation

The solution of the variational problem (6.1) can also be obtained from the (iterative) solution of a projected nonregular system. Consider the linear system

$$(\mathbf{P}\mathbf{A})\mathbf{v} = \mathbf{P}\mathbf{r}. \quad (6.7)$$

Here, $\mathbf{P} = \mathbf{Q}^\top \mathbf{Q} \in \mathbb{R}^{3N \times 3N}$ is the matrix associated with the orthogonal projection onto $\text{Im } \mathbf{Q}^\top$ and we have already observed that it is also the transformation matrix associated with the orthogonal projection $\mathcal{S}^1(\mathcal{T}_h)^3 \rightarrow \mathcal{K}_{\mathbf{m}_h}$. The following proposition clarifies the relation between (6.7) and the saddle point formulation (6.3).

Proposition 6.1.4. *Let $(\mathbf{v}, \boldsymbol{\lambda}) \in \mathbb{R}^{3N} \times \mathbb{R}^N$ be the unique solution of (6.3). Then, $\mathbf{v} \in \mathbb{R}^{3N}$ solves (6.7) as well as*

$$(\mathbf{P}\mathbf{A})\mathbf{v} = \mathbf{P}\mathbf{r}. \quad (6.8)$$

Conversely, let $\mathbf{v} \in \mathbb{R}^{3N}$ be a solution of (6.8). Then, there exists $\boldsymbol{\lambda} \in \mathbb{R}^N$ such that $(\mathbf{P}\mathbf{v}, \boldsymbol{\lambda}) \in \mathbb{R}^{3N} \times \mathbb{R}^N$ is the unique solution of (6.3).

Proof. Let $(\mathbf{v}, \boldsymbol{\lambda}) \in \mathbb{R}^{3N} \times \mathbb{R}^N$ be the unique solution of (6.3). Then, it holds that $\mathbf{A}\mathbf{v} + \mathbf{B}^\top \boldsymbol{\lambda} = \mathbf{r}$ and $\mathbf{B}\mathbf{v} = \mathbf{0}$. Since $\mathbf{B}\mathbf{B}^\top = \mathbf{I}_{N \times N}$, it follows that $\boldsymbol{\lambda} = \mathbf{B}\mathbf{B}^\top \boldsymbol{\lambda} = \mathbf{B}(\mathbf{r} - \mathbf{A}\mathbf{v})$. We deduce that $\mathbf{A}\mathbf{v} + \mathbf{B}^\top \mathbf{B}(\mathbf{r} - \mathbf{A}\mathbf{v}) = \mathbf{r}$. Rearranging the terms, we conclude that $(\mathbf{I}_{3N \times 3N} - \mathbf{B}^\top \mathbf{B})\mathbf{A}\mathbf{v} = (\mathbf{I}_{3N \times 3N} - \mathbf{B}^\top \mathbf{B})\mathbf{r}$. Since $\mathbf{I}_{3N \times 3N} - \mathbf{B}^\top \mathbf{B} = \mathbf{Q}^\top \mathbf{Q} = \mathbf{P}$, we obtain (6.7). Moreover, as $\mathbf{B}\mathbf{v} = \mathbf{0}$, we obtain that $\mathbf{P}\mathbf{v} = (\mathbf{I}_{3N \times 3N} - \mathbf{B}^\top \mathbf{B})\mathbf{v} = \mathbf{v}$. In particular, \mathbf{v} solves also (6.8).

Conversely, let $\mathbf{v} \in \mathbb{R}^{3N}$ be a solution of (6.8). Since $\mathbf{B}\mathbf{Q}^\top = \mathbf{0}$, it holds that $\mathbf{B}\mathbf{P}\mathbf{v} = \mathbf{B}\mathbf{Q}^\top \mathbf{Q}\mathbf{v} = \mathbf{0}$. Moreover, as $\mathbf{Q}\mathbf{Q}^\top = \mathbf{I}_{2N \times 2N}$, it holds that

$$\mathbf{Q}(\mathbf{r} - \mathbf{A}\mathbf{P}\mathbf{v}) = \mathbf{Q}\mathbf{Q}^\top \mathbf{Q}(\mathbf{r} - \mathbf{A}\mathbf{P}\mathbf{v}) = \mathbf{Q}\mathbf{P}(\mathbf{r} - \mathbf{A}\mathbf{P}\mathbf{v}) = \mathbf{Q}(\mathbf{P}\mathbf{r} - \mathbf{P}\mathbf{A}\mathbf{P}\mathbf{v}) \stackrel{(6.8)}{=} \mathbf{0}.$$

It follows that $\mathbf{r} - \mathbf{A}\mathbf{P}\mathbf{v} \in \ker \mathbf{Q} = (\text{Im } \mathbf{Q}^\top)^\perp = (\ker \mathbf{B})^\perp = \text{Im } \mathbf{B}^\top$, i.e., there exists $\boldsymbol{\lambda} \in \mathbb{R}^N$ such that $\mathbf{B}^\top \boldsymbol{\lambda} = \mathbf{r} - \mathbf{A}\mathbf{P}\mathbf{v}$. In particular, we conclude that $(\mathbf{P}\mathbf{v}, \boldsymbol{\lambda})$ is a solution of (6.3). \square

6.2 Numerical experiments

In this section, to support our theoretical findings, we present some preliminary numerical results. Deeper investigations aimed at a better understanding of the numerical performances of the tangent plane integrators analyzed in Chapter 4 appear to be necessary and will be one of the subjects of our future research.

The computations presented in this section were performed at the Institute for Analysis and Scientific Computing of TU Wien with NGS- μ MAG, a micromagnetic code mainly developed by B. STIFTNER. His invaluable assistance is thankfully acknowledged. The C++/Python code is a micromagnetic extension of the open-source finite element library NETGEN/NGSolve [178, 179, 2]. The computation of the stray field is based on the hybrid FEM-BEM method of [99] which requires the evaluation of boundary integral operators associated with the Laplace equation. This part of the code exploits the open-source Galerkin boundary element library BEM++ [192].

6.2.1 Standard vs. projection-free tangent plane schemes

For the unit cube $\Omega = (0, 1)^3$, we consider the initial boundary value problem

$$\begin{aligned} \partial_t \mathbf{m} &= -\mathbf{m} \times \mathbf{h}_{\text{eff}} + \alpha \mathbf{m} \times \partial_t \mathbf{m} && \text{in } \Omega_T, \\ \partial_n \mathbf{m} &= \mathbf{0} && \text{on } \Gamma_T, \\ \mathbf{m}(0) &= \mathbf{m}^0 && \text{in } \Omega, \end{aligned}$$

with $T = 5$ and $\alpha = 1$. The effective field includes the exchange contribution (with unit exchange length), the stray field, and a constant applied external field

$$\mathbf{h}_{\text{eff}} = \Delta \mathbf{m} + \mathbf{h}_s(\mathbf{m}) + \mathbf{f},$$

with $\mathbf{f} = (-2, -1/2, 0)^\top$. As for the initial condition, we consider the constant function defined by $\mathbf{m}^0(\mathbf{x}) = (1, 0, 0)^\top$ for all $\mathbf{x} \in \Omega$. The resulting dynamics of the magnetization is very simple and consists in a coherent rotation towards a perfect alignment with the applied external field; see Figure 6.3. This example was considered in [167] to analyze the numerical performance of an implicit-explicit extension of the midpoint scheme of [40].

For the spatial discretization, we consider a regular triangulation of Ω into 3072 tetrahedra, which corresponds to a mesh size of about $h \approx 0.2$. For the time discretization, we start with a uniform partition of the time interval into $M = 1250$ subintervals, which corresponds to an initial time-step size of $k_0 = 4 \cdot 10^{-3}$, and consider the sequence of time-step sizes obtained by halving 4 times the initial one, i.e., $k = 2^{-\ell} k_0$ with $0 \leq \ell \leq 4$. Since an analytical expression of the exact solution is not available, we use as reference solution the discrete solution obtained by two further bisections of the time-step size, i.e., $\mathbf{m}_{\text{ref}} = \mathbf{m}_{hk_{\text{ref}}}$ with $k_{\text{ref}} = 2^{-6} k_0 = 6.25 \cdot 10^{-5}$.

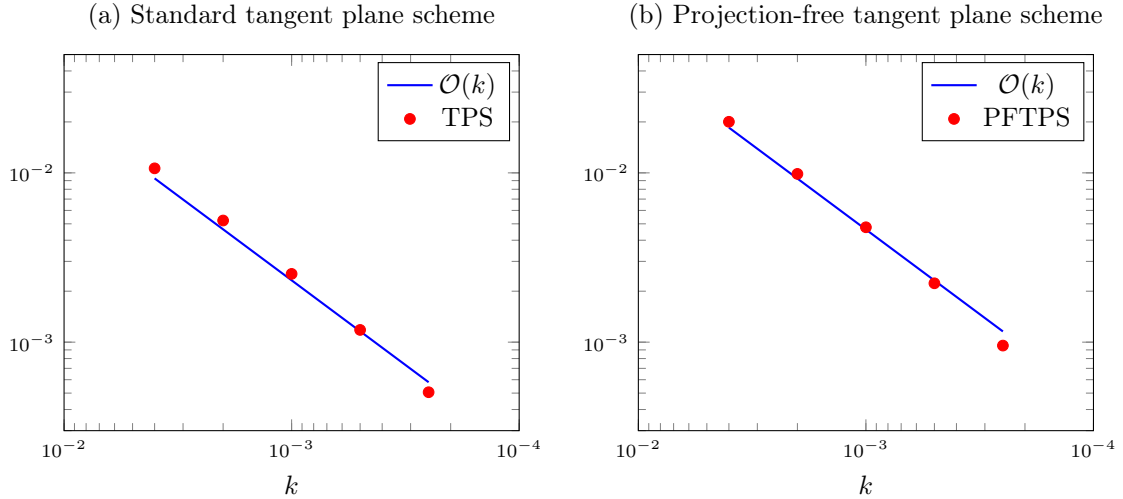


Figure 6.1: Empirical convergence rates of the tangent plane scheme ($\theta = 1$). Comparison between the standard version (a) and the projection-free version (b).

In Figure 6.1, for both the standard tangent plane scheme and its projection-free variant, we plot the computed empirical convergence rates of the error $\max_{1 \leq i \leq M} \|\mathbf{m}_h^i - \mathbf{m}_{\text{ref}}(t_i)\|_{L^2(\Omega)}$. In both cases, we observe a 1st-order convergence, which is in total agreement with the formal convergence rates predicted by the theory; see (4.11)–(4.12). As for the parameter θ , which modulates the ‘degree of implicitness’ of the method, the presented plots refer to the value $\theta = 1$, but analogous results were obtained for any other value $0 \leq \theta < 1$ that we tried.

In Figure 6.2, we numerically investigate the violation of the pointwise constraint occurring in the case of the projection-free tangent plane scheme. We compare the time evolution of the L^∞ -norm of the discrete solution for different values of the time-step size. The particular qualitative behavior of the functions depends on the model problem. We observe that, as the time-step size gets smaller, the plot of the function $t \mapsto \|\mathbf{m}_{hk}^-(t)\|_{L^\infty(\Omega)}$ is gradually closer to that of the constant function $f(t) = 1$.

6.2.2 μMAG standard problems

In order to test and compare the available micromagnetic codes, the Micromagnetic Modeling Activity Group [3], part of the Center for Theoretical and Computational Materials Science (CTCMS)

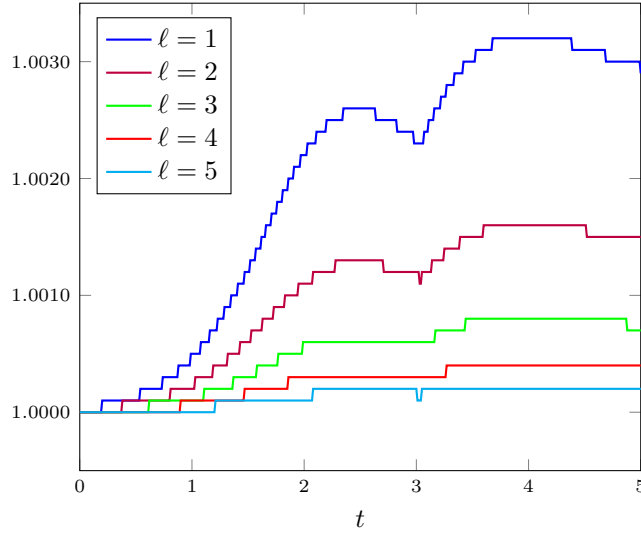


Figure 6.2: Projection-free tangent plane scheme ($\theta = 1$). Plot of the function $t \mapsto \|\mathbf{m}_{hk}^-(t)\|_{L^\infty(\Omega)}$ for different values of the time-step size $k = 2^{-\ell} k_0$, $1 \leq \ell \leq 5$.

of the National Institute of Standards and Technologies (NIST) of Gaithersburg (USA), has developed a set of 5 benchmark problems. In this section, we simulate two of the proposed problems (Standard problem #4 and Standard problem #5) and compare our results with those obtained by using OOMMF (Object-Oriented MicroMagnetic Framework), a FDM-FFT micromagnetic code developed by M. DONAHUE and D. PORTER at NIST [4, 82]. Because of the different nature of the considered methods (e.g., FEM vs. FDM for the spatial discretization, FFT vs. hybrid FEM-BEM method for the computation of the stray field, adaptive higher-order vs. uniform 1st order time-stepping), we cannot expect a perfect quantitative agreement of the simulation results. However, the comparison of the qualitative behavior of the solutions can give us some insights about the performance of our methods for the simulation of practically relevant problem sizes.

6.2.2.1 Standard problem #4

Standard problem #4, raised by R. MCMICHAEL, R. KOCH, and T. SCHREFL, and developed by J. EICKE and R. MCMICHAEL, is focused on dynamic aspects of micromagnetic computations.

The computational domain is a thin ferromagnetic film of length $L = 500$ nm, width $\ell = 125$ nm, and thickness $d = 3$ nm, aligned with the x , y , and z axes of a Cartesian coordinate system, respectively. The effective field to be considered in the Landau–Lifshitz–Gilbert equation (2.30) consists of the exchange contribution, the applied external field, and the stray field. The values of the involved material parameters mimic those of permalloy¹, i.e., $A = 1.3 \cdot 10^{-11}$ J/m for the exchange stiffness constant, $M_s = 8.0 \cdot 10^5$ A/m for the saturation magnetization, and $\alpha = 0.02$ for the Gilbert damping parameter. With these values, we obtain an exchange length of $\lambda_{\text{ex}} = 5.7$ nm. Since permalloy is a soft magnetic material, the magnetocrystalline anisotropy is negligible and therefore omitted.

The initial configuration of the magnetization is an equilibrium s-state, which can be obtained, e.g., after applying and slowly reducing a saturating field along the $(1, 1, 1)^\top$ direction to zero; see Figure 6.6(a). Then, for $t = 0$, a constant external field of magnitude $\mu_0 \mathbf{H}_{\text{ext}} = (-24.6, 4.3, 0)^\top$ mT, sufficient to reverse the magnetization of the thin film, is instantaneously applied to the initial configuration and the time evolution of the magnetization as the system moves towards the new equilibrium is analyzed; see Figure 6.6(b).

¹Permalloy is a nickel-iron magnetic alloy with about 20% iron and 80% nickel content, frequently used in magnetic storage devices.

To discretize the problem, we consider a regular partition of the computational domain into 17478 tetrahedra generated by NETGEN, which corresponds to a mesh size of about 5 nm. As for the time discretization, we consider a uniform partition of the time interval with time-step size of 0.2 ps. We compare our results, for both the standard tangent plane scheme and the projection-free version, with the simulation results obtained with OOMMF, available on the μ MAG homepage [3]. Their simulation results are based on a uniform partition of the computational domain into 187500 cubes with 1 nm edge. The time discretization employs an adaptive Runge–Kutta–Fehlberg method [83] with a maximal time-step size of 0.2 ps (thus comparable to ours).

In Figure 6.4, we show the time evolution of the three components of the spatially averaged magnetization of the sample. On the one hand, the results for the standard tangent plane scheme are in striking agreement with those of OOMMF. On the other hand, the curves obtained with the projection-free tangent plane scheme exhibit an evident offset, which becomes broader as time evolves. This can be ascribed to the omission of the nodal projection. The results for both the tangent plane integrators depicted in Figure 6.4 were obtained for the choice $\theta = 1$. Analogous results were obtained with $\theta = 1/2$. With these values for the discretization parameters, the choice $\theta = 0$ led to a completely different time evolution of the magnetization. This shows the stability issues of the explicit version of the method and underlines the necessity of the CFL condition revealed by the analysis.

6.2.2.2 Standard problem #5

Standard problem #5, a slight modification of the benchmark problem proposed in [158], aims at testing those micromagnetic solvers that include the effects of spin transfer between the magnetization and spin-polarized electric currents.

The computational domain is a rectangular magnetic film with dimensions $100 \text{ nm} \times 100 \text{ nm} \times 10 \text{ nm}$, aligned with the x , y , and z axes of a Cartesian coordinate system, with origin at the center of the film. The underlying model is the Zhang–Li extension of the LLG equation discussed in Section 2.3.3. The contributions included into the effective field and the material parameters are the same as in the previous section ($A = 1.3 \cdot 10^{-11} \text{ J/m}$, $M_s = 8.0 \cdot 10^5 \text{ A/m}$), except for the value of the Gilbert damping parameter ($\alpha = 0.1$). The magnetocrystalline anisotropy of the material is ignored also in this case.

The initial state is obtained by solving the Landau–Lifshitz–Gilbert equation (2.30) for the initial condition

$$\mathbf{m}^0(x, y, z) = \frac{(-y, x, R)^\top}{\sqrt{x^2 + y^2 + R^2}} \quad \text{with } R = 10 \text{ nm},$$

until the magnetization reaches the equilibrium configuration; see Figure 6.7(a). The resulting state is a magnetization vortex pattern. Then, for $t = 0$, a constant polarized electric current with associated spin velocity vector $\mathbf{v} = (-72.12, 0, 0)^\top \text{ A/m}$ is applied. The governing equation is the extended LLG equation (2.51), with ratio of adiabaticity set to $\xi = 0.05$. The time evolution of the magnetization as the system moves towards the new equilibrium is analyzed; see Figure 6.7(b).

To discretize the problem with the tangent plane scheme, we consider a tetrahedral triangulation of the computational domain into 25666 tetrahedra, which corresponds to a mesh size of about 5 nm. For the time discretization, we employ a uniform partition of the time interval with time-step size of 0.2 ps (40000 time-steps). Again, we compare our results with those obtained by OOMMF. The simulation results downloadable from the μ MAG homepage [3] refer to a uniform partition of the computational domain into 12500 cubes with 2 nm edge and 42350 adaptive time-steps.

In Figure 6.5, we show the time evolution of the first two components of the spatially averaged magnetization of the sample. The qualitative behavior of the time evolution of the magnetization is in agreement with the one simulated with OOMMF. For this problem, the difference between the standard tangent plane scheme and the projection-free version is not significant.

For the physical validation of our algorithms for the spin diffusion model (see Section 2.3.2 and Section 5.1) and the self-consistent model (see Section 2.3.4 and Section 5.2.4), we refer to our papers [7, 174, 8].

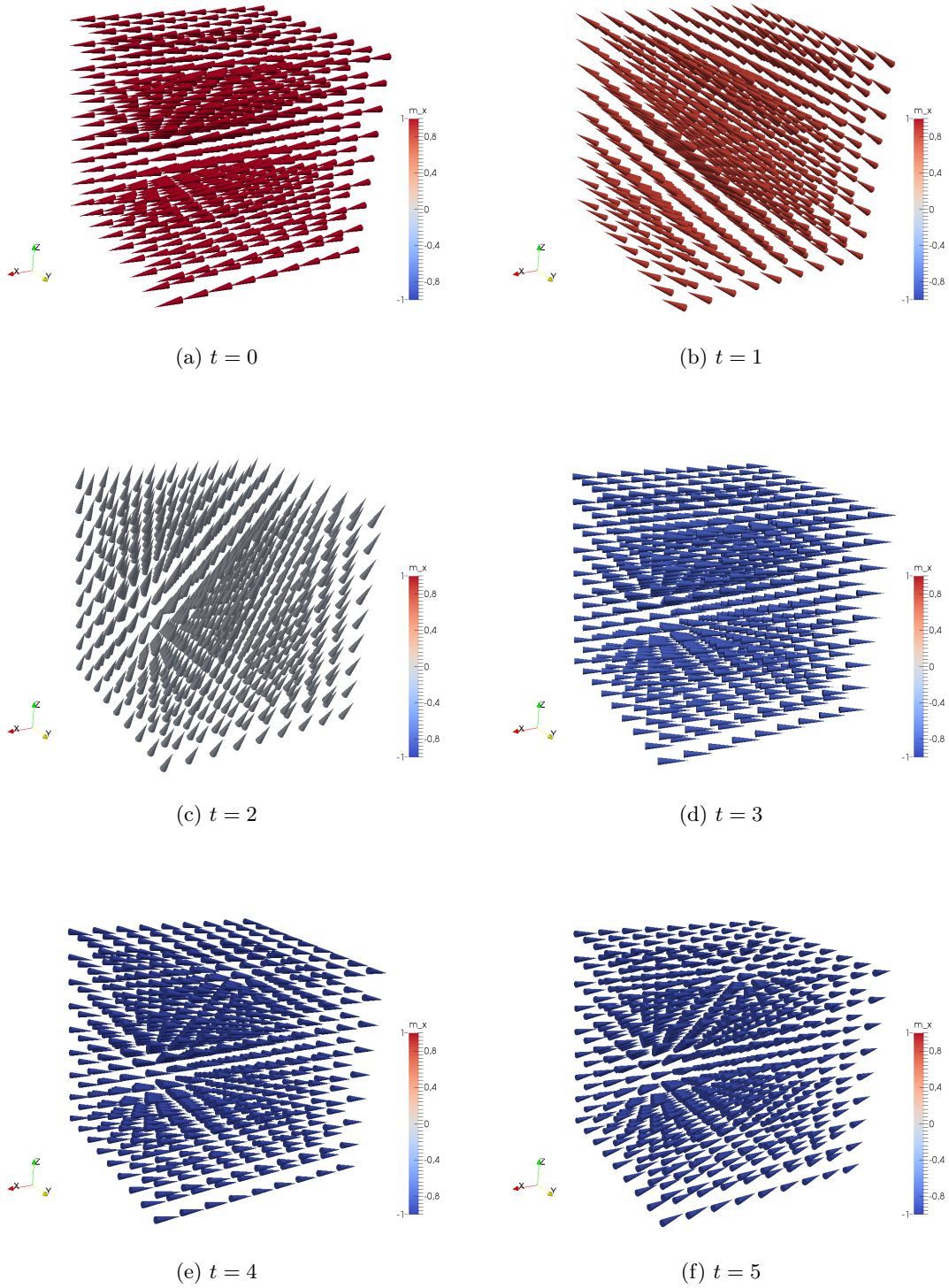


Figure 6.3: Snapshots of the magnetization dynamics for the model problem considered in Section 6.2.1.

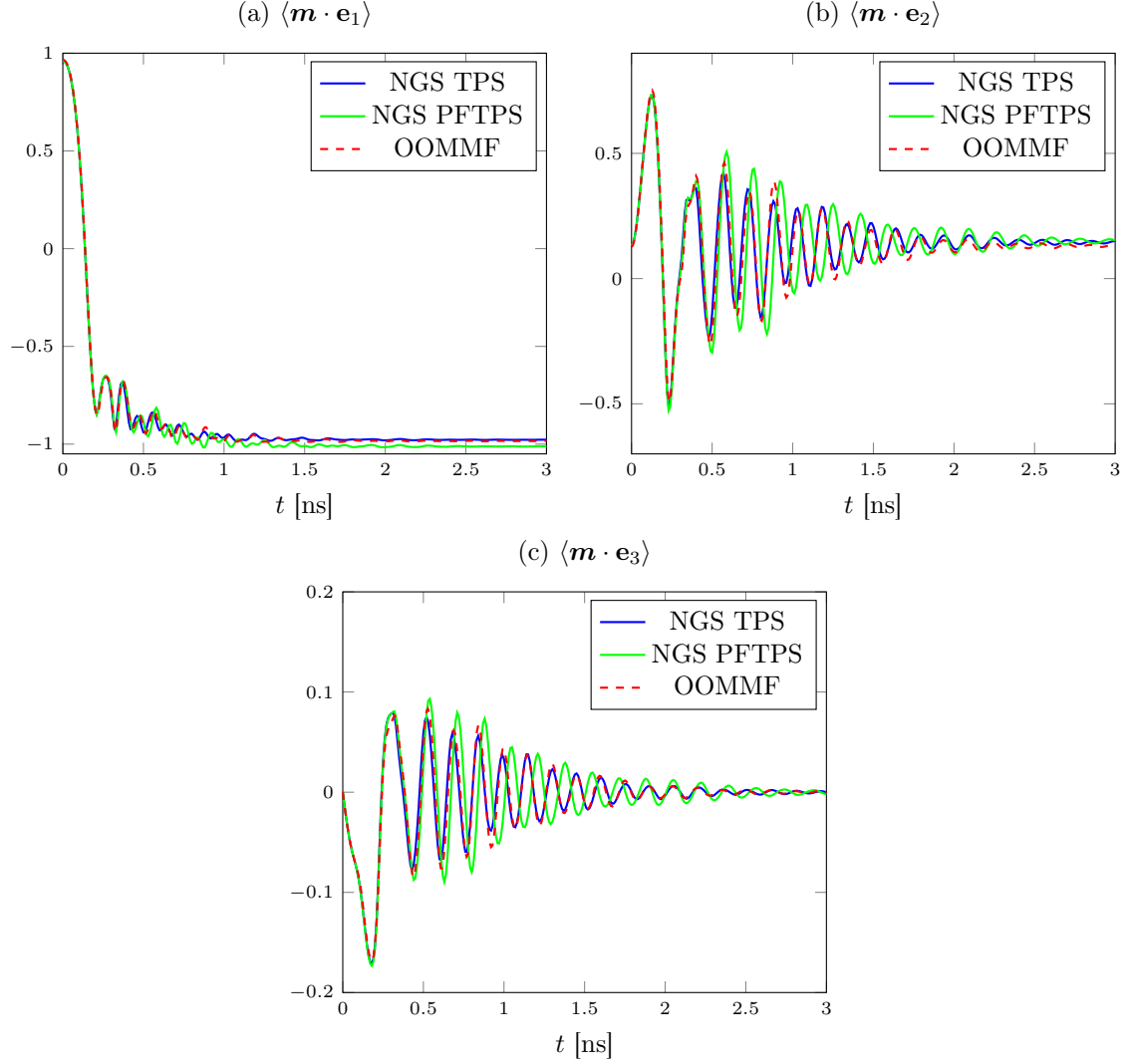


Figure 6.4: μ MAG standard problem #4. Time evolution of the three components of the spatially averaged magnetization of the sample, i.e., $\langle \mathbf{m}(t) \cdot \mathbf{e}_i \rangle = \frac{1}{N} \sum_{n=1}^N \mathbf{m}(\mathbf{z}_n, t) \cdot \mathbf{e}_i$ for $1 \leq i \leq 3$. Comparison of the results obtained with the standard tangent plane scheme (TPS), the projection-free tangent plane scheme (PFTPS), both implemented in NETGEN/NGSolve, and with OOMMF.

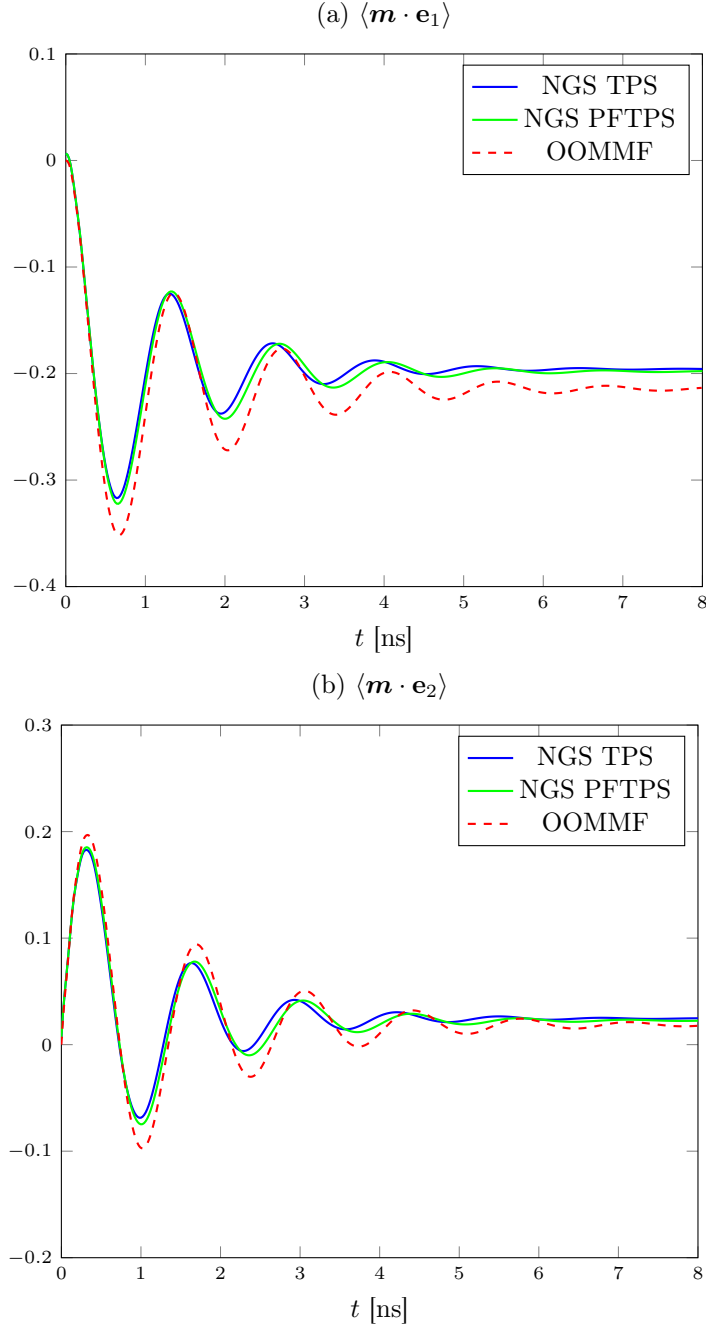
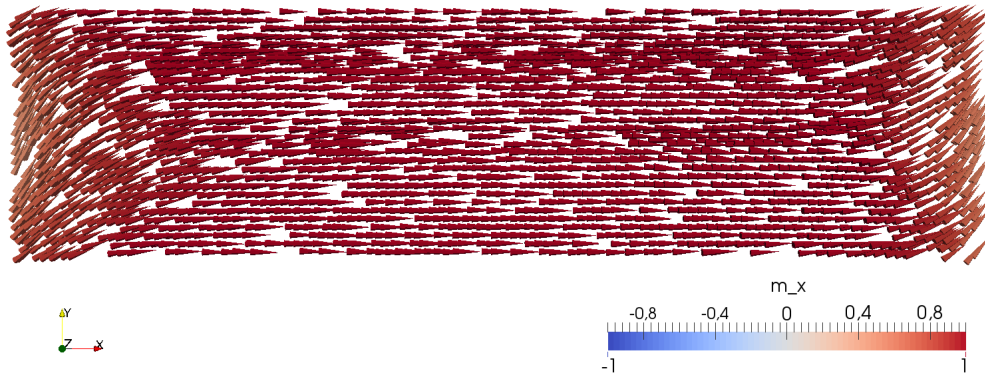
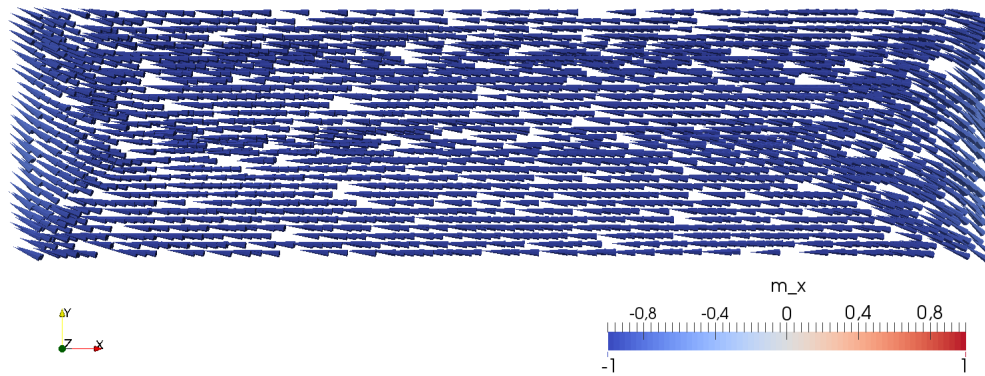


Figure 6.5: μ MAG standard problem #5. Time evolution of the first two components of the spatially averaged magnetization of the sample, i.e., $\langle \mathbf{m}(t) \cdot \mathbf{e}_i \rangle = \frac{1}{N} \sum_{n=1}^N \mathbf{m}(\mathbf{z}_n, t) \cdot \mathbf{e}_i$ for $1 \leq i \leq 2$. Comparison of the results obtained with the standard tangent plane scheme (TPS), the projection-free tangent plane scheme (PFTPS), both implemented in NETGEN/NGSolve, and with OOMMF.

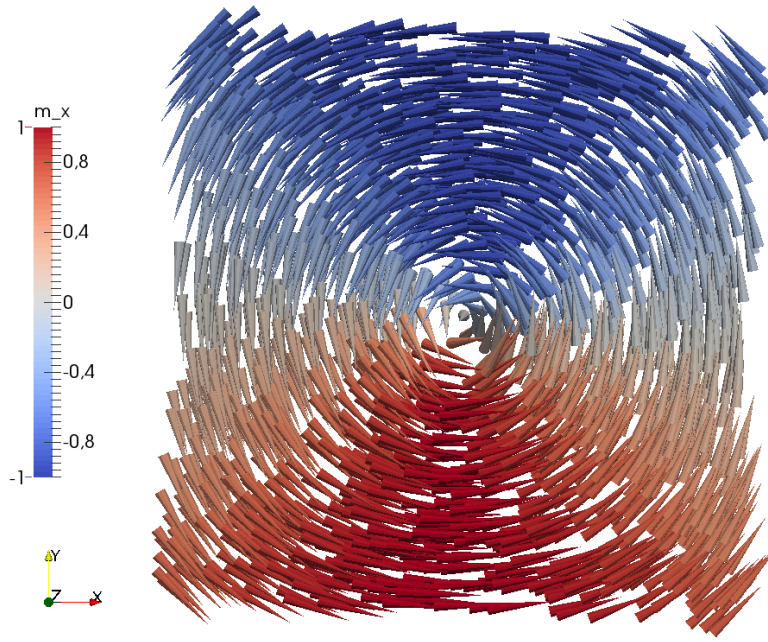


(a) Initial s-state at $t = 0$ ns.

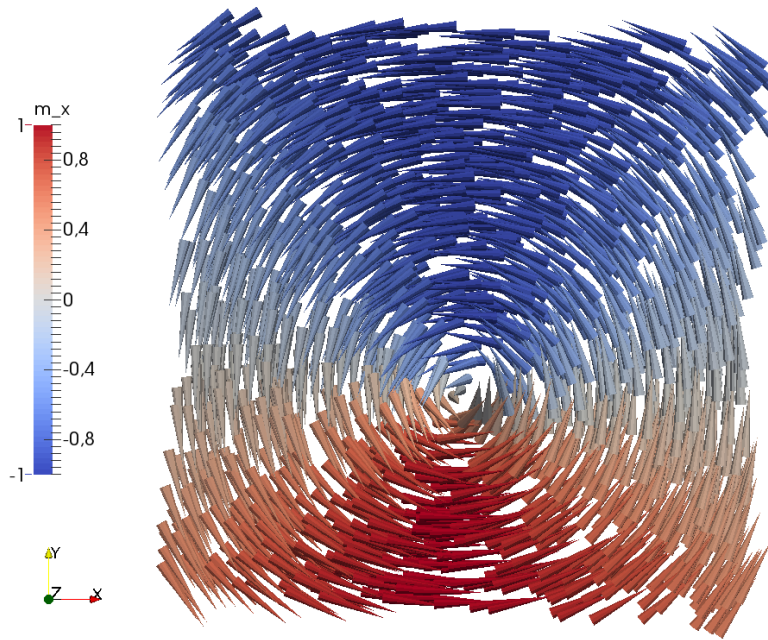


(b) Final equilibrium state at $t = 3$ ns.

Figure 6.6: Snapshots of the magnetization dynamics for μ MAG standard problem #4.



(a) Initial vortex state at $t = 0$ ns.



(b) Final equilibrium state at $t = 8$ ns.

Figure 6.7: Snapshots of the magnetization dynamics for μ MAG standard problem #5.

Chapter 7

Perspectives and future work

With this dissertation, we have tried to contribute to the study of reliable and effective numerical methods for the simulation of time-dependent micromagnetic phenomena. The main focus of our work has been on the development of (unconditionally) convergent integrators which are suitable for the efficient treatment of coupled systems of PDEs, in which the LLG equation is coupled with another equation that models a particular nonlocal effective field contribution. However, there are a number of possible extensions and improvements of the presented results, related interesting questions, and open problems that, in our opinion, are worth to be investigated. In this chapter, we aim to give a short outlook of some of them.

- **Numerical analysis of tangent plane integrators**

In Chapter 4, we have provided a unified analysis of the tangent plane scheme which combines and extends the results of the original papers [14, 39, 12, 16, 56, 6]. Future work will address some of the aspects not covered by the present dissertation, such as the derivation of a priori error estimates (recently proved in [93] for the projection-free variant of the scheme of [6], but still open for the standard version of the method) and a posteriori error estimates, which will be the starting point for the development of adaptive algorithms for the LLG equation. Preliminary results in this direction can be found, e.g., in [22, 23].

One difficult task concerns the development of higher-order methods in both time and space. State-of-the-art numerical integrators for the LLG equation used in computational physics are usually based on higher-order black-box adaptive time discretizations; see, e.g., [194]. An (almost) 2nd order version in time of the tangent plane scheme was introduced in [16, 15]. However, the proposed strategy is based on an implicit treatment of the lower-order effective field terms (including the nonlocal and expensive-to-compute stray field), which is not fully attractive from the computational point of view, as, in particular, it breaks the linearity of the scheme in the presence of nonlinear field contributions. Extensions to higher-order methods in space would also be of great interest. In this context, the main difficulties stem from the nonconvex pointwise constraint. For instance, to our knowledge, it is not clear if the result of Proposition 3.4.11, i.e., the fact that the nodal projection mapping does not increase the Dirichlet energy of piecewise linear polynomials for weakly acute triangulations, can be transferred to higher-order polynomials.

Moreover, practically relevant problem sizes require efficient iterative solvers for the involved linear systems. Together with D. PRAETORIUS and B. STIFTNER, we are currently analyzing the preconditioning for the solution strategies presented in Section 6.1; see [168]. The goal is to avoid the recomputation of the preconditioners in each time step of the time-marching scheme, which should be possible as long as the time discretization is sufficiently fine so that the magnetization does not change too rapidly.

- **Numerical analysis of the midpoint scheme of [40]**

Together with D. PRAETORIUS, and B. STIFTNER, we are investigating some open questions related to the midpoint scheme of [40]. We have recently shown that an implicit-explicit approach for the

effective field contributions can simultaneously mitigate the computational cost and preserve the formal 2nd order time convergence of the method [167]. Future work will address the development of efficient solution strategies for the nonlinear system of algebraic equations resulting from the method as well as the analysis of numerically decoupled time-marching schemes for coupled LLG-systems.

- **Numerical simulation of magnetic skyrmions**

The Dzyaloshinskii–Moriya (DM) interaction (page 13) is the most important ingredient for the enucleation and the stabilization of the class of soliton vortex-like structures that are usually referred to as magnetic skyrmions [157, 173, 175, 200, 127]. In the mathematical literature, the existence of isolated skyrmions emerging as energy minimizers of a simplified two-dimensional micromagnetic model was analyzed by C. MELCHER in [150]. Together with G. HRKAC, D. PRAETORIUS, and B. STIFTNER, we are currently investigating the extension of the tangent plane integrator, subject of this dissertation, and the midpoint scheme of [40] for the simulation of the LLG-driven dynamics of magnetic skyrmions [116]. Considering the DM interaction entails the modification of the boundary conditions for the LLG equation (see Remark 4.1.2), which in turn requires to adapt both the variational formulation (4.4) included in the definition of a weak solution (Definition 4.1.1) and the numerical algorithm by including a boundary term, for which a careful analysis is needed.

- **Stochastic Landau–Lifshitz–Gilbert equation and Landau–Lifshitz–Bloch equation**

In Section 1.1, as a motivation for our work, we have described how the spintronic extensions of the micromagnetic theory can be applied to the development of more performing recording devices. Another approach to simultaneously improve the competing requirements of high storage density, writeability, and thermal stability (the so-called magnetic recording trilemma [172]) is based on a technique usually referred to as heat-assisted magnetic recording (HAMR). In HAMR, during the writing process, the recording device is locally heated by a small laser, which reduces the coercivity of the medium and allows the recording head to write the data [146, 89, 195, 205].

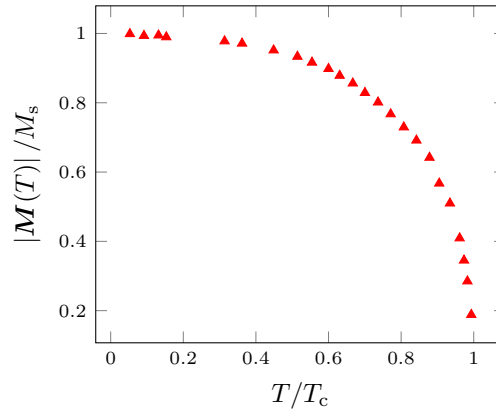


Figure 7.1: Spontaneous magnetization of nickel as a function of temperature. Experimental values by P. WEISS and R. FORRER [208].

The mathematical modeling of such processes is beyond the possibilities of the classical theory of micromagnetics, whose key hypothesis, the saturation assumption (2.8), is plausible only if the temperature is constant and far below the so-called Curie temperature T_c of the ferromagnetic material. Indeed, the spontaneous magnetization depends on many factors, e.g., the nature of the atoms and the crystal structure of the material (which determine how ‘strong’ and how ‘dense’ the magnetic moments are, respectively), but it is mostly affected by the temperature, since thermal fluctuations of the atoms represent an obstacle for the alignment of the magnetic moments.

Figure 7.1 shows the typical behavior of the spontaneous magnetization as a function of temperature in a ferromagnetic material. The spontaneous magnetization decreases if the temperature increases. Moreover, when the temperature reaches the Curie temperature of the material, the impact of the thermal fluctuations prevails over all the other effects, leading to total disorder, and thus zero spontaneous magnetization.

In order to model these phenomena, two main strategies have been proposed. On the one hand, the random fluctuation of the magnetization associated with the thermal agitation of the magnetic moments can be included into the model by adding a (stochastic) noise term to the effective field. This ‘thermal fluctuation field’, usually assumed to be uncorrelated in space and time, is characterized by zero mean and variance proportional to the temperature [55]. In the mathematical literature, different forms of the stochastic LLG equation have been considered from both the analytical [126, 59, 160, 60] and the numerical point of view. In particular, both the tangent plane scheme, subject of the present thesis, and the midpoint scheme [40] have been extended to stochastic forms of the LLG equation; see [13, 112] and [27, 25], respectively.

On the other hand, an alternative approach for nonzero-temperature micromagnetics consists in the study of extended macroscopic forms of the LLG equation which allow for longitudinal variations of the magnetization field. The papers [30, 31] extended the LLG equation by a term which can be tuned in order to prescribe a given temperature law for the modulus of the magnetization (which, in practical situations, will be chosen in order to fit the experimental data, e.g., those depicted in Figure 7.1). The equation is discretized by an extended version of the midpoint scheme of [40]. Another approach, very popular in the physical literature, is based on the derivation of the Fokker–Planck equation satisfied by the probability density function associated with the stochastic LLG equation [100]. The resulting equation, usually referred to as Landau–Lifshitz–Bloch (LLB) equation, is similar to the one considered in [30, 31], except from the fact that the term associated with the longitudinal variation of the magnetization is nonlinear. Preliminary analytical results for a simplified version of the LLB equation can be found in the recent paper [140].

In the frame of the project *Thermally controlled magnetization dynamics*, supported by the Vienna Science and Technology Fund (WWTF) under grant MA14-44, we are planning to address the development of numerical methods for nonzero-temperature micromagnetics. In particular, we aim to consider the coupling and the numerical integration of the LLB equation. As a first attempt, we will try to extend the midpoint scheme of [40].

- **Extension of the results to further models in metal spintronics**

In this dissertation we have considered several spintronic extensions of the micromagnetic theory. Together with C. ABERT, D. PRAETORIUS, and D. SUESS, we are planning to continue the work in this direction and to address the numerical integration of other LLG-based models in metal spintronics. Among others, we mention the mean field model of [66, 67], the unified drift-diffusion theory of [163], or models which extend LLG equation by torque terms originated by spin-orbit coupling effects, such as the spin Hall effect [85, 197, 91] and the Rashba effect [153, 144].

- **Numerical integration of LLG-based models in semiconductor spintronics**

The spintronic extensions of the micromagnetic theory considered throughout this work (see Section 2.3) can be classified into the field of metal spintronics. This is clear if one considers the phenomenological expression of the electric current density provided in (2.42), i.e.,

$$\mathbf{J}_e = \sigma \mathbf{E} - \beta' \frac{e}{\mu_B} D_0 \nabla \mathbf{s}^\top \mathbf{m}.$$

In the case of no-polarization, i.e., $\beta' = 0$, this reduces to the Ohm law (2.9c), which is appropriate for metallic conductors, in which the charge density is essentially constant, but not reasonable for semiconductors.

Together with A. JÜNGEL and D. PRAETORIUS, we are planning to investigate the extensions of the micromagnetic model for semiconductor spintronics, which, to our knowledge, is an open problem from both the modeling and the numerical point of view. A possible starting point is given

by the spinorial matrix drift-diffusion model of [165], analyzed in [121], and discretized by a finite volume method in the two-dimensional case in [64]. In the model, which consists of a nonlinear system of drift-diffusion equations for the charge density and the spin density that is further coupled to the electrostatic Maxwell equations for the electric potential, the magnetization is assumed to be constant. We will remove this assumption and start by considering the finite element discretization of the coupling of this system with the LLG equation, for which some preliminary analytical results are already available [210, 211]. We believe that our approach, based on the numerical decoupling of the time integration of the LLG equation and the coupled system, can be an effective tool for the treatment of the strong nonlinearities which characterize the problem.

Appendix A

Physical quantities, constants and units

For the convenience of the reader, in this appendix we collect the physical quantities and the physical constants considered throughout the thesis. We use physical units in the International System of Units (SI).

A.1 Physical quantities

Quantity	Symbol	Unit
Angular momentum	\mathbf{L}	J s
Anisotropy constant	K	J/m ³
Bloch parameter	δ_0	m
Bloch wall width	δ	m
Conductivity	σ, σ	A/(m V)
Curie temperature	T_c	K
Diffusion coefficient	D_0	m ² /s
Displacement	\mathbf{u}	m
DM constant	D	J/m ²
Electric charge density	ρ	C/m ³
Electric current density	\mathbf{J}_e, J_e	A/m ²
Electric displacement field	\mathbf{D}	C/m ²
Electric field	\mathbf{E}	V/m
Electric permittivity	ϵ, ϵ	F/m
Electric potential	V	V
Energy	\mathcal{E}	J
Exchange integral	J	J
Exchange length	λ_{ex}	m
Exchange stiffness constant	A	J/m
Gilbert damping parameter	α	–
Magnetic field	\mathbf{H}	A/m
Magnetic flux density	\mathbf{B}	T
Magnetic hardness parameter	q	–
Magnetic moment	$\boldsymbol{\mu}$	J/T
Magnetic permeability	μ	N/A ²
Magnetization	\mathbf{M}	A/m
Magnetization (normalized)	\mathbf{m}	–

Quantity	Symbol	Unit
Magnetostatic energy density	K_s	J/m ³
Magnetostatic potential	u	A
Mass density	κ	kg/m ³
Polarization parameters	β, β', P	–
Poynting vector	\mathbf{S}	W/m ²
Ratio of nonadiabacity	ξ	–
Saturation magnetization	M_s	A/m
Spin accumulation	s	A/m
Spin current density	\mathbf{J}_s	A/s
Spin diffusion length	λ_{sd}	m
Spin-flip relaxation time	τ_{sf}	s
Spin velocity vector	\mathbf{u}, \mathbf{v}	m/s
Stiffness tensor	\mathbf{C}	Pa
Strain tensor	$\boldsymbol{\varepsilon}$	–
Stress tensor	$\boldsymbol{\sigma}$	Pa
STT characteristic time	τ_J	s
Temperature	T	K
Torque	$\boldsymbol{\tau}$	J
Zhang–Li parameters	b_J, b_ξ	m ³ /C

A.2 Physical constants

Physical constant	Symbol	Value & Unit	Note
Bohr magneton	μ_B	$9.274\,009\,68 \cdot 10^{-24}$ A m ²	$\mu_B = e\hbar/(2m_e)$
Density of states at Fermi level	N_0	$1/(\text{J m}^3)$	$\sigma = e^2 N_0 D_0$
Electric charge of the electron	e	$1.602\,176\,620\,8 \cdot 10^{-19}$ A s	–
g-factor (of the electron)	g_e	2.0023193043617	–
Gyromagnetic ratio	γ	$-1.760\,859\,708 \cdot 10^{11}$ rad/(s T)	$\gamma = -g_e \mu_B / \hbar$
Mass of the electron	m_e	$9.109\,383\,56 \cdot 10^{-31}$ kg	–
Reduced Planck constant	\hbar	$1.054\,571\,800 \cdot 10^{-34}$ J s	–
Rescaled gyromagnetic ratio	γ_0	$2.212\,761\,569 \cdot 10^5$ m/(A s)	$\gamma_0 = -\gamma \mu_0$
Vacuum permeability	μ_0	$4\pi \cdot 10^{-7}$ N/A ²	–
Vacuum permittivity	ε_0	$8.854\,187\,817\,620 \cdot 10^{-12}$ F/m	–

Appendix B

Auxiliary results

The aim of this appendix is twofold: On the one hand, we define the notation used throughout the thesis. On the other hand, we recall several definitions and auxiliary results (in most cases omitting the proof).

B.1 Linear algebra

For the sake of simplicity, most of the forthcoming definitions and results are stated within the three-dimensional case, e.g., for vectors in \mathbb{R}^3 and matrices in $\mathbb{R}^{3 \times 3}$. Unless stated otherwise, all the vectors are column vectors.

Let $\mathbf{a}, \mathbf{b} \in \mathbb{R}^3$ be two vectors.

- The scalar product (or inner product) $\mathbf{a} \cdot \mathbf{b} \in \mathbb{R}$ is defined by

$$\mathbf{a} \cdot \mathbf{b} = \sum_{i=1}^3 a_i b_i.$$

- The vector product (or cross product) $\mathbf{a} \times \mathbf{b}$ is defined by

$$\mathbf{a} \times \mathbf{b} = (a_2 b_3 - a_3 b_2, a_3 b_1 - a_1 b_3, a_1 b_2 - a_2 b_1)^\top.$$

- The tensor product (or outer product) $\mathbf{a} \otimes \mathbf{b} \in \mathbb{R}^{3 \times 3}$ is defined by

$$(\mathbf{a} \otimes \mathbf{b})_{ij} = a_i b_j \quad \text{for all } 1 \leq i, j \leq 3.$$

Let $\mathbf{A}, \mathbf{B} \in \mathbb{R}^{3 \times 3}$ be two matrices.

- The Frobenius product $\mathbf{A} : \mathbf{B} \in \mathbb{R}$ is defined by

$$\mathbf{A} : \mathbf{B} = \sum_{i,j=1}^3 a_{ij} b_{ij}.$$

Let $\mathbf{A} \in \mathbb{R}^{m \times n}$ and $\mathbf{B} \in \mathbb{R}^{n \times p}$ be two matrices, and let $\mathbf{x} \in \mathbb{R}^n$ be a vector.

- The matrix-vector product $\mathbf{Ax} \in \mathbb{R}^m$ is defined by

$$(\mathbf{Ax})_i = \sum_{j=1}^n a_{ij} x_j \quad \text{for all } 1 \leq i \leq m.$$

- The matrix-matrix product $\mathbf{AB} \in \mathbb{R}^{m \times p}$ is defined by

$$(\mathbf{AB})_{ij} = \sum_{k=1}^n a_{ik} b_{kj} \quad \text{for all } 1 \leq i \leq m, 1 \leq j \leq p.$$

Let $\mathbf{A} \in \mathbb{R}^{m \times n}$ and $\mathbf{B} \in \mathbb{R}^{p \times q}$ be two matrices.

- The Kronecker product $\mathbf{A} \otimes \mathbf{B} \in \mathbb{R}^{mp \times nq}$ is the block matrix defined by

$$\mathbf{A} \otimes \mathbf{B} = \begin{pmatrix} a_{11}\mathbf{B} & \cdots & a_{1n}\mathbf{B} \\ \vdots & & \vdots \\ a_{m1}\mathbf{B} & \cdots & a_{mn}\mathbf{B} \end{pmatrix}.$$

Let $\boldsymbol{\lambda} = (\lambda_{ijkl})_{1 \leq i,j,k,\ell \leq 3}$ be a three-dimensional 4th order tensor.

- For a matrix $\mathbf{B} \in \mathbb{R}^{3 \times 3}$, the tensor-matrix product $\boldsymbol{\lambda}\mathbf{B} \in \mathbb{R}^{3 \times 3}$ is the matrix defined by

$$(\boldsymbol{\lambda}\mathbf{B})_{ij} = \sum_{k,\ell=1}^3 \lambda_{ijk\ell} B_{k\ell} \quad \text{for all } 1 \leq i, j \leq 3.$$

We denote by $|\cdot|$ both the Euclidean norm of a vector and Frobenius norm of a matrix, which are defined by $|\mathbf{a}| = \sqrt{\mathbf{a} \cdot \mathbf{a}}$ and $|\mathbf{A}| = \sqrt{\mathbf{A} : \mathbf{A}}$ for any vector $\mathbf{a} \in \mathbb{R}^n$ and any matrix $\mathbf{A} \in \mathbb{R}^{n \times n}$ ($n \geq 1$), respectively. This does not lead to ambiguities, since the meaning is clear from the argument. The above norms satisfy the following properties

$$|\mathbf{a} \cdot \mathbf{b}| \leq |\mathbf{a}| |\mathbf{b}|, \quad |\mathbf{a} \times \mathbf{b}| \leq |\mathbf{a}| |\mathbf{b}|, \quad |\mathbf{a} \otimes \mathbf{b}| = |\mathbf{a}| |\mathbf{b}| \quad \text{for all } \mathbf{a}, \mathbf{b} \in \mathbb{R}^3,$$

$$|\mathbf{A} : \mathbf{B}| \leq |\mathbf{A}| |\mathbf{B}| \quad \text{for all } \mathbf{A}, \mathbf{B} \in \mathbb{R}^{3 \times 3},$$

$$|\mathbf{A}\mathbf{x}| \leq |\mathbf{A}| |\mathbf{x}|, \quad |\mathbf{AB}| \leq |\mathbf{A}| |\mathbf{B}|, \quad |\mathbf{A} \otimes \mathbf{B}| = |\mathbf{A}| |\mathbf{B}| \quad \text{for all } \mathbf{A}, \mathbf{B} \in \mathbb{R}^{3 \times 3} \text{ and } \mathbf{x} \in \mathbb{R}^3.$$

A three-dimensional 4th order tensor $\boldsymbol{\lambda}$ is called symmetric if $\lambda_{ijkl} = \lambda_{jikl} = \lambda_{ijlk} = \lambda_{klij}$ for all $1 \leq i, j, k, \ell \leq 3$. We call $\boldsymbol{\lambda}$ positive definite if there exists $\lambda_* > 0$ such that $(\boldsymbol{\lambda}\mathbf{B}) : \mathbf{B} \geq \lambda_* |\mathbf{B}|^2$ for all $\mathbf{B} \in \mathbb{R}^{3 \times 3}$.

B.2 Useful (in)equalities

In the following proposition, we collect some useful vector identities involving the vector product.

Proposition B.2.1. *For all $\mathbf{a}, \mathbf{b}, \mathbf{c}, \mathbf{d} \in \mathbb{R}^3$, we have the following identities:*

- (i) $\mathbf{a} \times \mathbf{a} = \mathbf{0}$,
- (ii) $\mathbf{a} \times \mathbf{b} = -\mathbf{b} \times \mathbf{a}$,
- (iii) $(\mathbf{a} \times \mathbf{b}) \cdot \mathbf{a} = 0$,
- (iv) $(\mathbf{a} \times \mathbf{b}) \cdot \mathbf{c} = (\mathbf{c} \times \mathbf{a}) \cdot \mathbf{b} = (\mathbf{b} \times \mathbf{c}) \cdot \mathbf{a}$,
- (v) $\mathbf{a} \times (\mathbf{b} \times \mathbf{c}) + \mathbf{c} \times (\mathbf{a} \times \mathbf{b}) + \mathbf{b} \times (\mathbf{c} \times \mathbf{a}) = \mathbf{0}$ (*Jacobi identity*),
- (vi) $\mathbf{a} \times (\mathbf{b} \times \mathbf{c}) = (\mathbf{a} \cdot \mathbf{c})\mathbf{b} - (\mathbf{a} \cdot \mathbf{b})\mathbf{c}$ (*triple product expansion formula*),
- (vii) $(\mathbf{a} \times \mathbf{b}) \cdot (\mathbf{c} \times \mathbf{d}) = (\mathbf{a} \cdot \mathbf{c})(\mathbf{b} \cdot \mathbf{d}) - (\mathbf{a} \cdot \mathbf{d})(\mathbf{b} \cdot \mathbf{c})$ (*Lagrange identity*).

The Lagrange identity (vii) is the three-dimensional case of the more general Binet-Cauchy equality.

The following well-known inequality is sometimes called the *Peter-Paul inequality*. This name refers to the fact that a sharper estimate of the first term is achieved at the cost of losing some control of the second term. One must ‘rob Peter to pay Paul’.

Lemma B.2.2 (weighted Young's inequality). *For all $a, b \in \mathbb{R}$ and $\delta > 0$, it holds that*

$$ab \leq \frac{\delta}{2}a^2 + \frac{1}{2\delta}b^2.$$

Proof. Since $2xy \leq x^2 + y^2$ for all $x, y \in \mathbb{R}$, it follows that

$$ab \leq (\sqrt{\delta}a) \left(\frac{1}{\sqrt{\delta}}b \right) \leq \frac{\delta}{2}a^2 + \frac{1}{2\delta}b^2,$$

which is the requested inequality. \square

The following lemma states a simple algebraic trick which often simplifies the computation and the estimation of sums. It is named after N. H. ABEL.

Lemma B.2.3 (Abel's summation by parts). *Given an integer $j \geq 1$, let $\{\mathbf{a}_i\}_{0 \leq i \leq j} \subset \mathbb{R}^n$. Then, it holds that*

$$\sum_{i=0}^{j-1} (\mathbf{a}_{i+1} - \mathbf{a}_i) \cdot \mathbf{a}_{i+1} = \frac{1}{2} |\mathbf{a}_j|^2 - \frac{1}{2} |\mathbf{a}_0|^2 + \frac{1}{2} \sum_{i=0}^{j-1} |\mathbf{a}_{i+1} - \mathbf{a}_i|^2.$$

Proof. Let $0 \leq i \leq j-1$. It holds that

$$\begin{aligned} 2(\mathbf{a}_{i+1} - \mathbf{a}_i) \cdot \mathbf{a}_{i+1} &= |\mathbf{a}_{i+1}|^2 - \mathbf{a}_{i+1} \cdot \mathbf{a}_i + (\mathbf{a}_{i+1} - \mathbf{a}_i) \cdot \mathbf{a}_{i+1} \\ &= |\mathbf{a}_{i+1}|^2 - \mathbf{a}_{i+1} \cdot \mathbf{a}_i + (\mathbf{a}_{i+1} - \mathbf{a}_i) \cdot \mathbf{a}_{i+1} - |\mathbf{a}_i|^2 + |\mathbf{a}_i|^2 \\ &= |\mathbf{a}_{i+1}|^2 - |\mathbf{a}_i|^2 + (\mathbf{a}_{i+1} - \mathbf{a}_i) \cdot \mathbf{a}_{i+1} - (\mathbf{a}_{i+1} - \mathbf{a}_i) \cdot \mathbf{a}_i \\ &= |\mathbf{a}_{i+1}|^2 - |\mathbf{a}_i|^2 + |\mathbf{a}_{i+1} - \mathbf{a}_i|^2. \end{aligned}$$

Summation over $0 \leq i \leq j-1$ yields the assertion. \square

The following lemma is a discrete counterpart of Gronwall's inequality (also called Gronwall's lemma or Gronwall-Bellman inequality), an important tool to derive estimates in the theory of ordinary differential equations. The differential form of the result was proved by T. H. GRONWALL in 1919.

Lemma B.2.4 (discrete Gronwall lemma). *Let $\{\alpha_j\}_{j \geq 0}$, $\{\beta_j\}_{j \geq 0}$, and $\{w_j\}_{j \geq 0}$ be sequences of real numbers such that*

$$\alpha_j \leq \alpha_{j+1}, \quad \beta_j \geq 0, \quad \text{and} \quad w_j \leq \alpha_j + \sum_{i=0}^{j-1} \beta_i w_i \quad \text{for all } j \geq 0.$$

Then, it holds that

$$w_j \leq \alpha_j \exp \sum_{i=0}^{j-1} \beta_i \quad \text{for all } j \geq 0.$$

For the proof, we refer the interested reader to [199, Lemma 10.5].

B.3 Vector calculus

Let $\Omega \subset \mathbb{R}^3$ be an open set. The gradient of a scalar-valued function $f : \Omega \rightarrow \mathbb{R}$ is denoted by $\nabla f = (\partial_1 f, \partial_2 f, \partial_3 f)^\top$. For a vector-valued function $\mathbf{f} = (f_1, f_2, f_3)^\top : \Omega \rightarrow \mathbb{R}^3$, we denote the Jacobian by $\nabla \mathbf{f}$, i.e., $(\nabla \mathbf{f})_{ij} = \partial_j f_i$ for all $1 \leq i, j \leq 3$, the divergence by $\nabla \cdot \mathbf{f}$, and the curl by $\nabla \times \mathbf{f}$. The Laplace operator of f is denoted by $\Delta f = \nabla \cdot (\nabla f)$. We define the divergence $\nabla \cdot \mathbf{F}$ of a matrix-valued function $\mathbf{F} : \Omega \rightarrow \mathbb{R}^{3 \times 3}$ as the vector of the divergences of the rows of the matrix, i.e., $(\nabla \cdot \mathbf{F})_i = \nabla \cdot (F_{i1}, F_{i2}, F_{i3})^\top$ for all $1 \leq i \leq 3$. The Laplace operator of \mathbf{f} is denoted by $\Delta \mathbf{f} = \nabla \cdot (\nabla \mathbf{f})$ and coincides with the vector of the Laplace operator of the components of \mathbf{f} . It

follows that $\nabla \times (\nabla f) = 0$ and $\nabla \cdot (\nabla \times \mathbf{f}) = 0$. For the vector-valued functions $\mathbf{f}, \mathbf{h} : \Omega \rightarrow \mathbb{R}^3$, abusing our notation, we write

$$\nabla \mathbf{f} \times \mathbf{h} = (\partial_1 \mathbf{f} \times \mathbf{h}, \partial_2 \mathbf{f} \times \mathbf{h}, \partial_3 \mathbf{f} \times \mathbf{h}).$$

We define $(\mathbf{f} \cdot \nabla) \mathbf{h}$ by

$$[(\mathbf{f} \cdot \nabla) \mathbf{h}]_i = \sum_{k=1}^3 f_k \partial_k h_i = \mathbf{f} \cdot \nabla h_i \quad \text{for all } 1 \leq i \leq 3,$$

and note that $(\mathbf{f} \cdot \nabla) \mathbf{h}$ coincides with the matrix-vector product of $\nabla \mathbf{h}$ and \mathbf{f} . From the well-known product rule $\partial_i(fg) = \partial_i f g + f \partial_i g$, simple (but possibly lengthy) computations prove the identities collected in the following proposition.

Proposition B.3.1. *Let $\Omega \subset \mathbb{R}^3$ be an open set. For all sufficiently smooth functions $f, h : \Omega \rightarrow \mathbb{R}$, $\mathbf{f}, \mathbf{h} : \Omega \rightarrow \mathbb{R}^3$, we have the following product rules:*

- (i) $\nabla(fh) = f\nabla h + h\nabla f$,
- (ii) $\nabla(\mathbf{f} \cdot \mathbf{h}) = \nabla \mathbf{f}^\top \mathbf{h} + \nabla \mathbf{h}^\top \mathbf{f} = (\mathbf{f} \cdot \nabla) \mathbf{h} + (\mathbf{h} \cdot \nabla) \mathbf{f} + \mathbf{f} \times (\nabla \times \mathbf{h}) + \mathbf{h} \times (\nabla \times \mathbf{f})$,
- (iii) $\nabla(\mathbf{f} \times \mathbf{h}) = \nabla \mathbf{f} \times \mathbf{h} + \mathbf{f} \times \nabla \mathbf{h}$,
- (iv) $\nabla(f\mathbf{h}) = \mathbf{h} \otimes \nabla f + f\nabla \mathbf{h}$,
- (v) $\nabla \cdot (f\mathbf{h}) = \nabla f \cdot \mathbf{h} + f\nabla \cdot \mathbf{h}$,
- (vi) $\nabla \cdot (\mathbf{f} \times \mathbf{h}) = (\nabla \times \mathbf{f}) \cdot \mathbf{h} - (\nabla \times \mathbf{h}) \cdot \mathbf{f}$,
- (vii) $\nabla \cdot (\mathbf{f} \otimes \mathbf{h}) = (\nabla \cdot \mathbf{f}) \mathbf{h} + (\mathbf{f} \cdot \nabla) \mathbf{h}$,
- (viii) $\nabla \times (f\mathbf{h}) = \nabla f \times \mathbf{h} + f\nabla \times \mathbf{h}$,
- (ix) $\nabla \times (\mathbf{f} \times \mathbf{h}) = (\nabla \cdot \mathbf{h}) \mathbf{f} - (\nabla \cdot \mathbf{f}) \mathbf{h} + (\mathbf{h} \cdot \nabla) \mathbf{f} - (\mathbf{f} \cdot \nabla) \mathbf{h}$,
- (x) $\nabla \times (\nabla \times \mathbf{f}) = \nabla(\nabla \cdot \mathbf{f}) - \Delta \mathbf{f}$,
- (xi) $\nabla(|\mathbf{f}|) = |\mathbf{f}|^{-1} \nabla \mathbf{f}^\top \mathbf{f}$,
- (xii) $\nabla(\mathbf{f}/|\mathbf{f}|) = |\mathbf{f}|^{-1} (\mathbf{I} - |\mathbf{f}|^{-2} \mathbf{f} \otimes \mathbf{f}) \nabla \mathbf{f}$.

References

- [1] Hard disk drive. https://en.wikipedia.org/wiki/Hard_disk_drive. Accessed on October 10, 2016.
- [2] NGSolve Finite Element Library. <https://sourceforge.net/projects/ngsolve/>. Accessed on September 24, 2016.
- [3] NIST micromagnetic modeling activity group (μ MAG) website. <http://www.ctcms.nist.gov/~rdm/mumag.html>. Accessed on October 10, 2016.
- [4] The Object Oriented MicroMagnetic Framework (OOMMF) project at ITL/NIST. <http://math.nist.gov/oommf/>. Accessed on October 10, 2016.
- [5] ABERT, C., EXL, L., BRUCKNER, F., DREWS, A., AND SUESS, D. magnum.fe: A micromagnetic finite-element simulation code based on FEniCS. *J. Magn. Magn. Mater.* 345 (2013), 29–35.
- [6] ABERT, C., HRKAC, G., PAGE, M., PRAETORIUS, D., RUGGERI, M., AND SUESS, D. Spin-polarized transport in ferromagnetic multilayers: An unconditionally convergent FEM integrator. *Comput. Math. Appl.* 68, 6 (2014), 639–654.
- [7] ABERT, C., RUGGERI, M., BRUCKNER, F., VOGLER, C., HRKAC, G., PRAETORIUS, D., AND SUESS, D. A three-dimensional spin-diffusion model for micromagnetics. *Sci. Rep.* 5 (2015), 14855.
- [8] ABERT, C., RUGGERI, M., BRUCKNER, F., VOGLER, C., MANCHON, A., PRAETORIUS, D., AND SUESS, D. A self-consistent spin-diffusion model for micromagnetics. Accepted for publication in *Sci. Rep.*, preprint available at arXiv:1512.05519, 2016.
- [9] AHARONI, A. *Introduction to the theory of ferromagnetism*, second ed., vol. 109 of *International Series of Monographs on Physics*. Oxford University Press, 2001.
- [10] ALONSO RODRÍGUEZ, A., AND VALLI, A. *Eddy current approximation of Maxwell equations: Theory, algorithms and applications*, vol. 4 of *Modeling, Simulation and Applications*. Springer, 2010.
- [11] ALOUGES, F. A new algorithm for computing liquid crystal stable configurations: The harmonic mapping case. *SIAM J. Numer. Anal.* 34, 5 (1997), 1708–1726.
- [12] ALOUGES, F. A new finite element scheme for Landau–Lifchitz equations. *Discrete Contin. Dyn. Syst. Ser. S* 1, 2 (2008), 187–196.
- [13] ALOUGES, F., DE BOUARD, A., AND HOCQUET, A. A semi-discrete scheme for the stochastic Landau–Lifshitz equation. *Stoch. Partial Differ. Equ. Anal. Comput.* 2, 3 (2014), 281–315.
- [14] ALOUGES, F., AND JAISSE, P. Convergence of a finite element discretization for the Landau–Lifshitz equation in micromagnetism. *Math. Models Methods Appl. Sci.* 16, 2 (2006), 299–316.

- [15] ALOUGES, F., KRITSIKIS, E., STEINER, J., AND TOUSSAINT, J.-C. A convergent and precise finite element scheme for Landau–Lifschitz–Gilbert equation. *Numer. Math.* 128, 3 (2014), 407–430.
- [16] ALOUGES, F., KRITSIKIS, E., AND TOUSSAINT, J.-C. A convergent finite element approximation for Landau–Lifschitz–Gilbert equation. *Physica B* 407, 9 (2012), 1345–1349.
- [17] ALOUGES, F., AND SOYEUR, A. On global weak solutions for Landau–Lifshitz equations: Existence and nonuniqueness. *Nonlinear Anal.* 18, 11 (1992), 1071–1084.
- [18] ANSERMET, J.-P. Classical description of spin wave excitation by currents in bulk ferromagnets. *IEEE Trans. Magn.* 40, 2 (2004), 358–360.
- [19] BAIBICH, M. N., BROTO, J. M., FERT, A., VAN DAU, F. N., PETROFF, F., ETIENNE, P., CREUZET, G., FRIEDERICH, A., AND CHAZELAS, J. Giant magnetoresistance of (001)Fe/(001)Cr magnetic superlattices. *Phys. Rev. Lett.* 61, 21 (1988), 2472–2475.
- [20] BAÑAS, L. A numerical method for the Landau–Lifshitz equation with magnetostriction. *Math. Methods Appl. Sci.* 28, 16 (2005), 1939–1954.
- [21] BAÑAS, L. Numerical methods for the Landau–Lifshitz–Gilbert equation. In *Numerical analysis and its applications*, Z. Li, L. Vulkov, and J. Waśniewski, Eds., vol. 3401 of *Lecture Notes in Computer Science*. Springer, 2005, pp. 158–165.
- [22] BAÑAS, L. Adaptive methods for dynamical micromagnetics. In *Numerical Mathematics and Advanced Applications*, A. Bermúdez de Castro, D. Gómez, P. Quintela, and P. Salgado, Eds. Springer, 2006, pp. 531–538.
- [23] BAÑAS, L. Adaptive techniques for Landau–Lifshitz–Gilbert equation with magnetostriction. *J. Comput. Appl. Math.* 215, 2 (2008), 304–310.
- [24] BAÑAS, L., BARTELS, S., AND PROHL, A. A convergent implicit finite element discretization of the Maxwell–Landau–Lifshitz–Gilbert equation. *SIAM J. Numer. Anal.* 46, 3 (2008), 1399–1422.
- [25] BAÑAS, L., BRZEŹNIAK, Z., NEKLYUDOV, M., AND PROHL, A. A convergent finite-element-based discretization of the stochastic Landau–Lifshitz–Gilbert equation. *IMA J. Numer. Anal.* 34, 2 (2014), 502–549.
- [26] BAÑAS, L., BRZEŹNIAK, Z., NEKLYUDOV, M., AND PROHL, A. *Stochastic ferromagnetism: Analysis and numerics*, vol. 58 of *Studies in Mathematics*. De Gruyter, 2014.
- [27] BAÑAS, L., BRZEŹNIAK, Z., AND PROHL, A. Computational studies for the stochastic Landau–Lifshitz–Gilbert equation. *SIAM J. Sci. Comput.* 35, 1 (2013), B62–B81.
- [28] BAÑAS, L., PAGE, M., AND PRAETORIUS, D. A convergent linear finite element scheme for the Maxwell–Landau–Lifshitz–Gilbert equations. *Electron. Trans. Numer. Anal.* 44 (2015), 250–270.
- [29] BAÑAS, L., PAGE, M., PRAETORIUS, D., AND ROCHAT, J. A decoupled and unconditionally convergent linear FEM integrator for the Landau–Lifshitz–Gilbert equation with magnetostriction. *IMA J. Numer. Anal.* 34, 4 (2014), 1361–1385.
- [30] BAÑAS, L., PROHL, A., AND SLODIČKA, M. Modeling of thermally assisted magnetodynamics. *SIAM J. Numer. Anal.* 47, 1 (2008), 551–574.
- [31] BAÑAS, L., PROHL, A., AND SLODIČKA, M. Numerical scheme for augmented Landau–Lifshitz equation in heat assisted recording. *J. Comput. Appl. Math.* 236, 18 (2012), 4775–4787.

- [32] BANK, R. E., AND YSERENTANT, H. On the H^1 -stability of the L^2 -projection onto finite element spaces. *Numer. Math.* 126, 2 (2014), 361–381.
- [33] BARTELS, S. Stability and convergence of finite-element approximation schemes for harmonic maps. *SIAM J. Numer. Anal.* 43, 1 (2005), 220–238.
- [34] BARTELS, S. Constraint preserving, inexact solution of implicit discretizations of Landau–Lifshitz–Gilbert equations and consequences for convergence. *PAMM* 6, 1 (2006), 19–22.
- [35] BARTELS, S. Numerical analysis of a finite element scheme for the approximation of harmonic maps into surfaces. *Math. Comp.* 79, 61 (2010), 1263–1301.
- [36] BARTELS, S. *Numerical methods for nonlinear partial differential equations*, vol. 47 of *Springer Series in Computational Mathematics*. Springer, 2015.
- [37] BARTELS, S. Projection-free approximation of geometrically constrained partial differential equations. *Math. Comp.* 85, 299 (2016), 1033–1049.
- [38] BARTELS, S., FENG, X., AND PROHL, A. Finite element approximations of wave maps into spheres. *SIAM J. Numer. Anal.* 46, 1 (2007), 61–87.
- [39] BARTELS, S., KO, J., AND PROHL, A. Numerical analysis of an explicit approximation scheme for the Landau–Lifshitz–Gilbert equation. *Math. Comp.* 77, 262 (2008), 773–788.
- [40] BARTELS, S., AND PROHL, A. Convergence of an implicit finite element method for the Landau–Lifshitz–Gilbert equation. *SIAM J. Numer. Anal.* 44, 4 (2006), 1405–1419.
- [41] BARTELS, S., AND PROHL, A. Constraint preserving implicit finite element discretization of harmonic map flow into spheres. *Math. Comp.* 76, 260 (2007), 1847–1859.
- [42] BAZALIY, Y. B., JONES, B. A., AND ZHANG, S.-C. Modification of the Landau–Lifshitz equation in the presence of a spin-polarized current in colossal- and giant-magnetoresistive materials. *Phys. Rev. B* 57, 6 (1998), R3213–R3216.
- [43] BENZI, M., GOLUB, G. H., AND LIESEN, J. Numerical solution of saddle point problems. *Acta Numer.* 14 (2005), 1–137.
- [44] BERGER, L. Emission of spin waves by a magnetic multilayer traversed by a current. *Phys. Rev. B* 54, 13 (1996), 9353–9358.
- [45] BERGH, J., AND LÖFSTRÖM, J. *Interpolation space: An introduction*, vol. 223 of *Grundlehren der mathematischen Wissenschaften*. Springer, 1976.
- [46] BERTOTTI, G., MAGNI, A., MAYERGOYZ, I. D., AND SERPICO, C. Landau–Lifshitz magnetization dynamics and eddy currents in metallic thin films. *J. Appl. Phys.* 91, 10 (2002), 7559.
- [47] BERTOTTI, G., MAYERGOYZ, I. D., AND SERPICO, C. *Nonlinear magnetization dynamics in nanosystems*. Elsevier Series in Electromagnetism. Elsevier, 2009.
- [48] BETHUEL, F., CORON, J.-M., GHIDAGLIA, J.-M., AND SOYEUR, A. Heat flows and relaxed energies for harmonic maps. In *Nonlinear diffusion equations and their equilibrium states 3*, N. G. Lloyd, W. M. Ni, L. A. Peletier, and J. Serrin, Eds. Birkhäuser, 1992, pp. 99–109.
- [49] BINASCH, G., GRÜNBERG, P., SAURENBACH, F., AND ZINN, W. Enhanced magnetoresistance in layered magnetic structures with antiferromagnetic interlayer exchange. *Phys. Rev. B* 39, 7 (1989), 4828–4830.
- [50] BOFFI, D., BREZZI, F., AND FORTIN, M. *Mixed finite element methods and applications*, vol. 44 of *Springer Series in Computational Mathematics*. Springer, 2013.

- [51] BRAESS, D. *Finite elements: Theory, fast solvers, and applications in solid mechanics*, third ed. Cambridge University Press, 2007.
- [52] BRAMBLE, J. H., PASCIAK, J. E., AND STEINBACH, O. On the stability of the L^2 projection in $H^1(\Omega)$. *Math. Comp.* 71, 237 (2002), 147–156.
- [53] BRENNER, S. C., AND SCOTT, L. R. *The mathematical theory of finite element methods*, third ed., vol. 15 of *Texts in Applied Mathematics*. Springer, 2008.
- [54] BROWN, W. F. *Micromagnetics*. Interscience tracts on physics and astronomy. Interscience Publishers, 1963.
- [55] BROWN, W. F. Thermal fluctuations of a single-domain particle. *Phys. Rev.* 130, 5 (1963), 1677–1686.
- [56] BRUCKNER, F., FEISCHL, M., FÜHRER, T., GOLDENITS, P., PAGE, M., PRAETORIUS, D., RUGGERI, M., AND SUESS, D. Multiscale modeling in micromagnetics: Existence of solutions and numerical integration. *Math. Models Methods Appl. Sci.* 24, 13 (2014), 2627–2662.
- [57] BRUCKNER, F., VOGLER, C., BERGMAIR, B., HUBER, T., FUGER, M., SUESS, D., FEISCHL, M., FÜHRER, T., PAGE, M., AND PRAETORIUS, D. Combining micromagnetism and magnetostatic Maxwell equations for multiscale magnetic simulations. *J. Magn. Magn. Mater.* 343 (2013), 163–168.
- [58] BRUCKNER, F., VOGLER, C., FEISCHL, M., PRAETORIUS, D., BERGMAIR, B., HUBER, T., FUGER, M., AND SUESS, D. 3D FEM-BEM-coupling method to solve magnetostatic Maxwell equations. *J. Magn. Magn. Mater.* 324, 10 (2012), 1862–1866.
- [59] BRZEŹNIAK, Z., GOLDYS, B., AND JEGARAJ, T. Weak solutions of a stochastic Landau–Lifshitz–Gilbert equation. *Appl. Math. Res. Express. AMRX* 2013, 1 (2013), 1–33.
- [60] BRZEŹNIAK, Z., AND LI, L. Weak solutions of the stochastic Landau–Lifshitz–Gilbert equations with nonzero anisotropy energy. *Appl. Math. Res. Express. AMRX* 2016, 2 (2016), 334–375.
- [61] CARBOU, G., EFENDIEV, M. A., AND FABRIE, P. Global weak solutions for the Landau–Lifshitz equation with magnetostriction. *Math. Methods Appl. Sci.* 34, 10 (2011), 1274–1288.
- [62] CARBOU, G., AND FABRIE, P. Time average in micromagnetism. *J. Differential Equations* 147, 2 (1998), 383–409.
- [63] CARBOU, G., AND FABRIE, P. Regular solutions for Landau–Lifshitz equation in a bounded domain. *Differential Integral Equations* 14, 2 (2001), 213–229.
- [64] CHAINAIS-HILLAIRET, C., JÜNGEL, A., AND SHPARTKO, P. A finite-volume scheme for a spinorial matrix drift-diffusion model for semiconductors. *Numer. Methods Partial Differential Equations* 32, 3 (2015), 819–846.
- [65] CHAPPERT, C., FERT, A., AND VAN DAU, F. N. The emergence of spin electronics in data storage. *Nat. Mater.* 6, 11 (2007), 813–823.
- [66] CHEN, J., GARCÍA-CERVERA, C. J., AND YANG, X. Mean-field dynamics of the spin-magnetization coupling in ferromagnetic materials: Application to current-driven domain wall motions. *IEEE Trans. Magn.* 51, 6 (2015), 1400906.
- [67] CHEN, J., GARCÍA-CERVERA, C. J., AND YANG, X. A mean-field model for spin dynamics in multilayered ferromagnetic media. *Multiscale Model. Simul.* 13, 2 (2015), 551–570.

- [68] CIARLET, P. G. *The finite element method for elliptic problems*, vol. 4 of *Studies in mathematics and its applications*. Elsevier, 1988.
- [69] CIARLET, P. G. *Mathematical elasticity. Volume 1: Three dimensional elasticity*, vol. 20 of *Studies in mathematics and its applications*. Elsevier, 1988.
- [70] CIARLET, P. G., AND RAVIART, P.-A. Maximum principle and uniform convergence for the finite element method. *Comput. Methods Appl. Mech. Engrg.* 2, 1 (1973), 17–31.
- [71] CIMRÁK, I. Error estimates for a semi-implicit numerical scheme solving the Landau–Lifshitz equation with an exchange field. *IMA J. Numer. Anal.* 25, 3 (2005), 611–634.
- [72] CIMRÁK, I. Error analysis of a numerical scheme for 3D Maxwell–Landau–Lifshitz system. *Math. Methods Appl. Sci.* 30, 14 (2007), 1667–1683.
- [73] CIMRÁK, I. Existence, regularity and local uniqueness of the solutions to the Maxwell–Landau–Lifshitz system in three dimensions. *J. Math. Anal. Appl.* 329, 2 (2007), 1080–1093.
- [74] CIMRÁK, I. Regularity properties of the solutions to the 3D Maxwell–Landau–Lifshitz system in weighted Sobolev spaces. *J. Comput. Appl. Math.* 215, 2 (2008), 320–327.
- [75] CIMRÁK, I. A survey on the numerics and computations for the Landau–Lifshitz equation of micromagnetism. *Arch. Comput. Methods Eng.* 15, 3 (2008), 277–309.
- [76] CIMRÁK, I. Convergence result for the constraint preserving mid-point scheme for micromagnetism. *J. Comput. Appl. Math.* 228, 1 (2009), 238–246.
- [77] CIMRÁK, I., AND VAN KEER, R. Higher order regularity results in 3D for the Landau–Lifshitz equation with an exchange field. *Nonlinear Anal.* 68, 5 (2008), 1316–1331.
- [78] CORON, J.-M. Nonuniqueness for the heat flow of harmonic maps. *Ann. Inst. H. Poincaré Anal. Non Linéaire* 7, 4 (1990), 335–344.
- [79] D’AQUINO, M., SERPICO, C., AND MIANO, G. Geometrical integration of Landau–Lifshitz–Gilbert equation based on the mid-point rule. *J. Comput. Phys.* 209, 2 (2005), 730–753.
- [80] DAUGHTON, J. M. Magnetic tunneling applied to memory. *J. Appl. Phys.* 81, 8 (1997), 3758–3763.
- [81] DIENING, L., KREUZER, C., AND SCHWARZACHER, S. Convex hull property and maximum principle for finite element minimisers of general convex functionals. *Numer. Math.* 124, 4 (2013), 685–700.
- [82] DONAHUE, M. J., AND PORTER, D. G. OOMMF user’s guide, Version 1.0. Interagency Report NISTIR 6376, National Institute of Standards and Technology, Gaithersburg, MD, 1999.
- [83] DORMAND, J. R., AND PRINCE, P. J. A family of embedded Runge–Kutta formulae. *J. Comput. Appl. Math.* 6, 1 (1980), 19–26.
- [84] DUMAS, E., AND SUEUR, F. On the weak solutions to the Maxwell–Landau–Lifshitz equations and to the Hall-Magneto-Hydrodynamic equations. *Comm. Math. Phys.* 330, 3 (2014), 1179–1225.
- [85] DYAKONOV, M. I. Magnetoresistance due to edge spin accumulation. *Phys. Rev. Lett.* 99, 12 (2007), 126601.
- [86] DZYALOSHINSKII, I. A thermodynamic theory of ‘weak’ ferromagnetism of antiferromagnetics. *J. Phys. Chem. Solids* 4, 4 (1958), 241–255.

- [87] E, W., AND WANG, X.-P. Numerical methods for the Landau–Lifshitz equation. *SIAM J. Numer. Anal.* **38**, 5 (2000), 1647–1665.
- [88] EVANS, L. C. *Partial differential equations*, second ed., vol. 19 of *Graduate Studies in Mathematics*. American Mathematical Society, 2010.
- [89] EVANS, R. F. L., CHANTRELL, R. W., NOWAK, U., LYBERATOS, A., AND RICHTER, H. J. Thermally induced error: density limit for magnetic data storage. *Appl. Phys. Lett.* **100**, 10 (2012), 102402.
- [90] EVANS, R. F. L., HINZKE, D., ATXITIA, U., NOWAK, U., CHANTRELL, R. W., AND CHUBYKALO-FESENKO, O. Stochastic form of the Landau–Lifshitz–Bloch equation. *Phys. Rev. B* **85**, 1 (2012), 014433.
- [91] FEILER, L., SENTKER, K., BRINKER, M., KUHLMANN, N., STEIN, F.-U., AND MEIER, G. Inverse spin Hall effect voltage generation by nonlinear spin-wave excitation. *Phys. Rev. B* **93**, 6 (2016), 064408.
- [92] FEISCHL, M., AND TRAN, T. The Eddy Current–LLG equations. Part I: FEM-BEM coupling. Submitted for publication, preprint available at arXiv:1602.00744, 2016.
- [93] FEISCHL, M., AND TRAN, T. The Eddy Current–LLG equations. Part II: A priori error estimates. Submitted for publication, preprint available at arXiv:1602.00745, 2016.
- [94] FEISCHL, M., AND TRAN, T. Existence of arbitrarily smooth solutions of the LLG equation in 3D with natural boundary conditions. Submitted for publication, preprint available at arXiv:1606.00086, 2016.
- [95] FERT, A., CROS, V., AND SAMPAIO, J. Skyrmions on the track. *Nat. Nanotechnol.* **8**, 3 (2013), 152–156.
- [96] FIDLER, J., CHANTRELL, R. W., SCHREFL, T., AND WONGSAM, M. A. Micromagnetics: Basic principles. In *Encyclopedia of Materials: Science and Technology*, K. H. J. Buschow, R. W. Cahn, M. C. Flemings, B. Ilshner, E. J. Kramer, S. Mahajan, and P. Veyssi re, Eds., second ed. Elsevier, Oxford, 2001, pp. 5642–5650.
- [97] FIDLER, J., AND SCHREFL, T. Micromagnetic modelling - the current state of the art. *J. Phys. D: Appl. Phys.* **33**, 15 (2000), R135–R156.
- [98] FREDKIN, D. R., AND KOEHLER, T. R. Numerical micromagnetics by the finite element method. *IEEE Trans. Magn.* **23**, 5 (1987), 3385–3387.
- [99] FREDKIN, D. R., AND KOEHLER, T. R. Hybrid method for computing demagnetization fields. *IEEE Trans. Magn.* **26**, 2 (1990), 415–417.
- [100] GARANIN, D. A. Fokker–Planck and Landau–Lifshitz–Bloch equations for classical ferromagnets. *Phys. Rev. B* **55**, 5 (1997), 3050–3057.
- [101] GARC A-CERVERA, C. J. Numerical micromagnetics: A review. *Bol. Soc. Esp. Mat. Apl. SeMA* **39** (2007), 103–135.
- [102] GARC A-CERVERA, C. J., AND WANG, X.-P. Spin-polarized currents in ferromagnetic multilayers. *J. Comput. Phys.* **224**, 2 (2007), 699–711.
- [103] GARC A-CERVERA, C. J., AND WANG, X.-P. Spin-polarized transport: Existence of weak solutions. *Discrete Contin. Dyn. Syst. Ser. B* **7**, 1 (2007), 87–100.
- [104] GARC A-CERVERA, C. J., AND WANG, X.-P. A note on ‘Spin-polarized transport: Existence of weak solutions’. *Discrete Contin. Dyn. Syst. Ser. B* **20**, 8 (2015), 2761–2763.

- [105] GARCÍA-PALACIOS, J. L., AND LÁZARO, F. J. Langevin-dynamics study of the dynamical properties of small magnetic particles. *Phys. Rev. B* 58, 22 (1998), 14937–14958.
- [106] GILBARG, D., AND TRUDINGER, N. S. *Elliptic partial differential equations of second order*, second ed. Classics in Mathematics. Springer, 2011.
- [107] GILBERT, T. L. A Lagrangian formulation of the gyromagnetic equation of the magnetization fields. *Phys. Rev.* 100 (1955), 1243. Abstract only.
- [108] GILBERT, T. L. A phenomenological theory of damping in ferromagnetic materials. *IEEE Trans. Magn.* 40, 6 (2004), 3443–3449.
- [109] GOLDENITS, P. *Konvergente numerische Integration der Landau–Lifshitz–Gilbert Gleichung*. PhD thesis, TU Wien, 2012. In German.
- [110] GOLDENITS, P., HRKAC, G., PRAETORIUS, D., AND SUESS, D. An effective integrator for the Landau–Lifshitz–Gilbert equation. In *Proceedings of 7th Vienna International Conference on Mathematical Modelling* (2012), vol. 7 of *Mathematical Modelling*, International Federation of Automatic Control, pp. 493–497.
- [111] GOLDENITS, P., PRAETORIUS, D., AND SUESS, D. Convergent geometric integrator for the Landau–Lifshitz–Gilbert equation in micromagnetics. *PAMM* 11, 1 (2011), 775–776.
- [112] GOLDYS, B., LE, K.-N., AND TRAN, T. A finite element approximation for the stochastic Landau–lifshitz–gilbert equation. *J. Differential Equations* 260, 2 (2016), 937–970.
- [113] GUO, B., AND DING, S. *Landau–Lifshitz equations*, vol. 1 of *Frontiers of Research with the Chinese Academy of Sciences*. World Scientific, 2008.
- [114] GUO, B., AND HONG, M.-C. The Landau–Lifshitz equation of the ferromagnetic spin chain and harmonic maps. *Calc. Var. Partial Differential Equations* 1, 3 (1993), 311–334.
- [115] HOSOMI, M., YAMAGISHI, H., YAMAMOTO, T., BESSHO, K., HIGO, Y., YAMANE, K., YAMADA, H., SHOJI, M., HACHINO, H., FUKUMOTO, C., NAGAO, H., AND KANO, H. A novel nonvolatile memory with spin torque transfer magnetization switching: Spin-RAM. In *Proceedings of the IEEE International Electron Devices Meeting 2005. IEDM Technical Digest.* (2005), pp. 459–462.
- [116] HRKAC, G., PRAETORIUS, D., RUGGERI, M., AND STIFTNER, B. Convergent numerical simulations of magnetic skyrmions. In preparation, 2016.
- [117] HRKAC, G., SCHREFL, T., ERTL, O., SUESS, D., KIRSCHNER, M., DORFBAUER, F., AND FIDLER, J. Influence of eddy current on magnetization processes in submicrometer permalloy structures. *IEEE Trans. Magn.* 41, 10 (2005), 3097–3099.
- [118] HUBERT, A., AND SCHÄFER, R. *Magnetic domains: The analysis of magnetic microstructures*. Springer, 1998.
- [119] JACKSON, J. D. *Classical electrodynamics*, third ed. John Wiley & Sons, 1999.
- [120] JOHNSON, M., AND SILSBEE, R. H. Interfacial charge-spin coupling: Injection and detection of spin magnetization in metals. *Phys. Rev. Lett.* 55, 17 (1985), 1790–1793.
- [121] JÜNGEL, A., NEGULESCU, C., AND SHPARTKO, P. Bounded weak solutions to a matrix drift-diffusion model for spin-coherent electron transport in semiconductors. *Math. Models Methods Appl. Sci.* 25, 5 (2015), 929–958.
- [122] JÜNGEL, A., AND UNTERREITER, A. Discrete minimum and maximum principles for finite element approximations of non-monotone elliptic equations. *Numer. Math.* 99, 3 (2005), 485–508.

- [123] KARKULIK, M., PAVLICEK, D., AND PRAETORIUS, D. On 2D newest vertex bisection: Optimality of mesh-closure and H^1 -stability of L^2 -projection. *Constr. Approx.* 38, 2 (2013), 213–234.
- [124] KHVALKOVSKIY, A. V., ZVEZDIN, K. A., GORBUNOV, Y. V., CROS, V., GROLLIER, J., FERT, A., AND ZVEZDIN, A. K. High domain wall velocities due to spin currents perpendicular to the plane. *Phys. Rev. Lett.* 102, 6 (2009), 067206.
- [125] KOEHLER, T. R., AND FREDKIN, D. R. Finite element methods for micromagnetics. *IEEE Trans. Magn.* 28, 2 (1992), 1239–1244.
- [126] KOHN, R. V., REZNIKOFF, M. G., AND VANDEN-EIJNDEN, E. Magnetic elements at finite temperature and large deviation theory. *J. Nonlinear Sci.* 15, 4 (2005), 223–253.
- [127] KOMINEAS, S., AND PAPANICOLAOU, N. Skyrmion dynamics in chiral ferromagnets. *Phys. Rev. B* 92, 6 (2015), 064412.
- [128] KOROTOV, S., AND KŘÍŽEK, M. Acute type refinements of tetrahedral partitions of polyhedral domains. *SIAM J. Numer. Anal.* 39, 2 (2002), 724–733.
- [129] KOROTOV, S., AND KŘÍŽEK, M. Local nonobtuse tetrahedral refinements of a cube. *Appl. Math. Lett.* 16, 7 (2003), 1101–1104.
- [130] KOROTOV, S., AND KŘÍŽEK, M. Global and local refinement techniques yielding nonobtuse tetrahedral partitions. *Comput. Math. Appl.* 50, 7 (2005), 1105–1113.
- [131] KOROTOV, S., AND KŘÍŽEK, M. Nonobtuse local tetrahedral refinements towards a polygonal face/interface. *Appl. Math. Lett.* 24, 6 (2011), 817–821.
- [132] KOROTOV, S., AND KŘÍŽEK, M. Local nonobtuse tetrahedral refinements around an edge. *Appl. Math. Comput.* 219, 13 (2013), 7236–7240.
- [133] KOROTOV, S., KŘÍŽEK, M., AND NEITTAANMAKI, P. Weakened acute type condition for tetrahedral triangulations and the discrete maximum principle. *Math. Comp.* 70, 233 (2001), 107–119.
- [134] KRONMÜLLER, H. Theory of nucleation fields in inhomogeneous ferromagnets. *Phys. Status Solidi B* 144, 1 (1987), 385–396.
- [135] KRONMÜLLER, H. General micromagnetic theory. In *Handbook of Magnetism and Advanced Magnetic Materials*. John Wiley & Sons, Ltd, 2007.
- [136] KRONMÜLLER, H., AND FÄHNLE, M. *Micromagnetism and the Microstructure of Ferromagnetic Solids*. Cambridge University Press, 2009.
- [137] KRUŽÍK, M., AND PROHL, A. Recent developments in the modeling, analysis, and numerics of ferromagnetism. *SIAM Rev.* 48, 3 (2006), 439–483.
- [138] KŘÍŽEK, M., AND QUN, L. On diagonal dominance of stiffness matrices in 3D. *East-West J. Numer. Math.* 3, 1 (1995), 59–69.
- [139] LANDAU, L., AND LIFSHITZ, E. On the theory of the dispersion of magnetic permeability in ferromagnetic bodies. *Phys. Zeitsch. der Sow.* 8 (1935), 153–168.
- [140] LE, K.-N. Weak solutions of the Landau–lifshitz–bloch equation. *J. Differential Equations* 261, 12 (2016), 6699–6717.
- [141] LE, K.-N., PAGE, M., PRAETORIUS, D., AND TRAN, T. On a decoupled linear FEM integrator for eddy-current-LLG. *Appl. Anal.* 94, 5 (2015), 1051–1067.

- [142] LE, K.-N., AND TRAN, T. A convergent finite element approximation for the quasi-static Maxwell–Landau–Lifshitz–Gilbert equations. *Comput. Math. Appl.* 66, 8 (2013), 1389–1402.
- [143] LI, Z., AND ZHANG, S. Domain-wall dynamics and spin-wave excitations with spin-transfer torques. *Phys. Rev. Lett.* 92, 20 (2004), 207203.
- [144] MARTINEZ, E. The influence of the Rashba field on the current-induced domain wall dynamics: A full micromagnetic analysis, including surface roughness and thermal effects. *J. Appl. Phys.* 111, 7 (2012), 07D302.
- [145] MAXWELL, J. C. *A treatise on electricity and magnetism*, third ed. Dover Books on Physics. Dover Publications, 1954.
- [146] MAYER, L. Curie-point writing on magnetic films. *J. Appl. Phys.* 29, 6 (1958), 1003–1003.
- [147] MCLEAN, W. *Strongly elliptic systems and boundary integral equations*. Cambridge University Press, 2000.
- [148] MELCHER, C. Existence of partially regular solutions for Landau–Lifshitz equations in \mathbb{R}^3 . *Comm. Partial Differential Equations* 30, 4 (2005), 567–587.
- [149] MELCHER, C. Global solvability of the Cauchy problem for the Landau–Lifshitz–Gilbert equation in higher dimensions. *Indiana Univ. Math. J.* 61, 3 (2012), 1175–1200.
- [150] MELCHER, C. Chiral skyrmions in the plane. *Proc. R. Soc. A* 470, 2172 (2014).
- [151] MELCHER, C., AND PTASHNYK, M. Landau–Lifshitz–Slonczewski equations: Global weak and classical solutions. *SIAM J. Math. Anal.* 45, 1 (2013), 407–429.
- [152] MILTAT, J. E., AND DONAHUE, M. J. Numerical micromagnetics: Finite difference methods. In *Handbook of Magnetism and Advanced Magnetic Materials*. John Wiley & Sons, Ltd, 2007.
- [153] MIRON, I. M., MOORE, T., SZAMBOLICS, H., BUDA-PREJBEANU, L., AUFFRET, S., RODMACQ, B., PIZZINI, S., VOGEL, J., BONFIM, M., SCHUHL, A., AND GAUDIN, G. Fast current-induced domain-wall motion controlled by the rashba effect. *Nat. Mater.* 10, 6 (2011), 419–423.
- [154] MONK, P., AND SUN, J. Analysis of an eddy current and micromagnetic model. *Appl. Anal.* 85, 12 (2006), 1509–1525.
- [155] MONK, P. B., AND VACUS, O. Accurate discretization of a non-linear micromagnetic problem. *Comput. Methods Appl. Mech. Engrg.* 190, 40 (2001), 5243–5269.
- [156] MORIYA, T. Anisotropic superexchange interaction and weak ferromagnetism. *Phys. Rev.* 120, 91 (1960), 91.
- [157] NAGAOSA, N., AND TOKURA, Y. Topological properties and dynamics of magnetic skyrmions. *Nat. Nanotechnol.* 8, 12 (2013), 899–911.
- [158] NAJAFI, M., KRÜGER, B., BOHLENS, S., FRANCHIN, M., FANGOHR, H., VANHAVERBEKE, A., ALLENSPACH, R., BOLTE, M., MERKT, U., PFANNKUCHE, D., MÖLLER, D. P. F., AND MEIER, G. Proposal for a standard problem for micromagnetic simulations including spin-transfer torque. *J. Appl. Phys.* 105, 11 (2009), 113914.
- [159] NAKATANI, Y., UESAKA, Y., AND HAYASHI, N. Direct solution of the Landau–Lifshitz–Gilbert equation for micromagnetics. *ãAÖJpn. J. Appl. Phys* 28, 12R (1989), 2485.
- [160] NEKLYUDOV, M., AND PROHL, A. The role of noise in finite ensembles of nanomagnetic particles. *Arch. Ration. Mech. Anal.* 210, 499 (2013).

- [161] PAGE, M. *On dynamical micromagnetism*. PhD thesis, TU Wien, 2013.
- [162] PARKIN, S. S. P., HAYASHI, M., AND THOMAS, L. Magnetic domain-wall racetrack memory. *Science* 320, 5873 (2008), 190–194.
- [163] PETITJEAN, C., LUC, D., AND WAIN TAL, X. Unified drift-diffusion theory for transverse spin currents in spin valves, domain walls, and other textured magnets. *Phys. Rev. Lett.* 109, 11 (2012), 117204.
- [164] PODIO-GUIDUGLI, P. On dissipation mechanisms in micromagnetics. *Eur. Phys. J. B* 19, 3 (2001), 417–424.
- [165] POSSANNER, S., AND NEGULESCU, C. Diffusion limit of a generalized matrix Boltzmann equation for spin-polarized transport. *Kinet. Relat. Models* 4, 4 (2011), 1159–1191.
- [166] PRAETORIUS, D. Analysis of the operator $\Delta^{-1}\text{div}$ arising in magnetic models. *Z. Anal. Anwend.* 23, 3 (2004), 589–605.
- [167] PRAETORIUS, D., RUGGERI, M., AND STIFTNER, B. Convergence of an implicit-explicit midpoint scheme for computational micromagnetics. Submitted for publication, preprint available at arXiv:1611.02465, 2016.
- [168] PRAETORIUS, D., RUGGERI, M., AND STIFTNER, B. Iterative solution and preconditioning for the tangent plane scheme in computational micromagnetics. In preparation, 2016.
- [169] PROHL, A. *Computational micromagnetism*. Advances in numerical mathematics. B. G. Teubner, 2001.
- [170] QUARTERONI, A., AND VALLI, A. *Numerical approximation of partial differential equations*, vol. 23 of *Springer Series in Computational Mathematics*. Springer, 1994.
- [171] RADO, G. T., AND WEERTMAN, J. R. Spin-wave resonance in a ferromagnetic metal. *J. Phys. Chem. Solids* 11, 3–4 (1959), 315–333.
- [172] RICHTER, H. J. The transition from longitudinal to perpendicular recording. *J. Phys. D: Appl. Phys.* 40, 9 (2007), R149.
- [173] ROMMING, N., HANNEKEN, C., MENZEL, M., BICKEL, J. E., WOLTER, B., VON BERGMANN, K., KUBETZKA, A., AND WIESENDANGER, R. Writing and deleting single magnetic skyrmions. *Science* 341, 6146 (2013), 636–639.
- [174] RUGGERI, M., ABERT, C., HRKAC, G., SUESS, D., AND PRAETORIUS, D. Coupling of dynamical micromagnetism and a stationary spin drift-diffusion equation: A step towards a fully self-consistent spintronics framework. *Physica B* 486 (2016), 88–91.
- [175] SAMPAIO, J., CROS, V., ROHART, S., THIAVILLE, A., AND FERT, A. Nucleation, stability and current-induced motion of isolated magnetic skyrmions in nanostructures. *Nat. Nanotechnol.* 8, 11 (2013), 839–844.
- [176] SBIAA, R., AND CHANTRELL, R. W. Domain wall oscillations induced by spin torque in magnetic nanowires. *J. Appl. Phys.* 117, 5 (2015), 053907.
- [177] SCHABES, M. E., AND BERTRAM, H. N. Magnetization processes in ferromagnetic cubes. *J. Appl. Phys.* 64, 3 (1988), 1347–1357.
- [178] SCHÖBERL, J. NETGEN An advancing front 2D/3D-mesh generator based on abstract rules. *Comput. Vis. Sci.* 1, 1 (1997), 41–52.
- [179] SCHÖBERL, J. C++11 implementation of finite elements in NGSolve. ASC Report No. 30/2014, 2014.

- [180] SCHOLZ, W., FIDLER, J., SCHREFL, S., SUESS, D., DITTRICH, R., FORSTER, H., AND TSANTOS, V. Scalable parallel micromagnetic solvers for magnetic nanostructures. *Comput. Mater. Sci.* 28, 2 (2003), 366–383.
- [181] SCHREFL, T. Finite elements in numerical micromagnetics. Part I: granular hard magnets. *J. Magn. Magn. Mat.* 207, 1–3 (1999), 45–65.
- [182] SCHREFL, T. Finite elements in numerical micromagnetics. Part II: patterned magnetic elements. *J. Magn. Magn. Mat.* 207, 1–3 (1999), 66–77.
- [183] SCHREFL, T., FIDLER, J., SUESS, D., SCHOLZ, W., AND TSANTOS, V. Micromagnetic simulation of dynamic and thermal effects. In *Handbook of Advanced Magnetic Materials*, Y. Liu, D. J. Sellmyer, and D. Shindo, Eds. Springer, 2006, pp. 128–146.
- [184] SCHREFL, T., HRKAC, G., BANCE, S., GONCHAROV, A., FIDLER, J., AND SUESS, D. Micromagnetism of nanoscale materials. In *Magnetic materials: Current topics in amorphous wires, hard magnetic alloys, ceramics, characterization and modelling*, I. Betancourt, Ed. Research Signpost, 2007, pp. 33–48.
- [185] SCHREFL, T., HRKAC, G., BANCE, S., SUESS, D., ERTL, O., AND FIDLER, J. Numerical methods in micromagnetics (Finite element method). In *Handbook of Magnetism and Advanced Magnetic Materials*. John Wiley & Sons, Ltd, 2007.
- [186] SCHWAB, C., AND SAUTER, S. A. *Boundary Element Methods*, vol. 39 of *Springer Series in Computational Mathematics*. Springer, 2011.
- [187] SCOTT, L. R., AND ZHANG, S. Finite element interpolation of nonsmooth functions satisfying boundary conditions. *Math. Comp.* 54, 190 (1990), 483–493.
- [188] SHIR, C. C. Computations of the micromagnetic dynamics in domain walls. *J. Appl. Phys.* 49, 6 (1978), 3413–3421.
- [189] SHPIRO, A., LEVY, P. M., AND ZHANG, S. Self-consistent treatment of nonequilibrium spin torques in magnetic multilayers. *Phys. Rev. B* 67, 10 (2003), 104430.
- [190] SHU, Y. C., LIN, M. P., AND WU, K. C. Micromagnetic modeling of magnetostrictive materials under intrinsic stress. *Mech. Mater.* 36, 10 (2004), 975–997.
- [191] SLONCZEWSKI, J. C. Current-driven excitation of magnetic multilayers. *J. Magn. Magn. Mat.* 159, 1–2 (1996), L1–L7.
- [192] ŚMIGAJ, W., BETCKE, T., ARRIDGE, S., PHILLIPS, J., AND SCHWEIGER, M. Solving boundary integral problems with BEM++. *ACM Trans. Math. Softw.* 41, 2 (2015), 6:1–6:40.
- [193] STURMA, M., TOUSSAINT, J.-C., AND GUSAKOVA, D. Geometry effects on magnetization dynamics in circular cross-section wires. *J. Appl. Phys.* 117, 24 (2015), 243901.
- [194] SUESS, D., TSANTOS, V., SCHREFL, T., FIDLER, J., SCHOLZ, W., FORSTER, H., DITTRICH, R., AND MILES, J. J. Time resolved micromagnetics using a preconditioned time integration method. *J. Magn. Magn. Mater.* 248, 2 (2002), 298–311.
- [195] SUESS, D., VOGLER, C., ABERT, C., BRUCKNER, F., WINDL, R., BRETH, L., AND FIDLER, J. Fundamental limits in heat-assisted magnetic recording and methods to overcome it with exchange spring structures. *J. Appl. Phys.* 117, 16 (2015), 163913.
- [196] SUN, J., COLLINO, F., MONK, P. B., AND WANG, L. An eddy-current and micromagnetism model with applications to disk write heads. *Internat. J. Numer. Methods Engrg.* 60, 10 (2004), 1673–1698.

- [197] TANIGUCHI, T., GROLLIER, J., AND STILES, M. D. Spin-transfer torques generated by the anomalous Hall effect and anisotropic magnetoresistance. *Phys. Rev. Applied* 3, 4 (2015), 044001.
- [198] THIAVILLE, A., NAKATANI, Y., MILTAT, J., AND SUZUKI, Y. Micromagnetic understanding of current-driven domain wall motion in patterned nanowires. *Europhys. Lett.* 69, 6 (2005), 990–996.
- [199] THOMÉE, V. *Galerkin finite element methods for parabolic problems*, second ed., vol. 25 of *Springer Series in Computational Mathematics*. Springer, 2006.
- [200] TOMASELLO, R., MARTINEZ, E., ZIVIERI, R., TORRES, L., CARPENTIERI, M., AND FINOCCHIO, G. A strategy for the design of skyrmion racetrack memories. *Sci. Rep.* 4 (2014), 6784.
- [201] TROUILLOUD, P. L. Wall nucleation propagation for racetrack memory. Patent US 7768809, 2010.
- [202] VALET, T., AND FERT, A. Theory of the perpendicular magnetoresistance in magnetic multilayers. *Phys. Rev. B* 48, 10 (1993), 7099–7113.
- [203] VISINTIN, A. On Landau–Lifshitz’ equations for ferromagnetism. *Japan J. Appl. Math.* 2, 1 (1985), 69–84.
- [204] VOGLER, C., ABERT, C., BRUCKNER, F., SUESS, D., AND PRAETORIUS, D. Areal density optimizations for heat-assisted magnetic recording of high-density media. *J. Appl. Phys.* 119, 22 (2016), 223903.
- [205] VOGLER, C., ABERT, C., BRUCKNER, F., SUESS, D., AND PRAETORIUS, D. Heat-assisted magnetic recording of bit-patterned media beyond 10 Tb/in². *Appl. Phys. Lett.* 108, 10 (2016), 102406.
- [206] ŽUTIĆ, I., FABIAN, J., AND DAS SARMA, S. Spintronics: Fundamentals and applications. *Rev. Mod. Phys.* 76, 2 (2004), 323–410.
- [207] WANG, X.-P., GARCÍA-CERVERA, C. J., AND E, W. A Gauss-Seidel projection method for micromagnetics simulations. *J. Comput. Phys.* 171, 1 (2001), 357–372.
- [208] WEISS, P., AND FORRER, R. Aimantation et phénomène magnétocalorique du nickel. *Ann. Phys. (Paris)* 5 (1926), 153–213.
- [209] WOOD, R. Future hard disk drive systems. *J. Magn. Magn. Mater.* 321, 6 (2009), 555–561.
- [210] ZAMPONI, N. Analysis of a drift-diffusion model with velocity saturation for spin-polarized transport in semiconductors. *J. Math. Anal. Appl.* 420, 2 (2014), 1167–1181.
- [211] ZAMPONI, N., AND JÜNGEL, A. Analysis of a coupled spin drift-diffusion Maxwell–Landau–Lifshitz system. *J. Differential Equations* 260, 9 (2016), 6828–6854.
- [212] ZHANG, S., LEVY, P. M., AND FERT, A. Mechanisms of spin-polarized current-driven magnetization switching. *Phys. Rev. Lett.* 88, 23 (2002), 236601.
- [213] ZHANG, S., AND LI, Z. Roles of nonequilibrium conduction electrons on the magnetization dynamics of ferromagnets. *Phys. Rev. Lett.* 93, 12 (2004), 127204.

Curriculum Vitae

Michele Ruggeri

Personal information

Date of birth: April 12, 1988
Place of birth: Bergamo, Italy
Citizenship: Italian
Marital status: Married
Private address: Oswaldgasse 118/5/10, 1120, Vienna, Austria
Work address: TU Wien, Institute for Analysis and Scientific Computing (E101)
Wiedner Hauptstraße 8-10, 1040, Vienna, Austria
Mail: michele.ruggeri@tuwien.ac.at
Webpage: <http://www.asc.tuwien.ac.at/~mruggeri/>

Scientific interests

Numerical approximation of PDEs; finite element methods; discontinuous Galerkin methods; computational electromagnetism; computational micromagnetics; boundary element methods.

Employment

Since 06/2013: **TU Wien, Vienna, Austria**
University assistant
10/2009 – 06/2012: **University of Pavia, Pavia, Italy**
Tutor

Education

06/2013 – 11/2016: **TU Wien, Vienna, Austria**
(expected) PhD in Technical mathematics
Supervisor: Prof. Dirk Praetorius
10/2007 – 10/2013: **Institute for Advanced Study, Pavia, Italy**
Diploma in Sciences and technologies
Supervisors: Prof. Daniele Boffi, Prof. Franco Brezzi
10/2010 – 04/2013: **University of Pavia, Pavia, Italy**
Laurea Magistrale (M.Sc.) in Mathematics
Supervisor: Prof. Ilaria Perugia
10/2007 – 09/2010: **University of Pavia, Pavia, Italy**
Laurea (B.Sc.) in Mathematics
Supervisor: Prof. Ilaria Perugia
10/2007 – 07/2012: **Almo Collegio Borromeo, Pavia, Italy**

Awards

- Premio di Laurea Proff. *Silvio Cinquini e Maria Cinquini Cibrario*, for the best master thesis in mathematics presented in the period 01.09.2012/30.09.2014 at the University of Pavia.

Publications (articles, proceedings, and preprints)

8. D. Praetorius, M. Ruggeri, B. Stiftnr: *Convergence of an implicit-explicit midpoint scheme for computational micromagnetics*. Submitted, preprint available at arXiv:1611.02465 (2016).
7. C. Abert, M. Ruggeri, F. Bruckner, C. Vogler, A. Manchon, D. Praetorius, D. Suess: *A self-consistent spin-diffusion model for micromagnetics*. Accepted for publication in Sci. Rep. (2016).
6. M. Ruggeri, C. Abert, G. Hrkac, D. Suess, D. Praetorius: *Coupling of dynamical micromagnetism and a stationary spin drift-diffusion equation: A step towards a fully self-consistent spintronics framework*. Physica B 486 (2016), 88–91.
5. C. Abert, M. Ruggeri, F. Bruckner, C. Vogler, G. Hrkac, D. Praetorius, D. Suess: *A three-dimensional spin-diffusion model for micromagnetics*. Sci. Rep. 5 (2015), 14855.
4. D. Boffi, L. Gastaldi, M. Ruggeri: *Mixed formulation for interface problems with distributed Lagrange multiplier*, Comput. Math. Appl. 68 (2014), 2151–2166.
3. F. Bruckner, M. Feischl, T. Führer, P. Goldenits, M. Page, D. Praetorius, M. Ruggeri, D. Suess: *Multiscale modeling in micromagnetics: Existence of solutions and numerical integration*, Math. Models Methods Appl. Sci. 24 (2014), 2627–2662.
2. C. Abert, G. Hrkac, M. Page, D. Praetorius, M. Ruggeri, D. Suess: *Spin-polarized transport in ferromagnetic multilayers: An unconditionally convergent FEM integrator*, Comput. Math. Appl. 68 (2014), 639–654.
1. M. L. Della Vedova, M. Ruggeri, T. Facchinetti: *On real-time physical systems*, in Proceedings of 18th International Conference on Real-Time and Network Systems (RTNS), November 2010, Toulouse, France.

Additional information

- Known languages: Italian (mother tongue), English, German.
- Main software skills: Linux, Microsoft Windows, Mac OS, ECDL Core, LaTeX, HTML, Matlab, C, C++, Python.